THE SYNTHESIS AND CHARACTERIZATION OF XENON AND RELATED MAIN-GROUP ELEMENT DERIVATIVES OF THE $O=IF_4O-$ GROUP

BY

© T. ROBERT GEORGE SYVRET, B.Sc.

A Thesis
Submitted to the School of Graduate Studies
in Partial Fulfilment of the Requirements
for the Degree
Doctor of Philosophy

McMaster University
May 1987

$O=IF_4O-$ DERIVATIVES OF XENON AND RELATED MAIN-GROUP ELEMENTS

TO MY PARENTS,

MAUGE AND BIG JIM

DOCTOR OF PHILOSOPHY (1987) McMASTER UNIVERSITY
(Chemistry) Hamilton, Ontario

TITLE: $O=IF_4O-$ Derivatives of Xenon and Main-Group Elements

AUTHOR: T. Robert George Syvret, B.Sc. (McMaster University)

SUPERVISOR: Professor G. J. Schrobilgen

NUMBER OF PAGES: xix, 297

Abstract

With improved syntheses of the $O{=}IF_4O-$ group precursors, $HOIOF_4$ and IO_2F_3, an extensive derivative chemistry of the $O{=}IF_4O-$ group has begun to emerge. The xenon(II) derivatives, $FXeOIOF_4$ and $Xe(OIOF_4)_2$, have been shown by their solution ^{19}F and ^{129}Xe NMR spectra to result from the reaction between IO_2F_3 and XeF_2 in SO_2ClF, $CFCl_3$ and BrF_5 solvents. The covalently bonded $O{=}IF_4O-$ groups are shown to be equilibrium mixtures of their cis- and trans-isomers and are oxygen bonded to xenon. The solid derivative, cis, cis-$Xe(OIOF_4)_2$, has been isolated from the acid displacement reaction between $Xe(OTeF_5)_2$ and the stronger protonic acid mixture cis/trans-$HOIOF_4$ under neat conditions, or in $CFCl_3$ solvent. A mixture of the cis- and trans-derivatives of $FXeOIOF_4$ were prepared by the stoichiometric reaction of IO_2F_3 with XeF_2 in anhydrous HF, followed by removal of the solvent under vacuum. Both cis/trans-$FXeOIOF_4$ and cis, cis-$Xe(OIOF_4)_2$ were characterized by ^{19}F and ^{129}Xe NMR spectroscopy and low-temperature Raman spectroscopy. A comparison among ^{129}Xe NMR chemical shifts for mixed Xe(II) derivatives, $F_4OIOXeOSO_2F$ and $F_4OIOXeOTeF_5$ has resulted in an effective group electronegativity order $-OSO_2F$ > trans- $O{=}IF_4O-$ > cis- $O{=}IF_4O-$ > $-OTeF_5$.

The thermal decomposition reactions of $FXeOIOF_4$ and cis, cis-$Xe(OIOF_4)_2$ have been studied by ^{19}F NMR spectroscopy and Raman spectroscopy. In the latter case, the novel $O{=}IF_4O-$ derivative, $F_4OIOOIOF_4$, has been prepared by the controlled thermal decomposition of cis, cis-$Xe(OIOF_4)_2$ as well as from the reaction of IO_2F_3 and KrF_2, and characterized by ^{19}F NMR spectroscopy and Raman spectroscopy.

Higher oxidation state derivatives of xenon were, until the present work, known only for $-OTeF_5$. The $O=IF_4O-$ derivatives, $F_3XeOIOF_4$ and $OXeF_3OIOF_4$, have been identified by ^{129}Xe and ^{19}F NMR spectroscopy as the products of the insertion reactions between IO_2F_3 and XeF_4 and $XeOF_4$, respectively. In addition, the mixed Xe(VI) derivatives, $OXe(OIOF_4)_x(OTeF_5)_{4-x}$, resulting from the reaction of $HOIOF_4$ with $OXe(OTeF_5)_4$, have been identified in situ by ^{129}Xe NMR spectroscopy. The solid product isolated from the neat reaction of $HOIOF_4$ with $OXe(OTeF_5)_4$, has been shown by ^{129}Xe NMR spectroscopy in solution and Raman spectroscopy in the solid state, to consist of a mixture of cis- and trans-isomers of the novel Xe(VIII) derivative, $O_3Xe(OIOF_4)_x(OTeF_5)_{2-x}$.

Preliminary evidence obtained from Raman spectroscopy as well as ^{11}B and ^{125}Te NMR spectroscopy, suggests that novel $O=IF_4O-$ derivatives of boron, mercury and tellurium have also been formed.

ACKNOWLEDGEMENTS

I would like to thank my research supervisor, Dr. G.J. Schrobilgen, for his sincere interest in this work and for his constant support and encouragement throughout.

I would like to thank the members of my supervisory committee, Drs. Birchall and Lock, for their guidance and many useful suggestions. Thanks also to Dr. Gillespie for his participation as a member of my oral examining committee.

I gratefully acknowledge the technical assistance provided by Brian Sayer, Ian Thompson, Claus Schonfield and Lee Gowers as well as the masterful drafting performed by Dave Hodgson.

Financial support from McMaster University Chemistry Department, which provided scholarships (1982-1986), McMaster University, which provided Teaching Assistantships (1982-1986) and the Ontario Government, which provided Ontario Graduate Scholarships (1983-1985) is kindly acknowledged.

I wish to thank the many people at McMaster who have given me their valued friendship and because of whom, my memories of McMaster will always be pleasant ones. In particular, Lesley Devereux, Mar Björgvinsson, Dr. Veeragathy Manivannan (Manni), Mike Malott, Dr. O.E. Hileman Jr., Mr. Brooman, Mrs. Carol Dada and the lovely ladies, Linda and Kerstin.

My dearest friend, Steve Baynton (Tank), is thanked for

his loyal friendship that has lasted for so many years and has helped me endure some very rough times. Our friendship will always be cherished.

Finally, I wish to thank mom and dad for their continual love and support as well as Nan, Cass, my sisters Tina and Nancy, my brother Dave, Colleen, Davey and the amazing Danny. Without them, my life would be empty.

TABLE OF CONTENTS

Page

CHAPTER 1: INTRODUCTION

CHAPTER 2: EXPERIMENTAL

CHAPTER 3: AN IMPROVED SYNTHESIS OF $HOIOF_4$ AND DEFINITIVE ^{19}F NMR STUDY OF THE STRUCTURE OF IO_2F_3 AND THE cis- and trans-$HOIOF_4$ ISOMER RATIO

CHAPTER 4: THE PREPARATION OF $FXeOIOF_4$ AND $Xe(OIOF_4)_2$ AND THEIR CHARACTERIZATION BY NMR SPECTROSCOPY AND RAMAN SPECTROSCOPY

CHAPTER 5: THE DECOMPOSITION PRODUCTS OF cis/trans-$FXeOIOF_4$ AND cis, cis-Xe($OIOF_4$)$_2$ AND THE PREPARATION AND CHARACTERIZATION OF $F_4OIOOIOF_4$

CHAPTER 6: Xe(IV), (VI) AND (VIII) DERIVATIVES OF THE $-OIF_4O$ GROUP

CHAPTER 7: PRELIMINARY EVIDENCE FOR $-OIF_4O$ DERIVATIVES OF BORON, MERCURY AND TELLURIUM

CHAPTER 8: SUMMARY AND CONCLUSIONS

LIST OF TABLES

LIST OF FIGURES

Figure **Page**

Figure | Page

CHAPTER 1

INTRODUCTION

(A) HISTORICAL

Although the noble-gases had been known for more than 50 years prior to the discovery of the reactivity of xenon in 1962 by Neil S. Bartlett, their placement in Group 8 (Group 18 under the recently sanctioned I.U.P.A.C. revisions to the periodic table) did not occur widely until general acceptance of noble-gas reactivity was gained. During the whole period 1895-1933 after the discovery of argon by Ramsay and Rayleigh (1) in 1895 (Ramsay provided Moissan with about 100 ml of the gas so that he could react it with fluorine which Moissan had isolated in 1886), the myth of chemical inertness of the noble-gases was not all-powerful, as numerous attempts at making compounds of the noble-gases show (2-7). It is only after Yost and Kaye's (8) reported failure to form a xenon fluoride in 1933 using a discharge method which, some 30 years later, was shown to work in the hands of other experimentalists; and the attendant loss of faith by Linus Pauling who helped instigate the Yost and Kaye experiments at Caltech, that this myth ascended into a rigid dogma. No doubt, Pauling's influence and his becoming interested in more biological quests had a lot to do with this.

In other terms, the octet rule was not seen as a deterrent to the existence of noble-gas compounds until the mid-1930's. In fact, the famous "The Atom and the Molecule" paper by G.N. Lewis, with the octet theory, dates back to 1916 and Irving Langmuir's concept of the atoms as made of concentric electronic shells appeared in 1919. However, a paper by W. Kossel (9), also published in 1916, argued from the standpoint of a stable configuration of eight electrons, but could also make, in the same paper, the prediction of xenon and krypton fluorides. In the 1930's there was general acceptance by chemists of modern electronic theories of the atom as the basis for the periodic table. After 1933, when Linus Pauling himself started to assert the inertness of the noble-gases, the octet rule became entrenched and it became the common lot of the noble-gases to be allocated to Group 0 of the periodic table. What history shows is that the myth of chemical inertness of the noble-gases was not in full force until recently, when for instance, Neil Bartlett feared ridicule from his colleagues in the department and from his students (10).

The remaining episode is well known. After reporting that PtF_6 oxidizes O_2 to O_2^+, forming $[O_2]^+[PtF_6]^-$ (11,12), Bartlett (13) surmised that a similar reaction should occur with xenon, since the first ionization potential of xenon (1170 kJ mol^{-1}) is less than that of oxygen (1176 kJ mol^{-1}). The reaction of PtF_6 vapor and xenon gas at room temperature yielded an orange-yellow solid initially reported to be

$Xe^+[PtF_6]^-$ and was summarily communicated (13). Within months of the discovery of this first true compound of xenon, the binary fluorides XeF_2 (14-18), XeF_4 (19), XeF_6 (20,21) and KrF_2 (22) were reported by other workers. The immediate developments in noble-gas chemistry which followed these initial reports have resulted in the preparation of three binary fluorides, two oxides and five oxide fluorides of xenon, krypton difluoride and a fluoride(s) of radon. Much of this earlier work has been summarized in a number of comprehensive reviews on the subject (23-35). In addition to simple fluorides, oxides and oxide fluorides, a number of derivatives have been prepared as ionic complexes, molecular adducts or which contain pseudo-halogen type ligands of high effective group electronegativity.

(B) NOBLE-GAS FLUORIDES, OXIDE FLUORIDES AND OXIDES

(i) Xenon Fluorides: Preparation and Properties

Xenon difluoride can be prepared by one of two routes. The first route involves the photolysis of equimolar quantities of Xe and F_2 with ultra-violet light from either a mercury arc source (36) or from direct sunlight (37). Alternatively, XeF_2 is prepared when mixtures of Xe and F_2, in the ratio 2:1, are reacted at high pressure and temperature (38). The XeF_2 formed is a colorless, crystalline solid (m.p. 129°C) which has a vapor pressure of 4.6 Torr at 25°C (39). Vibrational analyses have shown that the linear molecular structure is present in both the solid and vapor state. Xenon difluoride dissolves in water to the extent of 25 g dm^{-3} at 0°C forming solutions which are marginally stable (half-life $\approx$ 7 h) in the absence of base. In base, hydrolysis is instantaneous (40). Aqueous XeF_2 is a powerful oxidant ($E° \approx 2.64$ V), oxidizing Ag(I) to Ag(II), Ce(III) to Ce(IV) and even bromate to perbromate (40-42). In the case of $[BrO_4]^-$, its preparation by oxidation of $[BrO_3]^-$ with XeF_2 forms the basis for the first synthesis of this novel anion (40,41). In base, XeF_2 oxidizes Xe(VI) to Xe(VIII) (42).

Xenon tetrafluoride is best prepared by heating a 1:5 mixture of Xe and F_2 to 400°C under ca. 7 atm. pressure for a one hour in a nickel can (43). The XeF_4, like XeF_2, is a colorless crystalline solid and has a square planar molecular geometry (D_{4h}, AX_4E_2 arrangement of lone pairs and bond pairs) in both the solid and vapor states. The solid has a melting point of 117°C and a vapor pressure of 2.5 Torr at 25°C (39). Xenon tetrafluoride is rapidly hydrolysed in water, yielding a variety of products which include XeO_3 (44,45).

Xenon hexafluoride is prepared as a pure compound by the heating of 1:20 mixtures of Xe and F_2, respectively, at 250 - 300°C for 16 hours under 50 - 60 atm. pressure (46). The XeF_6 formed is a colorless, crystalline solid (m.p. 49.5°C) with a vapor pressure of 27 Torr at 25°C (39). In the melt and vapor phases, XeF_6 is yellow to yellow-green. The structure of XeF_6 has been the subject of controversy since its discovery in 1963. In the crystalline state, at least four different phases of XeF_6 are known (47). The basic structural unit in each phase, however, consists of $[XeF_5]^+$ ions (C_{4v} symmetry) bridged by F^- ions. Three of the phases are tetramers, $[(XeF_5^+)F^-]_4$, while in the fourth, the unit cell contains 24 tetramers and 8 hexamers $[(XeF_5^+)F^-]_6$ (48). Electron-diffraction studies of XeF_6 vapor are consistent with the predictions of the valence shell electron-pair repulsion (VSEPR) rules (49) and a distorted octahedral arrangement of six fluorine atoms and one non-bonding lone pair around the central xenon (AX_6E) (50,51). The hydrolysis of XeF_6 is extremely vigorous, yielding either $XeOF_4$, XeO_2F_2 or XeO_3, depending on the quantity of H_2O used (42,52,53).

(ii) Xenon Oxide Fluorides: Preparation and Properties

There are five xenon oxide fluorides presently known: $XeOF_2$, $XeOF_4$, XeO_2F_2, XeO_3F_2 and XeO_2F_4. While all five oxide fluorides have been well characterized, it appears that only $XeOF_4$ is thermodynamically stable ($\Delta H_f° = -25.1$ kJ mol^{-1}) (54-61).

Prior to the isolation of pure $XeOF_2$ in 1977 (60), evidence for its existence had been reported on two previous occassions (45,62). In neither case, however, was the compound isolated in a pure state nor was any evidence for its structure given. Xenon oxide difluoride was first prepared in pure form by the reaction of finely divided XeF_4 with water, in HF solvent at low temperature (60). The Raman spectrum recorded on pure $XeOF_2$ was consistent with monomeric units of C_{2v} symmetry (AX_3E_2 arrangement) (60). Xenon oxide difluoride is a light-yellow solid which decomposes explosively at ca. 0°C.

Xenon oxide tetrafluoride can be prepared by the partial hydrolysis of XeF_6 (63), by the reaction of XeF_6 with either glass (63) or silica (20), or by the reaction of XeF_6 with one mole of water in HF solution (53). The compound is colorless in all physical states, low melting (-46.2°C), volatile (v.p. (25°C) = 35 Torr) and stable with respect to decomposition at room temperature (64). Its structure is consistent with monomeric ~~units (AX~~$_5$E arrangement) having C_{4v} symmetry.

Xenon dioxide difluoride has been prepared by the reaction of XeO_3 with $XeOF_4$ (65) or by the interaction of a 2:1 molar ratio of water to XeF_6 in HF solution (53). The colorless crystals of XeO_2F_2 (m.p. 30.8°C) have a volatility between that of XeO_3 and XeF_2 (65) and are mildly shock sensitive (ΔH_f° = +234 kJ mol^{-1} (61)). The structure of XeO_2F_2 has been shown by Raman spectroscopy and ^{19}F NMR spectroscopy, to consist of monomeric units (AX_4E arrangement) having C_{2v} symmetry (53) as predicted by VSEPR rules (49).

Xenon trioxide difluoride is best prepared by the reaction of XeF_6 with XeO_4 (66,67). The pale-yellow crystals of XeO_3F_2 are volatile at -78°C and are reported to melt at -54.1°C. Raman and infrared spectra, acquired by matrix-isolation techniques (67), are consistent with the D_{3h} symmetry

(AX_5 arrangement) predicted by Gillespie (68).

Xenon dioxide tetrafluoride, XeO_2F_4, has been reported as the product obtained in low yield from the reaction of XeF_6 with XeO_3F_2 in $XeOF_4$ solvent (66,69) and has been characterized by mass spectrometry. The structure and stability of XeO_2F_4 is of particular interest since the isoelectronic $[IO_2F_4]^-$ anion is known to exist as both a cis- and trans-isomer and to be very stable (Section D).

(iii) Xenon Oxides: Preparation and Properties

There are presently two neutral xenon oxide species known, XeO_3 and XeO_4. Xenon trioxide is formed in the hydrolysis of XeF_6, XeF_4, $XeOF_4$ or XeO_2F_2 as cited earlier. It can be obtained in pure form from the hydrolysis reaction, by removal of water and HF under vacuum (70). It is, however, a powerful explosive ($\Delta H_f° = +402 \pm 8$ kJ mol^{-1} (71)) and should only be prepared by experienced workers. Pure XeO_3 is very soluble in water, forming stable, yet powerfully oxidizing, solutions. Xenon tetroxide is prepared by the reaction of anhydrous sulfuric acid with sodium or barium perxenate (61,72). The tetroxide is the most volatile xenon compound known (v.p. (0°C) = 25 Torr). Xenon tetroxide vapor is explosive ($\Delta H_f° = +642.2$ kJ mol^{-1} (61)) in high concentrations at room temperature, and in the solid state, may explode at temperatures as low as -40°C.

(iv) Krypton and Radon Fluorides

Krypton difluoride cannot be prepared by direct fluorination of krypton gas at high pressures and temperatures as is the case for the fluorides of xenon (73). The high ionization potential of krypton (1351 kJ mol^{-1} (74)) requires the use of low-temperature, high-energy methods (22,75,76). Krypton difluoride can be prepared by electric glow discharge of Kr/F_2 mixtures at liquid oxygen temperature (-183°C) (22), photolysis of Kr/F_2 mixtures at liquid nitrogen temperatures (77,78) or by the use of hot-wire techniques (79). Krypton difluoride is a white crystalline solid which sublimes readily below 0°C, and at room temperature, has a vapor pressure estimated to be well above 100 Torr. The compound has an estimated half-life of four hours in the vapor state at room temperature, but can be maintained indefinitely at dry-ice temperature (53). The mean thermochemical bond energy is approximately 50 kJ mol^{-1} (53), which in fact, is the lowest bond energy of any fluoride. The extraordinary low-temperature fluorinating ability of KrF_2 is thus not unexpected. For example, the krypton difluoride derivatives, $[KrF]^+[AsF_6]^-$, $[Kr_2F_3]^+[AsF_6]^-$ and $[Kr_2F_3]^+[SbF_6]^-$ are capable of oxidizing BrF_5 to $[BrF_6]^+$ (80), a feat which the strong fluorinating agent, PtF_6, is unable to achieve even in the presence of ultraviolet light (53). Krypton difluoride oxidizes Au metal in HF to the Au(VI) species $[KrF]^+[AuF_6]^-$ from which is derived, upon pyrolysis, AuF_5 (81).

No krypton oxides or higher oxidation state krypton fluorides are known at this time. An early report that KrF_4 was formed by electric discharge of mixtures of Kr and F_2 (82) was later shown to be erroneous (22,83).

Radon-222 is the longest-lived radioactive isotope of Rn and is produced by the decay of radium having a half-life of 3.823 days, decaying by alpha emission. As a result, all radon chemistry is performed on the tracer scale. The first evidence for a radon fluoride was obtained when radon could not be pumped from a nickel reaction vessel after reaction with fluorine at 400°C (14,84,85). The hydrolysis of radon fluoride has been studied (86,87). Its behavior is analogous to KrF_2 and XeF_2, which suggests the fluoride is RnF_2 (86,87). No higher oxidation state radon fluorides, oxides or oxide fluorides are presently known.

(v) Derivatives of Noble-Gas Fluorides and Oxide Fluorides

The chemistry of noble-gas fluorides and oxide fluorides with respect to derivative formation is extensive in comparison to other main-group fluorides and oxide fluorides. Whereas the vast majority of examples are those derived from xenon, krypton and radon derivatives are also known. The noble-gas derivatives can be conveniently divided into three categories: (1) those formed in reactions of a noble-gas fluoride or oxide fluoride with a fluoride-ion donor (2) a fluoride-ion acceptor, and (3) those formed as covalent derivatives with ligand groups, other than fluorine or oxygen, of high electronegativity. The examples included in categories (1) and (2) will be dealt with only briefly here. Those examples in category (3) are considered in detail in Section (C) of this Chapter.

The fact that xenon fluorides and oxide fluorides form cationic species in the presence of fluoride-ion acceptors is well established. The reaction of 1:1 quantities of XeF_2 and a Lewis acid pentafluoride MF_5 (M = As, Sb, Ta, Nb, Ru, Os, Ir, V) results in the formation of ionic compounds of the general form $[XeF]^+[MF_6]^-$ (88-90) where the $[XeF]^+$ cation forms a weak covalent bond with the anion (fluorine-bridge). In some cases, where an excess of pentafluoride is used, more weakly basic polyanions are formed (88,91,92), resulting in compounds of the general form $[XeF]^+[M_2F_{11}]^-$ (M = Sb, Nb, Ta, Ir, Os, Ru, Rh). On the other hand, if excess XeF_2 is used, the V-shaped fluorine-bridged cation $[Xe_2F_3]^+$ (C_{2V}) is formed (90,92-94). Furthermore, dissolution of $[Xe_2F_3]^+[AsF_6]^-$ in HSO_3F solvent, results in the solvolysis and formation of the unique fluorosulfate-bridged species $[(FXe)_2SO_3F]^+[AsF_6]^-$ (95). Molecular adducts are formed when XeF_2 is allowed to react with a transition-metal oxide fluoride, MOF_4 (M = W, Mo), resulting in the species $XeF_2 \cdot nWOF_4$ (n = 1-4) and $XeF_2 \cdot MoF_4$ (96). In all cases, the basic structural unit consists of a linear F-Xe ·· F-M interaction. It has been reported that when XeF_2 or XeF_4 are reacted with CsF at high temperatures, an adduct of empirical composition $2CsF \cdot XeF_6$ is formed (97). This result suggests the occurrence of disproportionation processes on heating the lower fluorides of xenon in the presence of CsF to give xenon(VI). These xenon(VI) species would therefore be best represented by the ionic formulation $[XeF_8]^{2-}$. There are no examples presently known where XeF_2 or XeF_4 act as a fluoride-ion acceptors forming $[XeF_3]^-$ and $[XeF_5]^-$, respectively.

Xenon tetrafluoride forms cationic complexes with only the strongest Lewis acids. Bartlett <u>et al.</u> have reported that XeF_4 does not form stable adducts with either AsF_5 or IrF_5 in bromine pentafluoride solution (98) or with RuF_5 (99). Xenon tetrafluoride does, however, react with SbF_5 to give complexes containing the $[XeF_3]^+$ (C_{2v}, AX_3E_2 arrangement) cation weakly fluorine bridged to the counter-ions $[SbF_6]^-$ or $[Sb_2F_{11}]^-$ (100-105). In addition, XeF_4 forms a 1:1 and 1:2 adduct with the more weakly acidic acceptor BiF_5 in which the fluorine bridge interaction between $[BiF_6]^-$ or $[Bi_2F_{11}]^-$ and $[XeF_3]^+$ is substantially stronger than in the antimony compounds (90,106). Attempts to generate the complex cation, $[Xe_2F_7]^+$, using a strategy analogous to that used for the preparation of $[Xe_2F_3]^+$, were unsuccessful (101).

Xenon hexafluoride is an even stronger fluoride-ion donor than XeF_2 (98,107,108). The reaction of XeF_6 with fluoride-ion acceptors such as MF_5 (M = Sb, As, Pt, Ru, V), MF_4 (M = Pd, Ge, Sn) and MF_3 (M = B, Fe, Co) results in the formation of ionic complexes containing the $[XeF_5]^+$ (C_{4V}, AX_5E arrangement) cation and the corresponding anion (109,110). Xenon hexafluoride forms a fluorine-bridged cation $[Xe_2F_{11}]^+$, by analogy with $[Xe_2F_3]^+$ (92-94). The first report of a compound containing the $[Xe_2F_{11}]^+$ cation, $[Xe_2F_{11}]^+[AuF_6]^-$ (111,112), was of dual significance since both the cation, and the gold anion in the +5 oxidation state, were previously unknown.

Krypton difluoride, like XeF_2, behaves as a fluoride-ion donor towards fluoride-ion acceptors yielding the thermally unstable compounds $[KrF]^+[MF_6]^-$ and $[Kr_2F_3]^+[MF_6]^-$ (M = Sb, As) (113,114), $KrF_2 \cdot nMoOF_2$ (n = 1-3) (115) and $KrF_2 \cdot WOF_4$ (115). Krypton difluoride undergoes an oxidation-reduction reaction with PtF_6 forming $[KrF]^+[PtF_6]^-$ and F_2 (114). In addition, KrF_2 reacts with gold metal in HF solvent at room temperature, yielding the Au(V) compounds $[KrF]^+[AuF_6]^-$ and $[KrF]^+[Au_2F_{11}]^-$ (81).

A few derivatives of radon fluoride with fluoride-ion acceptors have now been reported and are summarized in a recent comprehensive review of radon chemistry (116).

The xenon oxide fluorides, $XeOF_4$ and XeO_2F_2, react with SbF_5 forming the species $[XeOF_3]^+[SbF_6]^-$, $[XeOF_3]^+[Sb_2F_{11}]^-$ and $[XeO_2F]^+[Sb_2F_{11}]^-$ (101,117). The ^{19}F NMR spectra recorded on SbF_5 solutions containing these species (101), shows in each case, that the structure of the cation conforms to that predicted by VSEPR rules (49).

The number of noble-gas anions is more limited. Of the binary fluorides, only XeF_6 forms anionic species when reacted with fluoride-ion donors. Xenon hexafluoride reacts with alkali metal fluorides to form $M^+[XeF_7]^-$ (M = Rb, Cs) and $M^+{}_2[XeF_8]^{2-}$ (M = Na, K, Rb, Cs) species (118,119). The $[NO]^+$ salt, $[NO^+]_2[XeF_8]^{2-}$, is formed in the reaction of XeF_6 with NOF (120,121). The X-ray structure of the $[NO]^+$ salt shows that the anion $[XeF_8]^{2-}$ assumes a square antiprismatic structure (D_{4d}) implying the non-bonding lone pair is stereochemically inactive. This contrasts with the structure of XeF_6, where the non-bonding electron lone pair is known to be stereochemically active (50,51).

The xenon oxide fluorides $XeOF_2$, XeO_2F_2 and $XeOF_4$ all exhibit fluoride-ion acceptor properties. The reaction of $XeOF_2$ with CsF, yields the bright yellow salt, $Cs^+[XeOF_3]^-$, which is stable at room temperature for up to several hours (60). Furthermore, the disproportionation of $XeOF_2$ in the presence of CsF, leads to the stable anion $[XeO_2F_3]^-$ (60), a derivative of XeO_2F_2. Xenon oxide tetrafluoride forms stable adducts with a number of fluoride ion donors including KF, RbF, CsF and NOF (86,121-123). In the case of the 1:1 CsF:$XeOF_4$ adduct, the basic structural unit is the $[XeOF_5]^-$ (AX_6E arrangement) anion. In addition, preparations at 3:1 molar ratios of CsF and $XeOF_4$, have led to the novel $[(XeOF_4)_3F]^-$ anion (123). Crystallographic analysis (123) has shown that the structure of this novel anion is consistent with a trigonal arrangement of three equivalent $XeOF_4$ molecules coordinated through the three Xe atoms to a central F^- ion.

Of the two xenon oxides, only XeO_3 forms a stable anion with fluoride-ion donors. Xenon trioxide reacts with CsF to form the $[XeO_3F]^-$ anion (124). This anion is stable at room temperature (124), in contrast to XeO_3, which is dangerously explosive (70).

(C) COMPOUNDS CONTAINING HIGHLY ELECTRONEGATIVE GROUPS OTHER THAN OXYGEN AND FLUORINE

(i) General

Highly electronegative ligand-groups resemble fluorine in its ability to stabilize high oxidation states of the elements, and in most cases, have the advantage of avoiding bridging which is frequently found in many fluorides. There are a few examples where a ligand-group (other than oxygen or fluorine) is known to bridge two, formally positive charged centers. Examples are $[(FXe)_2SO_3F]^+ [AsF_6]^-$ (95), $[AgOTeF_5(C_6H_5CH_3)_2]_2$ (125), $AgOTeF_5$ (125), $AgOTeF_5(CH_3CN)_x$ (125) and $Au(OTeF_5)_3$ (126).

In general, all of these ligand-groups satisfy the same set of criteria, i.e., all exist in the form of a moderate to strong monoprotic acid, all form positive chlorine derivatives and stable alkali metal salts and all have probable high group electronegativities. In the case of the pentafluoroorthotellurate group, $-OTeF_5$, the effective group electronegativity

(3.87 on the Pauling scale) is only slightly less than that of fluorine itself (127,128).

The chemistry of compounds containing the ligand-groups $-OSeF_5$ and, in particular, $-OTeF_5$ have been the most extensively studied, and their derivatives are now known for many of the chemical elements. It is beyond the scope of this work to discuss all of these derivatives in detail. Instead, the emphasis here will focus on the covalent ligand-group derivatives of the noble-gases. For a complete account of all the known derivatives, the reader is directed to a number of recent articles (129-131) written on the ligand properties of these groups, and a comprehensive review (132) of all known derivatives containing these groups.

(ii) Ligand-Group Derivatives of Xenon

In addition to the simple binary fluorides, oxides and oxide fluorides of xenon cited earlier, a number of derivatives are known in which xenon is covalently bonded to a ligand-group through either oxygen or nitrogen. Included in this list of ligands are $-OSO_2F$ (133,134), $-OTeF_5$ (135-142), $-OPOF_2$ (135,143), $-OSeF_5$ (144,145), $-OClO_3$ (133,134), $-OCOCF_3$ (138,146), $-OSO_2CF_3$ (134), $-ONO_2$ (147), $-N(SO_2F)_2$ (148-152) and $-N(SO_2CF_3)_2$ (153). The covalent xenon(II) derivatives $FXeBF_2$ (154) and $Xe(CF_3)_2$ (155) have also been reported, however, no definitive physical evidence was given to support their covalent Xe-B and Xe-C formulations. Thus, the existence of examples of either a Xe-B or a Xe-C bonded species still remains unknown.

Table 1.1 summarizes all the known covalent ligand group derivatives of xenon and their physical properties. From inspection of Table 1.1, it is evident that the $-OTeF_5$ group is second only to oxygen and fluorine in its ability to stabilize the +4 and +6 oxidation states of xenon. Until the present work, no other ligand-group had demonstrated this ability. A report by Eisenberg and DesMarteau (156) that XeF_4 and XeF_6 react with HSO_3F to give $F_2Xe(OSO_2F)_2$ and $F_4Xe(OSO_2F)_2$, respectively, was later shown to be in error (109,157). Xenon(VI) fluorosulfate F_5XeOSO_2F is known (109, 157), however, this compound is best described as an ionic complex containing the $[XeF_5]^+$ and $[SO_3F]^-$ ions.

The thermal stabilities of ligand-group derivatives of xenon vary, but in any case, are less stable than those of their corresponding binary fluorides or oxide fluorides. This fact is clearly illustrated by comparing the decomposition temperatures for XeF_4 (300°C) and $Xe(OTeF_5)_4$ (72°C). The vast difference in stabilities presumably arises from the fact that the peroxide $F_5TeO-OTeF_5$ is formed much more readily than F_2 (equations 1.1 and 1.2) as well as the relative bond strengths, i.e. Xe-O < Xe-F.

$$XeF_4 \xrightarrow{300-600°C} XeF_2 + F_2 \qquad (1.1)$$

Table 1.1

Known Ligand-Group Derivatives of Xenon and Their Physical Properties

Compound	Appearance at Room Temperature	Physical Properties and Stability	Ref.
$FXeOTeF_5$	pale-yellow liquid	m.p. -24°C b.p. 53°C	135
$Xe(OTeF_5)_2$	white solid	m.p. 35-37 °C	136
$Xe(OTeF_5)_4$	pale-yellow solid	m.p. 72°C with decomposition	139
$OXe(OTeF_5)_4$	white solid	m.p. 56°C	140
$O_2Xe(OTeF_5)_2$	white solid	decomposes above 0°C	142
$[Xe(OTeF_5)_6]^a$	red/violet solid at -40°C	decomposes above -10°C	140
$FXeOSO_2F$	white solid yellow-green melt	m.p. 36.6°C	133
$Xe(OSO_2F)_2$	yellow solid	m.p. 43-45°C	133
$FXeOPOF_2$/ $Xe(OPOF_2)_2$	pale-yellow solids	decompose at room temperature	143
$FXeOClO_3$	white solid	m.p. 16.5°C	134
$Xe(OClO_3)_2$	pale-yellow solid	decomposes above -20°C	133

Table 1.1 Continued

Compound	Appearance at Room Temperature	Physical Properties and Stability	Ref.
$FXeOCOCF_3$/ $Xe(OCOCF_3)_2$	pale-yellow solids	explode above -20°C	138
$FXeOSO_2CF_3$	yellow solid at 0°C	decomposes slowly at 0°C	134
$FXeOSeF_5$	pale-yellow liquid	m.p. ≈ -13°C	144
$Xe(OSeF_5)_2$	yellow solid	m.p. 69°C	144
$FXeN(SO_2F)_2$/ $Xe[N(SO_2F)_2]_2$	white solids	decompose slowly at room temperature	150 151
$Xe[N(SO_2CF_3)_2]_2$	white solid	stable at room temperature for days	153
$FXeONO_2$/ $Xe(ONO_2)_2$	[red-brown solids][b]	decompose rapidly at room temperature	147

a: Evidence for $Xe(OTeF_5)_6$ is based on decomposition products (140) and preliminary X-ray analysis (141).

b: Evidence for $FXeONO_2$ and $Xe(ONO_2)_2$ is based on decomposition products only (147).

$$Xe(OTeF_5)_4 \xrightarrow{72°C} Xe(OTeF_5)_2 + F_5TeO{-}OTeF_5 \quad (1.2)$$

Furthermore, thermal stability of the xenon(II) derivatives increases in the order $-OSO_2F < -OSeF_5 < -OTeF_5$, and is consistent with the decreasing stability of the corresponding peroxides. This trend is exemplified by the $-OClO_3$ and $-OCOCF_3$ derivatives of xenon(II). Whereas $Xe(OClO_3)_2$ decomposes above -20°C and $Xe(OCOCF_3)_2$ detonates above -20°C, the corresponding decomposition products, Cl_2O_7 and $F_3OCOOCOCF_3$, are stable up to their boiling points, (Cl_2O_7 b.p. = 82°C (158), $F_3OCOOCOCF_3$ b.p. = 40°C (159)) if not shocked.

(iii) Preparation of Ligand-Group Derivatives of Xenon

The syntheses of covalently bonded ligand-group derivatives of xenon can be accomplished in a variety of ways. DesMarteau and Eisenberg (143) have produced difluorophosphate, $-OPOF_2$, derivatives of xenon(II) by direct reaction of xenon difluoride with μ-oxobis(phosphoryldifluoride), $P_2O_3F_4$, in trichlorofluoromethane $CFCl_3$ solvent at 22°C according to equations (1.3) and (1.4).

$$XeF_2 + P_2O_3F_4 \xrightarrow[CFCl_3]{22°C} FXeOPOF_2 + POF_3 \quad (1.3)$$

$$XeF_2 + 2\ P_2O_3F_4 \xrightarrow[CFCl_3]{22°C} Xe(OPOF_2)_2 + 2\ POF_3 \quad (1.4)$$

The derivatization proceeds with net insertion of the PO_2F moiety into the Xe-F bond, yielding either the mono-substituted or di-substituted derivatives according to the stoichiometric reactions (1.3) and (1.4). The work of DesMarteau and Eisenberg (143) had represented the only example, prior to the present work, where an oxide fluoride precursor was used to prepare xenon(II) derivatives by means of the insertion method. For the other ligand-groups where an oxide fluoride precursor is known, such as for the $-OTeF_5$ group (TeO_2F_8 (160,161)) or the $-OSeF_5$ group (SeO_2F_8 (160,161)), insertion methods have not been employed and alternative methods have been used for preparing xenon(II) derivatives.

The synthetic method which has proven most general for the preparation of xenon(II) derivatives involves the direct interaction of XeF_2 with the corresponding ligand-group's protonic acid leading to HF displacement. An example of a HF displacement reaction, generalized for any ligand-group acid RH, is given by equation (1.5).

$$XeF_2 + n\,RH \rightleftharpoons F_{2-n}XeR_n + n\,HF \qquad (1.5)$$

The key components in equation (1.5) are the volatility of HF at low temperature (v.p. HF (-45°C) = 40 mm Hg (159)), which is pumped off forcing the reaction to completion, and the acid strength of RH. The latter method has been used in the preparation of $-OTeF_5$ (135-138), $-OSeF_5$ (144), $-OSO_2F$ (133,134), $-OClO_3$ (133,134), $-OPOF_2$ (135), $-OCOCF_3$ (138,146) and $-N(SO_2F)_2$ (148-152) derivatives of xenon(II).

The boron derivative, $B(OTeF_5)_3$, was first prepared in 1973 by Sladky et al. (162) according to equation (1.6).

$$BCl_3 + 3\ HOTeF_5 \longrightarrow B(OTeF_5)_3 + 3\ HCl \quad (1.6)$$

Since then, this reagent has proven to offer the most convenient route to $-OTeF_5$ derivatives of xenon, and in fact, represents the only method for preparing xenon(IV) (139,141) and xenon(VI) derivatives (140-142). When a xenon fluoride or oxide fluoride is allowed to react at low temperature with stoichiometric amounts of the ligand transfer reagent $B(OTeF_5)_3$ in an inert solvent, the corresponding $-OTeF_5$ derivative is generated quantitatively, with elimination of BF_3 gas. Equation (1.7) illustrates this preparative method using XeF_2 as an example.

$$XeF_2 + 2/3\ B(OTeF_5)_3 \xrightarrow[CFCl_3]{0\,°C} Xe(OTeF_5)_2 + 2/3\ BF_3 \uparrow \quad (1.7)$$

A ligand transfer reagent has also been used in the preparation of the nitrogen-bonded derivative $Xe[N(SO_2CF_3)_2]_2$. DesMarteau (153) has shown that by reacting the silylimide precursor $Me_3SiN(SO_2CF_3)_2$, prepared according to equation (1.8), with XeF_2 (equation (1.9)), the desired product is attained in high yield. In addition, formation of HF, which is a major problem in promoting side reactions, is eliminated.

$$\mathrm{Me_3SiH} + \mathrm{(CF_3SO_2)_2NH} \xrightarrow{-195\ \mathrm{to}\ 22^\circ\mathrm{C}} \mathrm{Me_3SiN(SO_2CF_3)_2} + \mathrm{H_2}\uparrow \qquad (1.8)$$

$$2\ \mathrm{Me_3SiN(SO_2CF_3)_2} + \mathrm{XeF_2} \xrightarrow[\mathrm{CF_2Cl_2}]{-22\ \mathrm{to}\ 10^\circ\mathrm{C}} \mathrm{Xe[N(SO_2CF_3)_2]_2} + \mathrm{Xe}\uparrow + 2\ \mathrm{Me_3SiF} \qquad (1.9)$$

This represents the only method where a metathesis reaction, apart from H/F metathesis, which occurs in the acid displacement scheme (1.5), has been used to prepare xenon derivatives.

(iv) Major Physical Methods Used in the Characterization of Noble-Gas Derivatives

Characterization of covalent ligand-group derivatives of xenon has been accomplished by the application of a wide range of physical methods. These methods include multinuclear magnetic resonance spectroscopy (NMR), infrared and Raman spectroscopy, mass spectrometry, Mössbauer spectroscopy and X-ray crystallography. The method of characterization used is dictated by the physical properties of the xenon derivative, and in particular, the thermodynamic stability of the derivative under the conditions required by a particular physical technique.

NMR Spectroscopy

The characterization of xenon derivatives in solution is best achieved through the use of multinuclear magnetic resonance spectroscopy (NMR). With the availability of state-of-the-art pulse Fourier-transform spectrometers, the potential exists for studying, directly, most nuclei involved in ligand-groups which bond to or are alleged to bond to a noble-gas. Included in this list of nuclei are ^{11}B, ^{13}C, ^{15}N, ^{17}O, ^{19}F, ^{31}P, ^{77}Se, ^{125}Te and ^{129}Xe.

Xenon-129 is an ideal nucleus to study by Fourier-transform techniques insofar as it has a high natural abundance (26.44%), is a non-quadrupolar nuclide ($I = \frac{1}{2}$) and possesses a receptivity that is 31.6 times that of natural abundance ^{13}C (58). From the stand-point of gross structural determinations for xenon derivatives, the ^{129}Xe resonance of the central Xe atom provides the most structural information based on nuclear spin-spin coupling multiplicities. For instance, although a large number of xenon species possessing terminal Xe-F bonds have been adequately characterized in solution using ^{19}F NMR spectroscopy and the coupling patterns arising from ^{19}F-^{19}F and ^{129}Xe-^{19}F couplings (^{129}Xe satellite spectra, usually a doublet due to a single fluorine directly bonded xenon) (94,95,109,135,138,144,148-152,163), there exist a considerable number of derivatives in which the xenon is bonded exclusively to atoms other than fluorine, e.g. $Xe(OTeF_5)_2$. Effective characterization of these derivatives frequently cannot be based solely on the ^{19}F NMR resonance since, the ligating atom itself or its homonuclear spin-spin couplings or those with ^{129}Xe cannot be readily observed without expensive and time consuming enrichment procedures. For instance, the ^{129}Xe

resonances and accompanying ^{125}Te satellite multiplicities in the ^{129}Xe spectrum, were used to provide definitive evidence for Xe(OTeF$_5$)$_4$ (139,141), OXe(OTeF$_5$)$_4$ (140-142) and O$_2$Xe(OTeF$_5$)$_2$ (142) in solution. The ^{129}Xe resonance has been observed for all xenon derivatives of -OTeF$_5$ (127,139-142,164), -OSeF$_5$ (164), -OSO$_2$F (58) and -N(SO$_2$F)$_2$ (149-152). Complimentary structural information for these species has been obtained from the ^{19}F and ^{125}Te resonances of -OTeF$_5$ derivatives (127,135-138), the ^{19}F resonance of -OSO$_2$F derivatives (94,109), the ^{19}F and ^{77}Se resonances of -OSeF$_5$ derivatives (144,163) and from the ^{19}F (148-152), ^{15}N (150-152) and ^{17}O (150) resonances of -N(SO$_2$F)$_2$ derivatives. In the case of FXeN(SO$_2$F)$_2$ (150), ^{15}N and ^{129}Xe NMR spectroscopy on 30% ^{15}N-enriched samples were used to provide the first definitive proof for a Xe-N bond in solution based on the observation of the one-bond ^{129}Xe-^{15}N spin-spin coupling in the ^{129}Xe and ^{15}N spectra.

In addition to gross structural considerations, ^{129}Xe chemical shifts can provide information relating to the formal oxidation state of the xenon nucleus (58). Using the Ramsey theory of magnetic screening (165), the total shielding of the any nucleus (σ_T) can be represented by local diamagnetic (σ_d) and paramagnetic (σ_p) contributions as illustrated in equation (1.10). The diamagnetic contribution (σ_d) involves the free

$$\sigma_T = \sigma_d + \sigma_p \qquad (1.10)$$

rotation of electrons about the nucleus and is positive while the paramagnetic term (σp) describes the restriction to this rotation caused by other electrons and other nuclei in the molecule and is negative. In the case of xenon, approximations are made in which the long-range contributions to the shielding of the xenon nucleus from other nuclei are neglected (166). The paramagnetic shielding term (σp) thus represents the contribution from the electrons on xenon only and changes in the local electron environment, which accompany changes in oxidation state, affect the paramagnetic contribution (σ_p) to the shielding. The effective magnetic field at the nucleus (B) is influenced by the effect of the shielding term (σT) on the static applied magnetic field (B_o). These terms are related by equation (1.11). Furthermore, the resonance frequency ν

$$B = B_o(1-\sigma T) \qquad (1.11)$$

(Larmor frequency) is related to the static magnetic field (B_o), the shielding term σT and the magnetogyric ratio for Xe (γ_{Xe}) by expression (1.12). The net result is the resonance

$$\nu = \frac{\gamma_{Xe}}{2\pi} B_o(1-\sigma T) \qquad (1.12)$$

frequency (^{129}Xe chemical shift) occurs progressively to higher frequency as the paramagnetic shielding term (σp)

increases (becomes more negative) in going from the (+2) to (+8) oxidation states.

Xenon-129 and ^{19}F NMR chemical shifts as well as $^{129}Xe-^{19}F$ spin-spin coupling constants, are sensitive probes for assessing the ionicity of the terminal Xe-F bond and the covalency of the xenon-ligand atom bond (58,167). In xenon(II) species containing a terminal Xe-F bond, the Xe-F group is regarded as being bonded either to a fluorine, as in XeF_2, to an oxygen as in $FXeSO_2F$, or to a nitrogen, as in $FXeN(SO_2F)_2$. A near linear correlation exists between the ^{19}F chemical shifts and both the ^{129}Xe chemical shifts and $^{129}Xe-^{19}F$ coupling constants of these species. Furthermore, a decrease in ^{19}F chemical shift and $^{129}Xe-^{19}F$ coupling constant is consistent with a greater degree of ionic character in the terminal Xe-F bond. In addition, a decrease in ^{129}Xe chemical shift indicates an increasingly more covalent xenon-ligand atom bond. More recently, the correlation between ^{129}Xe chemical shifts and xenon-ligand atom bond covalency, has been used to determine the effective electronegativity of the $-OTeF_5$ group (127). These correlations are further addressed in Chapter 4 with emphasis on chemical shifts and ligand-group electronegativity, and have been extended to include the novel xenon(II) derivatives of the $-OIF_4O$ group prepared for the first time in the course of this work.

Although the magnitudes of $^{129}Xe-^{19}F$ spin-spin coupling constants might be expected to provide further information on bonding in xenon species, the theories of spin-spin coupling constants, which have been used successfully in the case of lighter elements, are not directly applicable to heavier nuclei such as xenon (167). The interaction of nuclear spins with the surrounding electrons give rise to spin-spin coupling. In general, the Fermi contact term, which describes the magnitude of the coupling between the electron and nuclear spin moments, and whose magnitude increases with increasing s-electron density at the nucleus, is assumed to be dominant over dipolar and spin-orbital effects. The generalized expression of the Fermi contact term for a n-bond coupling between two atoms (A) and (B) is given by equation (1.13).

$$ {}^{n}J_{AB} = \frac{16\pi^2}{9h}\left(\frac{g\beta h}{2\pi}\right)^2 \gamma_A\gamma_B\left|\Psi_{ns,A}(0)\right|^2\left|\Psi_{ns,B}(0)\right|^2\pi_{A,B} \quad (1.13) $$

where all symbols have their usual meanings and/or values. $\Psi_{ns,A}(0)^2$ and $\Psi_{ns,B}(0)^2$ are the s-electron densities for the ns valence orbitals at the nuclei of atoms A and B. π_{AB} is is the mutual polarizability of the ns orbitals on A and B, and γ_A and γ_B are the magnetogyric ratios for atoms A and B, respectively. This results in reasonable qualitative agreement between $J(^{129}Xe-^{19}F)$ and the localized MO description of the Xe-F bond. The lack of good quantitative agreement has been attributed to dipolar contributions to J_{XeF} (167).

Xenon-129 chemical shifts are sensitive to changes in solvent polarity and temperature. These solvent and temperature effects are most prominent for Xe(II) and decrease in the order Xe(II) > Xe(IV) > Xe(VI) (58). This effect is thought to arise from the interaction of the solvent with either the lone electron-pairs on the xenon nucleus, or alternatively, with the atom bound directly to xenon. In the first case, this effect is expected to be greatest for Xe(II) with three lone electron-pairs and only minimal for Xe(VIII) with no lone electron-pairs. The ^{129}Xe NMR spectrum of XeF_2 has been recorded in HF, BrF_5 and SO_2ClF solvents at 25°C (58). The ^{129}Xe chemical shifts are: HF, $\delta^{129}Xe = -1592$ ppm; BrF_5, $\delta^{129}Xe = -1750$ ppm; SO_2ClF, $\delta^{129}Xe = -1905$ ppm. As the solvent polarity increases in the order $SO_2ClF < BrF_5 < HF$, the ^{129}Xe chemical shift is also found to increase which implies that XeF_2 may be solvated through one of its fluorines, giving rise to increased $[XeF]^+$ character and a high frequency shift of the ^{129}Xe resonance, with increasing solvent polarity. The chemical shift of XeF_2 in BrF_5 is also temperature dependent (XeF_2: $\delta^{129}Xe$ (25°C) = -1750, (-40°C) = -1708), shifting to high frequency with decreasing temperature. This effect is consistent with a higher degree of association between XeF_2 and BrF_5 solvent at lower temperatures as expected.

The temperature effects outlined above can have a detrimental effect on the resolution one can attain in recording ^{129}Xe NMR spectra of, in particular, xenon(II) species. In addition to temperature effects, the use of high-field NMR spectrometers can result in substantial line broadening and consequently, the loss of resolution and long range spin-spin coupling information. The line broadening at high magnetic fields can be attributed to relaxation dominated by shielding anisotropy (SA) which is field dependent and becomes significant for heavy nuclei such as xenon. The contribution to the components of the spin-lattice relaxation (T_1) arising from SA is inversely proportional to the square of the external magnetic field B_0 and is defined in equation (1.14), where ω is the resonance frequency, γ is the magneto-

$$T_1 = \frac{15(1 + \omega^2\tau_c^2)}{\gamma^2 B_0^2(\sigma_\parallel - \sigma_\perp)^2\ 2\tau_c} \qquad (1.14)$$

gyric ratio, τ_c is the molecular correlation time, and $\sigma_\parallel$ and $\sigma_\perp$ refer to the shielding along and perpendicular to the symmetry axis, respectively. An increase in B_0, is accompanied by a decrease in T_1, which implies the lifetime of the spin state is correspondingly shortened and the resonance line broadened.

Raman Spectroscopy

Vibrational spectroscopy, and in particular Raman spectroscopy, has been used in the characterization of ligand-group derivatives of xenon. Ligand-group derivatives of xenon are ideally suited for study by Raman spectroscopy insofar as they generally contain large and polarizable atoms, and the spectrum can usually be recorded directly in the reaction vessel. Infrared spectroscopy, on the other hand, suffers from the fact that special sample handling devices are usually required, the materials of which are generally susceptible to oxidation by the xenon derivatives. In a number of cases (134,143,168), Raman spectroscopy has provided the sole basis for characterization, while for a majority of derivatives, vibrational information has been ancillary, serving only to verify the characterization made by other techniques.

Full characterization of ligand-group derivatives of xenon by mass spectrometry is often hampered by complex fragmentations of the ligand-group and difficulties with thermal stability and sampling. In some cases (139,140,144) however, observation of the molecular ion M^+ can be used to infer the molecular weight of the derivative, e.g., in the case of $Xe(OTeF_5)_4$, m/e = 859, $[Xe(OTeF_5)_3]^+$ (144).

Mössbauer spectra have been measured for both ^{129}Xe and ^{83}Kr in a number of derivatives of xenon (127,169,170), and krypton (170,171). Included here are a small number of ligand-group derivatives of xenon containing the $-OTeF_5$ group (127). The method suffers from the fact that the isomer-shift, a measure of s-electron density, exhibits very little sensitivity to s-electron character in the bonding to the central xenon atom and formal xenon oxidation state (127). The quadrupole splittings are, however, sensitive to changes in electronic environment around the central nucleus and can aid in the assessment of the overall molecular geometry.

The most definitive structural analysis of any molecule is provided by X-ray crystallography. Despite the large number of neutral, ligand-group derivatives of xenon, only four have been characterized by crystallographic studies! Included here are the neutral species $FXeN(SO_2F)_2$ (150,151), $FXeOSO_2F$ (173) and $Xe(OSeF_5)_2$ (174). In addition, the structure of $[XeN(SO_2F)_2]^+[Sb_3F_{16}]^-$ has recently been determined (175). In each structure, the L-Xe-L moiety is approximately linear. Preliminary X-ray measurements have also been made on the $Xe(OTeF_5)_2$ (137) and $Xe(OTeF_5)_6$ (141) molecules. In the case of $Xe(OTeF_5)_2$, structural disorder within the unit cell has prevented a rigorous crystallographic determination.

(v) Reactions of Xenon Ligand-Group Derivatives

The reactions of ligand-group derivatives of xenon can be divided into two categories. The xenon derivative can serve as a fluoride-ion donor with an appropriate Lewis acid or it can oxidatively add one or more ligand-groups to an oxidizable moiety.

The reaction of FXeL (L = $-OTeF_5$ or $-N(SO_2F)_2$) with AsF_5 at low-temperature yields cationic species of the form $[XeL]^+[AsF_6]^-$ (149,175-178). Dissolution of $[XeOTeF_5]^+[AsF_6]^-$

in BrF_5 at low temperature, yields among other species, the fluorine-bridged cation $[FXeFXeOTeF_5]^+$ (178). Similarily, the fluorine-bridged species $F[XeN(SO_2F)_2]_2{}^+[AsF_6]^-$ is formed when $[XeN(SO_2F)_2]^+[AsF_6]^-$ is warmed to room temperature under a dynamic vacuum without ensuant AsF_5 elimination (175). The salts $[XeOTeF_5]^+[Sb_2F_{11}]^-$ (178) and $[XeN(SO_2F)_2]^+[Sb_3F_{16}]^-$ (175), are formed when AsF_5 is displaced from the corresponding $[AsF_6]^-$ salts upon dissolution in the stronger Lewis acid SbF_5. The cation $[XeOSO_2F]^+$, is formed when $[XeOTeF_5]^+$ is dissolved in HSO_3F (178). The reaction proceeds with displacement of $HOTeF_5$ by the stronger acid HSO_3F.

In addition to reactions with Lewis acids, the ligand-group derivatives of xenon can act as oxidative ligand transfer reagents as illustrated by $Xe(OTeF_5)_2$ in equation (1.15).

$$Xe(OTeF_5)_2 + M \longrightarrow M(OTeF_5)_2 + Xe\uparrow \qquad (1.15)$$

This method has been used for the preparation of cis- and trans-$F_4Te(OTeF_5)_2$ (179), $Te(OTeF_5)_6$ (179,180), $I(OTeF_5)_5$ (129,181) and various $-OTeF_5$ substituted fluorocarbons (182,183).

(vi) Krypton Ligand-Group Derivatives

The synthesis of krypton derivatives containing highly electronegative ligand-groups is considerably more difficult than those of the analogous xenon derivatives. The reaction of KrF_2 with $B(OTeF_5)_3$ at -100°C has been investigated (140,141) but no isolable krypton product was recovered. Formation of $F_5TeOOTeF_5$ and the reductive elimination of krypton gas in this case does, however, imply the intermediacy of an $-OTeF_5$ derivative of krypton(II), namely $Kr(OTeF_5)_2$. In addition, the fact that neither TeF_6 nor O_2 was formed in this reaction, which would be expected if KrF_2 oxidatively fluorinated the $-OTeF_5$ group, supports the formation of a $Kr(OTeF_5)_2$ intermediate. The $-OSeF_5$ ligand is reported to behave similarily when allowed to react with KrF_2 (140,141).

(D) THE OXYTETRAFLUOROIODINE(VII) OXIDE GROUP, $-OIF_4O$

(i) General

Prior to the present work, the $-OIF_4O$ group had been little studied with respect to derivative formation. The limited list of previously known $-OIF_4O$ group derivatives includes $HOIOF_4$ (184-186), $K^+[IO_2F_4]^-$ (187), $Cs^+[IO_2F_4]^-$ (186,188), $FOIOF_4$ (186,189) and $ClOIOF_4$ (186). All of these derivatives exist in the form of cis- and trans- isomers except $K^+[IO_2F_4]^-$, which is formed exclusively as the trans-isomer. The preparation and properties of these derivatives are described below.

(ii) Preparation and Physical Properties of $-OIF_4O$ Derivatives

Tetrafluoro-orthoperiodic acid $HOIOF_4$ and the $-OIF_4O$

group precursor IO_2F_3, were first prepared in 1969 by Englebrecht and Peterfy (184,185) according to equations (1.16) to (1.18).

$$Ba_3H_4(IO_6)_2 + 14\ HSO_3F \longrightarrow 2\ HOIOF_4 + 8\ H_2SO_4 + 3\ Ba(SO_3F)_2 \qquad (1.16)$$

$$HOIOF_4 + SO_3 \longrightarrow IO_2F_3 + HSO_3F \qquad (1.17)$$

$$HF + IO_2F_3 \longrightarrow HOIOF_4 \qquad (1.18)$$

In addition, Christe et al. (186) have prepared $HOIOF_4$ by displacement of the acid from $Cs^+[IO_2F_4]^-$ with HF (see below).

Both $HOIOF_4$ and IO_2F_3 exist in more than one isomeric form. Whereas $HOIOF_4$ clearly exists as an equilibrium mixture of cis- and trans-isomers (185), the structure of IO_2F_3 is not as straight-forward and has been the subject of numerous investigations. These include an X-ray crystal structure (190), two vibrational studies (191,192), a mass spectrometry and electric diffraction study (193), three independent ^{19}F NMR investigations (184,185,192,194) and an Ab Initio SCF calculation (195). Despite the discrepencies in conclusions drawn from the aforementioned studies, IO_2F_3 has been shown to exist as an oxygen-bridged dimer in the solid state by X-ray crystallography (190) and it is generally accepted that IO_2F_3 exists with some degree of polymerization through oxygen bridges in the gas phase and in solution. This matter is further addressed in Chapter 3.

Both $HOIOF_4$ (m.p. 36.0°C, b.p. 154°C) and IO_2F_3 (m.p. 41.0°C) are crystalline solids at room temperature. Although IO_2F_3 can be handled in vacuum (v.p. IO_2F_3 (21°C) = 5.33 Torr), the vapor pressure of $HOIOF_4$ is prohibitively low for transfer in vacuum (v.p. $HOIOF_4$ (21°C) = 1.40 Torr). The standard enthalpy of formation of IO_2F_3 has been determined as -1320 ± 17 kJ mol^{-1} (196). Both $HOIOF_4$ and IO_2F_3 slowly attack glass and quartz at room temperature, and thus, must be handled in inert fluoroplastic ware. Both are strong oxidants, reacting explosively with organics. Only IO_2F_3 is photosensitive (192), decomposing to IOF_3 and oxygen according to equation (1.19).

$$IO_2F_3 \xrightarrow{h\nu} IOF_3 + \tfrac{1}{2}\, O_2\uparrow \qquad (1.19)$$

The published reaction chemistry of $HOIOF_4$ and IO_2F_3 is limited. In 1971, Engelbrecht et al. (185,197) reported that $HOIOF_4$ interacts with alkali-metal fluorides or trifluoroacetates to yield the corresponding salts, however, no physical data were given. From the reaction of IO_2F_3 with SbF_5 they were able to isolate a white crystalline solid (m.p. 102°C) which they interpreted as a polymeric structure containing both cis- and trans-oxygen bridges between $-IO_2F_4-$ and $-SbF_4-$ units. The crystal structure of this adduct has been reported (198), and is consistent with a distorted, oxygen-bridged dimer with two antimony atoms and two iodine atoms at the corners of a rhombus.

In 1975, Aubke et al. (188) reported that IO_2F_3 reacts with the fluoride-ion donors CsF and FNO_2 and the fluoride-ion acceptors SbF_5 and AsF_5, yielding, in all cases, the 1:1 adducts. An incomplete vibrational spectrum and an elemental analysis were given in support of the CsF/IO_2F_3 adduct, which were incorrectly interpreted as arising solely from the cis-$[IO_2F_4]^-$ ion (186). Data from a ^{121}Sb Mössbauer spectrum and a Raman spectrum, were given in support of the IO_2F_3/SbF_5 adduct. No physical data was provided for the FNO_2 and AsF_5 adducts.

Gillespie and Krasznai (187) have investigated the Lewis acid-base properties of IO_2F_3 with AsF_5, SbF_5, NbF_5, TaF_5, IF_5 and IOF_3. The adducts formed, based on ^{19}F NMR and Raman spectroscopic results, were shown to be oxygen-bridged polymers of the type $(IO_2F_4 \cdot MF_4)_n$ and $(IO_2F_4 \cdot IOF_2)_n$.

There are two compounds presently known which contain the $[IO_2F_4]^-$ anion. Christe et al. (186) have prepared pure mixtures of cis- and trans- $Cs^+[IO_2F_4]^-$ according to equation (1.20). They have also investigated the direct fluorination of

$$Cs^+[IO_4]^- + 4\ HF \xrightleftharpoons{HF} Cs^+[IO_2F_4]^- + 2\ H_2O \qquad (1.20)$$

$Cs^+[IO_4]^-$ with BrF_5, ClF_5 and elemental fluorine (186), but in each case, the products were contaminated with residual amounts of iodine fluorides or oxide fluorides. The cis- and trans-isomers of $Cs^+[IO_2F_4]^-$, formed according to equation (1.20), have been fully characterized by ^{19}F NMR spectroscopy and Raman and infrared spectroscopy (186). The white solid (m.p. 117°C) can be stored indefinately at room temperature and does not attack glass or quartz.

Gillespie and Krasznai (187) have reported that solutions of $K^+[IO_4]^-$ in IF_5 contain cis- and trans-$[IO_2F_4]^-$. They were able to isolate $K^+[IO_2F_4]^-$ which was shown to exist as the trans-isomer in the solid state and in CH_3CN solution, and in a cis-/trans- equilibrium in IF_5-solution by Raman and ^{19}F NMR spectroscopy.

Christe et al. (186,189) have prepared the first known iodine hypofluorite, $FOIOF_4$, according to equation (1.21).

$$[NF_4]^+[SbF_6]^- + Cs^+[IO_2F_4]^- \xrightarrow[-78°C]{HF} Cs^+[SbF_6]^- + NF_3 + FOIOF_4 \qquad (1.21)$$

The precipitate, $Cs^+[SbF_6]^-$ was filtered off at -78°C and the remaining solution was allowed to warm to room temperature. The solution slowly decomposed yielding NF_3 and a mixture of cis- and trans-$FOIOF_4$. The hypofluorites have been characterized by ^{19}F NMR spectroscopy, infrared and Raman spectroscopy and by mass spectrometry (186). Mixtures of cis- and trans-$FOIOF_4$

(m.p. -33.1°C) are extremely volatile (v.p. (0°C) = 244 Torr) and are colorless as a gas, pale-yellow as a liquid and white as a solid. The mixture of hypofluorites are marginally stable at room temperature, decomposing to IOF_5 and O_2, but have a tendency to detonate if shocked.

Attempts to form adducts of $FOIOF_4$ with CsF or SbF_5 were unsuccessful (186). Furthermore, attempts to add $FOIOF_4$ across the C=C double bond in C_2F_4 resulted in fluorination and oxygenation of the fluorocarbon (186).

The hypochlorite $ClOIOF_4$ has been reported (186). The main evidence in support of this derivative is an infrared spectrum which is similar to that of $FOIOF_4$. The only exceptions being that the O-F stretch is replaced by a band assigned to a O-Cl stretch, and the I=O, I-F and I-O stretching modes in $FOIOF_4$ are shifted slightly to lower frequency in the spectrum of the hypochlorite. The compound was found to be highly reactive and thermally unstable decomposing to IF_5 and other products which were not characterized.

(E) PURPOSE OF THE PRESENT WORK

The purpose of the present work was to extend both the chemistry of the $-OIF_4O$ group and that of xenon through the preparation of new $-OIF_4O$ derivatives of the main-group elements, with particular emphasis to be placed on the derivatives of xenon.

The emphasis on derivative formation with xenon was chosen for a number of reasons. An analogous xenon chemistry of the $-OTeF_5$ group for Xe(II), Xe(IV) and Xe(VI) had already been established prior to the outset of the present work. Furthermore, the $-OTeF_5$ derivatives of xenon had been the most extensively studied of any main-group element, and in fact, the number of these derivatives for the lighter main-group elements is limited. The physical and chemical properties of these derivatives would provide the basis for comparison, by analogy, with any new xenon derivatives of $-OIF_4O$ formed. In addition, the positive oxidation states of xenon ranging from Xe(II) to Xe(VIII) and the associated high electron affinities provide a means by which the stability of the $-OIF_4O$ group could be assessed under extreme oxidizing conditions.

It was first planned to develop and optimize a convenient route for the preparation of large quantities of the $-OIF_4O$ group precursors $HOIOF_4$ and IO_2F_3, which was lacking prior to this work and to better characterize IO_2F_3 in solution. Secondly, it was intended to establish the existence of new $-OIF_4O$ derivatives of xenon in solution with extensive use of ^{129}Xe and ^{19}F NMR spectroscopy. Methods would then be devised to isolate these species for characterization of the pure compounds in the solid state by Raman spectroscopy. A number of these new species could then hopefully function as $-OIF_4O$ group precursors, and be used subsequently in the preparation of new $-OIF_4O$ derivatives. Finally, the intention was to correlate the physical properties of the new derivatives with those of other ligand groups, and in this way, make definitive statements on the $-OIF_4O$ ligand-group's properties, including electronegativity.

CHAPTER 2

EXPERIMENTAL

(A) VACUUM TECHNIQUES

(i) Vacuum Systems and Inert Atmospheres

Nearly all of the compounds used in the course of this work were moisture and/or oxygen sensitive thus requiring that they be handled under anhydrous conditions in vacuum systems or in the inert atmospheres (N_2 atmosphere) of dryboxes. Two vacuum lines were in common use. For manipulations involving volatile reagents or products, or for the transfer of solvents, a general purpose vacuum line constructed largely from 316 stainless steel and nickel and equipped with 316 stainless steel valves (Autoclave Engineers Inc., HT-70123) was used. A second line, constructed out of Pyrex glass, was used for drying of reaction vessels and NMR tubes and for the preparation of IO_2F_3.

Pressures in the metal vacuum line were measured using two Ashcroft "Duragauge" model 8439 Bourdon tube gauges reading 0 to 30 pound/sq. in. absolute. Pressures in the glass vacuum line were measured using a mercury manometer.

Vacuum was attained by using mechanical vacuum fore pumps (Precision Scientific Co.) in series with mercury diffusion pumps. Two mechanical pumps were incorporated in the metal line. One, a roughing pump, was used for initial evacuation of the apparatus and removal of volatile fluorinated compounds. The second pump, used in combination with a mercury diffusion pump, provided the vacuum source (ca. 10^{-4} Torr) for the manifold. One mechanical vacuum pump in combination with a mercury diffusion pump, was incorporated in the glass line providing vacuum (ca. 10^{-6} Torr) for manipulations carried out on this line. In order to protect the pumps on the metal line, all volatile fluorinated compounds were dynamically pumped, by means of the roughing pump, through a copper tube (ca. 60 x 15 cm) packed with soda lime (Fisher Scientific, 4-8 mesh) absorbent.

Air-sensitive substances of low volatility were handled in nitrogen-filled dryboxes (Vacuum Atmospheres model DLX or S. Blickman Inc. model 44121). Drybox moisture and oxygen levels were routinely less than 0.01 ppm in the Vacuum Atmospheres box, which was equipped with a moisture monitor.

(ii) Preparative Apparatus and Sample Tubing

All synthetic procedures were performed in apparatus constructed from either nickel metal, glass, Kel-F or FEP. Sample preparations were carried out in vessels fashioned from lengths of FEP tubing (Chemplast Inc.) equipped with Kel-F bodied valves encased in aluminum housings. All vessels were seasoned with liquid HF to which ca. 1 atm. of F_2 had been added for ca. 1 hour and then pumped on the vacuum line for 1-2 days prior to use. For bulk preparations, (> 2g), 3/4" o.d. FEP tubes, heat-sealed at one end and heat-flared (45° SAE) at the other end, were used. For small scale preparations (<2 g), 1/4" o.d. FEP tubes, heat-sealed at one end and flared (45° SAE) at the other end were used.

Nuclear magnetic resonance (NMR) spectra were recorded in either Pyrex glass (10 mm o.d. thin-wall or 5 mm o.d. thin-wall or medium-wall, Wilmad Glass Co.) or in FEP tubes (9 mm o.d. or 4 mm o.d.). The 9 mm o.d. FEP NMR tubes were fabricated from lengths of 10 mm o.d. FEP tubing by reducing their diameter to 9 mm o.d. in a heated brass form with mechanical pressure. One end of the tube was heat-sealed by pushing it into the end of a thin-walled 10 mm o.d. glass NMR tube previously heated in a Bunsen flame. The other end was heat-flared (45° SAE) for attachment to a Kel-F valve. The 4 mm o.d. FEP NMR tubes were fabricated from lengths of FEP tubing which had one end heat-sealed by pushing the tube into the end of a heated thin-walled 5 mm o.d. glass NMR tube and the other end heat-flared (45° SAE) for attachment to a Kel-F valve. The sample tubes used for recording NMR spectra were loaded either under vacuum or in an inert atmosphere drybox and then heat-sealed under vacuum, using either an oxygen torch for the glass tubes or a small diameter Nichrome wire-resistance furnace for the FEP tubes.

All vacuum transfers were carried out through adaptors and/or connectors fabricated from FEP or Kel-F. All tubing was inter-connected using 1/4" Teflon unions (Swagelok) and Teflon compression fittings (back and front ferrules, Hoke Controls). The fluoroplastic valves and connectors, have been described in greater detail elsewhere (53).

(B) PREPARATION AND PURIFICATION OF STARTING MATERIALS

(i) Solvents

The preparation and/or purification of solvents used in the course of this work are described below. All solvents were transferred under vacuum except SbF_5, which was transferred in a drybox using an all glass syringe.

Sulfurylchlorofluoride, SO_2ClF, (Columbia Organic Chemicals), was purified by distillation onto SbF_5 to remove SO_2 contaminants as previously described (115). It was distilled from SbF_5 and stored over dry KF in a glass storage bulb to remove residual SbF_5 and HF and used directly from the storage vessel thereafter.

Trichlorofluoromethane, $CFCl_3$, (Canadian Liquid Air) and perfluoromethylcyclohexane, C_7F_{14}, (SCM Chemicals) were dried by periodic shaking with anhydrous P_4O_{10} over a period of several days prior to use and were stored over anhydrous P_4O_{10} in glass storage bulbs until used.

Bromine pentafluoride, BrF_5, (Matheson) was purified as described earlier (53) and stored over dry KF in a 3/4" Kel-F storage tube equipped with a Kel-F valve.

Antimony pentafluoride SbF_5 (Ozark-Mahoning Co.) was purified by vacuum distillation in an all-glass apparatus and stored in FEP bottles at room temperature in a desiccator over P_4O_{10}.

Anhydrous hydrogen fluoride, HF, (Harshaw Chemical Co.) was purified by treatment with 5 atmospheres of F_2 gas in a nickel can for a period of 1 month, converting residual water to HF and O_2 gas. After the specified time period, water-free HF was vacuum distilled into a dry Kel-F storage vessel and stored at room temperature. All transfers were made under vacuum on a metal vacuum line through all-fluoroplastic connections.

(ii) Reagents for the Preparation of $HOIOF_4$ and IO_2F_3

Fluorosulfuric acid, HSO_3F, (Allied Chemical Co.) was purified by double distillation under an atmosphere of dry nitrogen. The apparatus and procedure are described in detail elsewhere (199). The fractions boiling at 163 to 165°C were collected in 250 ml conical flasks fitted with extended ground-glass joints and caps lubricated with Kel-F grease and stored below 0°C in a refrigerator. All transfers of HSO_3F were made in an inert atmosphere drybox or in a glove bag flushed with dry nitrogen.

Periodic acid, H_5IO_6, (99%, Aldrich Chemical Co.) was used without further purification.

Potassium sulfate, K_2SO_4, (99%, Merck or Fisher Scientific) was dried in an oven at 200°C for 1 week and then transferred to a glass vessel and pumped on a vacuum line for 2 days prior to use.

Oleum, H_2SO_4/SO_3, (65% by weight SO_3) was prepared in volumes of 100 ml by adding 65 g of liquid SO_3 (J.T. Baker Co.) dropwise to 35 g of H_2SO_4 (J.T. Baker Co.), 96%, contained in a 250 ml conical flask. The flask was then capped and stored at room temperature until used.

(iii) Preparation of $HOIOF_4$ and IO_2F_3

The apparatus used for the preparation of $HOIOF_4$ and IO_2F_3 is illustrated in Figures 2.1 to 2.3. In a typical experiment, 100 ml of HSO_3F (1.75 moles) was introduced into the FEP bottle which had previously been flushed overnight with dry nitrogen, in a glove bag also flushed overnight with dry nitrogen. The Teflon cap was installed and the bottle and contents were then transferred to a fumehood for final assembly according to Figure 2.1. The FEP bottle was immersed in an ice bath and stirred mechanically with a Teflon coated magnetic stir bar. The mixture was then flushed for 1 hour with a stream of dry nitrogen connected through the gas entry port on the Teflon cap. The FEP transfer cone containing 99.6 g of H_5IO_6 was then installed, completing the preparative apparatus as depicted in Figure 2.1. A small portion of H_5IO_6 (approximately 3-4 g) was introduced to the liquid and stirred until dissolved. The addition was repeated until all the H_5IO_6 had been added, requiring a total of 1¼ to 1½ hours to

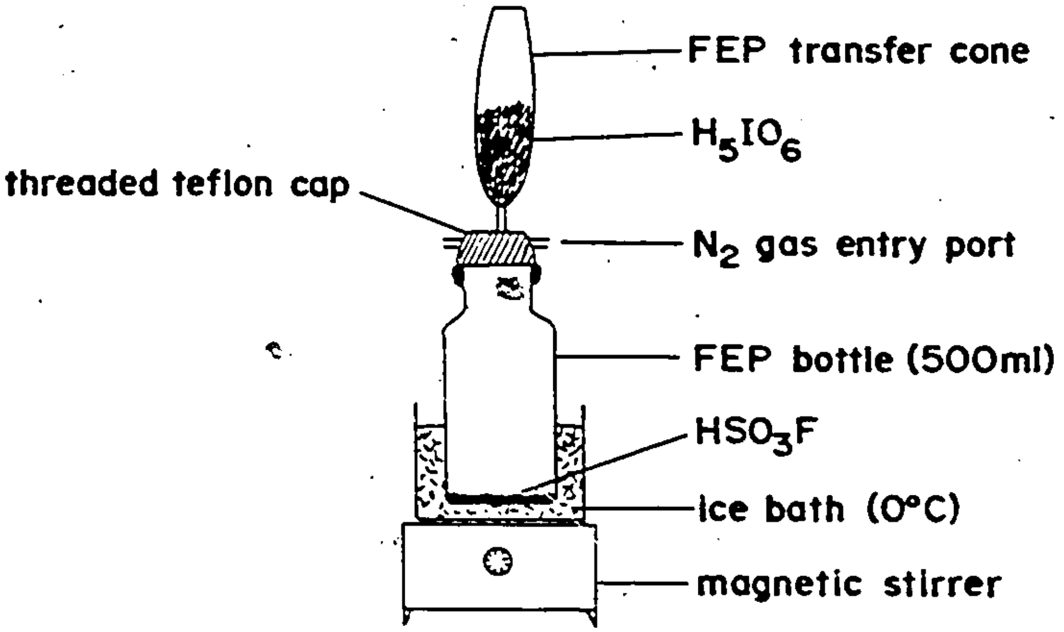

Figure 2.1

The apparatus used for the preparation of $HOIOF_4$.

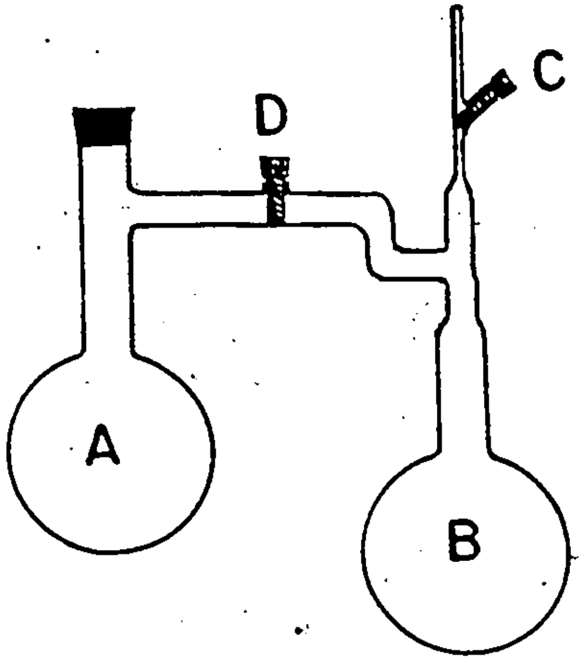

Figure 2.2

The $HOIOF_4$ distillation apparatus. Valves (C) and (D) are Rotaflo valves. Bulbs (A) and (B) are 250 ml Pyrex glass.

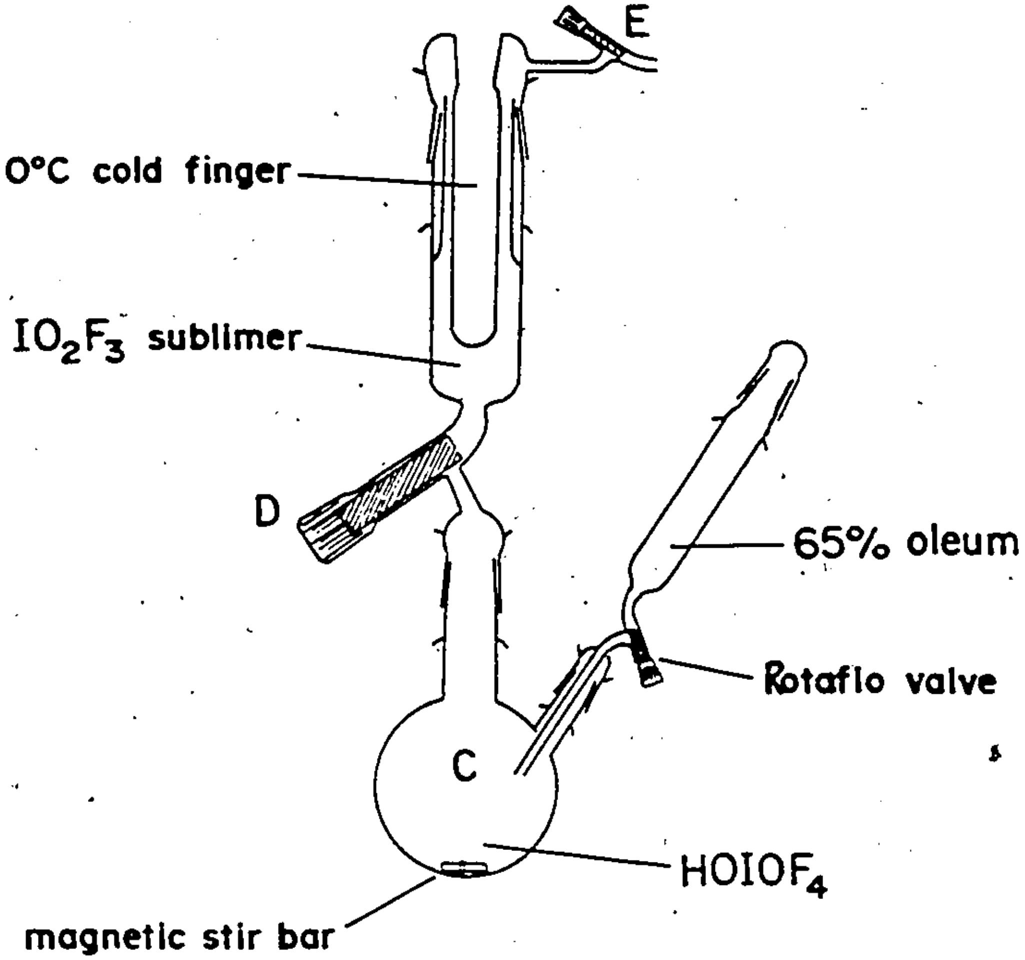

Figure 2.3

The IO_2F_3 sublimation apparatus. Bulb (C) is 500 ml Pyrex. Valves (D) and (E) are Rotaflo valves.

complete. After the addition of H_5IO_6 was complete, the FEP transfer cone was quickly removed and replaced with the Teflon cap (with both gas ports now sealed with Teflon plugs). The mixture was then stirred for 24 hours as the temperature was allowed to rise from 0°C to room temperature. The FEP bottle was then moved to a glove bag, flushed with dry nitrogen and the contents transferred into bulb A of the $HOIOF_4$ distillation apparatus depicted in Figure 2.2. Bulb B was periodically flamed over the course of 24 to 48 hours while under dynamic vacuum. Bulb B was then cooled to -196°C and evacuated through valve C. While the $HOIOF_4/HSO_3F$ mixture was stirring, valve D, connecting bulb A and bulb B, was opened. The $HOIOF_4$ statically distilled from bulb A and was condensed in the glass arm leading to bulb B. With valve D closed, the $HOIOF_4$ was melted from the glass arm into bulb B. This procedure was repeated over the course of 48 hours or until no more $HOIOF_4$ would transfer. The apparatus was then removed to a glove bag, flushed with dry nitrogen and the contents of bulb B transferred into bulb C of the IO_2F_3 generation apparatus illustrated in Figure 2.3. The contents of bulb A (mostly H_2SO_4 and HSO_3F) were discarded. Bulb C was removed from the glove bag and the sublimation apparatus assembled according to Figure 2.3. Small additions of 65% oleum (approximately 1 ml) were added to the contents of bulb C while being stirred mechanically with a Teflon coated stir bar. After the 1 ml addition was complete, valve D was opened, valve E closed and

IO_2F_3 sublimed from bulb C condensing onto the cold finger chilled with ice water. After the sublimation was complete, with valve D then closed and valve E open, the IO_2F_3 was pumped into an FEP U-trap cooled to -196°C. Another addition of 65% oleum was made and the procedure for recovery of IO_2F_3 repeated. It is important that the additions of 65% oleum be made slowly and in small quantities. If, in the course of a single oleum addition, it was made too rapidly, or if too much oleum was added per addition, a bright-yellow solid separated which prevented the further recovery of IO_2F_3. This yellow solid, thought to be an iodine(VII) fluorosulfate, is discussed in Chapter 3. As the IO_2F_3 recovery neared completion, the yellow solid began to form and steadily increased in quantity and ultimately inhibited the formation of IO_2F_3. The contents of bulb C were left standing at room temperature to allow the yellow solid to settle. Following this, bulb C was transferred to a glove bag flushed with dry nitrogen, and the liquid portion decanted and stored in a 250 ml stoppered conical flask. The $HOIOF_4$ which remained in the supernatant was then subsequently recovered by repeating the $HOIOF_4/HSO_3F$ distillation procedure outlined above. The IO_2F_3 collected in the FEP U-trap was purified by pumping through a column of previously vacuum dried K_2SO_4 supported on a glass frit, which served to remove any residual strong acid contaminants. The highest yield of purified IO_2F_3 recovered using this method was 83 g (88%). The purified material was stored in a FEP tube under 2 atm of dry nitrogen at dry ice temperature and shielded from exposure to light. All subsequent transfers of IO_2F_3 were made under static vacuum through fluoroplastic valves and fittings. The procedure outlined above represents the reaction conditions developed during the course of this work and optimized with the aid of a ^{19}F NMR study (see Chapter 3).

If pure $HOIOF_4$ was required, a 1:1 mole ratio of IO_2F_3 and anhydrous HF were allowed to react at room temperature in an FEP reaction vessel. Formation of $HOIOF_4$ is signaled by a change of color of the IO_2F_3/HF mixture from yellow to colorless and/or by evidence of $HOIOF_4$ crystallization. The $HOIOF_4$ produced was either a colorless crystalline solid or, if a slight excess of HF was used, a colorless liquid with a freezing point slightly below room temperature. The product was stored in an FEP vessel under 2 atm of dry nitrogen at -78°C. All subsequent transfers were made in a drybox. Transfer of the liquid was accomplished with the aid of an FEP pipette drawn from a length of ¼" FEP tubing.

(iv) Preparation of Noble-Gas Fluorides and Oxide Fluorides

Fluorine (Air Products and Chemicals, Inc.) containing ca. 0.2% HF was used during the course of this work. Hydrogen fluoride was effectively removed, prior to F_2 usage, by passing the fluorine through a Matheson model 68-1008 hydrogen fluoride trap. The trap consists of a brass cylinder packed with porous sodium fluoride pellets and surrounded by an insulated Nichrome resistance. The activity of sodium fluoride was maintained by periodic heating at 250 to 300°C, while purging with dry nitrogen gas.

Xenon gas (Linde, research grade, 99%) and krypton gas (Matheson, research grade, 99.99%) were used directly from their respective cylinders on a metal vacuum line.

The method used for the preparation of xenon difluoride XeF_2 was similar to that used by of Malm and Chernick (43) for the preparation of XeF_4. Two parts xenon and one part fluorine were allowed to react in a nickel can (249 ml) at 400°C for 7 hours. In a typical preparation, xenon (0.236 mole) and fluorine (0.118 mole) were condensed into a nickel can (249 ml) at -196°C. The can and contents were then allowed to warm to room temperature. At room temperature, the total pressure in the can was ca. 34.4 atm. An electric furnace, preheated to 400°C was placed around the nickel can and maintained there for 7 hours. The initial pressure in the can at 400°C, assuming no reaction, was ca. 78.5 atm. After the specified time period, the furnace was removed and the can and contents were allowed to cool to room temperature in the air. The can and contents were then further cooled to -196°C at which temperature any excess fluorine was pumped off. The can and contents were warmed to -78°C and excess xenon (0.118 mole) was condensed into a storage cylinder at -196°C. The XeF_2 was collected by pumping the contents of the nickel can through a cold trap at -78°C. The yield of XeF_2 was 19.86 g (99.3%).

The purity of the product was checked by recording the Raman spectrum in the range 450 to 600 cm^{-1}. Xenon difluoride has a strong line at 496 cm^{-1} whereas the most likely impurity, XeF_4, has two strong lines at 502 and 543 cm^{-1}. The amount of XeF_4 found in any of the preparations was generally estimated to be less than 0.5%. The product was stored under an atmosphere of dry nitrogen in an FEP storage vessel at room temperature. All XeF_2 transfers were made as a solid in an inert atmosphere drybox.

Xenon tetrafluoride XeF_4 was prepared in a manner similar to that described by Malm and Chernick (43). The procedure has been described in detail elsewhere (53). The purity of the product was checked by recording the Raman spectrum in the range 450 to 700 cm^{-1}. The most likely impurities are XeF_2, which has a strong band at 496 cm^{-1}, and XeF_6, which has strong bands at 583, 636 and 656 cm^{-1}. While in none of the preparations were appreciable quantities of XeF_2 detected, the product was always found to contain small amounts of XeF_6. The XeF_6 could be removed by flash distillation at room temperature owing to its high vapor pressure in comparison to that of XeF_4. The product was stored under an atmosphere of dry nitrogen [illegible] a FEP storage vessel at room temperature. All transfers were made as a solid in an inert atmosphere drybox.

Xenon hexafluoride XeF_6 was prepared according to the method of Malm and Chernick (46). Details of the procedure are given elsewhere (53). The purity of the product was checked by recording the Raman spectrum in the range 500 to 950 cm^{-1}. The most likely impurities are $XeOF_4$ having strong lines at 919, 566 and 530 cm^{-1} and XeF_4, having lines at 543 and 502 cm^{-1}. The $XeOF_4$ contaminant, which was generally slight, was removed by flash distillation at room temperature. Its removal is judged complete by the absence of pre-melting in the bulk XeF_6. Xenon hexafluoride is colorless as a solid (m.p. 45°C) when pure but is light-yellow in appearance when pre-melting occurs. The product was stored under an atmosphere of dry nitrogen in a FEP storage vessel at room temperature. All transfers were made under vacuum through all stainless steel, nickel or fluoroplastic fittings.

Krypton difluoride KrF_2 was prepared by the electrical discharge method described by Schreiner _et al._ (22) and has been described in detail elsewhere (53). The product was stored in an FEP storage vessel pressurized to 2 atm at -78°C. All transfers were made under vacuum through all stainless steel, nickel or fluoroplastic fittings.

Xenon oxide tetrafluoride $XeOF_4$ was prepared by the interaction of 1 mole of XeF_6 with 1 mole of H_2O in a nickel can. The product was stored over dry NaF (for HF removal) in an FEP storage vessel pressurized to 2 atm with dry nitrogen at room temperature. All transfers were made under vacuum,

(v) Reagents for the Preparation of -$OTeF_5$ Derivatives

Boron trichloride BCl_3 (Matheson) was condensed from a steel lecture cylinder into a 250 ml glass bulb fitted with a Rotaflo valve. Prior to use, several volatile "heads", consisting of mostly HCl, were removed by expansion into a static vacuum manifold and discarded.

Pentafluoro-orthotelluric acid, $HOTeF_5$, was prepared from the reaction of $Te(OH)_6$ (BDH Chemicals Ltd.) with 7 moles of HSO_3F. This synthesis has been described earlier (200) with the only exception being that the previous work used 11 moles of HSO_3F. Pure $HOTeF_5$ was obtained by overnight hydrolysis of the resulting $HOTeF_5/FO_2SOTeF_5$ mixture in concentrated (96%) H_2SO_4 at 60°C. Pure $HOTeF_5$ was sublimed into a Kel-F storage vessel equipped with a Kel-F valve and stored at room temperature. All transfers involving $HOTeF_5$ were made under vacuum on either glass or metal vacuum lines.

Boron tris(pentafluoro-orthotellurate(VI)), $B(OTeF_5)_3$, was prepared according to the method previously described (162). Typical quantities of reactants used were: BCl_3, 8.8130 g (75.22 mmol); $HOTeF_5$, 54.1951 g (229.62 mmol). The product was stored under an atmosphere of dry nitrogen in a glass bulb or an FEP storage vessel at room temperature. All transfers were made as a solid or by pouring the molten compound (m.p. 37°C).

Mercuric fluoride, HgF_2, was prepared by the oxidative fluorination of elemental mercury (Johnson Matthey & Mallory, triply distilled) with XeF_2 in anhydrous HF solvent. In a typical preparation, XeF_2, 1.1330 g (6.69 mmol), was transfered to an FEP reaction vessel in a drybox. After removing from the drybox, anhydrous HF (ca. 10 ml) was added and the reaction vessel taken back into the drybox and cooled to -196°C in a Dewar of liquid nitrogen. Mercury, 1.2665 g (6.31 mmol), previously dried under vacuum, was added while maintaining the reaction vessel at -196°C. The tube was quickly removed from the drybox and immersed in a Dewar containing dry ice and acetone (-78°C). Upon warming from -78°C to ambient temperature, the reaction proceeded rapidly and smoothly with intermittent cooling in dry ice-acetone bath to allow the xenon gas generated in the reaction to be pumped off in vacuum at -78°C. When gas evolution ceased, the tube and contents were warmed to room temperature for an additional 1 hour followed by the removal of HF and excess XeF_2 under vacuum. The product was pumped on for 24 hours at room temperature and stored in its FEP storage tube under an atmosphere of dry nitrogen at room temperature. All transfers were made as a solid in an inert atmosphere drybox.

Tellurium tetrafluoride, TeF_4, was prepared according to the procedure described by Seppelt _et al._ (179) by the reaction of SF_4 (Air Products and Chemicals, Inc.) and TeO_2 (BDH Chemicals, 99%) in a Monel vessel. The product was stored at room temperature in a glass storage tube. All transfers were made as a solid.

(vi) Preparation of $-OTeF_5$ Derivatives

Xenon(II) bis(pentafluoro-orthotellurate(VI)), $Xe(OTeF_5)_2$, was prepared by the stoichiometric reaction of XeF_2 and $B(OTeF_5)_3$ in an FEP vessel equipped with a Kel-F valve. In a typical preparation, $B(OTeF_5)_3$ 8.0825 g (11.12 mmol) was introduced into a FEP reaction vessel in a drybox. After removing the vessel from the dry box, ca. 10 ml of $CFCl_3$ solvent was vacuum distilled into the reaction vessel. The tube was then returned to the drybox and cooled to -196°C in a Dewar of liquid nitrogen. Xenon difluoride, 2.8027 g (16.56 mmol), was added to the FEP reaction vessel maintained at -196°C. The reaction vessel was quickly transfered from the drybox to a vacuum line while cold. After evacuating the tube and contents at -196°C, the tube was opened to an isolated section of the vacuum line and pressurized to ca. 1 atm with dry nitrogen. The tube was then allowed to warm slowly in order to solublize the $B(OTeF_5)_3$ and initiate the reaction (XeF_2 is only sparingly soluble in $CFCl_3$). The progress of the reaction was monitored by evolution of BF_3 gas. The tube was intermittedly cooled throughout the reaction when the evolution of BF_3 gas became too rapid. After ½ hour the gas evolution ceased and the reaction was complete. The tube was cooled to 0°C and pumped to remove the $CFCl_3$ solvent. Pumping was continued for 1 hour at 0°C and then warmed to room temperature and again pumped for a further 4 to 5 hours. The yield was 9.57 g (95%) of $Xe(OTeF_5)_2$. The yield is reduced substantially if the $B(OTeF_5)_3$ and $CFCl_3$ mixture was allowed to stand at room temperature for prolonged periods of time. The purity of the product was checked by Raman spectroscopy. The absence of lines at 740 and 725 cm^{-1} due to $B(OTeF_5)_3$ or at 496 cm^{-1} due to XeF_2, which are the most intense bands in the spectra of these compounds, and comparison with the published Raman spectrum of $Xe(OTeF_5)_2$ (178), indicated that the final product was pure. The compound was stored at -78°C in an FEP storage vessel under 2 atm of dry nitrogen. All transfers were made as a solid in an inert atmosphere drybox.

Xenon(II) fluoride pentafluoro-orthotellurate(VI), $FXeOTeF_5$, was prepared by the stoichiometric reaction of XeF_2 and $Xe(OTeF_5)_2$ in SO_2ClF solvent at 0°C. The procedure is analogous to that for the preparation of $FXeOIOF_4$ described below. A typical preparation consisted of the following quantities of reactants: XeF_2, 0.5032 g (2.97 mmol); $Xe(OTeF_5)_2$, 1.7873 g (2.94 mmol); SO_2ClF, ca. 6 ml. The product was isolated by removal of the solvent under vacuum and used immediately thereafter.

Xenon(IV) tetrakis(pentafluoro-orthotellurate(VI)), $Xe(OTeF_5)_4$, was prepared by the reaction of stoichiometric amounts of XeF_4 and $B(OTeF_5)_3$ in $CFCl_3$ solvent. The procedure is identical to that for the preparation of $Xe(OTeF_5)_2$ described above. Owing to slow attack of the solvent by the product, the reaction mixture was never allowed to warm above 0°C. Typical preparations involved the following quantities of reactants: $B(OTeF_5)_3$, 6.4941 g (8.94 mmol); XeF_4, 1.3234 g (6.38 mmol); $CFCl_3$, ca. 10 ml. The purity of the product was checked by recording the Raman spectrum. The absence of lines at 502 and 543 cm^{-1} (XeF_4), 725 and 740 cm^{-1} ($B(OTeF_5)_3$), 440 cm^{-1} ($Xe(OTeF_5)_2$) as well as by comparison with the published Raman spectrum of $Xe(OTeF_5)_4$ (142), confirmed the purity of the product. The compound was stored in an FEP storage vessel at -78°C under 2 atm of dry nitrogen. All transfers were made as a solid in an inert atmosphere drybox.

Xenon(VI) oxide tetrakis(pentafluoro-orthotellurate(VI), $OXe(OTeF_5)_4$, was prepared by the reaction of stoichiometric amounts of $XeOF_4$ and $B(OTeF_5)_3$ in $CFCl_3$ solvent. The procedure was analogous to that of the preparation of $Xe(OTeF_5)_4$ described above. Typical preparations involved the following quantities of reactants: $XeOF_4$, 1.7527 g (7.849 mmol); $B(OTeF_5)_3$, 7.9336 g (10.92 mmol); $CFCl_3$, ca. 10 ml. The purity of the product was checked by recording the Raman spectrum and comparing the results with those obtained by Schrobilgen and Schumacher (142). The product was stored in an FEP storage tube at -78°C under 2 atm of dry nitrogen. All transfers were made as a solid in an inert atmosphere drybox.

Mercury(II) bis(pentafluoro-orthotellurate(VI)), $Hg(OTeF_5)_2$, was prepared by the stoichiometric reaction of HgF_2 with $B(OTeF_5)_3$ in $CFCl_3$ solvent. The procedure is similar to that for the preparation of $Xe(OTeF_5)_2$ described above. A typical preparation involved the following quantities of reactants: HgF_2, 0.3379 g (1.42 mmol); $B(OTeF_5)_3$, 0.7120 g (0.98 mmol); $CFCl_3$, ca. 6 ml. The product was stored in an FEP storage vessel under an atmosphere of dry nitrogen at room temperature. All transfers were made as a solid in an inert atmosphere drybox.

Tellurium(IV) tetrakis(pentafluoro-orthotellurate(VI)), $Te(OTeF_5)_4$, was prepared as previously described by Seppelt <u>et al.</u> (179). The product was stored in an FEP storage vessel under an atmosphere of dry nitrogen at room temperature. A typical preparation involved the following quantities of reactants: TeF_4, 0.4497 g (2.21 mmol); $B(OTeF_5)_3$, 2.1838 g (3.01 mmol). All transfers were made as a solid in an inert atmosphere drybox.

(C) PREPARATION OF $-OIF_4O$ DERIVATIVES

(i) Preparation of cis, cis-$Xe(OIOF_4)_2$

The cis, cis-isomer of xenon(II) bis(oxytetrafluoroiodine(VII) oxide), $Xe(OIOF_4)_2$, was prepared as a pure compound by the displacement of $HOTeF_5$ from $Xe(OTeF_5)_2$ with stoichiometric amounts of the stronger protonic acid $HOIOF_4$. These reactions were performed either neat or in $CFCl_3$ solvent. In a typical experiment, $HOIOF_4$, 0.8810 g (3.74 mmol), was transfered in a drybox into a 9 mm o.d. FEP NMR tube equipped with a Kel-F valve. The tube was cooled to -196°C in a Dewar of liquid nitrogen. A pre-weighed amount of $Xe(OTeF_5)_2$, 1.0740 g (1.77 mmol), was then transferred to the FEP tube immersed in liquid nitrogen. After the transfer was complete, the tube was closed and quickly removed from the dry box while cold and transfered to a Dewar of liquid nitrogen. The tube and contents were immediately pumped on at -196°C to remove the pressure of nitrogen that had built up from handling the open tube in the dry box. In preparations where a solvent was used, such as $CFCl_3$, the solvent was statically distilled in at this point. The amount of solvent condensed at liquid nitrogen temperature was typically 4 to 5 ml, but, in any case, enough was added to completely solubilize the reactants. The temperature of the tube and contents was then raised to 0°C in an ice water bath for approximately 15 minutes. For reactions performed with neat $HOIOF_4$, the temperature was raised to approximately 10°C in order to liquify the $HOIOF_4$ and initiate reaction. The contents were mixed throughout the time of reaction and periodically cooled with liquid nitrogen to control the rate of reaction. As the reaction proceeded the mixture went from colorless to yellow with some gas evolution always being observed. After the reaction was deemed complete (ca. 10 min.), the tube was checked for non-condensibles first at -196°C (O_2) and then at -78°C (Xe). In this procedure, the tube was opened to an isolated section of the vacuum line (52 ml) equipped with a pressure gauge. The preparations involving $CFCl_3$ solvent generally showed small oxygen and xenon pressures (≈ .1 atm O_2, .2 atm Xe). Preparations performed neat generally showed smaller pressures of xenon and little or no oxygen (< .1 atm O_2, ≈ .1 atm Xe). The product was then isolated by pumping at 0°C for approximately 1 hour to remove the solvent and $HOTeF_5$ formed in the reaction. The slightly wetted solid was pumped for a further 24 hours between 0°C and room temperature in order to remove any residual $HOIOF_4$. The tube was then pressurized to 2 atm with dry nitrogen and stored at -78°C until used. The yield was typically 90 to 95% when the reaction was performed neat whereas when done in $CFCl_3$ solvent, the yields never exceeded 40%. In both cases the solid product was shown to consist of only cis, cis-$Xe(OIOF_4)_2$ by low-temperature Raman spectroscopy (Chapter 4). The reaction carried out in C_7F_{14} produced only xenon and oxygen gas, a mixture of volatile substances presumably CF_4, C_2F_6 and other fluorinated hydrocarbons and iodine(V) species IOF_3, IF_5 and IO_2F. The reaction performed in SO_2ClF yielded a very small amount of product (mg quantities) but mostly oxygen, xenon, and the iodine(V) species IOF_3, IF_5 and IO_2F, identified by recording the low-temperature Raman spectrum of the solid product and the ^{19}F NMR spectrum of the product dissolved in $CFCl_3$ solvent.

(ii) Attempted Preparation of $Xe(OIOF_4)_2$ by HF Displacement

Attempts to prepare $Xe(OIOF_4)_2$ by the stoichiometric reaction of XeF_2 and $HOIOF_4$ in HF, SO_2ClF or $CFCl_3$ solvent were unsuccessful. The procedure used in each of these attempts is identical to that discussed above with the only exceptions being that XeF_2 replaces $Xe(OTeF_5)_2$ and the solvents used were either HF, SO_2ClF or $CFCl_3$. In a typical attempt, $HOIOF_4$, 3.0228 g (12.81 mmol), and XeF_2, 1.0305 g (6.09 mmol), were combined at -196°C in a drybox. After removing the reaction tube from the drybox, solvent (ca. 10 ml) was added and the tube evacuated at -196°C. The contents were allowed to react at 0°C for 15 minutes with periodic cooling and agitation. After the specified reaction time the tube was monitored for non-condensibles as outlined above. During the removal of solvent under vacuum at 0°C, gas evolution was vigorous and was controlled by intermittent cooling with liquid nitrogen. In the attempts using HF solvent, after the HF had been completely removed, a small amount of liquid, identified as $HOIOF_4$ and IF_5, by recording the ^{19}F NMR spectrum, and a white solid, identified as IO_2F, by recording the low temperature Raman spectrum, were the only products. In the attempts using $CFCl_3$ or SO_2ClF solvents, complete solvent removal was accompanied by detonations presumably the result of formation of one or more unstable chlorine oxides.

(iii) Preparation of cis- and trans-$FXeOIOF_4$

Xenon(II) fluoride oxytetrafluoroiodine(VII) oxide was prepared as a homogenous mixture of cis- and trans-isomers by the direct interaction of IO_2F_3 with XeF_2 in HF solvent. In a typical preparation, IO_2F_3 2.6848 g (12.44 mmol), and XeF_2, 2.1361 g (12.62 m mol), were combined in a 9 mm o.d. FEP NMR tube at -196°C in a drybox. After removing the reaction tube from the drybox while being kept cold, HF (ca. 10 ml) was added and the tube evacuated at -196°C. The contents were allowed to react between -10°C and 0°C for approximately ½ hour. The tube was frequently agitated during the course of the reaction to solubilize the reactants and periodically cooled in liquid nitrogen to control the rate of reaction. The mixture went from initially being colorless to yellow when the reaction was complete. The solvent was then removed under vacuum at -50°C resulting in a yellow liquid having a melting point between 0 and -5°C. The vessel containing the product was pressurized with 2 atm of dry nitrogen and stored at -78°C until used.

A second method used to prepare cis/trans-$FXeOIOF_4$ was by reaction of a stoichiometric amount of cis, cis-$Xe(OIOF_4)_2$ with XeF_2 in SO_2ClF solvent at 0°C. In this preparation, cis, cis-$Xe(OIOF_4)_2$, 1.0633 g (1.77 mmol), contained in a 9 mm o.d. FEP NMR tube was cooled to -196°C and then rapidly transfered to a drybox where it was immediately immersed in a Dewar of liquid nitrogen. Xenon difluoride, 0.2985 g (1.76 mmol), was added at -196°C and the tube removed from the drybox while still cold and cooled to -196°C. The solvent, SO_2ClF (ca. 6 ml), was condensed into the reaction tube under vacuum at -196°C. The mixture was allowed to react at 0°C for approximately 1 hour with vigorous agitation. Once no more solid was evident, the tube was cooled and the solvent removed at -78°C, leaving a yellow liquid consisting of a mixture of cis- and trans-isomers of $FXeOIOF_4$. The tube was pumped for a further 10 minutes at 0°C and then pressurized with 2 atm of dry nitrogen and stored at -78°C until used.

(iv) Attempted Preparation of $[XeOIOF_4]^+[AsF_6]^-$

Arsenic pentafluoride, AsF_5, was prepared by the reaction of ASF_3 (201) with a 10% molar excess of fluorine in a nickel can at 200°C for 16 hours.

In an attempt to prepare the title compound, an excess of AsF_5 (ca. 6-fold) was condensed at dry-ice temperature onto approximately 0.5 g of $FXeOIOF_4$ contained in a ¼" o.d. FEP reaction tube. The reactants remained in contact for ca. 10 minutes at -78°C before being warmed slowly to 0°C. As the mixture was warmed, the AsF_5 was allowed to expand into an isolated section (ca. 52 ml volume) of the metal vacuum manifold to a pressure of 1.0-1.3 atm absolute. The bulk sample slowly fused with a concurrent color change from light-yellow to a deeper yellow. The mixture was held at 0°C for ca. 5 minutes and was periodically agitated during this time to facilitate mixing. The mixture was cooled to -78°C and monitored for O_2 and Xe gases. As no O_2 or Xe gas was apparent, the cycle was repeated three times followed by the removal of excess AsF_5 at 0°C. During the removal of AsF_5 the tube was periodically chilled with liquid nitrogen to prevent "frothing" of the mixture up the tube and into the attached Kel-F valve. After the AsF_5 had been completely removed, a light-yellow powder remained which when exposed to an additional 0.3 atm of AsF_5, became wetted. Pumping at 0°C again resulted in the deposit of the pale-yellow solid. The tube was pressurized to 2 atm with dry nitrogen at -78°C and the Raman spectrum recorded in situ at -196°C.

(v) Reaction of $HOIOF_4$ with $OXe(OTeF_5)_4$

Mixed xenon(VI) derivatives of the general form $OXe(OTeF_5)_x(OIOF_4)_{4-x}$ (x=0-3) have been observed in $CFCl_3$ solvent by ^{129}Xe NMR spectroscopy during the course of this work. In addition, when stoichiometric amounts of neat $HOIOF_4$ and $OXe(OTeF_5)_4$ are allowed to react and the volatiles removed, mixed xenon(VIII) derivatives of the general form $XeO_3(OTeF_5)_x(OIOF_4)_{2-x}$ (x=0,1) are isolated. In a typical preparation of the xenon(VIII) derivatives, $HOIOF_4$, 0.6660 g (2.82 mmol), was placed in a 9 mm o.d. FEP NMR tube and transfered to a drybox. At -196°C, $OXe(OTeF_5)_4$, 0.7659 g (0.70 mmol), was added to the FEP reaction tube. After quickly removing the tube from the drybox, it was cooled to -196°C and pumped on a vacuum line for ca. 10 minutes. The mixture was slowly warmed to 0°C with frequent shaking and with intermittent cooling in liquid nitrogen. After 15 minutes the tube was pumped out at 0°C to remove $HOTeF_5$ resulting in a slightly pale-yellow solid depositing. The tube was pumped for a further 34 hours at 0°C and then pressurized with 2 atm of dry nitrogen at -78°C. The Raman spectrum was recorded in the reaction tube at -196°C followed by storage at -78°C. The ^{129}Xe NMR spectrum was recorded on the sample in $CFCl_3$ solvent at 5°C.

(vi) Preparation of $F_4OIOOIOF_4$

The title compound has been prepared by the controlled decomposition of cis, cis-$Xe(OIOF_4)_2$. In this preparation, an FEP tube containing cis, cis-$Xe(OIOF_4)_2$, maintained at -78°C, was connected to an FEP U-tube equipped with a 4mm o.d. FEP NMR tube side-arm (Figure 2.4) and pumped for 18 hours to ensure dryness of all connections. Following the specified drying time, the FEP NMR tube was warmed to 0°C in an ice water bath while being pumped on through the U-tube which was cooled to -196°C in a Dewar of liquid nitrogen. The decomposition proceeded smoothly over the period of 1-2 hours resulting in the formation of a "plug" of white material in the FEP U-tube. After the decomposition was complete, milligram quantities of a white powder, later identified by Raman spectroscopy as IO_2F, remained in the FEP NMR tube. The U-tube containing the decomposition products was warmed to -78°C in a dry-ice/acetone slush bath. It was then opened to the manifold to check for xenon pressure while being maintained at -78°C. In each preparation, pressures of xenon ranging from 0.45 to 0.55 atm absolute were observed, depending on the amount of $Xe(OIOF_4)_2$

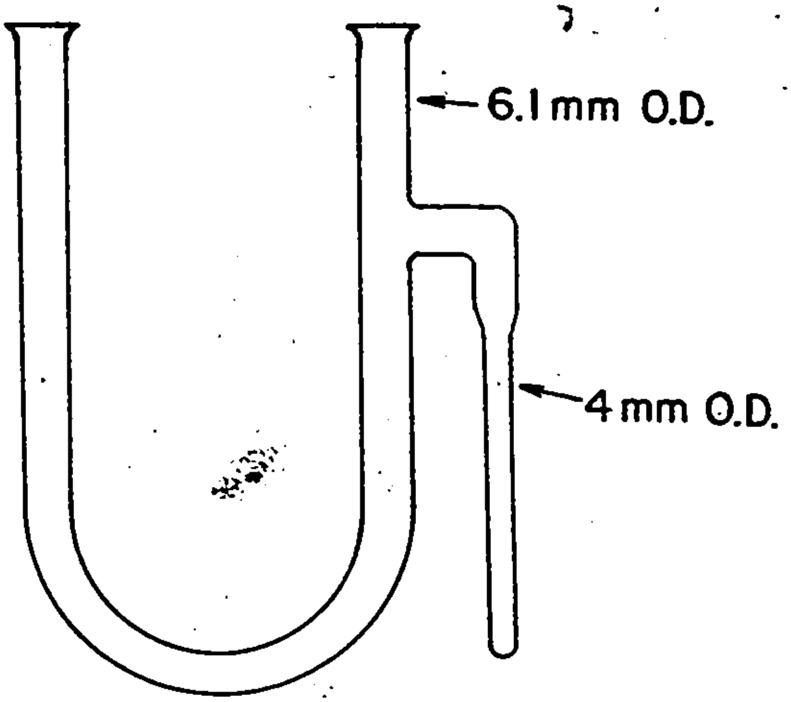

Figure 2.4

The FEP U-tube with 4 mm o.d. side-arm used for trapping $F_4OIOOIOF_4$ generated in the decomposition of cis, cis-$Xe(OIOF_4)_2$.

used. The U-tube was then pumped for ca. 5 minutes at -78°C to remove xenon. The contents of the U-tube, consisting of a finely divided white solid, were then carefully tipped into the 4 mm o.d. side-arm (Figure 2.4) while maintaining the complete unit at -78°C. The U-tube was pressurized with 2 atm of dry nitrogen and stored at -78°C until used. Raman spectra were recorded on the neat white solid at -196°C either in the FEP side-arm or by transferring the white solid at -196°C to a 3 mm o.d. glass capillary tube in an inert atmosphere drybox. Fluorine-19 NMR spectra were recorded in $CFCl_3$ solvent at -40°C by first vacuum distilling $CFCl_3$ solvent into the FEP side-arm containing the product and then heat-sealing the tube under vacuum with a Nichrome resistance furnace. The FEP tube containing the product and $CFCl_3$ solvent then served as the NMR sample tube.

The peroxide has also been prepared and studied in situ by ^{19}F NMR spectroscopy at -40°C. In this experiment, a sample of cis, cis-$Xe(OIOF_4)_2$, dissolved in SO_2ClF solvent, was warmed to 0°C from -196°C and held at 0°C for ca. 10 minutes after which time the ^{19}F NMR spectrum was recorded at -40°C. This cycle was repeated three times (after warm ups of 70, 130 and 520 minutes) with the ^{19}F NMR spectrum recorded after each warm up.

(vii) Preparation of $B(OIOF_4)_x(OTeF_5)_{3-x}$

A mixed boron derivative of the general form

$B(OIOF_4)_x(OTeF_5)_{3-x}$ has been prepared and isolated by the stoichiometric reaction of neat $HOIOF_4$ with $B(OTeF_5)_3$. In a typical preparation, $HOIOF_4$, 2.1538 g (9.13 mmol), was transfered into an FEP tube in an inert atmosphere drybox. The tube was then cooled to -196°C in a Dewar of liquid nitrogen and $B(OTeF_5)_3$, 2.1920 g (3.02 mmol), was added while maintaining the tube at -196°C. The tube was quickly removed from the drybox and immediately cooled to -196°C. The tube and contents were evacuated at -196°C followed by warming, in a static vacuum, to 0°C in an ice-water bath. The contents were allowed to react at 0°C for ca. 10 minutes. During the reaction time, no gas evolution was apparent and the color of the reaction mixture progressed from colorless to bright-yellow. After the specified time, the tube was connected to a vacuum line and pumped on at 0°C for ca. 1 hour after which time a bright-yellow and slightly viscous liquid remained. The tube was then pumped on overnight between 0 and 10°C with no apparent changes in the physical properties of the substance. The liquid was dissolved in ca. 4 ml of $CFCl_3$ solvent (distilled in) and then heat-sealed under dynamic vacuum. The tube and contents were stored at -196°C until ^{11}B and ^{19}F NMR spectra could be recorded.

(viii) Preparation of $Hg(OIOF_4)_2$

A mixture of cis- and trans-$Hg(OIOF_4)_2$ has been prepared by the stoichiometric reaction of $HOIOF_4$ with

$Hg(OTeF_5)_2$ in $CFCl_3$ solvent at 0°C. The experimental procedure is analogous to that used for the acid displacement reaction performed on $Xe(OTeF_5)_2$ with $HOIOF_4$ in $CFCl_3$ discussed previously. In a typical preparation, the following quantities of reactants were used: $HOIOF_4$, 0.3742 g (1.59 mmol); $Hg(OTeF_5)_2$, 0.5115 g (0.76 mmol). The FEP tube containing the pale-yellow product was pressurized with 2 atm of dry nitrogen at -78°C and the Raman spectrum was recorded at -196°C. The product was stored in its FEP tube at -78°C.

(ix) Attempted Preparation of $Te(OIOF_4)_4$ and $Te(OIOF_4)_6$

Attempts to prepare the title compounds either by IO_2F_3 insertion reactions with TeF_4 or by acid displacement reactions of $HOIOF_4$ with $Te(OTeF_5)_4$ or $Te(OTeF_5)_6$ have been made. Although the products have not been fully characterized (Chapter 7), preliminary Raman studies have indicated that Te(IV) derivatives, $Te(OIOF_4)_x(OTeF_5)_{4-x}$ ($x=1-3$), may have been generated. The most promising of these attempts involves the reaction of excess IO_2F_3 (8 moles) with TeF_4 (1 mole) in SO_2ClF solvent at room temperature. In this preparation, IO_2F_3, 0.7083 g (3.28 mmol), and TeF_4, 0.0808 g (0.40 mmol) were combined in an FEP tube at -196°C in a drybox as described previously. The solvent, SO_2ClF, was distilled into the reaction vessel at -196°C, also as previously described. The tube and contents were allowed to warm to and were maintained at room temperature for ca. ½ hour during which time most of the TeF_4 dissolved and the color of the reaction mixture, which was initially yellow, faded. In addition, no gas evolution was observed at any time. After the specified reaction time, the volatiles were pumped off at 0°C for [illegible] hour which resulted in the deposition of a pale-yellow solid. The tube and contents were pumped on overnight at room temperature resulting in a white-solid remaining. The tube was pressurized to 2 atm with dry nitrogen and the Raman spectrum was recorded at -196°C in the FEP tube. The results are discussed in Chapter 7.

(x) Reactions Studied In Situ by NMR Spectroscopy

In addition to the reactions discussed previously in which the isolation of single products was attempted and/or attained, some systems were first studied *in situ* by NMR spectroscopy. These studies were intended to provide the basis upon which subsequent assignments of these species, generated in other systems, could be made and to aid in arriving at strategies for the isolation of products. Below are listed the mixtures of reactants, together with their solvents, which were studied *in situ* by NMR spectroscopy:

Xenon-129 and/or ^{19}F NMR Spectroscopy

A) IO_2F_3	B) XeF_2	Ratio A:B
IO_2F_3/XeF_2 in SO_2ClF at -5°C		
0.8399 g (3.89 mmol)	0.7511 g (4.44 mmol)	0.877:1
1.3380 g (6.20 mmol)	0.5328 g (3.15 mmol)	1.969:1

1.6729 g (7.75 mmol)	0.3713 g (2.19 mmol)	3.530:1
IO_2F_3/XeF_2 in $CFCl_3$ at 24°C		
0.7439 g (3.45 mmol)	0.3529 g (2.09 mmol)	1.653:1
0.5901 g (2.73 mmol)	0.1240 g (0.73 mmol)	3.700:1
IO_2F_3/XeF_2 in BrF_5 at 0°C		
1.0836 g (5.02 mmol)	0.4258 g (2.52 mmol)	1.996:1

A) IO_2F_3	B) XeF_4	Ratio 1:2
IO_2F_3/XeF_4 in $CFCl_3$ at 24°C		
0.6897 g (3.20 mmol)	0.3348 g (1.62 mmol)	1.978:1
IO_2F_3/XeF_4 in BrF_5 at 0°C		
1.0022 g (4.64 mmol)	0.4802 g (2.32 mmol)	2.004:1

A) IO_2F_3	B) $XeOF_4$	Ratio A:B
$IO_2F_3/XeOF_4$ in $CFCl_3$ at 0°C		
0.3892 g (1.80 mmol)	0.4990 g (2.24 mmol)	0.804:1

A) IO_2F_3	B) KrF_2	Ratio A:B
KrF_2/IO_2F_3 in BrF_5 at -45°C		
excess	< (A)	> 1
< (B)	excess	< 1

KrF_2/IO_2F_3 in SO_2ClF at -45°C		
excess	< (A)	> 1
< (B)	excess	< 1

(exact quantities of reagents could not be determined)

A) $HOIOF_4$	B) $Xe(OTeF_5)_2$	Ratio A:B
$HOIOF_4/Xe(OTeF_5)_2$ in $CFCl_3$ at 21°C		
0.0831 g (0.35 mmol)	0.1965 g (0.32 mmol)	1.094:1

A) $HOIOF_4$	B) $Xe(OTeF_5)_4$	Ratio A:B
$HOIOF_4/Xe(OTeF_5)_4$ in $CFCl_3$ at -5°C		
0.1212 g (0.51 mmol)	0.2330 g (0.22 mmol)	2.394:1
0.2875 g (1.22 mmol)	0.2983 g (0.28 mmol)	4.357:1
0.2548 g (1.08 mmol)	0.1589 g (0.15 mmol)	7.378:1

A) $HOIOF_4$	B) $OXe(OTeF_5)_4$	Ratio A:B
$HOIOF_4/OXe(OTeF_5)_4$ in $CFCl_3$ at -35°C		
1.0207 g (4.33 mmol)	1.0894 g (0.99 mmol)	4.375:1

<u>Tellurium-125 NMR Spectroscopy</u>

A) $HOIOF_4$	B) TeF_4	Ratio A:B
$HOIOF_4/TeF_4$ in SO_2 at -10°C		
1.5014 g (6.37 mmol)	0.4024 g (1.98 mmol)	3.220:1

The procedure that was followed for preparing NMR samples was the same in each case. Reagents were loaded into the NMR tubes at low temperature (-196°C) either by vacuum distillation (IO_2F_3, KrF_2, XeF_6 and $XeOF_4$) or in an inert atmosphere drybox (XeF_2, XeF_4, $Xe(OTeF_5)_2$, $Xe(OTeF_5)_4$, $OXe(OTeF_5)_4$ and TeF_4). While maintaining the NMR sample cold, ca. 1.5-2.5 ml, of solvent was transfered to the tube under vacuum at -196°C, except for SbF_5, which was transfered to the cold tube using an all-glass syringe in an inert atmosphere drybox.

(D) INSTRUMENTATION

(i) Nuclear Magnetic Resonance Spectroscopy

All NMR spectra were recorded unlocked (field drift < 0.1 Hz h^{-1}) with the use of a Bruker WM-250 spectrometer equipped with a 5.8719 T cryomagnet and an Aspect 2000 computer. For variable temperature measurements, samples were kept cold (-196 or -78°C) until immediately prior to their placement in the probe. Samples were generally warmed only enough to liquify and solubilize or partially solubilize the contents and were then quickly placed in the pre-cooled probe. Prior to data accumulation, the tubes were allowed to equilibrate in the probe for periods of 1-3 minutes while spinning. Temperatures were periodically checked by placing a copper-constantan thermocouple into the sampling region of the probe. Temperatures were considered to be accurate to within ± 1°C.

Spectra were obtained in either precision 10 mm o.d. thin-walled glass NMR tubes (Wilmad Glass Co.) (^{129}Xe, ^{19}F and ^{11}B), 5 mm o.d. (^{19}F) or in FEP NMR tubes (described above), of 9 mm o.d. (^{129}Xe, ^{19}F, ^{125}Te) or 4 mm o.d. (^{19}F). The samples recorded in FEP tubes were placed inside precision 10 mm o.d. or 5 mm o.d. glass NMR tubes during the acquisition of spectra.

Spectra were obtained for ^{129}Xe, ^{125}Te, and ^{11}B on the same 10 mm probe (broad-banded over the frequency range 23-103 MHz) tuned to 69.56, 78.90 and 80.32 MHz, respectively. Fluorine-19 spectra using 10 mm o.d. tubes, were obtained with the use of the proton decoupler coils retuned to 235.36 MHz as the observe coils. Fluorine-19 spectra using 5 mm o.d. tubes, were obtained with the use of a combination ^{1}H/^{19}F probe and a fixed frequency transmitter.

All spectra were obtained on natural abundance compounds. Xenon-129 spectra were obtained in 400-10000 scans at a spectral width of 50 KHz (16K, 6.1 Hz/data point, 0.164 s acquisition time; 32K, 3.1 Hz/data point, 0.328 s acquisition time) or 100 KHz (32K, 6.1 Hz/data point, 0.164 s acquisition time). Fluorine-19 spectra were obtained in 64-1600 scans at a spectral width of 100 KHz (16K, 12.2 Hz/data point, 0.082 s acquisition time; 32K, 6.1 Hz/data point, 0.164 s acquisition time) or 150 KHz (32K, 9.2 Hz/data point, 0.109 s acquistion time). In some instances ^{19}F free induction decays accumulated at a spectral width of 100 KHz and in a 32K memory, were zero-filled to 64K for processing, yielding a data point resolution of 3.1 Hz. Both ^{11}B and ^{125}Te spectra were obtained in 100,000 scans at a spectra width of 100 KHz (32K, 6.1 Hz/data point, 0.164-s acquisition time). Pulse widths corresponding to bulk magnetization tip angles, θ = 90°, were 2 (^{19}F), 22 (^{129}Xe), 20 (^{11}B) and 25 μs (^{125}Te). Line-broadening parameters used in exponential multiplication of the free induction decays were set equal to or less than their respective data point resolutions. In some cases, resolution was further enhanced by transforming the free induction decays from a time to a frequency domain with use of a Gaussian fit rather than the convential Lorentzian fit. In these instances, a Gaussian broadening between 0.1 and 0.5 and a line-broadening equal to the negative of the respective data point resolution, were applied to the free induction decays prior to Gaussian multiplication and Fourier transform.

Line-broadening effects in the ^{129}Xe spectra due to shielding anisotropy (SA), were found to be a considerable nuisance in the course of this work. In particular, the long range spin - spin coupling patterns could not be resolved in the ^{129}Xe NMR spectra of the cis-isomers of $FXeOIOF_4$ and $Xe(OIOF_4)_2$ (Chapter 4) and this is attributed, in the most part, to line-broadening due to SA.

The respective nuclei were referenced with respect to neat samples of $XeOF_4$ (^{129}Xe), $CFCl_3$ (^{19}F) $(CH_3)_2Te$ (^{125}Te) and BCl_3 (^{11}B) at 24°C. A positive chemical shift was assigned to any resonance occuring to high frequency of the reference substance.

(ii) Raman Spectroscopy

A Coherent Model Innova 90 argon ion laser giving up to 3.5 W at 5145 Å was used to excite the Raman spectra. The spectrometer was a Spex Industries Model 14018 double monochromator equipped with 1800 grooves/mm Holographic gratings. Slit widths depended on the scattering efficiency of the sample but were typically set between 50 and 100 μm. The scanning rate used was 0.5 cm^{-1} s^{-1}. The typical power range used was between 0.4 and 1 W. All Raman shifts quoted are believed to be accurate to ± 2 cm^{-1}. Cylindrical sample tubes were mounted vertically. The angle between the laser beam and sample tube was 45°, and Raman scattered radiation was observed at 45° to the laser beam or 90° to the sample tube. Low-temperature spectra were recorded by mounting the sample vertically in an unsilvered Pyrex glass Dewar filled with liquid nitrogen. All spectra were obtained directly in either FEP or glass reaction vessels.

CHAPTER 3

AN IMPROVED SYNTHESIS OF $HOIOF_4$ AND DEFINITIVE ^{19}F NMR STUDY OF THE STRUCTURE OF IO_2F_3 AND THE cis- and trans-$HOIOF_4$ ISOMER RATIO

(A) INTRODUCTION

Prior to the commencement of this research, the chemistry of the $-OIF_4O$ group was limited to the preparation of cis- and trans-isomers of $HOIOF_4$ (184,185,186), $K^+IO_2F_4^-$ (187), $Cs^+IO_2F_4^-$ (186,189), $FOIOF_4$ (186,189) and $ClOIOF_4$ (186). The purpose of this work from the outset was to extend the chemistry of the $-OIF_4O$ group to other main-group derivatives. In light of this objective, it was first necessary to prepare substantial quantities of $HOIOF_4$ and IO_2F_3, which were seemingly best suited to function as precursors for $-OIF_4O$ derivatives. Secondly, it was necessary to study the solvent and temperature dependences of the cis:trans isomer ratio in $HOIOF_4$ and the solution structure of IO_2F_3. This would serve as a basis for characterizing new $-OIF_4O$ derivatives in solution and the detection of unreacted $HOIOF_4$ and IO_2F_3. To this end, a new synthesis was developed for $HOIOF_4$, monitored and optimized with the aid of a ^{19}F NMR study. In addition, a ^{19}F NMR study of the solvent and temperature dependences of the cis:trans isomer ratio in $HOIOF_4$ and a definitive structural analysis of IO_2F_3 in solution were undertaken. These studies and their results are discussed in this Chapter.

(B) RESULTS AND DISCUSSION

(i) An Improved Synthesis of $HOIOF_4$

Tetrafluoro-orthoperiodic acid $HOIOF_4$ and iodine dioxide trifluoride IO_2F_3 were first prepared in 80% yields by Engelbrecht and Peterfy (184,185) according to equations (3.1) - (3.3).

$$2\ Na_3H_2IO_6 + 3\ Ba(NO_3)_2 \rightleftharpoons Ba_3H_4(IO_6)_2 + 6\ NaNO_3 \qquad (3.1)$$

$$Ba_3H_4(IO_6)_2 + 14\ HSO_3F \rightleftharpoons 2\ HOIOF_4 + 8\ H_2SO_4 + 3\ Ba(SO_3F)_2 \qquad (3.2)$$

$$HOIOF_4 + SO_3 \longrightarrow IO_2F_3 + HSO_3F \qquad (3.3)$$

Attempts in the course of the present work to generate $HOIOF_4$ in high yield according to this method were unsuccessful, with a maximum attained yield of only 42%. In addition, this synthesis has two principal drawbacks; an additional step requiring the preparation of the barium periodate salt according to equation (3.1) and, the large quantity of HSO_3F used, 7 moles of HSO_3F for every mole of $HOIOF_4$ (equation 3.2). The only other published method leading to the recovery of pure $HOIOF_4$ is that of Christe <u>et al.</u> (186) who have prepared and isolated $HOIOF_4$ on a small scale by way of a metathesis utilizing $Cs^+[IO_2F_4]^-$ as the $-OIF_4O$ source according to equations (3.4) - (3.6).

$$Cs^+[IO_4]^- + 4\ HF \rightleftharpoons Cs^+[IO_2F_4]^- + 2\ H_2O \qquad (3.4)$$

$$Cs^+[IO_2F_4]^- + 2\ HF \rightleftharpoons Cs^+[HF_2]^- + HOIOF_4 \qquad (3.5)$$

$$Cs^+[HF_2]^- + BiF_5 \rightleftharpoons Cs^+[BiF_6]^- + HF \qquad (3.6)$$

The salt, $Cs^+[IO_2F_4]^-$ is prepared by HF solvolysis from $Cs^+[IO_4]^-$ (equation 3.4) followed by the removal of excess HF and H_2O under vacuum. The method can suffer from incomplete solvolysis resulting in some $Cs^+[IO_4]^-$ contamination (see Chapter 2). The latter can be removed, however, by fluorination with BrF_5 to give pure $Cs^+[IO_2F_4]^-$. The $[BiF_6]^-$ salt formed in the last step of the procedure is removed by filtration and the resulting $HOIOF_4/HF$ mixture is separated by fractional distillation. This method, which leads to the preparation of pure $HOIOF_4$ in gram quantities, is not feasible for the preparation of larger quantities of $HOIOF_4$ owing to the number of steps involved and difficulties encountered in preparing large amounts of pure BiF_5 (202,203) and pure $Cs^+[IO_2F_4]^-$ (186,188) (equation 3.4).

In the present work, $HOIOF_4$ is prepared in high yield (88%) according to equilibrium (3.7) and recovered and purified using the method of Engelbrecht and Peterfy (184,185) (equations 3.3 and 3.8).

$$H_5IO_6 + n\ HSO_3F \rightleftharpoons (HO)_{5-n}IOF_n + n\ H_2SO_4 \qquad (3.7)$$

$$HF + IO_2F_3 \longrightarrow HOIOF_4 \qquad (3.8)$$

The experimental details of this improved synthetic procedure are given in Chapter 2. This method offers several advantages, namely:

(1) H_5IO_6 (99%) is commercially available whereas the method of Engelbrecht and Peterfy (equations 3.1 -

3.3) and Christe et al. (equations 3.4 - 3.6) both require the preparation of iodine(VII) salt precursors.

(2) equilibrium (3.7) requires only 4 moles of HSO_3F whereas equation (3.2) requires 7 moles of HSO_3F per mole of $HOIOF_4$ formed.

(3) and the problems associated with the insoluble products $Ba(SO_3F)_2$ and $Cs^+[BiF_6]^-$ (equations 3.2 and 3.6) are eliminated.

The reactions and equilibria associated with the synthesis of $HOIOF_4$ according to equilibrium (3.7) were monitored by ^{19}F NMR at four stages throughout the preparation, namely:

Stage (1) on the reaction mixture after addition of H_5IO_6 to HSO_3F was complete and the mixture had presumably attained equilibrium.

Stage (2) on the residue remaining after $HOIOF_4$ was statically distilled from the original mixture.

Stage (3) on the $HOIOF_4$ which was statically distilled from the original mixture and used for the SO_3 titration according to equation (3.3).

Stage (4) and on the liquid portion of the reaction mixture which remained after the final SO_3 addition and presumably when all $HOIOF_4$ had been converted to IO_2F_3 and subsequently removed.

The results at each stage are important to the overall understanding of the conversion of H_5IO_6 to $HOIOF_4$ and have aided in refining the reaction conditions (see Chapter 2) and in optimizing the yield of pure $HOIOF_4$. These findings are discussed below.

At Stage (1), that is after the H_5IO_6/HSO_3F mixture had attained equilibrium in an inert FEP vessel (24 hours), the ^{19}F NMR spectrum (Fig 3.1) showed the presence of five distinct species. The ^{19}F NMR parameters and integrated ratios of the species are summarized in Table 3.1. The assignments are based on the earlier work of Selig and Elgad (204) who studied the solvolysis of periodate and the partial hydrolysis of iodine heptafluoride in anhydrous HF. Their ^{19}F NMR results indicate the following equilibrium exists in anhydrous HF:

$$[IO_4]^- + x\,HF \rightleftharpoons (HO)_xIOF_{5-x} \qquad x = 1-4 \qquad (3.9)$$

with the species cis- and trans-$HOIOF_4$, mer-$(HO)_2IOF_3$, cis- and trans-$(HO)_3IOF_2$ and $(HO)_4IOF$ being identified. The most prominent feature of the spectrum at Stage (1) is the large proportion of the higher fluorinated species present. With 96% of all species having undergone at least three successive fluorinations, it is evident that equilibrium (3.7) lies far to the right. In addition, the low intensities of ^{19}F NMR singlets attributable to the lower fluorinated species cis- or trans-$(HO)_3IOF_2$ and $(HO)_4IOF$ also serve to support the view that

Figure 3.1

The room temperature ^{19}F NMR spectrum (235.36 MHz) of an equilibrium mixture of iodine (VII) oxide fluoride acids resulting from the HSO_3F solvolysis of H_5IO_6. The peak assignments are given below.

Peak	Spin System	Species
A	A_2X_2	cis-$HOIOF_4$
B	A_4	trans-$HOIOF_4$
C	AX_2	mer-$(HO)_2IOF_3$
D	A_3	fac-$(HO)_2IOF_3$
E	A_2	cis-$(HO)_3IOF_2$

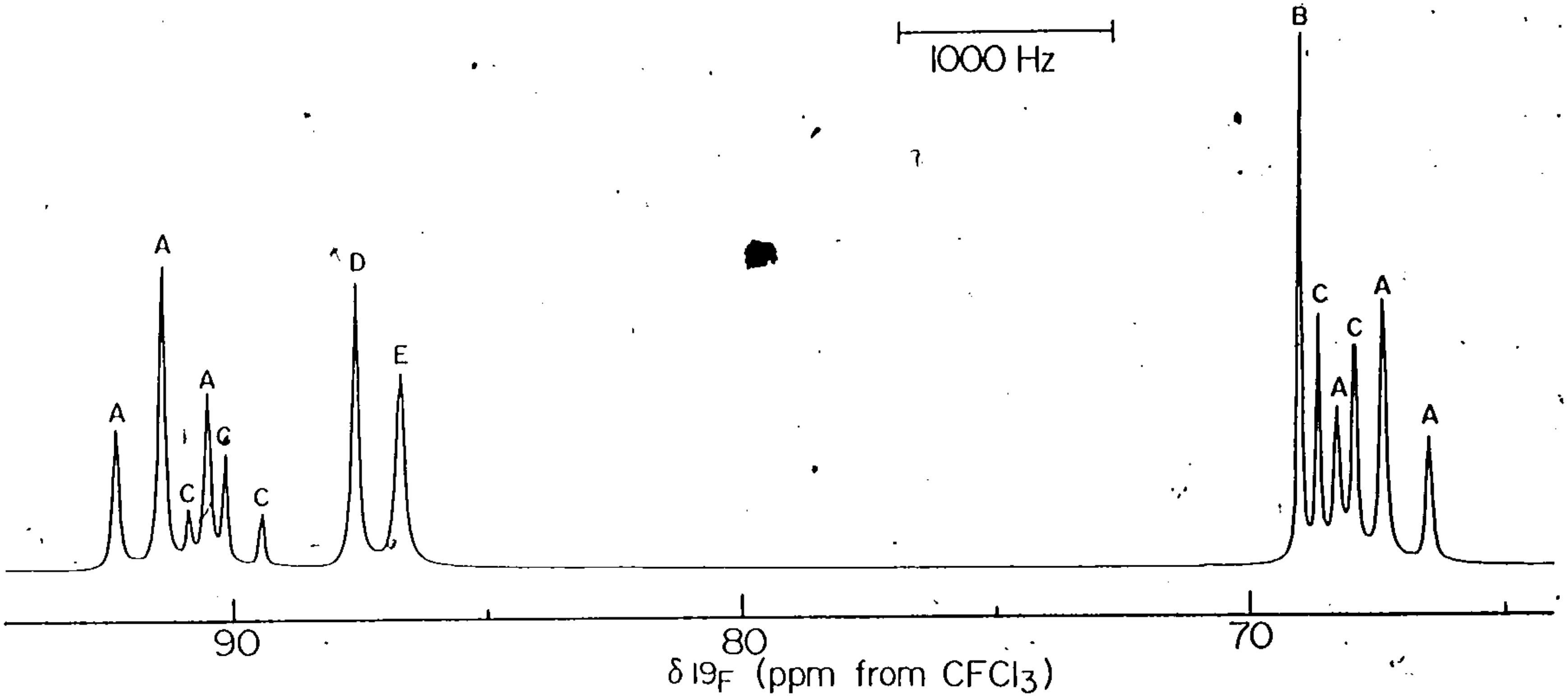
1000 Hz
A
A
C
A
G
C
D
E
B
C
A
C
A
A
90
80
70
δ 19F (ppm from CFCl3)

Table 3.1

Fluorine-19 NMR Parameters (235.36 MHz) for the Species Generated During the HSO_3F Solvolysis of H_5IO_6

Species	Spin System	δ $^{19}F^a$ (ppm)	$^2J_{FF}$ (Hz)	Integrated. Ratio	Fluorinated Species Present
trans-$HOIOF_4$	A_4	68.90	-	4.8	19.8%
cis-$HOIOF_4$	A_2X_2	(A) 91.46 (X) 67.30	213 213	14.8	60.2%
mer-$(HO)_2IOF_3$	AX_2	(A) 90.09 (X) 68.11	167 167	2.7	11.0%
fac-$(HO)_2IOF_3$	A_3	87.48	-	1.3	5.0%
cis-$(HO)_3IOF_2$	A_2	86.78	-	1.0	4.0%

a: Measured at 24°C and referenced with respect to neat $CFCl_3$ at 24°C.

equilibrium (3.7) lies far to the right.

The assignment of the higher fluorinated species is straight forward based on the spin multiplicities and the integrated ratios of the resonance peaks (Table 3.1) while the assignment of the weak singlet at $\delta^{19}F$ = 86.78 ppm must remain as tentative. It is possible that this peak represents one of either cis-$(HO)_3IOF_2$, trans-$(HO)_3IOF_2$, $(HO)_4IOF$ or a seven-coordinate species of the form $(HO)_xIF_{7-x}$ x = 1-6. It is unlikely that the monofluorinated species $(HO)_4IOF$ would exist in such an equilibrium in the absence of a difluorinated species and thus it is ruled out as a possibility. In addition, and as is the case for IF_7, a seven-coordinate species would be expected to undergo rapid intramolecular exchange averaging of its fluorine environments to give a singlet in its ^{19}F NMR spectrum. It is assumed, however, that six-coordinate species should be favored over seven-coordinate species and it then follows that the singlet at $\delta^{19}F$ = 86.78 ppm could be either cis- or trans-$(HO)_3IOF_2$. In view of the shielding trends exhibited by cis- and trans-$HOIOF_4$ (185,204,205) and mer- and fac-$(HO)_2IOF_3$ (204,205), the singlet at $\delta^{19}F$ = 86.78 ppm is assigned to cis-$(HO)_3IOF_2$. This assignment stems from the observation that the chemical shift of a fluorine in a position trans to another fluorine occurs at lower frequency than a fluorine trans to a hydroxyl group or to a doubly-bonded oxygen.

At Stage (2), the effectiveness of the $HOIOF_4$ removal step was determined by recording the ^{19}F NMR spectrum of an aliquot of the residue remaining after the $HOIOF_4$ was statically distilled out. The important feature of the NMR spectrum at Stage (2) is the abundance of the lower fluorinated species, indicating effective removal of cis- and trans-$HOIOF_4$. Of the total fluorinated iodine(VII) species remaining after distillation, 68% are the trifluorinated species mer-$(HO)_2IOF_3$ (8%) and fac-$(HO)_2IOF_3$ (60%), 21% are the difluorinated species cis-$(HO)_3IOF_2$ (13%) and trans-$(HO)_3IOF_2$ (8%) and 11% are the tetrafluorinated species cis-$HOIOF_4$ (3%) and trans-$HOIOF_4$ (8%). The removal of cis- and trans-$HOIOF_4$ leads to the enhancement of the ^{19}F NMR signals due to the lower fluorinated species and thus permits assignment of the new singlet ($\delta^{19}F$ = 69.52 ppm) to trans-$(HO)_3IOF_2$. The 11% of species remaining as $HOIOF_4$ does not necessarily indicate incomplete removal of $HOIOF_4$ by distillation. Equilibrium (3.7) may be slowly attained, in which case it is possible that all cis- and trans-$HOIOF_4$ had been removed when the distillation was stopped. A subsequent slow reattainment of equilibrium (3.7) could then follow since there were both HSO_3F and lower fluorinated species $(HO)_xIOF_{5-x}$ (x = 2,3) still remaining in the reaction mixture. The net result is further fluorination of the lower fluorinated species accounting for the residual $HOIOF_4$ observed in the ^{19}F NMR spectra of these mixtures after distillation. The relative amounts of $HOIOF_4$ remaining were found to vary with the time interval between stopping the distillation and taking an aliquot for ^{19}F NMR, and indeed were found to increase with increasing time interval.

At Stage (3), the $HOIOF_4/HSO_3F$ distillate was monitored by ^{19}F NMR to confirm its purity. The ^{19}F NMR spectrum was simple, corresponding to a mixture of cis- and trans-$HOIOF_4$ and HSO_3F. The two acids are unavoidably co-distilled owing to the similarity of their vapor pressure curves (Figure 3.2 and 3.3) at room temperature (e.g., HSO_3F, v.p. (21°C) = 2.09 mm Hg (206) : $HOIOF_4$, v.p. (21°C) = 1.40 mm Hg (185)). At lower temperatures, the rate of distillation is prohibitively slow and at 89°C the two vapor pressure curves cross.

At Stage (4), IO_2F_3 is generated by the addition of 65% oleum to the $HSO_3F/HOIOF_4$ distillate. Fluorine-19 NMR was used to monitor the fluorine-containing species remaining in the liquid portion of the reaction mixture after the final SO_3 addition. At this point in the overall synthetic scheme, the slow titration of $HOIOF_4$ with 1 ml aliquots of 65% oleum yields equimolar amounts of HSO_3F ~~and~~ IO_2F_3 according to equation (3.3). The latter is volatile at room temperature (IO_2F_3 v.p. (21°C) = 5.34 mm Hg (185)) and is sublimed from the mixture under reduced pressure onto a cold finger chilled with ice water. However, if the amount of SO_3 significantly exceeds 1 ml per addition, or if the addition is too rapid compared to the rate of IO_2F_3 sublimation (see Chapter 2), a pale-yellow solid precipitates. Characterization of this solid by Raman spectroscopy cannot be considered totally conclusive as the spectra recorded consisted of broad and poorly resolved bands and are complicated by many resonances in the I-F, S-F and I-O

Figure 3.2

Vapor Pressure Versus Temperature Curves for $HOIOF_4$ and HSO_3F. Temperature Range: 0-100°C.

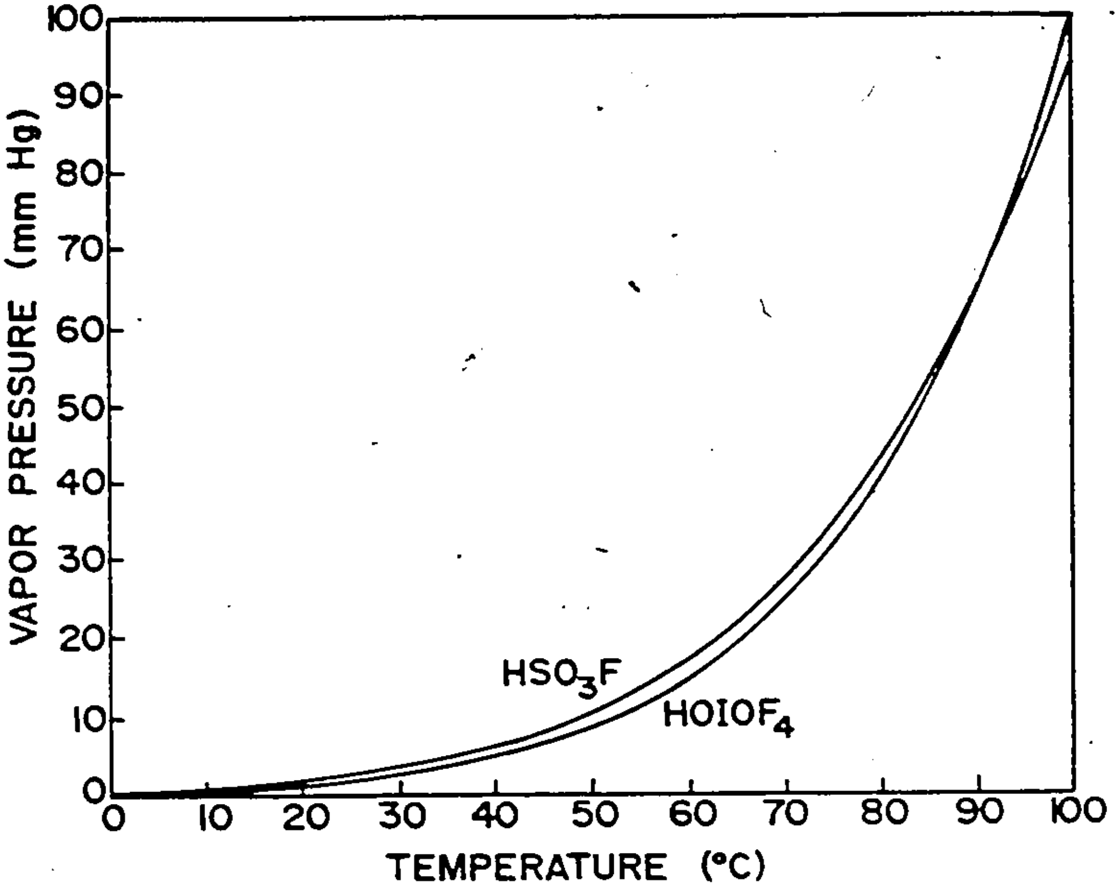

VAPOR PRESSURE (mm Hg)
0
10
20
30
40
50
60
70
80
90
100
TEMPERATURE (°C)
0
10
20
30
40
50
60
70
80
90
100
HSO$_3$F
HOIOF$_4$

Figure 3.3

Vapor Pressure Versus Temperature Curves for $HOIOF_4$ and HSO_3F. Temperature Range: 70-100°C.

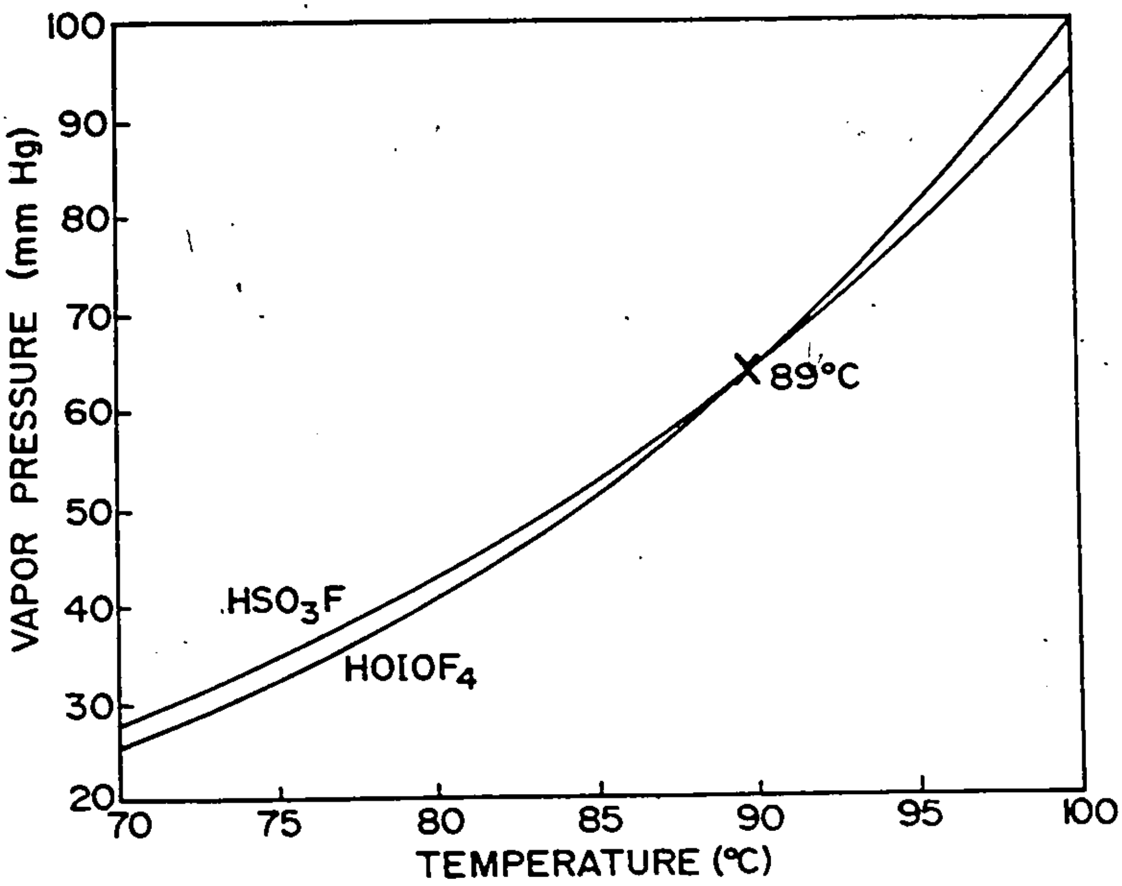
VAPOR PRESSURE (mm Hg)
100
90
80
70
60
50
40
30
20
70
75
80
85
90
95
100
TEMPERATURE (°C)
HSO_3F
$HOIOF_4$
89°C

stretching regions (550 - 960 cm^{-1}). The results of the Raman study do, however, indicate the pale-yellow solid could represent a mixture of iodine(VII) fluorosulfates resulting from SO_3 insertion into I-F bonds (see below). The presence of vibrational bands in the SO_2 stretching region (1050 - 1320 cm^{-1}) also supports this proposal. The appearance of broad bands may simply be due to a mixture of isomers with similar or even possibly coincident vibrational frequencies and/or may be a result of considerable mixing between I-F and I-O vibrations. Table 3.2 lists the approximate vibrational frequencies and possible assignments for the Raman spectrum recorded on the pale-yellow solid at room temperature. Assignments for the low frequency (< 350 cm^{-1}) vibrational modes cannot be made with any certainty and are therefore not attempted. The 380 - 405 cm^{-1} peak in the spectrum is assigned to an O-I-O bending mode(s) by analogy with the value reported for the corresponding mode in $IO_2F_4^-$ (399 cm^{-1}) (204), $K^+IO_2F_2^-$ (358 cm^{-1}) (207) and IO_2SO_3F (428 cm^{-1}) (207). The 555 cm^{-1} peak is assigned to a combination of I-O stretching and S-F deformation modes by analogy with the corresponding I-O stretching modes in $(IOF_2SO_3F)_n$ (423cm^{-1}) (208), I_2O_5 (503 cm^{-1}) (209) and HOI_3O_7 (459 cm^{-1}) (209) and S-F deformation modes in IO_2SO_3F (562 cm^{-1}) (207) and $(IOF_2SO_3F)_n$ (581 cm^{-1}) (208). The region of the spectrum from 625 cm^{-1} to 690 cm^{-1} is assigned to overlapping I-F stretching modes by analogy with the values reported for the same modes in other iodine(VII) oxide fluorides IOF_5 (640 cm^{-1}, 647 cm^{-1} and

Table 3.2

Vibrational Frequencies from the Room Temperature Raman Spectrum Recorded on the Pale-Yellow Solid which Precipitates at Stage (4) of the $HOIOF_4$ Synthesis

Frequency (cm^{-1})		Tentative Assignment
128	(br,W)	
200	(br,W)	
260	(br,W)	
320	(br,W)	
349	(br,M)	
380 - 405	(br,S)	δ O-I-O
555	(br,S)	ν I-O, S-F wag
633 - 655	(br,S)	ν I-F
775 - 795	(br,W)	
835 - 850	(br,S)	ν S-F
900 - 910	(br,S)	ν I=O
950 - 960	(br,M)	
1078	(br,M)	SO_2 sym
1155	(br,M)	SO_2 asym
1318	(br,W)	SO_2 sym

br: broad

S = strong, M = moderate, W = weak

680 cm^{-1}) (210,211), $HOIOF_4$ (629 cm^{-1}, 655 cm^{-1} and 670 cm^{-1}) (186,208) and IO_2F_3 (627 cm^{-1}, 659 cm^{-1} and 688 cm^{-1}) (208). The region of the spectrum assigned to S-F stretching modes (835 - 850 cm^{-1}) is higher than the corresponding mode in the SO_3F^- ion (741 cm^{-1}) (212) but is similar to that of the S-F stretching modes in IO_2SO_3F (843 cm^{-1}) (207) and $(IOF_2SO_3F)_n$ (848 cm^{-1}) (208). The I=O region is assigned to the stretches appearing at 900 - 910 cm^{-1} and 960 cm^{-1} in comparison to the values reported for the I=O stretching modes in $(IOF_2SO_3F)_n$ (933 cm^{-1} and 954 cm^{-1}) (208), IO_2F_3 (916 cm^{-1}) (208) and IOF_5 (927 cm^{-1}) (210,211). The bands at 1078, 1155 and 1318 cm^{-1} are assigned to SO_2 stretching modes in comparison to the same modes in $(IOF_2SO_3F)_n$ (1071, 1190 and 1316 cm^{-1}) (208) and IO_2SO_3F (1070, 1170 and 1335 cm^{-1}) (207).

The ^{19}F NMR results at Stage 4 show that of the total fluorinated iodine(VII) species, the majority remain as cis-$HOIOF_4$ (A_2X_2) (δF_A = 91.08 ppm, δF_X = 67.55 ppm, $^2J_{AX}$ = 214 Hz), trans-$HOIOF_4$ (A_4) (δF_A = 69.10 ppm) and IO_2F_3 (AX_2) (δF_A = 66.02 ppm, δF_X = 100.01 ppm, $^2J_{AX}$ = 176 Hz) in the approximate ratio 9:3:1. In addition to $HOIOF_4$ and IO_2F_3, two sharp singlets at $\delta^{19}F$ = 102.94 ppm and $\delta^{19}F$ = 96.42 ppm and two sets of two broadened singlets of near-equal intensities centered at $\delta^{19}F$ = 87.26 ppm (line separation 530 Hz) and $\delta^{19}F$ = 81.50 ppm (line separation 450 Hz), respectively, represent the remainder of fluorinated iodine(VII) species. The exact nature of these minor components is unknown. The chemical shifts seem to indicate that these resonances are due to F-on-I(VII) (204,205,208,213) (chemical shift range +170 ppm to +65 ppm) as opposed to F-on-I(V) (208) (chemical shift range +62 ppm to +12 ppm). In addition, the 530 Hz and 450 Hz spacings would be too large for $^2J_{FF}$ in an iodine oxide fluoride or an iodine fluoride (c.f. $^2J_{FF}$: IF_5 = 85 Hz (213), IOF_5 = 280 Hz (213), IO_2F_3 = 176 Hz (185)). It is possible, as the concentration of SO_3 is increased during the course of the titration with 65% oleum, to have SO_3 insert into an iodine(VII) oxide fluoride I-F bond. This would in turn generate a series of fluorosulfate derivatives analogous to the insertion of SO_3 into Sb-F bonds of SbF_5 (214,215). The F-on-S(VI) resonance of the fluorosulfate derivatives could be present in this case, however, they may be obscured by the intense HSO_3F solvent resonance. One such possibility is given in equation (3.10).

$$(HO)_2IOF_3 + SO_3 \longrightarrow (HO)_2IOF_2SO_3F \qquad (3.10)$$

The ^{19}F NMR spectrum at Stage (4) illustrates two important points; the conversion of $HOIOF_4$ to IO_2F_3 according to equation (3.3) does not go to completion nor is the removal of IO_2F_3 by static sublimation quantitative. Furthermore, as the SO_3 concentration increases, the rate of formation of the pale-yellow precipitate is enhanced over that of IO_2F_3, and eventually becomes the dominant process. This process competes with IO_2F_3 formation to the extent that no more can be recovered through static distillation and the sublimation of IO_2F_3 ceases.

The synthetic procedure developed here has been used repeatedly during the course of this work to prepare $HOIOF_4$ and IO_2F_3 on a large scale. The preparation of xenon and other $-OIF_4O$ derivatives are discussed in subsequent chapters. The success of these preparations was largely due to the availability of pure $HOIOF_4$ and IO_2F_3 as starting materials.

(ii) The cis- and trans-$HOIOF_4$ Isomer Ratio Dependence on Solvent and Temperature: A ^{19}F NMR Study

Both $HOIOF_4$ and IO_2F_3 exist in more than one isomeric form (184,185). While $HOIOF_4$ clearly exists in either the cis- (C_{2v}, structure 3.1) or trans- (D_{4h}, structure 3.2) isomeric forms, the structure of IO_2F_3 is not as straightforward and has been the subject of numerous papers (184,185,190-192,194,197). The latter point is addressed in the following section. Engelbrecht <u>et al.</u> (185) have measured the enthalpy of the isomerization process (3.11) and found it to be only 0.92 Kcal mol^{-1}.

$$\text{cis-}HOIOF_4 \rightleftharpoons \text{trans-}HOIOF_4 \qquad (3.11)$$

It is therefore not surprising that both isomers coexist in solution, except at very low temperatures (205). Figure 3.4 illustrates a typical ^{19}F NMR spectrum of $HOIOF_4$ recorded in $CFCl_3$ solvent showing the two isomers cis-$HOIOF_4$ (spin system A_2X_2) and trans-$HOIOF_4$ (spin system A_4).

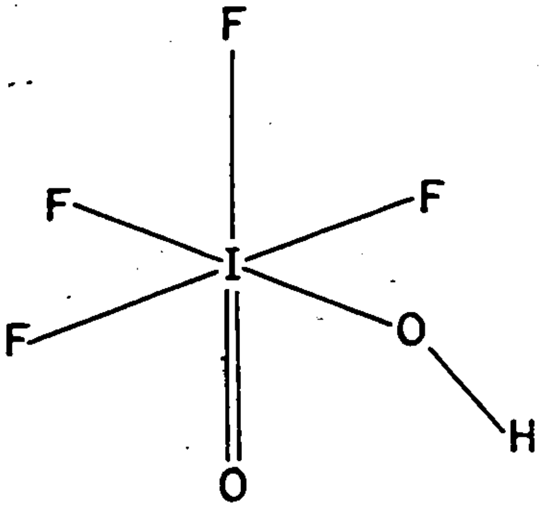

3.1

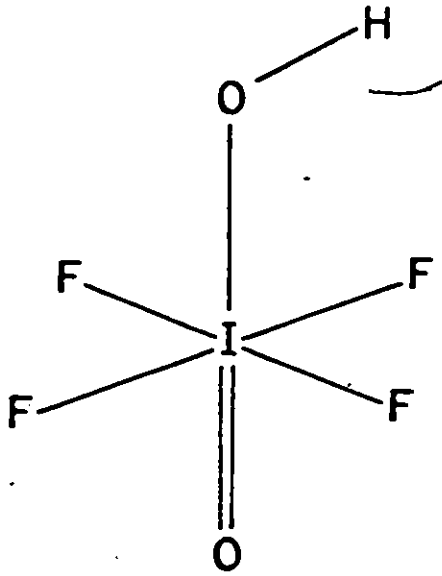

3.2

Figure 3.4

The ^{19}F NMR spectrum (235.36 MHz) of $HOIOF_4$ recorded in $CFCl_3$ solvent at -30°C.

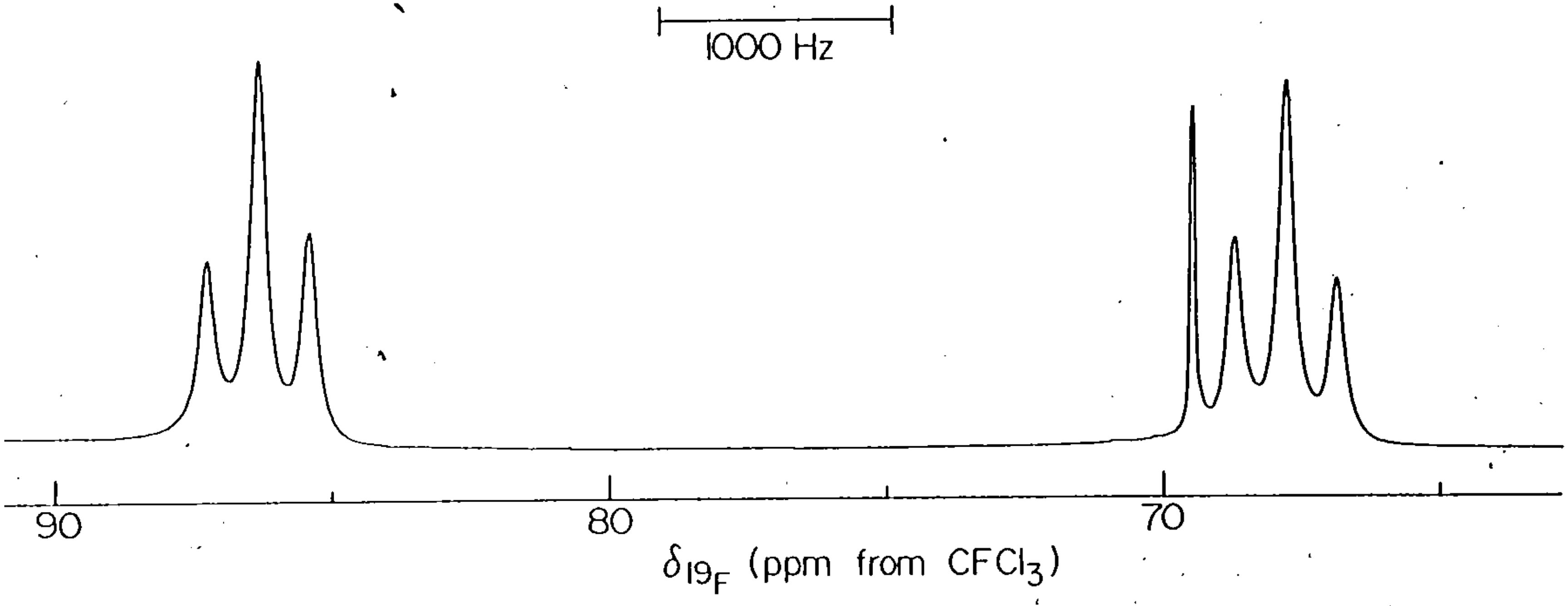
1000 Hz
90
80
70
δ_{19_F} (ppm from $CFCl_3$)

In 1971, Engelbrecht <u>et al.</u> (185) described the preparation and physical properties of $HOIOF_4$ and IO_2F_3. In this account, the cis:trans isomer ratio of $HOIOF_4$ was measured by ^{19}F NMR in HSO_3F solvent at 47 and 148°C and found to be 3:1 and 2:1, respectively. This report first established that the cis:trans-$HOIOF_4$ isomer ratio is, not suprisingly, dependent on temperature. Engelbrecht <u>et al.</u> (216) have also reported that the cis:trans-isomer ratio of $HOIOF_4$ was solvent dependent, however, the details of this investigation have not been published. Krasznai (208) measured the ^{19}F NMR spectrum of $HOIOF_4$ as a melt at 50°C and as a solution in HSO_3F at -75°C, however, the cis:trans-isomer ratio was not determined. In the most recent published work on the synthesis and properties of $HOIOF_4$, Christe <u>et al.</u> (186) reported the ^{19}F NMR parameters of $HOIOF_4$ in CH_3CN at -70°C. The spectrum was not published and again no mention was given to the cis:trans-isomer ratio dependence on solvent and temperature.

In light of the limited amount of information available on isomer ratio dependences, a variable temperature ^{19}F NMR investigation of $HOIOF_4$ dissolved in a number of solvents was undertaken. This investigation was intended to establish a collection of ^{19}F NMR chemical shifts and $^2J_{FF}$ coupling constants for $HOIOF_4$ as a solute in a number of solvents at different temperatures. This could then be used in subsequent experiments to identify $HOIOF_4$. The determination of the cis- and trans-$HOIOF_4$ isomer ratio dependence on both temperature and solvent medium could also aid in the identification of cis- and trans-isomers of other $-OIF_4O$ group derivatives. The results of this investigation are summarized in Table 3.3. From an inspection of Table 3.3, a cis:trans-isomer ratio temperature dependence is observed for all solvents investigated but is perhaps best illustrated by the measurements made in $CFCl_3$ solvent. As the temperature was decreased, the ratio of cis:trans-$HOIOF_4$ progressed from 6.31:1 at 25°C to greater than 50:1 at -60°C and finally to exclusively the cis-isomer at -90°C. In the other solvents measured, the trend is similar, however, the variation in the cis:trans-isomer ratio is not as pronounced. For measurements made at the same temperature but in different solvents, the cis:trans-isomer ratio increased as the polarity of the solvent decreased. This trend is illustrated in the values obtained at 25°C. At 25°C, the cis:trans-isomer ratio increased from 2.98:1 in SO_2 solvent (SO_2: μ = 1.60 D (217)) to 6.31:1 in $CFCl_3$ solvent ($CFCl_3$: μ = 0.45 D (217)). On the basis of structure alone, cis-$HOIOF_4$ is expected to be the more polar of the two isomers and would seemingly be favored over trans-$HOIOF_4$ as the solvent becomes increasingly polar. However, the electronegativity of trans-OIF_4O was determined to be greater than that of cis-OIF_4O (Chapter 4) and as such, the acidity of trans-$HOIOF_4$ is assumed to be greater than the acidity of cis-$HOIOF_4$. As a result, trans-$HOIOF_4$ is expected to be stabilized as the dielectric constant of the solvent increases (dielectric constants: $CFCl_3$ (29°C) = 2.28 (159); SO_2 (20°C) =

Table 3.3: Fluorine-19 NMR Data for $HOIOF_4$ Dissolved in Different Solvents at Different Temperatures

Solvent/ Temperature (°C)	$\delta^{19}F_A$ (ppm)^a (cis)	$\delta^{19}F_X$ (ppm)^a (cis)	$\delta^{19}F$ (ppm)^a (trans)	$^2J_{FF}$ (Hz)	Ratio cis:trans
C_7F_{14} (25°C)	85.54	64.39	66.70	213	4.0:1
$CFCl_3$ (25°C)	87.17	68.18	70.70	212	6.3:1
SO_2ClF (25°C)	89.33	69.01	71.54	189	3.5:1
SO_2 (25°C)	94.55	72.52	74.03	b	3.0:1
C_7F_{14} (-10°C)	82.38	63.69	66.17	212	4.5:1
$CFCl_3$ (-10°C)	86.65	67.69	69.81	211	b
SO_2ClF (-10°C)	87.90	67.90	70.64	212	3.8:1
$CFCl_3$ (-30°C)	86.27	67.85	69.52	214	[12:1]
SO_2ClF (-30°C)	89.20	70.47	71.63	214	≈ 4:1
$CFCl_3$ (-40°C)	86.56	67.84	69.39	215	[23:1]
SO_2ClF (-40°C)	89.55	68.21	69.41	214	4.2:1

Continued

Table 3.3: Continued

Solvent/ Temperature (°C)	$\delta^{19}F_A$ (ppm)[a] (cis)	$\delta^{19}F_X$ (ppm)[a] (cis)	$\delta^{19}F$ (ppm)[a] (trans)	$^2J_{FF}$ (Hz)	Ratio cis:trans
$CFCl_3$ (-60°C)	85.03	68.03	69.54	214	[50:1]
SO_2ClF (-60°C)	87.89	67.99	69.67	214	4.4:1
SO_2 (-76°C)	94.44	72.58	73.47	214	≈ 6:1
$CFCl_3$ (-90°C)	84.38	68.36	insol.	217	all cis
SO_2ClF (-90°C)	86.84	68.52	70.45	214	[25:1]

a: Recorded at 235.36 MHz and referenced with respect to external $CFCl_3$ at 24°C.

b: Not resolved.

[ ] Some precipitate present at this temperature.

14.1 (159)). The $^2J_{FF}$ coupling constant for cis-$HOIOF_4$ does not vary appreciably with temperature and only varies slightly with a change in solvent medium. The average $^2J_{FF}$ coupling constant for cis-$HOIOF_4$ measured in $CFCl_3$ solvent ranges from 212 Hz at 25°C to 217 Hz at -90°C. With optimum resolution of 6.1 Hz/data point (see Chapter 2), a 5 Hz change in coupling constant cannot be considered significant. The difference in $^2J_{FF}$ coupling constant for cis-$HOIOF_4$ is greatest at 25°C and when measurements made in $CFCl_3$ and SO_2ClF solvents are compared. The average $^2J_{FF}$ coupling constant ranges from 189 Hz in SO_2ClF solvent to 212 Hz in $CFCl_3$ solvent at 25°C. This effect seems to be linked to the increased coordinating ability of SO_2ClF over $CFCl_3$, which is manifested by a weakened $^{19}F_A$ - $^{19}F_X$ through space spin-spin interaction and a smaller $^2J_{FF}$ coupling constant. This solvent effect is expected to be more pronounced on going from SO_2 solvent to $CFCl_3$ solvent at 25°C, however, the exchange of cis-$HOIOF_4$ fluorine environments in SO_2 solvent at 25°C is rapid, and the coupling is not resolved. The exchange of fluorine environments in the cis-isomer could be attributed to strong coordination of the more strongly basic SO_2 molecule to give a seven-coordinate intermediate which would facilitate intramolecular exchange among fluorine environments.

The ^{19}F chemical shifts for cis- and trans-$HOIOF_4$ are found to vary with both temperature and solvent medium. In general, as the temperature is decreased, the difference in ^{19}F chemical shifts between equatorial and axial fluorines in cis-$HOIOF_4$ decreases. In $CFCl_3$ solvent for instance, the equatorial fluorines of cis-$HOIOF_4$ become increasingly shielded as the temperature is lowered, shifting from 87.17 ppm at 25°C to 84.38 ppm at -90°C while the resonance due to the axial fluorines remains approximately fixed (within ± 0.26 ppm). Similar trends are observed in SO_2ClF and C_7F_{14} solvents. Measurements made in the different solvents at the same temperature indicate that all fluorine environments in cis- and trans-$HOIOF_4$ become deshielded as the solvent polarity (solvent coordinating ability) increases (c.f. $\delta^{19}F_A$ (cis) at 25°C: $CFCl_3$ (87.17 ppm), SO_2ClF (89.33 ppm) and SO_2 (94.55 ppm)). In this case, the solvent apparently acts as a π-acid, accepting π-electron density from the fluorines resulting in deshielding of the ^{19}F resonance.

(iii) The Solution Structure of IO_2F_3: A ^{19}F NMR Study

The structure of IO_2F_3 in solution and in the solid, melt and gas phases, has been the subject of numerous publications (184,185,190-192,194,197). The first ^{19}F NMR study of IO_2F_3 as a melt was published by Engelbrecht and Peterfy (184,185) who concluded the melt consisted of a mixture of IO_2F_3 monomers with C_{2V} (structure 3.3) and C_S (structure 3.4) symmetries. This report quoted ^{19}F NMR chemical shift data for the respective IO_2F_3 isomers, however, the trace of the 56.4 MHz ^{19}F spectrum was not published. In 1974, Beattie and van Schalkwyk (194) published the 94.1 MHz ^{19}F NMR spectrum of an IO_2F_3 melt at 90°C

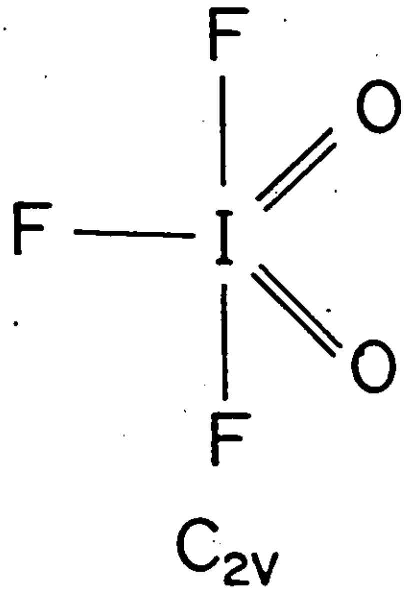

3.3

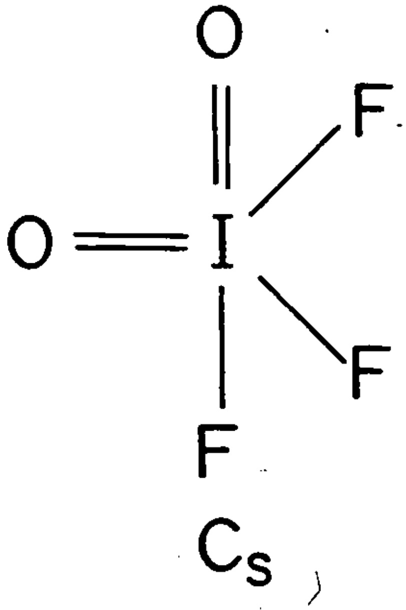

3.4

and of a solution of IO_2F_3 in perfluoromethylcyclohexane (C_7F_{14}) solvent at -50°C. More recently, Beattie et al. (191) published the results of molecular weight and vibrational studies on IO_2F_3 in the solid, melt and gas phases. Based on their observations, they concluded that IO_2F_3 consists of cis-oxygen bridged polymers in all phases, pure, and in C_7F_{14} solvent at -50°C. In 1975, Gillespie and Krasznai (192) published the results of their 94.1 MHz ^{19}F NMR and Raman spectroscopic investigations of the structure of IO_2F_3 as a melt at 51°C and as a solution in BrF_5 solvent at -45°C. Their ^{19}F NMR spectrum consisted of two AX_2 spectra with the A portions partially resolved and the X_2 portions completely overlapping. Their conclusions were different from those of Engelbrecht and Peterfy (184,185) and Beattie et al. (191,194). Gillespie and Krasznai (192) concluded the most probable structure of IO_2F_3 in BrF_5 solvent at -45°C is a cyclic trimer (structure 3.5) with the I_3O_3 ring in a boat conformation. In 1977, Smart (190) reported the structure of IO_2F_3 consisted of centrosymmetric oxygen bridged dimers (structure 3.6) based on a X-ray structure determination.

In view of the discrepencies found among three independent NMR studies (184,185,192,194), two vibrational studies (191,192) and a X-ray structure determination (190), a definitive high-resolution, high-field ^{19}F NMR investigation of the solution structure of IO_2F_3 was undertaken in this work. The use of high-field ^{19}F NMR (235.36 MHz) was expected to provide the field dispersion necessary to resolve the A and A' and X_2 and

X_2' portions of the spectrum. That is, ^{19}F NMR spectra recorded at 235.36 MHz provides a field dispersion equal to 2.5 and 4.3 times that of the same spectra recorded at 94.1 and 56.4 MHz, respectively, in the previous studies.

The 235.36 MHz ^{19}F NMR spectrum of IO_2F_3 in BrF_5 at -40°C is illustrated in Figure 3.5 and shows two well resolved first order spin systems labelled AX_2 and $A'X_2'$. The ^{19}F NMR chemical shifts and $^2J_{FF}$ coupling constants for spectra recorded on solutions of IO_2F_3 in various solvents are summarized in Table 3.4. The ^{19}F NMR spectrum depicted in Figure 3.5 can be interpreted under first order conditions since the R-factor (defined in equation 3.12) for the AX_2 and $A'X_2'$ spectra is 0.02 .

$$R = \frac{J}{V_o \ \delta_A - \delta_X} \qquad (3.12)$$

where

J = Coupling constant in Hz between the X and A fluorines.
V_o = Fluorine-19 resonance frequency (235.36 MHz).
δ_A, δ_X = Chemical shifts of the A and X fluorines referenced with respect to external $CFCl_3$ at 24°C.

The separation between the A ($\delta^{19}F$ = 67.2 ppm) and A' ($\delta^{19}F$ = 68.4 ppm) portions of the spectrum is 1.2 ppm (268 Hz) while the separation between the X_2 ($\delta^{19}F$ = 106.8 ppm) and X_2' ($\delta^{19}F$ = 106.5 ppm) portions of the spectrum is 0.3 ppm (74 Hz). This suggests that the fluorines responsible for the A and A' and

Figure 3.5

Fluorine-19 NMR Spectrum (235.36 MHz) of IO_2F_3 dissolved in BrF_5 Solvent Recorded at -40°C.

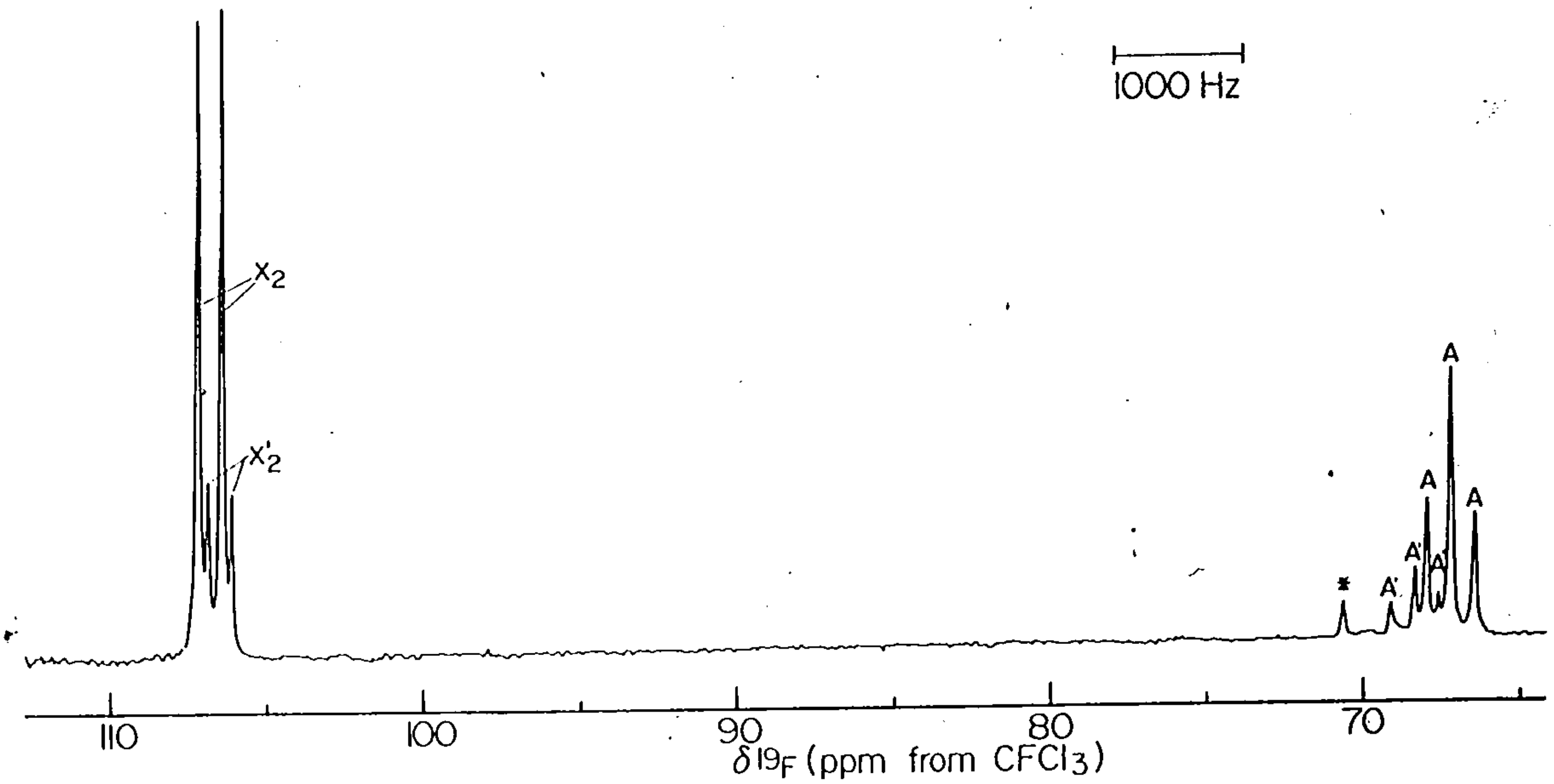
1000 Hz
X2
X'2
A
A
A
A'
A'
*
110
100
90
80
70
δ19F (ppm from CFCl3)

Table 3.4

Fluorine-19 NMR Parameters (235.36 MHz) for Solutions of IO_2F_3 in Different Solvents at Different Temperatures

Solvent and Temperature		$\delta^{19}F$ (ppm)^a	$^2J_{FF}$ (Hz)	R^b
BrF_5	X	106.8	179	0.02
(-40°C)	A	67.2	178	
	X'	106.5	180	0.02
	A'	68.4	183	
$CFCl_3$	X	108.6	174	0.02
(-10°C)	A	69.9	173	
	X'	108.2	178	0.02
	A'	69.4	178	
SO_2ClF	X	107.1	175	0.02
(-10°C)	A	67.9	173	
	X'	106.7	178	0.02
	A'	68.5	178	
C_7F_{14}	X	104.5	174	0.02
(-10°C)	A	64.6	173	
	X'	104.0	177	0.02
	A'	65.1	177	

a: Referenced with respect to neat $CFCl_3$ at 25°C.

b: Calculated from equation (3.12).

the X_2 and X_2' spectra are in very similar chemical environments. In addition, the similarity in average coupling constants for the AX_2 (178 Hz) and $A'X_2'$ (182 Hz) spectra also serves to reinforce this idea. The two AX_2 spectra in Figure 3.5 clearly represent two unique sets of two fluorines in one environment and one in another (ratio 2:1). The findings in this work are not consistent with a mixture of IO_2F_3 monomers (C_{2v}, structure 3.3 and C_s, structure 3.4) as suggested by Engelbrecht and Peterfy (184,185) or a cyclic trimer of IO_2F_3 (structure 3.5) as suggested by Gillespie and Krasznai (192). Instead, the results of this work suggest the structure of IO_2F_3 in solution is an equilibrium mixture of cis-oxygen bridged dimers (structure 3.7 and structure 3.8) whose ratio varies with temperature. The basis for these conclusions are discussed below.

Fluorine-19 NMR chemical shifts and $^2J_{FF}$ coupling constants have been measured for all iodine(VII) oxide fluoride acids (184-186,204,205,208), for all iodine(VII) oxide fluorides except IO_3F (185,189,191,192,194,197,204,205,208,213) and for the related $HOTeF_5$ molecule (218). The structure of the aforementioned oxide fluorides and oxide fluoride acids are based on octahedra with fluorines bonded trans to another fluorine, to a double-bonded oxygen or to a hydroxyl group. In all cases, except for IO_2F_3, a fluorine bonded trans to another fluorine has its chemical shift to low frequency of a fluorine bonded trans to a double-bonded oxygen and a fluorine bonded trans to a double-bonded oxygen occurs to low frequency of a fluorine bonded trans

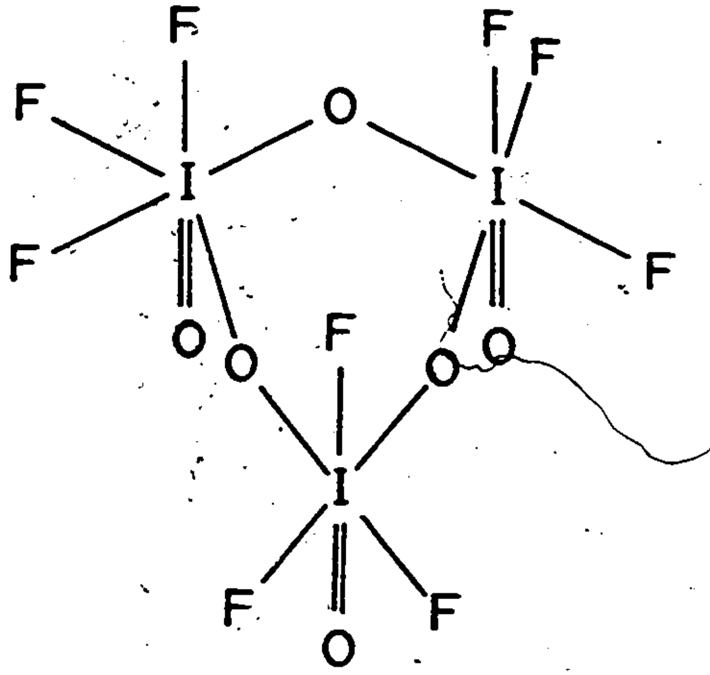

3.5

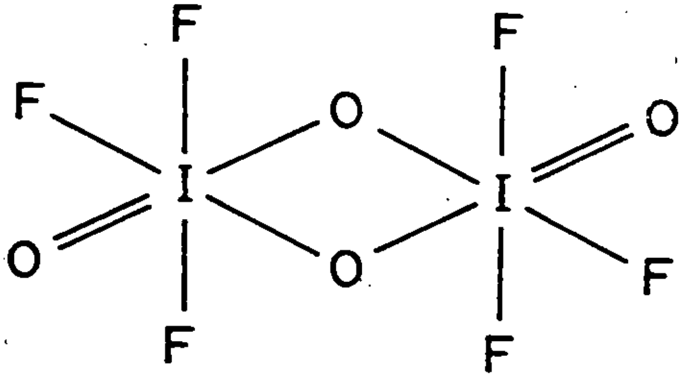

3.6

to a hydroxyl group. In light of this trend, the expected ^{19}F NMR spectrum for the IO_2F_3 monomers (C_{2v}, structure 3.3 and C_s, structure 3.4) would be two AX_2 spectra with the A portions (triplets) occuring to high frequency of the X_2 portions (doublets). This is clearly the reverse to the results found in this work and to the results obtained in three independent studies cited earlier. For this reason, the structure of IO_2F_3 in solution cannot be a simple equilibrium mixture of C_{2v} and C_s monomers.

A cyclic trimer of IO_2F_3 has nine geometric isomers and eighty-nine possible conformational isomers with the I_3O_3 ring in either a planar, boat or chair conformation (192). If IO_2F_3 existed as only one cyclic trimer isomer in solution such as structure 3.5, in the boat conformation, the ^{19}F NMR spectrum would consist of two AX_2 spectra in the ratio 2:1. Furthermore, the previously established shielding trends discussed above suggest the A and A' portions of the spectra should occur to low frequency of the X_2 and X_2' portions, respectively. In the spectrum published by Gillespie and Krasznai (192), the A portions of the two AX_2 spectra are to low frequency of the X_2 portions. In addition, they report that the ratio of the two A portions (triplets) in the spectrum was 2:1 and this ratio was independent of both temperature and solvent. This is in direct contrast to the results found in the present work. The intensity ratio of the AX_2 to $A'X_2'$ spectra measured by high-field ^{19}F NMR (235.36 MHz) in this work, was found to vary with both temperature and solvent medium. For example, the ratio of AX_2 to $A'X_2'$ spectra recorded in C_7F_{14}, $CFCl_3$ and SO_2ClF solvents at -10°C was 1:1.5 while the same ratio in BrF_5 solvent at -40°C was 4:1. On the basis of these results, the conclusions of Gillespie and Krasznai (192) must be viewed with considerable skepticism.

Structures 3.6 - 3.10 illustrate all possible cis-oxygen bridged dimers of IO_2F_3 resulting from positioning the two I=O bonds either in axial positions or in the equatorial plane and cis and trans with respect to either the I-O-I bridges or the I-I axis. Each of the isomer structures 3.6 - 3.9 is expected to display one unique AX_2 spectrum whereas the isomer corresponding to structure 3.10 is expected to display two unique AX_2 spectra. For structure 3.10, the doublet and triplet for one AX_2 spectrum should be in the ratio 2:1 while for the second, the ratio is expected to be 1:2. This is not the result found for the ^{19}F spectrum recorded in BrF_5 solvent at -40°C and thus structure 3.10 is excluded as a possibility. Structures 3.6 and 3.9 each have two different fluorine environments; one fluorine trans to a single-bonded oxygen and two fluorines trans to each other. On the basis of the ^{19}F shielding trends established previously for iodine(VII) oxide fluorides (189,204,205,213), the doublet representing the fluorines trans to one another is expected to occur to low frequency of the triplet corresponding to the fluorine trans to the single-bonded oxygen. This is opposite to the result depicted in Figure 3.5 where the doublets occur to high frequency of the triplets and, for this reason, structures

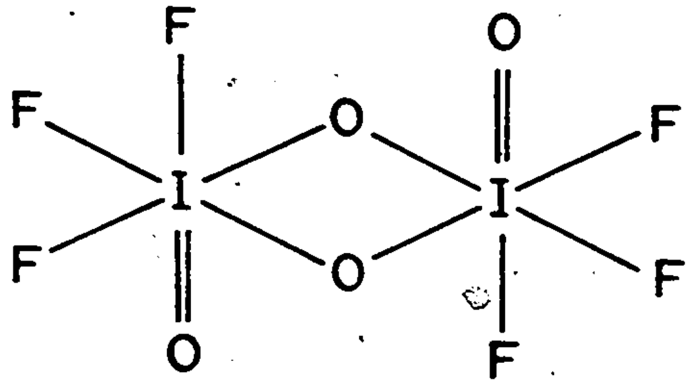

3.7

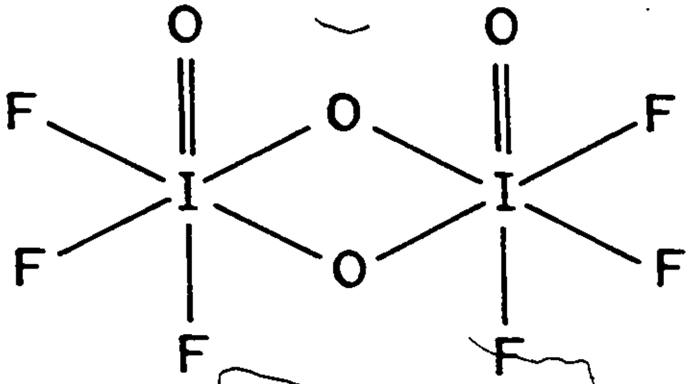

3.8

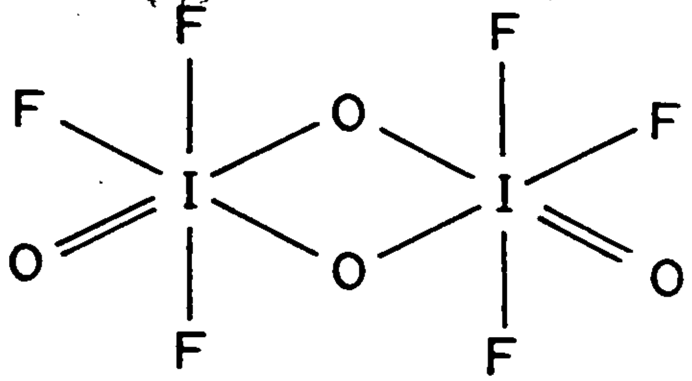

3.9

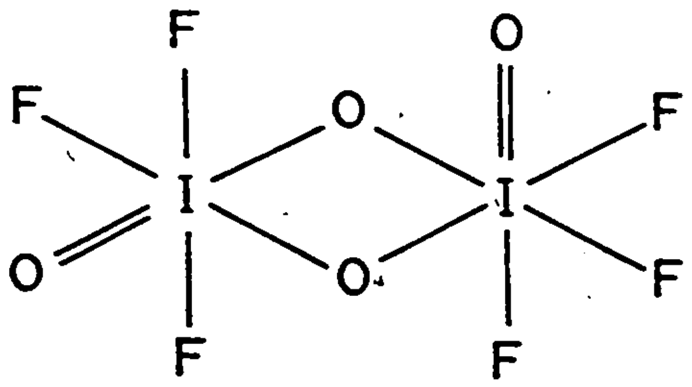

3.10

3.6 and 3.9 are eliminated as possible structures for the IO_2F_3 dimer in solution.

In structures 3.7 and 3.8, there are two different fluorine environments in the ratio 2:1. There are two fluorines in each of the first set of environments that are bonded trans to a single-bonded oxygen and one fluorine in each of the second set of environments bonded trans to a double-bonded oxygen. The ^{19}F NMR spectrum of each isomer is expected to be an AX_2 with the A portion occuring to low frequency of the X_2 portion. Furthermore, structures 3.7 and 3.8 are expected to yield two unique, yet very similar, AX_2 spectra. The structure of IO_2F_3 in BrF_5 solution at -40°C is therefore best represented as an equilibrium mixture of cis-oxygen bridged dimers (structures 3.7 and 3.8). It is difficult to assign the two AX_2 spectra to either structure 3.7 or 3.8 with any certainty. In a previous section of this chapter, the cis:trans-$HOIOF_4$ isomer ratio was found to vary as a function of temperature. As the temperature was decreased, the ratio of cis:trans-$HOIOF_4$ was enhanced suggesting the more polar of the two isomers (cis-$HOIOF_4$) is favored thermodynamically at low temperature. If the present assignment were to be made on this basis alone, structure 3.8 ($\mu > 0$) is assigned to the AX_2 spectrum which is favored at low temperature whereas structure 3.7 ($\mu \approx 0$) is assigned to the $A'X_2'$ spectrum since this is the one favored at higher temperatures (ratio AX_2:$A'X_2'$: -10°C (1:1.5), -40°C (4:1)).

(C) SUMMARY AND CONCLUSIONS

The conclusions established in this work regarding the structure of IO_2F_3 in solution are based on high-field (235.36 MHz) ^{19}F NMR results. These conclusions are definitive and are different from those of Engelbrecht and Peterfy (184,185) and Gillespie and Krasznai (192) for reasons given earlier. The results of the X-ray structure determination of IO_2F_3 by Smart (190) suggest the structure is a centrosymmetric oxygen bridged dimer (structure 3.6). The average bond lengths reported for the dimer do not vary appreciably ($I-F_{ax}$, 183.9 (0.2); $I-F_{eq}$, 179.5 (0.4); $I=O_{eq}$, 174.0 (0.4) pm) and discriminating between fluorines and double-bonded oxygens based on the structural data provided may be unjustified. The positions of the fluorines and double-bonded oxygens in this structure may in fact be populationally disordered, in which case the results of Smart's (190) structural determination would parallel the findings in this work.

The findings of Beattie et al. (191,194) suggest the structure of IO_2F_3 in the solid, melt and gas phases and in C_7F_{14} solvent at -50°C is based on cis-oxygen bridged polymers. In addition, the ratio of the apparent molecular weight of IO_2F_3 in the gas phase to that calculated for the monomer was found to range from 1.7 to 2.4. The findings of Beattie et al. (191,194), in the most part, corroborate the conclusions made here.

CHAPTER 4

THE PREPARATION OF $FXeOIOF_4$ AND $Xe(OIOF_4)_2$ AND THEIR CHARACTERIZATION BY NMR SPECTROSCOPY AND RAMAN SPECTROSCOPY

(A) INTRODUCTION

In addition to the simple binary fluoride XeF_2 (14-18), a number of ligands are known to form covalent derivatives. Included in this list of ligands are $-OSO_2F$ (133), $-OTeF_5$ (135,136), $-OPOF_2$ (143), $-OSeF_5$ (144), $-OClO_3$ (133,134), $-OCOCF_3$ (138), $-ONO_2$ (147), $-N(SO_2F)_2$ (150,151) and $-N(SO_2CF_3)_2$ (153). In general, all of these ligand groups satisfy the same set of criteria; i.e., all exist in the form of a moderate to strong monoprotic acid, all form positive chlorine derivatives and stable alkali metal salts and all have probable high group electronegativities.

The syntheses of covalently bonded xenon(II) derivatives can be accomplished in a variety of ways. The synthetic regimen which has proven most useful for xenon(II) derivatives involves the direct interaction of XeF_2 with the corresponding ligand group's monoprotic acid in a HF displacement according to equation (1.5). The latter approach can also be extended to include acid displacements from derivatives other than a fluoride, and has been employed for the first time in this work. In the case of the F_5TeO-derivatives, the ligand transfer reagent, $B(OTeF_5)_3$, provides the most convenient route to derivatization by reaction of XeF_2 with $B(OTeF_5)_3$ in a suitable solvent medium (equation 1.7) and elimination of BF_3 gas. A third route involves the insertion of an oxide fluoride ligand precursor into the Xe-F bond, i.e., the reaction of $P_2O_3F_4$ with XeF_2 to form the $O=PF_2O-$ derivatives $FXeOPF_2O$ (equation 1.3) and $Xe(OPF_2O)_2$ (equation 1.4).

Although the $-OIF_4O$ group has been little studied with respect to derivative formation, all of the aforementioned criteria (see Chapter 1) for stable xenon(II) derivatives have been met from among the limited list of previously known $-OIF_4O$ group derivatives, namely, $HOIOF_4$ (184-186), $K^+[IO_2F_4]^-$ (187), $Cs^+[IO_2F_4]^-$ (186,188), $FOIOF_4$ (186,189) and $ClOIOF_4$ (186). In the present work the formation of xenon(II) derivatives of the $-OIF_4O$ group has been investigated by several routes. Extensive use has been made of ^{129}Xe and ^{19}F NMR spectroscopy for characterization of these novel species in solution, as well as Raman spectroscopy, for characterization of the pure phases in the solid state. The results of these investigations are discussed in this Chapter.

(B) IDENTIFICATION OF XENON(II) DERIVATIVES OF $-OIF_4O$ IN SOLUTION: A ^{129}Xe AND ^{19}F NMR STUDY

(i) General

In this study, XeF_2/IO_2F_3 mixtures were investigated in SO_2ClF, $CFCl_3$ and BrF_5 solvents by ^{129}Xe and ^{19}F NMR spectroscopy. In all of the samples investigated, there was evidence of insoluble material as well as gas evolution as the reactions proceeded. For these reasons it was not possible to assess the results of these reactions in terms of equilibrium constants. Rather, the reactions are discussed in terms of initial XeF_2 : IO_2F_3 ratios and in terms of the resulting distribution of $-OIF_4O$ isomers as measured in solution by ^{129}Xe NMR spectroscopy.

(ii) • Structural Elucidation by Xenon-129 NMR Spectroscopy

The structures of xenon(II) derivatives in solution can be assessed through the use of ^{129}Xe NMR spectroscopy. The trends in ^{129}Xe chemical shifts and ^{129}Xe-^{19}F spin-spin coupling constants have already been well established with respect to the formal oxidation state of the central xenon nucleus, the relative ionicity of the xenon-ligand bonds and in terms of solvation and temperature effects (57,167). These trends as well as multiplicities in the ^{129}Xe NMR spectrum arising from one-bond and three-bond ^{129}Xe-^{19}F spin-spin couplings have been used in this work to show that IO_2F_3 inserts into the Xe-F bond to give pseudo-octahedral cis- and trans-OIF_4O oxygen-bonded derivatives of xenon(II) (structures 4.1 to 4.5) according to equations (4.1) and (4.2).

$$IO_2F_3 + XeF_2 \xrightleftharpoons[BrF_5 \text{ or } CFCl_3]{SO_2ClF} FXeOIOF_4 \qquad (4.1)$$

$$IO_2F_3 + FXeOIOF_4 \xrightleftharpoons[CFCl_3]{SO_2ClF \text{ or}} Xe(OIOF_4)_2 \qquad (4.2)$$

The basis for these conclusions are illustrated by the XeF_2/IO_2F_3 mixtures investigated in SO_2ClF solvent.

At low XeF_2 to IO_2F_3 ratios (1 : 0.877), the ^{129}Xe NMR spectrum recorded in SO_2ClF solvent at -5°C showed evidence for three doublet resonances at high frequency as well as four multiplet resonances at low frequency (Table 4.1). The three high-frequency doublets were assumed to have originated from three different species possessing terminal Xe-F bonds and were assigned to the trans- and cis-isomers of $FXeOIOF_4$ structures 4.1 and 4.2, respectively, and the fluorosulfate derivative $FXeOSO_2F$ (structure 4.6). The latter species, as well as the related mixed bis-isomers, namely, cis-$F_4OIOXeOSO_2F$ (structure 4.7) and trans-$F_4OIOXeOSO_2F$ (structure 4.8) presumably result from the reaction of $FXeOIOF_4$ with SO_2ClF solvent according to equations (4.3) and (4.4). (The chlorine products formed

$$SO_2ClF + FXeOIOF_4 \longrightarrow FXeOSO_2F + IOF_3 + [ClF] \qquad (4.3)$$

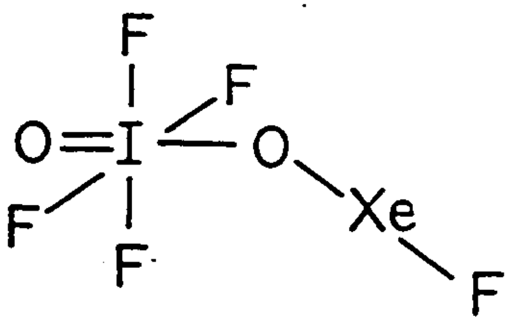

4.1

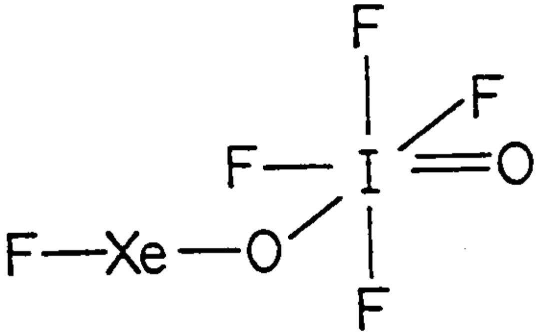

4.2

$$FXeOSO_2F \; + \; IO_2F_3 \; \rightleftharpoons \; F_4OIOXeOSO_2F \qquad (4.4)$$

products formed according to equation 4.3 have not been identified. The ClF included in equation 4.3 merely represents the amount of chlorine and fluorine needed for a charge balance and material balance of equation 4.3). The resonances assigned to cis- and trans-$FXeOIOF_4$ and $FXeOSO_2F$ were found to predominate at this low XeF_2 : IO_2F_3 ratio. The four multiplet resonances occuring at low frequency with respect to the high-frequency doublets, were much less intense and could not be assigned with any certainty at this ratio. In the absence of any apparent short-range spin-spin coupling, they were tentatively assigned to trans, trans-$Xe(OIOF_4)_2$ (structure 4.3), cis, trans-$Xe(OIOF_4)_2$ (structure 4.4), cis, cis-$Xe(OIOF_4)_2$ (structure 4.5) and cis-$F_4OIOXeOSO_2F$ (structure 4.7) pending verification at lower XeF_2 to IO_2F_3 ratios.

In an effort to enhance the intensity of the high-frequency resonances believed to represent the bis-isomers, a XeF_2 : IO_2F_3 mixture corresponding to the molar ratio 1 : 1.969 was prepared in SO_2ClF solvent. Again, resonances due to the cis- and trans-isomers of $FXeOIOF_4$ as well as $FXeOSO_2F$ were the most prominent species observed in the spectrum. The cummulative integrated ratio of the three isomers assigned to $Xe(OIOF_4)_2$, to that of the two isomers of $FXeOIOF_4$, was 1 : 76 at -5°C, and suggests equilibrium (4.2) lies far to the left in SO_2ClF solvent.

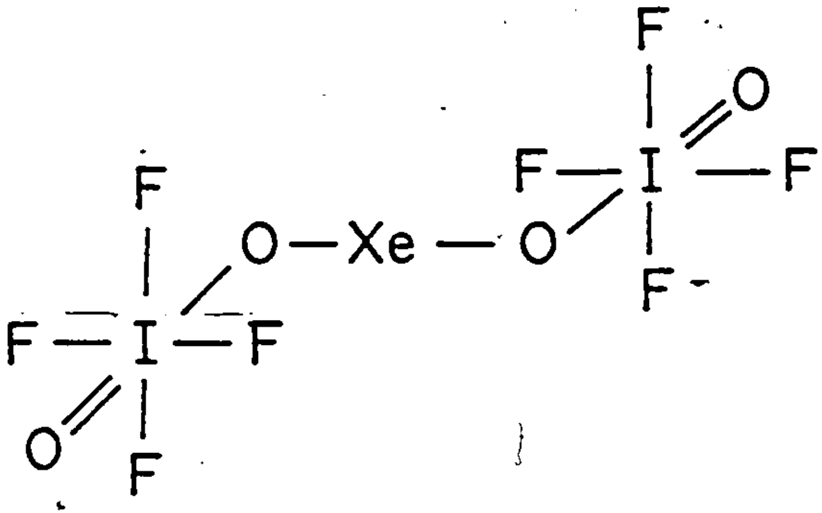

4.3

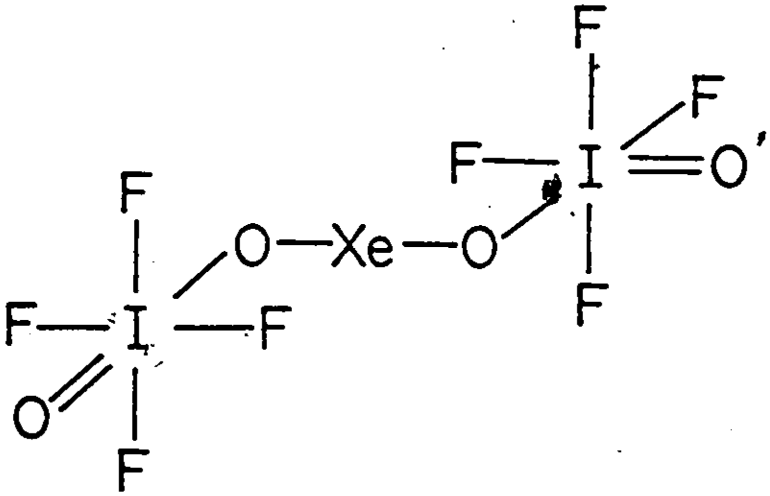

4.4

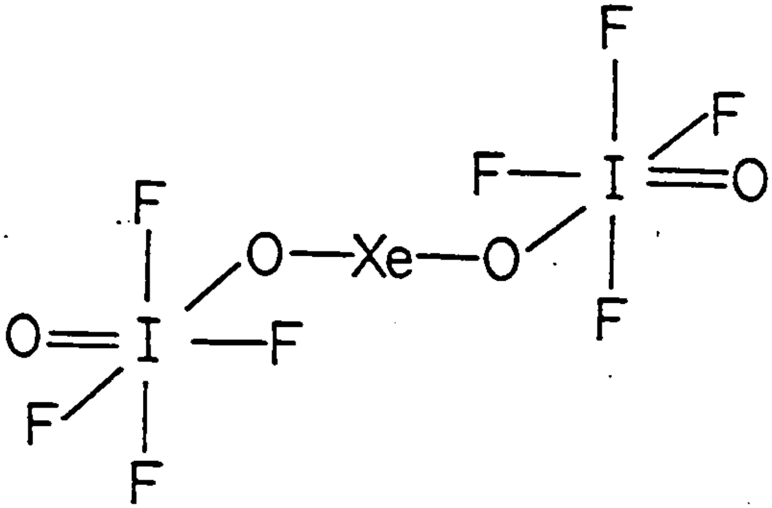

4.5

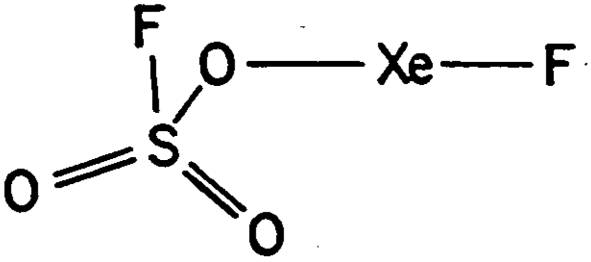

4.6

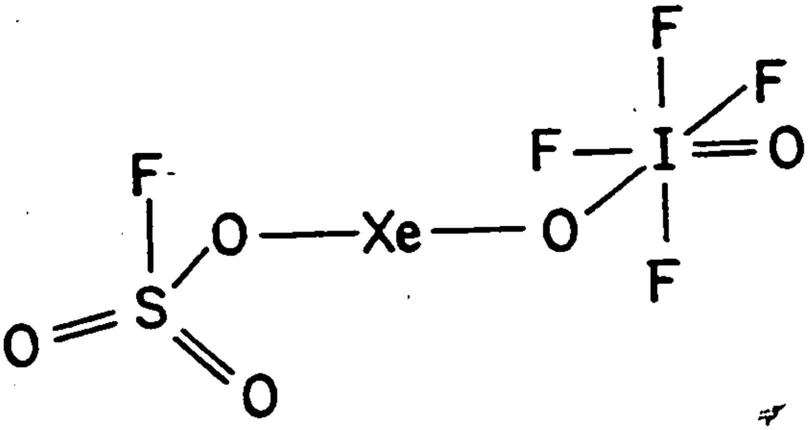

4.7

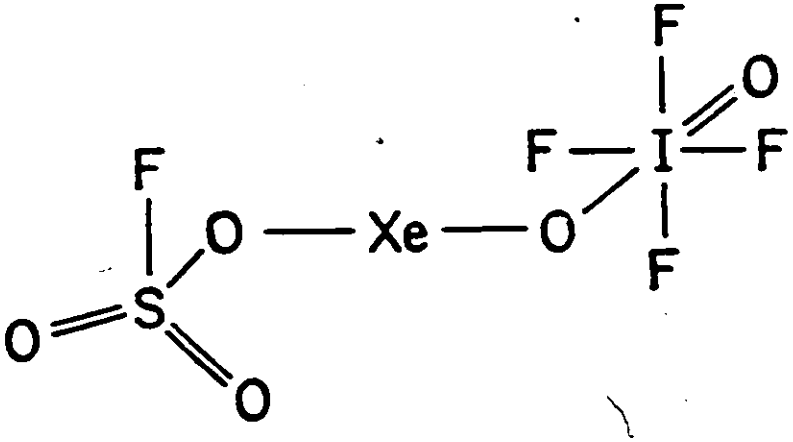

4.8

At high IO_2F_3 : XeF_2 ratios in SO_2ClF, useful NMR spectra of all $-OIF_4O$ species could be obtained. In fact, the $Xe(OIOF_4)_2$: $FXeOIOF_4$ ratio was increased even further where the initial XeF_2 : IO_2F_3 ratio was 1 : 3.530, and the cis, cis-, cis, trans- and trans, trans-isomers of $Xe(OIOF_4)_2$ were found to be in the relative ratio 1.00 : 7.62 : 9.46, respectively, and the ratio of trans- to cis-$FXeOIOF_4$ was found to be 1.66 : 1. In addition, resonances arising from cis- and trans-isomers of $F_4OIOXeOSO_2F$ are also evident. The ^{129}Xe NMR spectrum of a 1 : 3.53 XeF_2 to IO_2F_3 mixture recorded in SO_2ClF solvent at -5°C is depicted in Figure 4.1. The ^{129}Xe NMR chemical shifts as well as the $J(^{129}Xe-^{19}F)$ coupling constants are summarized in Table 4.1. Figure 4.1 clearly shows the three high-frequency doublets labelled (A), (B) and (C) as well as the five low-frequency multiplet resonances labelled (D) - (H).

The assignments for the doublet resonances are straight forward based on spin-multiplicity considerations and established ^{129}Xe chemical shift trends (57,167). The assignment of the high-frequency doublet (A) ($\delta^{129}Xe$ = -1724.1 ppm, $^{1}J(^{129}Xe-^{19}F)$ = 5867 Hz) to $FXeOSO_2F$ is based upon ^{129}Xe chemical shifts and $^{1}J(^{129}Xe-^{19}F)$ coupling constants reported previously (57) for this species. The doublet labelled (B) ($\delta^{129}Xe$ = -1741.9 ppm) is depicted on an expanded scale in Figure 4.2 which clearly shows the large doublet ($^{1}J(^{129}Xe-^{19}F)$ = 5923 Hz) indicative of a one-bond Xe-F coupling as well as

Table 4.1

Xenon-129 NMR Parameters for the IO_2F_3/XeF_2 System Recorded in SO_2ClF, BrF_5 and $CFCl_3$ Solvents

Solvent/ Temperature	Ratio $XeF_2:IO_2F_3$	$\delta^{129}Xe$ (ppm)[a]	$^1J(^{129}Xe-^{19}F)$ (Hz)	$^3J(^{129}Xe-^{19}F)$ (Hz)
trans-FXeOIOF4				
SO_2ClF (-5°C)	1:0.877	-1739.8	5907	42
SO_2ClF (-5°C)	1:1.969	-1741.8	5909	42
SO_2ClF (-5°C)	1:3.530	-1741.9	5923	42
$CFCl_3$ (24°C)	1:1.653	-1856.7	5876	43
$CFCl_3$ (24°C)	1:3.700	-1850.5	5883	b
BrF_5 (0°C)	1:1.996	-1720.5	5910	b
cis-$FXeOIOF_4$				
SO_2ClF (-5°C)	1:0.877	-1863.9	5865	b
SO_2ClF (-5°C)	1:1.969	-1868.5	5866	b
SO_2ClF (-5°C)	1:3.530	-1862.5	5879	b
$CFCl_3$ (24°C)	1:1.653	-1966.1	5848	b
$CFCl_3$ (24°C)	1:3.700	-1957.8	5850	b
BrF_5 (0°C)	1:1.996	-1823.5	5803	b
$FXeOSO_2F$				
SO_2ClF (-5°C)	1:0.877	-1725.1	5854	b
SO_2ClF (-5°C)	1:1.969	-1726.3	5856	b
SO_2ClF (-5°C)	1:3.350	-1724.1	5867	b

continued ...

Table 4.1 continued

Solvent/ Temperature	Ratio $XeF_2:IO_2F_3$	$\delta^{129}Xe$ (ppm)[a]	$^1J(^{129}Xe-^{19}F)$ (Hz)	$^3J(^{129}Xe-^{19}F)$ (Hz)
trans, trans-$Xe(OIOF_4)_2$				
SO_2ClF (-5°C)	1:0.877	-1856.4		
SO_2ClF (-5°C)	1:1.969	-1859.0		
SO_2ClF (-5°C)	1:3.350	-1866.8		38
$CFCl_3$ (24°C)	1:1.653	-1990.6		38
$CFCl_3$ (24°C)	1:3.700	-1998.6		b
cis, trans-$Xe(OIOF_4)_2$				
SO_2ClF (-5°C)	1:0.877	-1982.4		
SO_2ClF (-5°C)	1:1.969	-1985.3		
SO_2ClF (-5°C)	1:3.350	-1993.2		19
$CFCl_3$ (24°C)	1:1.653	-2116.3		
$CFCl_3$ (24°C)	1:3.700	-2123.6		
cis, cis-$Xe(OIOF_4)_2$				
SO2ClF (-5°C)	1:1.969	-2102.0		
SO_2ClF (-5°C)	1:3.350	-2109.6		
$CFCl_3$ (24°C)	1:1.653	-2231.0		
$CFCl_3$ (24°C)	1:3.700	-2240.4		
trans-$F_4OIOXeOSO_2F$				
SO_2ClF (-5°C)	1:3.350	-1834.2		
cis-$F_4OIOXeOSO_2F$				
SO_2ClF (-5°C)	1:0.877	-1951.0		
SO_2ClF (-5°C)	1:3.350	-1961.8		

a: Referenced with respect to neat external $XeOF_4$ at 24°C.

b: Coupling not resolved.

Figure 4.1

Xenon-129 NMR spectrum of a 1:3.530 molar mixture of XeF_2 and IO_2F_3 recorded in SO_2ClF solvent at -5°C. The peak assignments are below.

Peak	Assignment
A	$FXeOSO_2F$
B	trans-$FXeOIOF_4$
C	cis-$FXeOIOF_4$
D	trans-$F_4OIOXeOSO_2F$
E	trans, trans-$Xe(OIOF_4)_2$
F	cis-$F_4OIOXeOSO_2F$
G	cis, trans-$Xe(OIOF_4)_2$
H	cis, cis-$Xe(OIOF_4)_2$

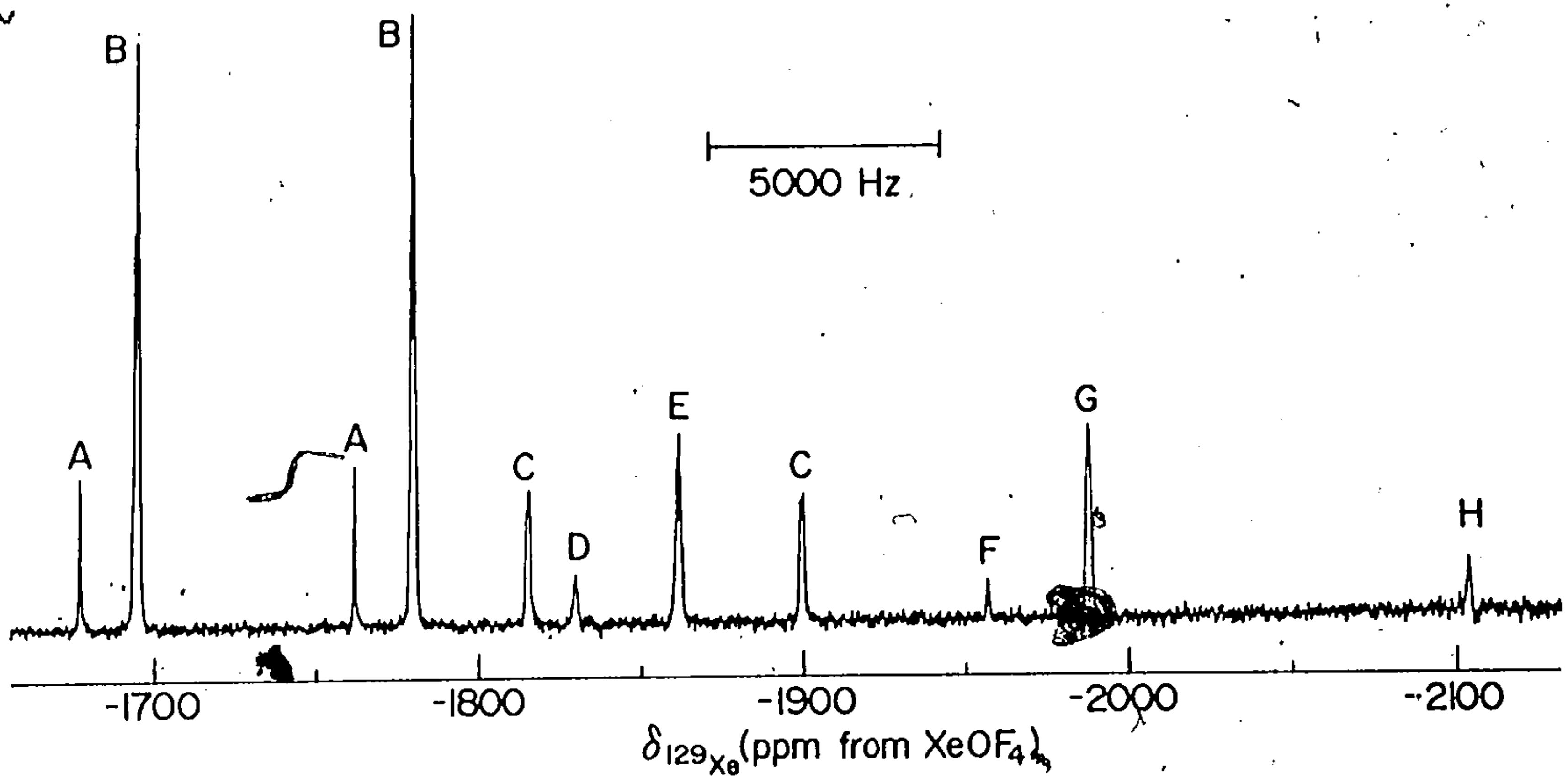
B
B
A
A
C
D
E
C
F
G
H
5000 Hz
-1700
-1800
-1900
-2000
-2100
$\delta_{^{129}Xe}$ (ppm from $XeOF_4$)

Figure 4.2

Xenon-129 NMR spectrum of a 1:3.530 XeF_2/IO_2F_3 mixture recorded in SO_2ClF solvent at -5°C showing the doublet of quintets ($\delta^{129}Xe$ = -1741.9 ppm) representing trans-$FXeOIOF_4$.

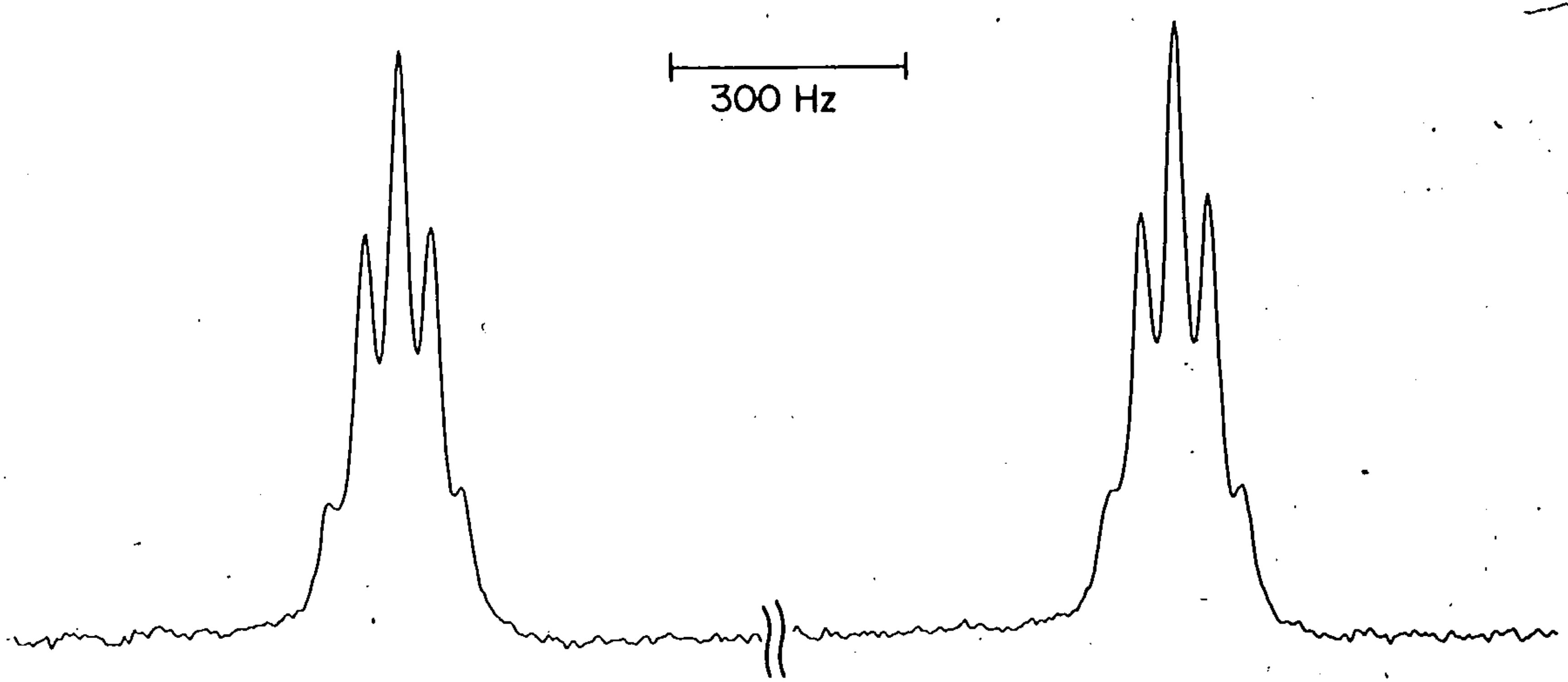
300 Hz

quintet fine structure (42 Hz) which results from the three-bond spin-spin coupling of four equivalent fluorines on the trans-OIF_4O group to the central xenon nucleus. The one-bond Xe-F coupling (5923 Hz) is similar in magnitude to other one-bond Xe-F couplings reported previously, i.e., $FXeOTeF_5$ (SO_2ClF, 26°C, 5743 Hz (127)), $FXeOSO_2F$ (HSO_3F, -84°C, 5975 Hz (57,167)), $FXeOSeF_5$ ($CFCl_3$, -40°C, 5790 Hz (144)) and $FXeN(SO_2F)_2$ (BrF_5, -58°C, 5586 (150)). The three-bond Xe-F coupling (42 Hz) is consistent with the analogous couplings reported for other pseudo-octahedral species, i.e., $FXeOTeF_5$ (34 Hz (127)) and $FXeOSeF_5$ (37 Hz (167). The remaining doublet of multiplets ($\delta^{129}Xe$ = -1862.5 ppm) labelled (C) in Figure 4.1 and illustrated on an expanded scale in Figure 4.3, is assigned to cis-$FXeOIOF_4$ by virtue of its one-bond Xe-F coupling (($^1J^{129}Xe-^{19}F$) = 5879 Hz) and the multiplet fine structure which is expected to arise from the three-bond spin-spin coupling of four fluorines in three magnetically non-equivalent environments to the central ^{129}Xe nucleus; a binomial doublet of doublets of triplets (AMX_2 pattern).

The multiplet resonances arising from the bis-isomers are assigned in the following manner: The resonance labelled (E) ($\delta^{129}Xe$ = -1866.8 ppm) in Figure 4.1 is depicted on an expanded scale in Figure 4.4. The expanded scale spectrum shows an odd-line multiplet with seven lines resolved ($^3J(^{129}Xe-^{19}F)$ = 38 Hz). The bis-isomer, trans, trans-$Xe(OIOF_4)_2$, is expected to display a binomial 1:8:28:56:

Figure 4.3

Xenon-129 NMR spectrum of a 1:3.530 XeF_2/IO_2F_3 mixture recorded in SO_2ClF solvent at -5°C showing the doublet of multiplets ($\delta^{129}Xe$ = -1862.5 ppm) representing cis-$FXeOIOF_4$.

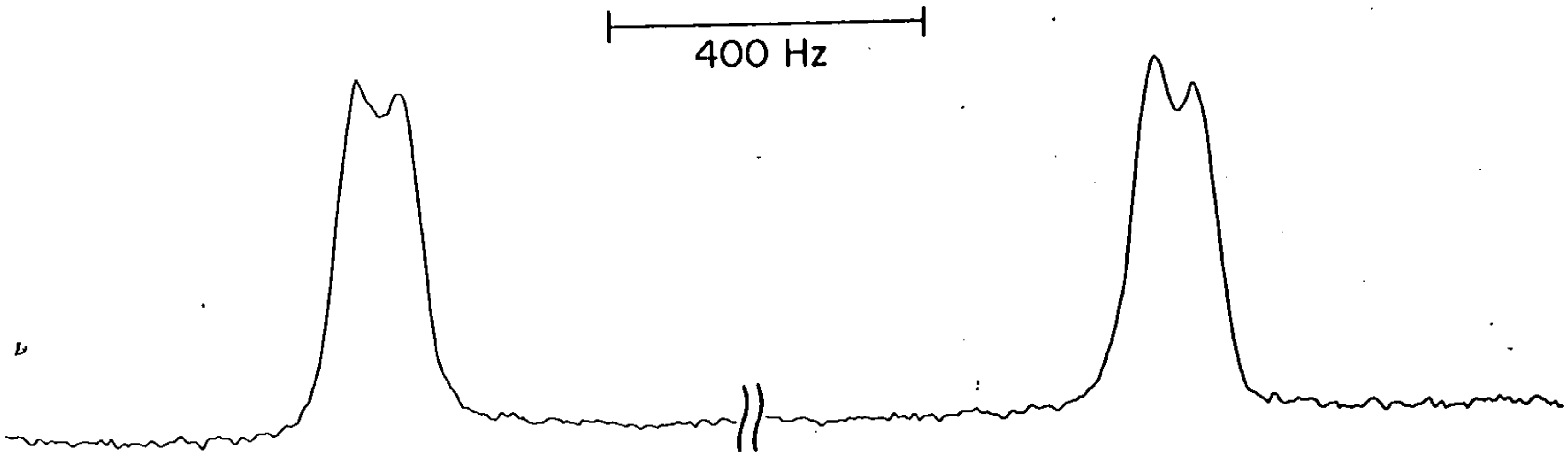
400 Hz

Figure 4.4

Xenon-129 NMR spectrum of a 1:3.530 XeF_2/IO_2F_3 mixture recorded in SO_2ClF solvent at -5°C showing the nonet ($\delta^{129}Xe$ = -1866.8 ppm) representing trans, trans-$Xe(OIOF_4)_2$.

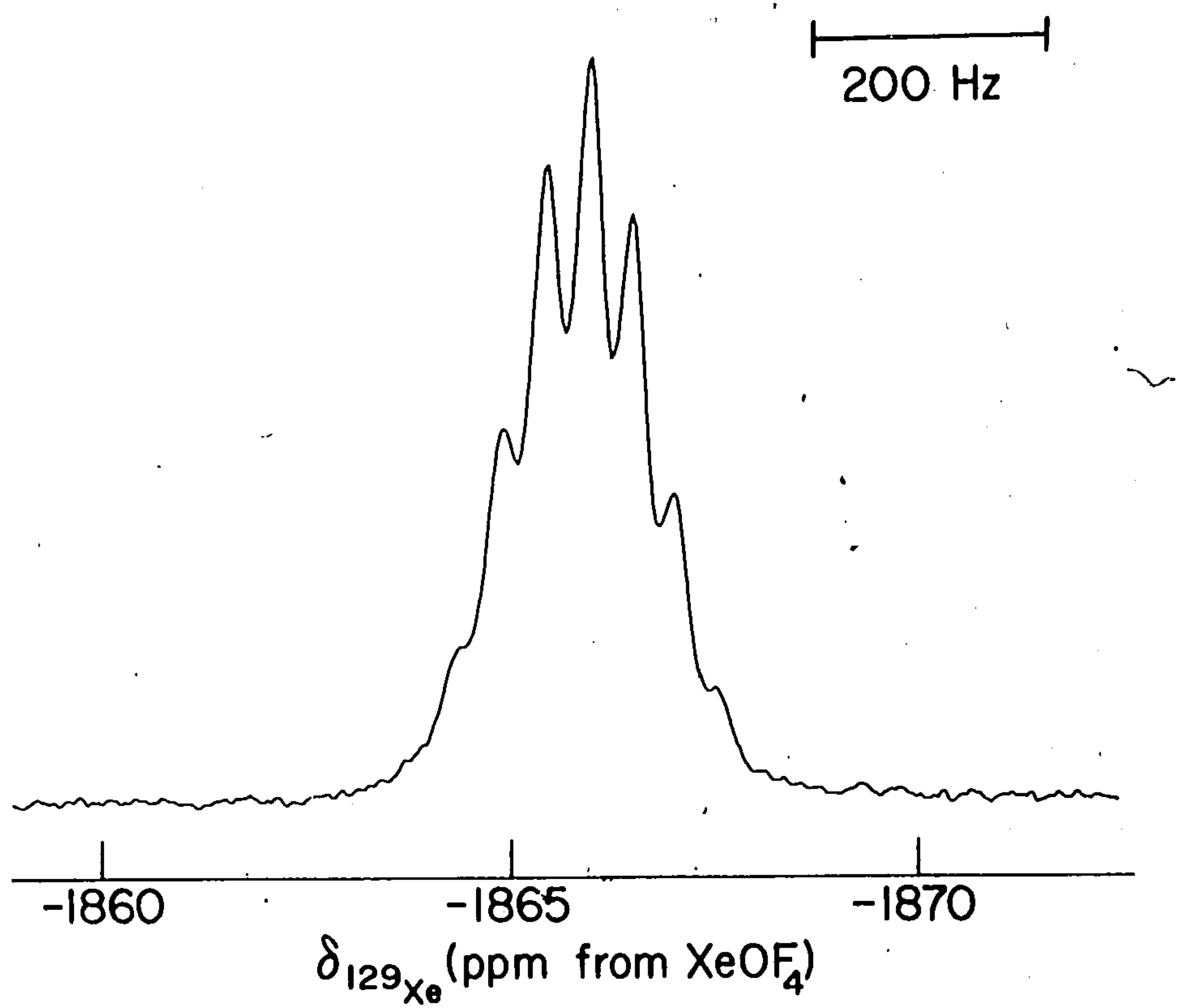
200 Hz
-1860
-1865
-1870
$\delta_{^{129}Xe}$ (ppm from $XeOF_4$)

70:56:28:8:1 nonet in its ^{129}Xe NMR spectrum resulting from the spin-spin coupling of eight equivalent fluorines on two $-OIF_4O$ groups bonded to the central xenon atom. The fact that only seven lines are resolved is a consequence of the low relative intensities of the two outermost lines of the nonet. The multiplet resonances in Figure 4.1 labelled (G) (δ^{129}Xe = -1993.2 ppm) and (H) (δ^{129}Xe = -2109.6 ppm) show partially resolved multiplet fine structure and were assigned to the bis-isomers cis, trans-$Xe(OIOF_4)_2$ and cis, cis-$Xe(OIOF_4)_2$, respectively. These assignments stem from the fact that a cis-OIF_4O group, having three non-equivalent fluorine environments, does not show a well resolved long range spin-spin coupling by analogy with a similar observation for cis-$FXeOIOF_4$. In addition, by comparison of the position of cis-$FXeOIOF_4$ to low frequency of trans-$FXeOIOF_4$, the bis-isomers containing one (G) or two (H) cis-OIF_4O groups, are expected to resonate to low frequency of trans, trans-$Xe(OIOF_4)_2$. A similar criteria was applied to the assignment of the multiplet resonances (D) (δ^{129}Xe = -1834.2 ppm) and (F) (δ^{129}Xe = -1961.8 ppm) to trans-$F_4OIOXeOSO_2F$ and cis-$F_4OIOXeOSO_2F$, respectively. Further evidence in support of the assignment of resonance (D) to trans-$F_4OIOXeOSO_2F$ comes from the resolved fine structure ($^3J(^{129}Xe-^{19}F)$ = 37 Hz) resulting from the three-bond spin-spin coupling of four equivalent fluorines on the trans-OIF_4O-group to the central ^{129}Xe nucleus and the absence of a three-bond coupling between the fluorine on sulfur and xenon. The later coupling can, however, be resolved under favorable circumstances in $FXeOSO_2F$ (vide infra). These assignments have been corroborated through the ^{129}Xe NMR studies on the pure derivatives to be discussed in a subsequent section.

(iii) Solvent Effects on the Cis:Trans Isomer Ratio

In order to test the solvent effect on the XeF_2/IO_2F_3 system and at the same time circumvent the problem of solvent reactivity, a 1 : 1.653 XeF_2 to IO_2F_3 mixture was prepared in $CFCl_3$ solvent. The ^{129}Xe chemical shifts and $^{129}Xe-^{19}F$ coupling constants are summarized in Table 4.1. The ^{129}Xe NMR spectrum recorded in $CFCl_3$ solvent at 24°C is depicted in Figure 4.5. In this spectrum there is no evidence for the fluorosulfate derivatives (structures 4.6 to 4.8), precluding the possibility that the IO_2F_3 used for the reactions carried out in SO_2ClF solvent was contaminated with HSO_3F in the course of its preparation (Chapter 2), which then would have reacted with XeF_2 (133,134) according to equation (4.5), also yielding $FXeOSO_2F$. The assignments for the cis- and trans-isomers of

$$XeF_2 + HSO_3F \rightleftharpoons FXeOSO_2F + HF \qquad (4.5)$$

$FXeOIOF_4$ and $Xe(OIOF_4)_2$, made in the SO_2ClF solvent system, are further supported in this spectrum. The doublet of quintets (B) and the unresolved AMX_2 pattern on each doublet line

Figure 4.5

Xenon-129 NMR spectrum of a 1:1.653 XeF_2/IO_2F_3 mixture recorded in $CFCl_3$ solvent at 24°C. The peak assignments are given below.

Peak	Assignment
B	trans-$FXeOIOF_4$
C	cis-$FXeOIOF_4$
E	trans, trans-$Xe(OIOF_4)_2$
G	cis, trans-$Xe(OIOF_4)_2$
H	cis, cis-$Xe(OIOF_4)_2$

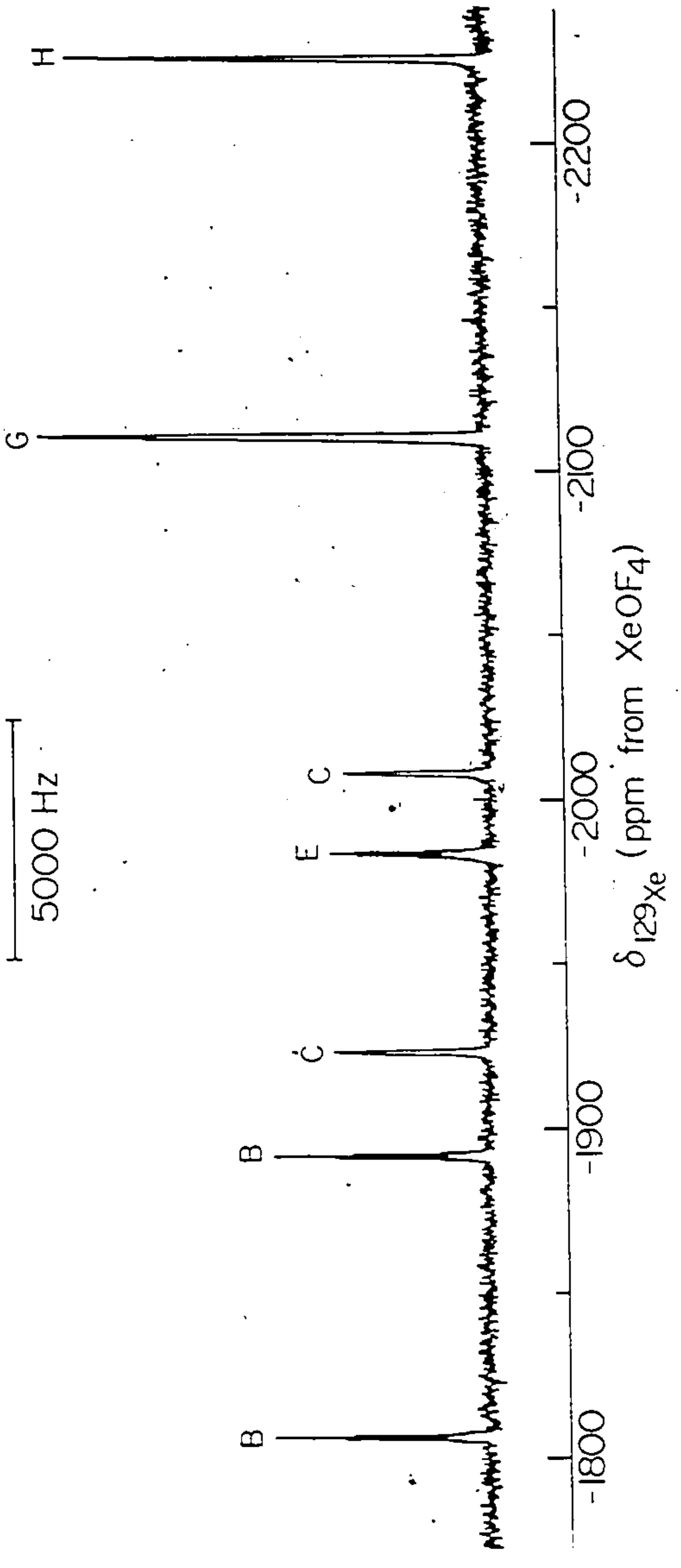
H
G
C
E
C
B
B
5000 Hz
-2200
-2100
-2000
-1900
-1800
$\delta_{^{129}Xe}$ (ppm from $XeOF_4$)

arising from the three-bond coupling to cis- and trans-fluorines on iodine(VII) (C), represent trans- and cis-$FXeOIOF_4$, respectively. The assignments for the multiplet resonances (E), (G) and (H) made previously, are again supported by the existence of resolved or unresolved three-bond xenon-fluorine spin-spin couplings and by the position of the cis-isomers to low frequency of trans-isomers. Figures 4.6 and 4.7 illustrate the multiplet resonances (G) and (H) on an expanded scale. Figure 4.6 clearly shows some resolved fine structure on the ^{129}Xe resonance of cis, trans-$Xe(OIOF_4)_2$, with at least eleven lines (19 Hz spacings) resulting from the overlapping three-bond spin-spin coupling of four equivalent fluorines on the trans-OIF_4O group and the four fluorines in three magnetically non-equivalent fluorine environments on the cis-OIF_4O group.

The relative ratio of $Xe(OIOF_4)_2$ to $FXeOIOF_4$ in this spectrum is significantly enhanced to 1 : 1.6 at 24°C and a XeF_2 to IO_2F_3 ratio of 1 : 1.969 compared to 1 : 76 in SO_2ClF solvent at -5°C. In addition, the cis-isomer of the -OIF_4O group is favored over that of the trans-isomer. This is reflected through the integrated ratios of the $Xe(OIOF_4)_2$ derivatives to give a trans, trans : cis, cis ratio of 1 : 2.7 and a trans : cis ratio of 1 : 1.3 for the $FXeOIOF_4$ derivatives.

The ^{129}Xe NMR spectrum of a 1 : 3.700 molar mixture of XeF_2 : IO_2F_3 recorded in $CFCl_3$ solvent at 21°C is illustrated

Figure 4.6

Xenon-129 NMR spectrum of a 1:1.653 XeF_2/IO_2F_3 mixture recorded in $CFCl_3$ solvent at 24°C showing the multiplet ($\delta^{129}Xe$ = -2116.3 ppm) representing cis, trans-$Xe(OIOF_4)_2$.

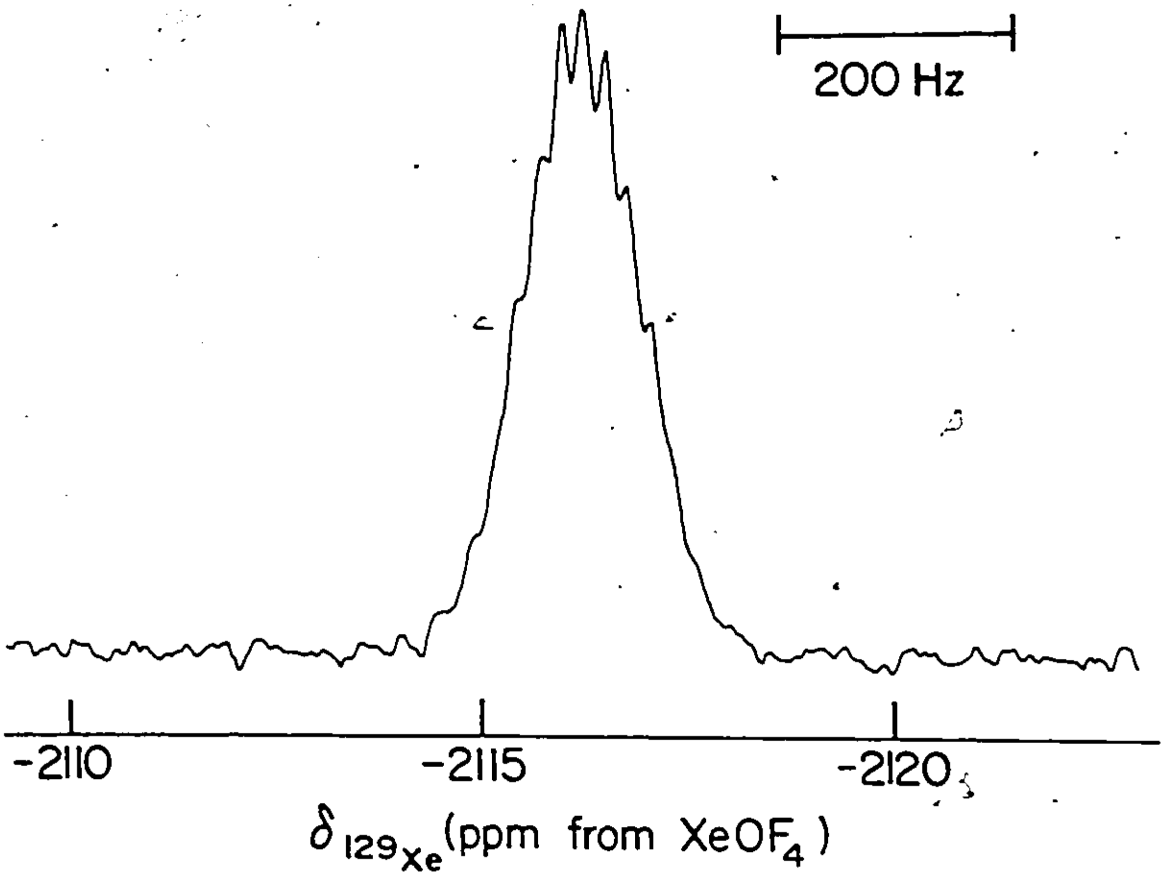
200 Hz
-2110
-2115
-2120
$\delta_{^{129}Xe}$ (ppm from $XeOF_4$)

Figure 4.7

Xenon-129 NMR spectrum of a 1:1.653 XeF_2/IO_2F_3 mixture recorded in $CFCl_3$ solvent at 24°C showing the multiplet ($\delta^{129}Xe$ = -2231.0 ppm) representing cis, cis-$Xe(OIOF_4)_2$.

6.

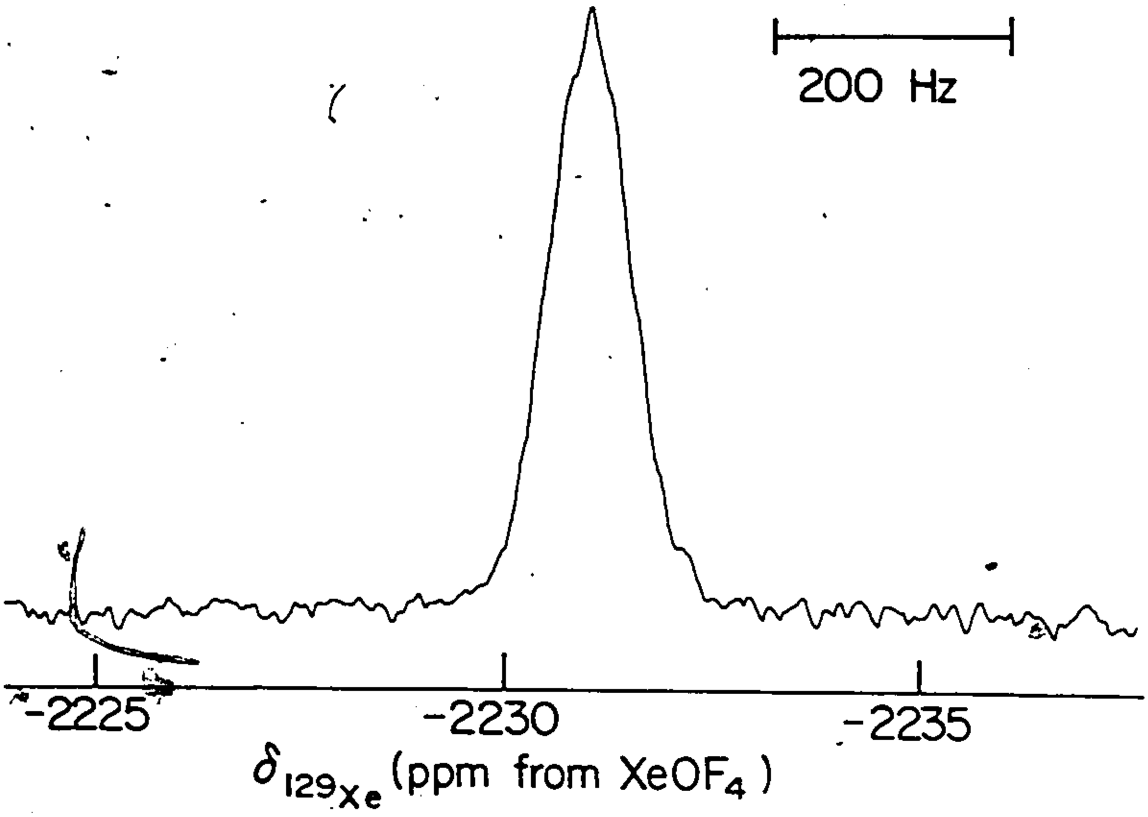

Figure 4.8

Xenon-129 NMR spectrum of a 1:3.700 XeF_2/IO_2F_3 mixture recorded in $CFCl_3$ solvent at 24°C. The peak assignments are given below.

Peak	Assignment
B	trans-$FXeOIOF_4$
C	cis-$FXeOIOF_4$
E	trans, trans-$Xe(OIOF_4)_2$
G	cis, trans-$Xe(OIOF_4)_2$
H	cis, cis-$Xe(OIOF_4)_2$

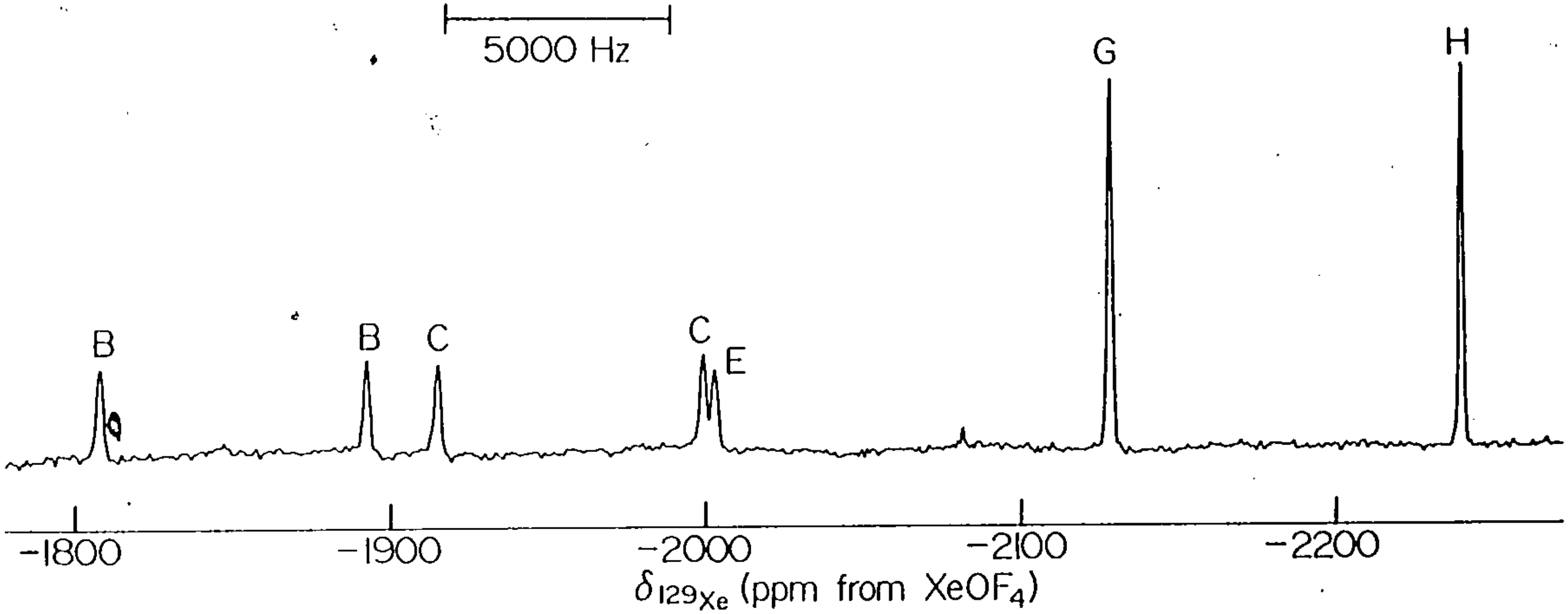
5000 Hz
B
B
C
C
E
G
H
-1800
-1900
-2000
-2100
-2200
$\delta_{^{129}Xe}$ (ppm from $XeOF_4$)

in Figure 4.8. This spectrum was recorded immediately following the combination of reactants and shows resonances representing cis, cis-, cis, trans-, and trans, trans-$Xe(OIOF_4)_2$ in the approximate ratio 5.09 : 4.85 : 1, respectively, and resonances due to cis- and trans-isomers of $FXeOIOF_4$ in the approximate ratio 1 : 1. The ratio of mono-isomers to bis-isomers was approximately 1 : 3. After approximately ½ hour at 24°C, the mixture had presumably attained equilibrium and displayed resonances representing the cis, cis- and cis, trans-isomers of $Xe(OIOF_4)_2$ in the ratio 10 : 1, respectively, and a small amount of cis-$FXeOIOF_4$ (< 5%). This suggests that the solvent polarity has a dual effect in these systems. With increasing solvent polarity, the ratio of mono-species is enhanced over that of bis-species and the trans-isomers of $-OIF_4O$ are favored over those of the cis-isomers of the $-OIF_4O$ group. This result parallels the work on the cis- and trans-isomer ratio dependences of $HOIOF_4$ discussed in Chapter 3 as well as the work of others cited therein.

To test the effect of further increasing the solvent polarity, a 1 : 1.996 molar mixture of XeF_2 : IO_2F_3 was prepared in BrF_5 solvent. The ^{129}Xe spectrum recorded at 0°C showed only cis- and trans-isomers of $FXeOIOF_4$ (Table 4.1) in the ratio 1 : 3.7, respectively, as well as XeF_2. Furthermore, the ratio of XeF_2 to cis- and trans-isomers of $FXeOIOF_4$ was 2.5 : 1. This result suggests that equilibrium (4.1) lies even further to the left in BrF_5 solvent than in SO_2ClF

solvent.

The ^{129}Xe NMR results for the XeF_2/IO_2F_3 system have demonstrated that the ratio of mono-species to bis-species and the ratio of cis- to trans-isomers of these species exhibit a marked dependence on the polarity of the solvent medium as well as the ratio of XeF_2 to IO_2F_3. In general, as the XeF_2 to IO_2F_3 ratio decreases, the formation of bis-isomers is favored over the formation of mono-isomers as expected. As the polarity of the solvent increases, i.e., from $CFCl_3$ to BrF_5, the formation of mono-species is favored over the formation of bis-species. In fact, in BrF_5 solvent the more polar cis- and trans-isomers of $FXeOIOF_4$ exist exclusively in equilibrium with XeF_2 with no evidence for the formation of bis-isomers. Moreover, the populations of the more polar cis-isomers in both the mono- and bis-derivatives are seen to likewise increase with solvent polarity. This result has been extrapolated to the more polar HF solvent system in which the successful preparation of $FXeOIOF_4$ was accomplished from the reaction of stoichiometric amounts of XeF_2 and IO_2F_3 in HF solvent.

The ^{129}Xe chemical shifts for the bis-isomers of the $-OIF_4O$ group are additive, progressing to lower frequency with increasing cis- substitution. For instance, a $XeF_2 : IO_2F_3$ mixture corresponding to a 1 : 3.53 molar ratio recorded in SO_2ClF at -5°C, yields ^{129}Xe chemical shifts of -1866.8 ppm for trans, trans-$Xe(OIOF_4)_2$, -1993.2 ppm for cis, trans-$Xe(OIOF_4)_2$ and -2109.6 ppm for cis, cis-$Xe(OIOF_4)_2$. Furthermore, substitution of one trans-ligand with one cis-ligand, i.e. on going from trans, trans- to cis, trans-Xe$(OIOF_4)_2$, results in a shift of the ^{129}Xe NMR resonance 126 ppm to lower frequency and with substitution of the second trans-ligand, the ^{129}Xe NMR resonance is shifted a further 117 ppm to lower frequency. This near additivity is found to be independent of solvent medium and of temperature. This sequence is consistent with a greater degree of deshielding of the xenon nucleus by the trans-ligand which implies that the trans-OIF_4O group is more electronegative than the cis-OIF_4O group. This is further supported by the ^{129}Xe resonance of trans-$FXeOIOF_4$ which occurs an average of 117 ppm to high frequency with respect to cis-$FXeOIOF_4$ in all solvents and at all temperatures investigated. A fuller discussion of group electronegativity trends is to be found in Section (C) of this Chapter.

Although ^{19}F NMR spectra were recorded on all of the XeF_2/IO_2F_3 mixtures investigated, these results will not be discussed here. The mixtures of $-OIF_4O$ derivatives resulted in complex ^{19}F spectra in the F-on-I(VII) region resulting from the partially overlapping resonances due to different cis- and trans-isomers of $FXeOIOF_4$ and $Xe(OIOF_4)_2$ as well as those of IO_2F_3. The resonances which could be identified are summarized in Table 4.2. However, a complete assignment of the ^{19}F NMR spectra for the $-OIF_4O$ derivatives has been made on samples of the pure isomers and is discussed in detail in Section C.

Table 4.2

Fluorine-19 NMR Results for the XeF_2/IO_2F_3 System

Species	Ratio $XeF_2:IO_2F_3$	$\delta^{19}F$(ppm)^a F-on-Xe	$\delta^{19}F$(ppm)^a F-on-I	Solvent	Temp (°C)
$FXeOIOF_4$	1:0.877	-168.4	71.6	SO_2ClF	
(trans-)	1:1.969	-168.0	71.9	SO_2CIF	-5
	1:1.653	-164.8	79.9	$CFCl_3$	24
	1:3.530	-168.9	72.0	SO_2Cl	-5
$FXeOIOF_4$	1:0.877	-158.4	b	SO_2ClF	-5
(cis-)	1:1.969	-158.2	b	SO_2ClF	-5
	1:1.653	-156.3	b	$CFCl_3$	24
	1:3.530	-159.4	b	SO_2ClF	-5
$Xe(OIOF_4)_2$	1:0.877	-	76.7	SO_2ClF	-5
(tr-/tr-)	1:1.969	-	77.1	SO_2ClF	-5
	1:1.653	-	-	$CFCl_3$	24
	1:3.530	-	76.9	SO_2ClF	-5
$Xe(OIOF_4)_2$	1:0.877	-	-	SO_2ClF	-5
(cis-/tr-)	1:1.969	-	76.4	SO_2ClF	-5
	1:1.653	-	79.2	$CFCl_3$	24
	1:3.530	-	76.1	SO_2ClF	-5
$Xe(OIOF_4)_2$	1:0.877	-	-	SO_2ClF	-5
(cis-cis-)	1:1.969	-	b	SO_2ClF	-5
	1:1.653	-	b	$CFCl_3$	24
	1:3.530	-	b	SO_2ClF	-5

a: Referenced with respect to external $CFCl_3$ at 24°C.

b: Overlapping or non-resolved resonances.

(C) THE PREPARATION, ISOLATION AND CHARACTERIZATION OF cis, cis-$Xe(OIOF_4)_2$ AND cis- AND trans-$FXeOIOF_4$

(i) General

The ^{129}Xe NMR investigations of the IO_2F_3/XeF_2 systems have demonstrated the existence of covalent xenon(II) derivatives of the $-OIF_4O$ group in solution. In an effort to more fully characterize these novel species as pure compounds in solution by ^{129}Xe and ^{19}F NMR spectroscopy and in the solid state by Raman spectroscopy, the isolation of these derivatives was attempted. The preparation, isolation and characterization of cis, cis-$Xe(OIOF_4)_2$ and a mixture of cis- and trans-$FXeOIOF_4$ are discussed in detail in this section.

(ii) Initial Attempts to Isolate $Xe(OIOF_4)_2$

Several attempts to isolate the solid derivative, $Xe(OIOF_4)_2$, from mixtures of XeF_2 and either IO_2F_3 or $HOIOF_4$ were unsuccessful. These attempts involved the stoichiometric reaction of either IO_2F_3 or $HOIOF_4$ with XeF_2 in $CFCl_3$ or SO_2ClF solvent. In each case, the reactants were combined at low temperature (-196°C) and then allowed to react for approximately 10 minutes at 0°C. During removal of the solvent at 0°C, a moist pale-yellow solid separated which detonated violently near dryness. Presumably, iodine(VII) is capable of oxidizing chlorine in both $CFCl_3$ and SO_2ClF generating one or more of the known thermally unstable chlorine oxide fluorides or oxides, i.e., ClO_2 (219). During removal of the solvent, these unstable species are apparently concentrated and detonate near dryness. An attempt to prepare $Xe(OIOF_4)_2$ by reacting excess $HOIOF_4$ with XeF_2 in $CFCl_3$ solvent did not result in a detonation, but rather, it yielded a non-volatile white powder as well as a clear volatile liquid identified as IF_5 by ^{19}F NMR spectroscopy ($\delta^{19}F$ = 58.9 ppm, $^{2}J(FF)$ = 81 Hz). Although a Raman spectrum was recorded, the identity of the white powder has not been confirmed. By comparison with the Raman spectra of IO_2F (220), IOF_3 (220), IO_2F_3 (208) and $IOF_3 \cdot IO_2F_3$, it was shown to be none of these species. A Raman spectrum recorded on the white powder at -196°C yielded three bands in the I=O stretching region at 821, 848 and 872 cm^{-1}, as well as two very intense bands in the F-on-I stretching region at 666 and 684 cm^{-1}. These findings suggest that up to three different species containing I=O bondsare present and that at least one of these species contains I-F bond(s). In addition, the bulk of the sample cannot be readily assigned to the expected decomposition products of $Xe(OIOF_4)_2$, i.e., IO_2F (ν_{sym} (I=O) = 807 cm^{-1} (220)), IOF_3 (ν_{sym} (I=O) = 883 cm^{-1} (220)) or solid IF_5 (ν_{sym} (I-F) = 568 cm^{-1} (221)). The same experiment was performed by Christe (222) who obtained a white powder which we identified as IO_2F.

Attempts to prepare $Xe(OIOF_4)_2$ by displacement of HF from XeF_2 in HF solvent have been unsuccessful. In this attempt, stoichiometric amounts (2:1) of $HOIOF_4$ and XeF_2 were allowed to react in HF solvent at 0°C. Removal of HF under vacuum at 0°C resulted in deposition of a viscous and colorless liquid, but no $Xe(OIOF_4)_2$ or $FXeOIOF_4$ could be detected. The liquid was identified as a mixture of $HOIOF_4$, IO_2F and IF_5 by recording the ^{19}F NMR spectrum in SO_2ClF solvent at -40°C.

(iii) The Preparation and Isolation of cis, cis-$Xe(OIOF_4)_2$

The successful preparation and isolation of solid cis, cis-$Xe(OIOF_4)_2$ has been accomplished by the low-temperature displacement of $HOTeF_5$ from $Xe(OTeF_5)_2$ with the stronger protonic acid $HOIOF_4$ according to equation (4.6). (Acid

$$Xe(OTeF_5)_2 + 2\ HOIOF_4 \xrightarrow[\text{or neat}]{\substack{0°C \\ CFCl_3}} Xe(OIOF_4)_2 + 2\ HOTeF_5 \quad (4.6)$$

strengths have been determined for a number of strong acids in acetic acid yielding pK values of 9.2 for $HOTeF_5$ and 5.8 for $HOIOF_4$ (223). In the same work, a pK value of 6.1 for HSO_3F was reported which implies the acid strength of $HOIOF_4$ is greater than that of HSO_3F. This latter result is somewhat surprising and contradicts the group electronegativity trends established in this work.) This acid displacement reaction proceeds smoothly at 0°C as a neat mixture of the two reactants or, alternatively, in $CFCl_3$ solvent. Preparations performed with neat reactants had yields typically over 90% whereas in $CFCl_3$ solvent, the yields were substantially lower owing to side reactions which presumably occur between $HOIOF_4$, $F_4OIOXeOTeF_5$, $Xe(OIOF_4)_2$ and $CFCl_3$ solvent. It is assumed the chlorines in chlorine containing solvents are rapidly attacked by these strong oxidant species at temperatures of 0°C or above. Preparations attempted in SO_2ClF or C_7F_{14} solvents yielded no $Xe(OIOF_4)_2$, but rather, a mixture of decomposition products (see Chapter 2). The identity of cis,-cis-$Xe(OIOF_4)_2$ was established by recording the low-temperature Raman spectrum of the solid and in solution in BrF_5, $CFCl_3$ or SO_2ClF solvents by ^{129}Xe and ^{19}F NMR spectroscopy. These results are discussed in subsequent sections of this Chapter.

The cis,-cis-isomer of $Xe(OIOF_4)_2$ is pale-yellow as a solid at room temperature, colorless as a solid at -196°C, has a negligible vapor pressure below its decompostion temperature of 0°C and decomposes instantly at room temperature under a static vacuum yielding Xe, O_2, IF_5 and IOF_3 according to equation (4.7). This decomposition, which is accompanied by

$$Xe(OIOF4)_2 \longrightarrow Xe \uparrow + 3/2\ O_2 \uparrow + IF_5 + IOF_3 \qquad (4.7)$$

the emission of white light, is thought to proceed by a free radical mechanism and formation of excited-state oxygen. This process is accelerated by the build up of radical initiator under a static vacuum. The compound can, however, be handled under dynamic vacuum near room temperature or under a pressure of dry nitrogen for extended periods of time below 0°C, and can be stored indefinately, without decomposition, in FEP vessels under 2 atm of dry nitrogen at dry-ice temperature. The decomposition routes of cis, cis-Xe(OIOF$_4$)$_2$ have been studied in more detail by ^{19}F NMR spectroscopy and by Raman spectroscopy and are discussed in detail in Chapter 5.

(iv) Characterization of cis, cis-Xe(OIOF$_4$)$_2$ in Solution by ^{129}Xe and ^{19}F NMR Spectroscopy

The structural characterization of cis, cis-Xe(OIOF$_4$)$_2$ in solution was accomplished by redissolving the compound in either BrF$_5$, CFCl$_3$ or SO$_2$ClF solvent and recording the low-temperature ^{129}Xe and ^{19}F NMR spectra. The quality of spectra were found to depend heavily on the choice of solvent medium and on the temperature at which the spectra were recorded. Although it was illustrated in a previous section of this Chapter that the cis-isomer of -OIF$_4$O was favored in solvents of low polarity, i.e., CFCl$_3$, the use of CFCl$_3$ solvent was avoided for a number of reasons. It was discovered during the course of this work that pure cis, cis-Xe(OIOF$_4$)$_2$ was of limited solubility in CFCl$_3$, except at temperatures greater than 0°C. Above 0°C, cis, cis-Xe(OIOF$_4$)$_2$ was found to be unstable with respect to decomposition in all solvents investigated, but especially in CFCl$_3$ due to solvent attack. The solubility of the pure compound was found to be high in BrF$_5$ and SO$_2$ClF solvents at temperatures as low as -40°C. The majority of NMR spectra were therefore recorded at -40°C in these solvents.

The ^{129}Xe NMR parameters for the $Xe(OIOF_4)_2$ isomers recorded in $CFCl_3$, SO_2ClF and BrF_5 solvents are summarized in Table 4.3. The ^{129}Xe NMR spectrum of cis, cis-$Xe(OIOF_4)_2$ redissolved in SO_2ClF solvent at -40°C is depicted in Figure 4.9. In this spectrum there is evidence for four xenon(II) derivatives, the most abundant species being cis, cis-$Xe(OIOF_4)_2$ ($\delta^{129}Xe$ = -2076.0 ppm), cis, trans-$Xe(OIOF_4)_2$ ($\delta^{129}Xe$ = -1929.8 ppm) and cis-$F_4OIOXeOSO_2F$ ($\delta^{129}Xe$ = -1961.7 ppm) in the ratio 6.3:1.9:1, respectively. A peak corresponding to trans, trans-$Xe(OIOF_4)_2$ ($\delta^{129}Xe$ = -1802.7 ppm) is also evident at very low intensity. Since pure cis, cis-$Xe(OIOF_4)_2$ was used to prepare all NMR samples investigated, the cis, trans- and trans, trans-isomers of $Xe(OIOF_4)_2$ must evolve from an isomerization of one or more cis-ligands on the xenon(II) derivative. The mixed derivative $F_4OIOXeOSO_2F$, must result from a series of reactions initiated by the decompostion of cis, cis-$Xe(OIOF_4)_2$ (Chapter 5). In all of the spectra recorded on pure cis, cis- $Xe(OIOF_4)_2$ redissolved in $CFCl_3$, SO_2ClF and BrF_5 solvents, there was evidence for isomerization of this isomer. The ratio of cis- to trans-isomers was found to vary with the solvent medium and with the temperature at which the spectra were recorded, but in any case, was consistent with the isomer ratio trends established in the IO_2F_3/XeF_2 systems discussed previously.

Table 4.3

Xenon-129 NMR Parameters for cis/trans-$FXeOIOF_4$ and $Xe(OIOF_4)_2$ Recorded at -40°C in SO_2ClF and BrF_5 Solvents

Solvent	$\delta^{129}Xe$(ppm)[a]	$^1J(^{129}Xe-^{19}F)$ (Hz)	$^3J(^{129}Xe-^{19}F)$ (Hz)
cis-$FXeOIOF_4$			
BrF_5	-1798.21	5814	41
SO_2ClF	-1824.44	5851	b
trans-$FXeOIOF_4$			
BrF_5	-1702.81	5868	37
SO_2ClF	-1701.50	5893	b
trans, trans-$Xe(OIOF_4)_2$			
BrF_5	-1871.40	-	b
SO_2ClF	-1802.68	-	b
cis, trans-$Xe(OIOF_4)_2$			
BrF_5	-1929.21	-	b
SO_2ClF	-1929.79	-	b
cis, cis-$Xe(OIOF_4)_2$			
BrF_5	-2059.46	-	b
SO_2ClF	-2076.03	-	b

a: Recorded at 69.56 MHz and referenced with respect to neat external $XeOF_4$ at 24°C.

b: Coupling not resolved.

Figure 4.9

Xenon-129 NMR spectrum recorded on cis, cis-$Xe(OIOF_4)_2$ dissolved in SO_2ClF solvent at -40°C. The peak assignments are given below.

Peak	Assignment
F	cis-$F_4OIOXeOSO_2F$
G	cis, trans-$Xe(OIOF_4)_2$
H	cis, cis-$Xe(OIOF_4)_2$

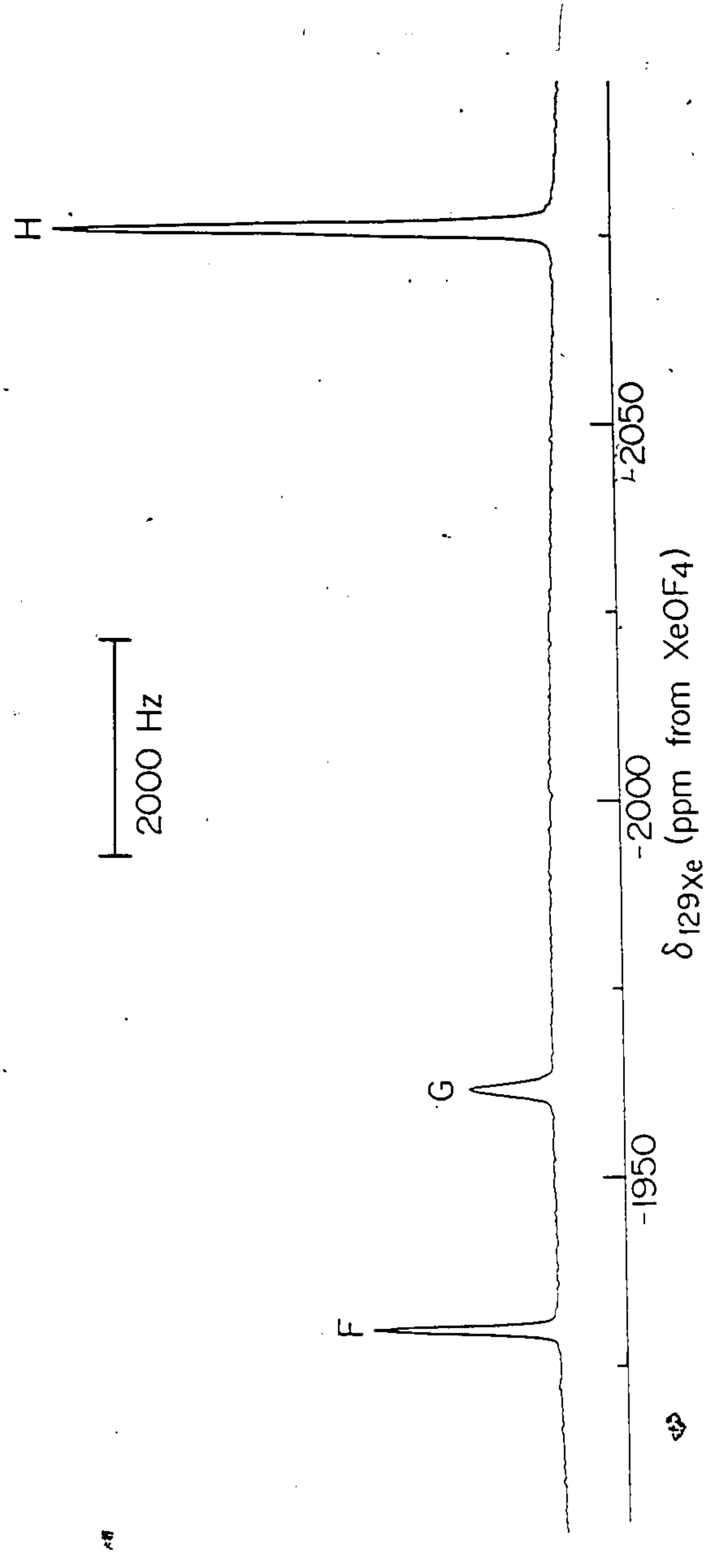
H
G
F
2000 Hz
-2050
-2000
-1950
$\delta_{^{129}Xe}$ (ppm from $XeOF_4$)

Fluorine-19 NMR spectra of samples of pure cis, cis-$Xe(OIOF_4)_2$ were recorded in the same solvent media and under the same temperature conditions as the ^{129}Xe spectra. In all cases, the ^{19}F NMR result was consistent with the conclusions derived from the ^{129}Xe study. The ^{19}F NMR results are summarized in Table 4.4 and in Figures 4.10 and 4.11 which show the ^{19}F NMR spectra of cis, cis-$Xe(OIOF_4)_2$ recorded at -40°C in SO_2ClF and BrF_5 solvents. Both spectra display a series of partially resolved multiplet resonances, which have been assigned by taking into account the ^{19}F shielding trends given in Chapter 3 and the spin-spin couplings among fluorines in three magnetically non-equivalent fluorine environments associated with a cis-OIF_4O group. Structure 4.9 depicts a pseudo-octahedral -OIF_4O group in the cis-configuration in which three magnetically non-equivalent fluorine environments are labelled F_1, F_2 and F_3. From the ^{19}F NMR shielding trends presented in Chapter 3, a fluorine trans- to another fluorine resonates at lower frequency than a fluorine trans- to a double-bonded oxygen and to even lower frequency than a fluorine trans- to a single-bonded oxygen. The ^{19}F NMR resonances of the environments labelled F_1, F_2 and F_3 are therefore expected to occur to high frequency in the order $F_1 < F_2 < F_3$. Furthermore, and under first order conditions, the multiplicity patterns for the three fluorine environments are expected to consist of a doublet of doublets, a doublet of triplets and a doublet of triplets in the ratio 2:1:1, for F_1,

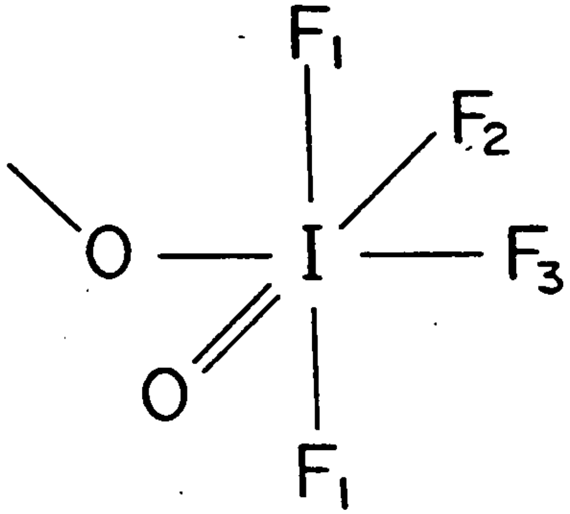

4.9

Table 4.4

Fluorine-19 NMR Parameters for a Mixture of cis- and trans-isomers of $FXeOIOF_4$ and cis, cis-$Xe(OIOF_4)_2$ Recorded at -40°C in SO_2ClF and BrF_5

Solvent	$\delta^{19}F$(ppm)^a		$^2J_{FF}$ (Hz)		$^1J(^{19}F-^{129}Xe)$ (Hz)
cis-$FXeOIOF_4$					
SO_2ClF	F	-158.5	$^4J_{FF}$	26	5852
SO_2ClF	F^1	103.3	(1,2)	284	-
SO_2ClF	F_2	86.6	(1,3)	240	-
SO_2ClF	F_3	70.3	(2,3)	191	-
BrF_5	F	-161.7		-	5816
BrF_5	F_1	101.5	(1,2)	280	-
BrF_5	F_2	85.8	(1,3)	234	-
BrF_5	F_3	70.4	(2,3)	193	-
trans-$FXeOIOF_4$					
SO_2ClF	F-on-Xe	-168.5		-	5893
SO_2ClF	F-on-I	71.3		-	-
BrF_5	F-on-Xe	-170.1		-	5877
BrF_5	F-on-I	75.1		-	-
cis, cis-$Xe(OIOF_4)_2$					
SO_2ClF	F_1	104.1	(1,2)	274	-
SO_2ClF	F_2	82.4	(1,3)	238	-
SO_2ClF	F_3	74.0	(2,3)	190	-
BrF_5	F_1	102.8	(1,2)	287	-
BrF_5	F_2	81.9	(1,3)	241	-
BrF_5	F_3	73.6	(2,3)	191	-

a: Recorded at 235.36 MHz and referenced with respect to external $CFCl_3$ at 24°C. Labels F_1, F_2 and F_3 correspond to the fluorine environments defined by structure 4.9.

Figure 4.10

Fluorine-19 NMR spectrum recorded on cis, cis-$Xe(OIOF_4)_2$ dissolved in SO_2ClF solvent at -40°C. The peak assignments are given below.

Peak	Assignment
C	cis, cis-$Xe(OIOF_4)_2$
D	cis, trans-$Xe(OIOF_4)_2$
F	trans, trans-$Xe(OIOF_4)_2$
G	cis, cis-$F_4OIOOIOF_4$
S	solvent

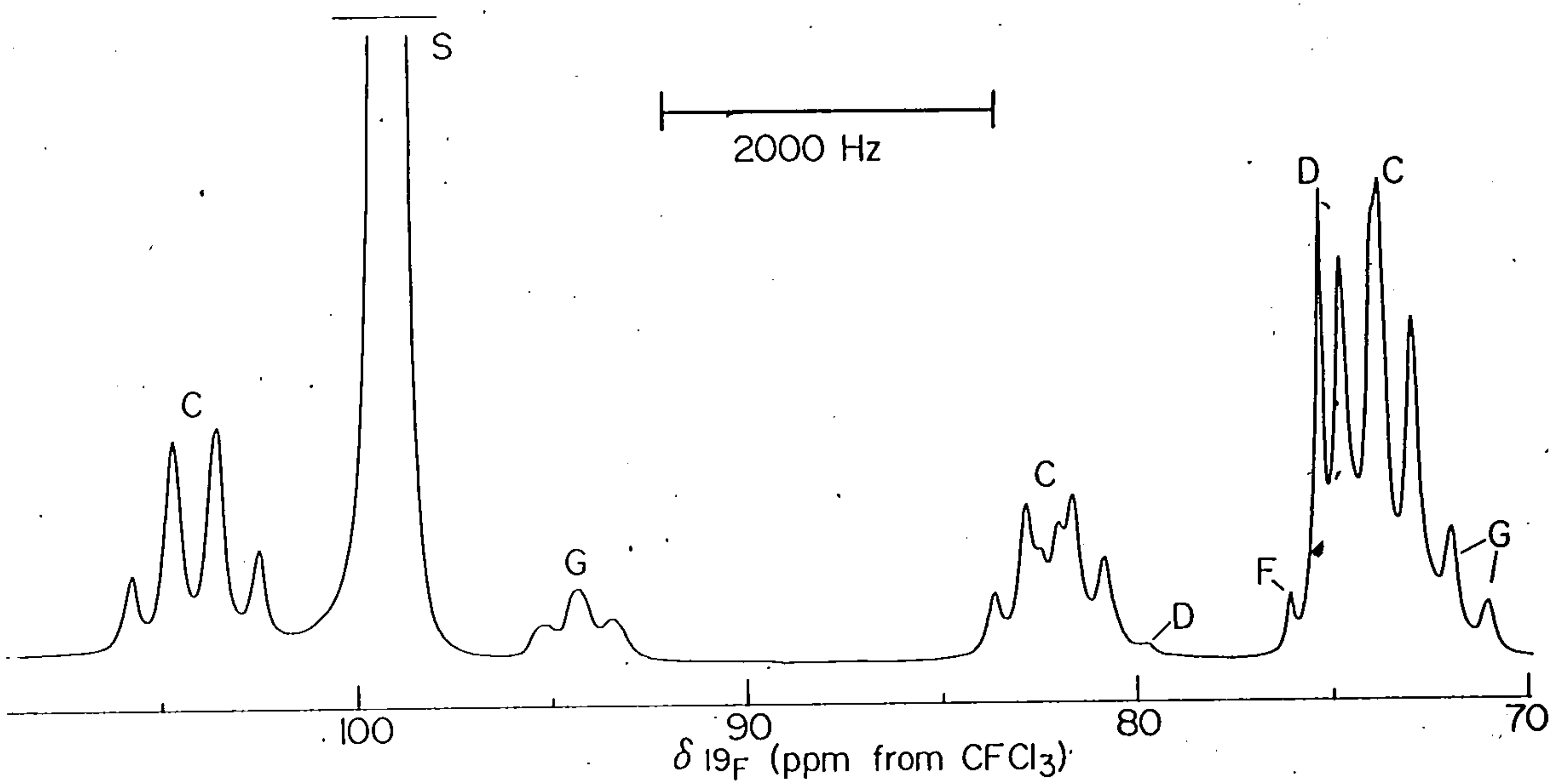
S
2000 Hz
C
G
C
D
D
C
F
G
100
90
80
70
δ ^{19}F (ppm from CFCl$_3$)

Figure 4.11

Fluorine-19 NMR spectrum recorded on cis, cis-$Xe(OIOF_4)_2$ dissolved in BrF_5 solvent at -40°C. The peak assignments are given below.

Peak	Assignment
A	cis-$FXeOIOF_4$
C	cis, cis-$Xe(OIOF_4)_2$
D	cis, trans-$Xe(OIOF_4)_2$
G	cis, cis-$F_4OIOOIOF_4$

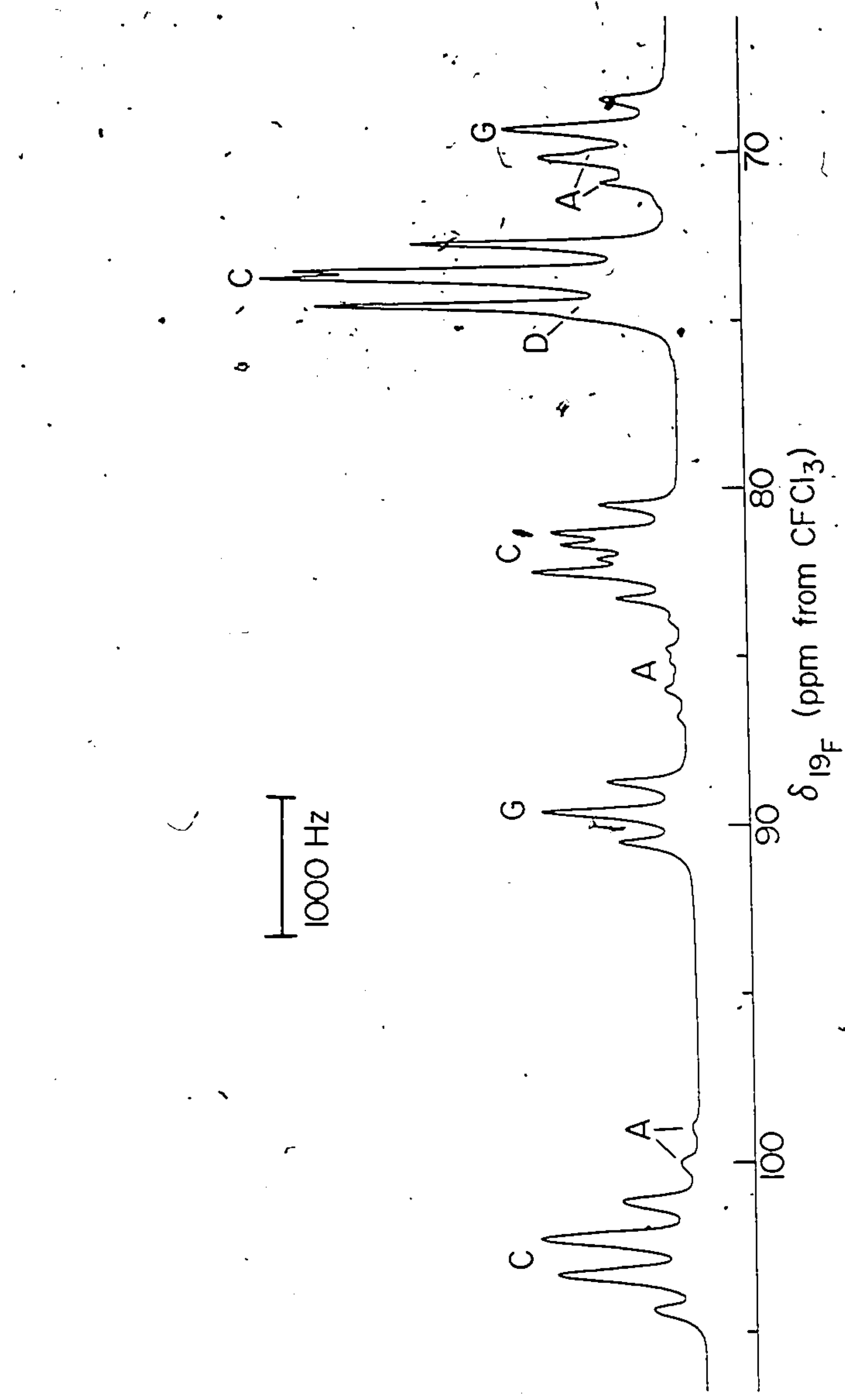C
A
G
C
A
C
D
A
G
1000 Hz
100
90
80
70
$\delta_{^{19}F}$ (ppm from $CFCl_3$)

F_2 and F_3, respectively. A trans-OIF_4O group has only one fluorine environment and is expected to yield a singlet resonance in the ^{19}F NMR spectrum.

The ^{19}F NMR spectrum recorded in SO_2ClF solvent and depicted in Figure 4.10 shows three partially resolved multiplets (C) in the ratio 1:1:2 which are assigned to the three fluorine environments associated with cis, cis-$Xe(OIOF_4)_2$, namely, F_1 ($\delta^{19}F$ = 104.1 ppm; $^2J_{FF}$ = 274 Hz) and F_2 ($\delta^{19}F$ = 82.4 ppm; $^2J_{FF}$ = 238 Hz) with each environment giving rise to a partially resolved doublet of triplets; and F_3 ($\delta^{19}F$ = 74.0 ppm; $^2J_{FF}$ = 190 Hz), a partially resolved doublet of doublets. In addition, two singlets of much lower intensity are evident which are assigned to the four equivalent fluorines of cis, trans-$Xe(OIOF_4)_2$ and the eight equivalent fluorines of trans, trans-$Xe(OIOF_4)_2$. Furthermore, a singlet representing SO_2ClF solvent (S) ($\delta^{19}F$ = 99.1 ppm) and an A_2X_2 pattern corresponding to the decomposition product, cis, cis-$F_4OIOOIF_4O$ (G) ($\delta^{19}F$ = 94.5, 72.2 ppm; $^2J_{FF}$ = 214 Hz) are also observed. The ^{19}F NMR chemical shifts reported here for cis, cis-$Xe(OIOF_4)_2$ fall within the range of all presently known F-on-I(VII) chemical shifts (170 to 65 ppm) (204,205,208,213). In addition, the $^2J_{FF}$ coupling constants are similar to those reported for other iodine(VII) oxide fluorides, i.e., IOF_5 = 280 (213), IO_2F_3 = 176 (185), cis-$[IO_2F_4]^-$ = 204 (186) and cis-$HOIOF_4$ = 214 Hz (205).

The ^{19}F NMR spectrum recorded in BrF_5 solvent is essentially the same, differing only in the ^{19}F chemical shifts and $^{2}J_{FF}$ coupling constants (Table 4.4) and the appearance of a small amount of cis-$FXeOIOF_4$ which presumably results from the dissociation of $Xe(OIOF_4)_2$ according to the reverse of equation (4.2). An AX_2 pattern arising from IO_2F_3, which is also formed in this dissociation, is observed at low-intensity and is partially obscured by the resonances assigned to the cis-OIF_4O groups. In BrF_5 solvent, the ^{19}F NMR chemical shifts for the three environments occur to lower frequency when recorded in the less polar solvent, SO_2ClF. This is consistent with the solvent-dependent shielding trends and solvent effects found for the fluorine environments of IO_2F_3 in Chapter 3. In both Figures 4.10 and 4.11, the magnitude of the two-bond coupling constants $^{2}J_{FF}$ decrease in the order $^{2}J(F_1-F_2) > ^{2}J(F_1-F_3) > ^{2}J(F_2-F_3)$. This implies that the strength of the fluorine-fluorine interaction decreases in the order $F_1-F_2 > F_1-F_3 > F_2-F_3$ which would be consistent with the anticipated bond lengths $I-F_1 < I-F_2 < I-F_3$.

(v) Characterization of cis, cis-$Xe(OIOF_4)_2$ in the Solid State by Low-Temperature Raman Spectroscopy

Pure cis, cis-$Xe(OIOF_4)_2$ has been characterized in the solid state by low temperature Raman spectroscopy. The Raman spectrum recorded on the solid at -196°C is depicted in Figure 4.12. Table 4.5 provides a summary of the vibrational frequencies with intensities and tentative assignments.

The cis- Xe-OIOF$_4$ fragment of symmetry C$_s$ should possess 18 fundamental modes classified as 12 A' + 6 A", all of which are Raman active. In addition, three modes associated with the O-Xe-O moiety, of which one mode is redundant with a mode in the Xe-OIOF$_4$ fragment, should yield a total of 20 Raman active bands. With complete intramolecular coupling, a total of 39 Raman active bands are expected. The spectrum depicted in Figure 4.12 shows 19 bands (100 - 900 cm^{-1}) which leads to the conclusion that there is no observable factor-group splitting or strong intra-molecular coupling. The high-frequency region (>400 cm^{-1}) of the spectrum can, in the most part, be assigned by comparison with the vibrational spectra for other iodine oxide fluorides, namely, FOIOF$_4$ (186), [IO$_2$F$_4$]$^-$ (186), IO$_2$F$_3$ (192) and IOF$_5$ (210,211). Although assignments are proposed for the low-frequency region (<400 cm^{-1}), these assignments are made without the benefit of assigned -OIF$_4$O derivative spectra from which comparisons could be made. Consequently, these assignments are deemed to be tentative in the absence of $^{16}O/^{18}O$ isotopic data.

The band at 889 cm^{-1} is assigned to the symmetric I=O of the cis-OIF$_4$O group by comparison with the frequencies of the corresponding modes in IOF$_5$ (927 cm^{-1}) (210,211), cis-FOIOF$_4$ (914 cm^{-1}) (186) and cis-[IO$_2$F$_4$]$^-$ (856 cm^{-1}) (186). The presence of only one band in the I=O stretching region supports a single -OIF$_4$O isomer and the fact that this band shows no splitting or broadening confirms the absence of

Table 4.5

Vibrational Frequencies and Tentative Assignments for the Raman Spectrum Recorded on Pure cis, cis-$Xe(OIOF_4)_2$

Frequency,[a] cm^{-1}	Tentative Assignment
889 (32)	ν I=O
745 (8)	
688 (56)	ν sym $(IF_2)_{ax}$
668 (38)	ν asym $(IF_2)_{eq}$
646 (18)	ν asym $(IF_2)_{ax}$
625 (1)	
614 (54)	ν sym $(IF_2)_{eq}$
579 (1)	
464 (100)	ν sym (Xe-O-I), ν sym (XeO_2)[b]
443 (3)	ν asym (Xe-O-I), ν asym (XeO_2)[b]
377 (3)	
368 (14)	δ (IO_2)
352 (15)	mixed F-I-O, F-I-F bends
339 (10)	
317 (4)	
272 (48)	
228 (2)	
216 (2)	
148 (78)	δ (O-Xe-O), δ (Xe-O-I)[b]
82 (35), 73 (3), 58 (6), 39 (28), 26 (46), 73 (3)	External Modes (lattice vibrations)

a: Raman spectrum recorded at -196°C in an FEP tube.

b: These modes are presumably strongly coupled.

Figure 4.12

Raman spectrum recorded on cis, cis-Xe(OIOF$_4$)$_2$ in an FEP tube at -196°C. * denotes an FEP band.

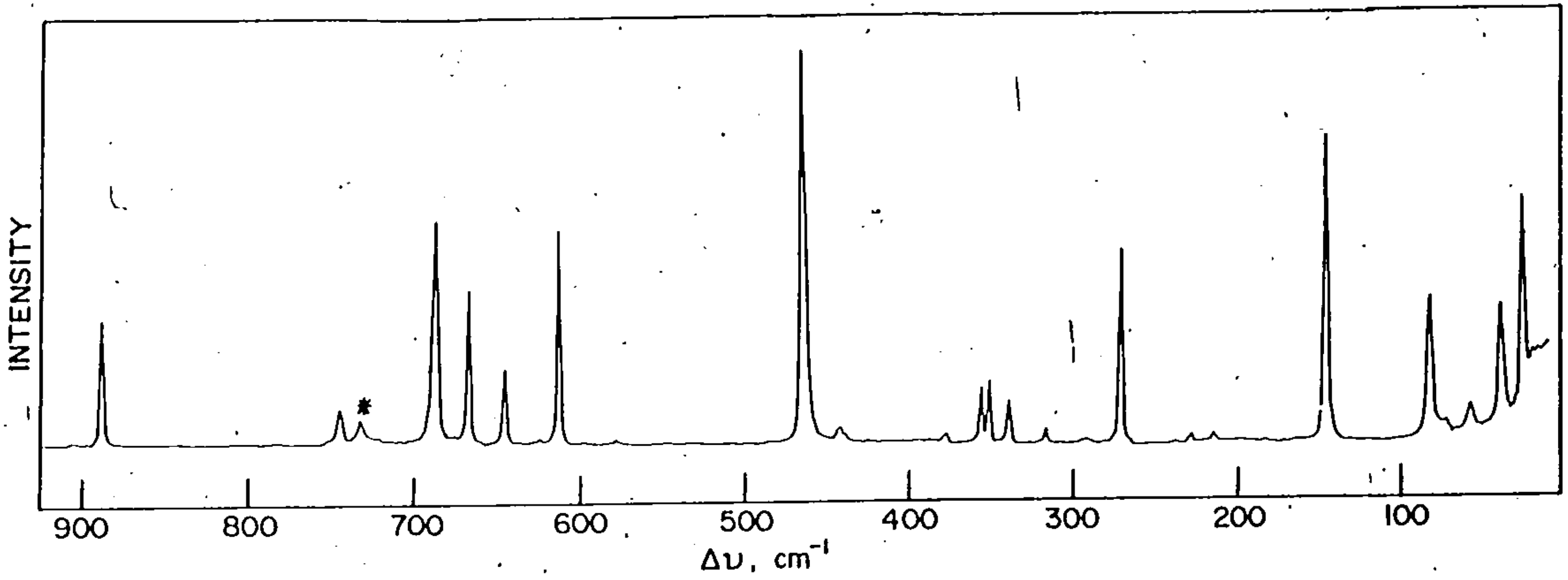
INTENSITY
*
900
800
700
600
500
400
300
200
100
Δυ, cm⁻¹

factor-group splitting or intramolecular coupling. The bands in the region of the spectrum between 614 and 688 cm^{-1} are assigned to I-F stretching modes by comparison with the same regions in the spectra of the iodine oxide fluorides cited earlier. The bands at 614 and 668 cm^{-1} are assigned to the symmetric and asymmetric I-F equatorial stretches, respectively, by analogy with the corresponding modes in IO_2F_3 (192) at 624 and 687 cm^{-1}. The bands at 688 and 646 are assigned to the symmetric and asymmetric I-F axial stretches, respectively, by considering the fact that in IOF_5 (210), IO_2F_3 (192) and cis-$FOIOF_4$ (186), the axial I-F stretches occur at higher frequency than their equatorial counterparts. The bands at 464 and 443 cm^{-1} are assigned to the strongly-coupled symmetric Xe-O-I/XeO_2 and asymmetric Xe-O-I/XeO_2 stretching modes, respectively, by comparison with the positions and intensities of the same modes in $Xe(OTeF_5)_2$, which occur at 440 and 428 cm-1, respectively (178). The band at 148 cm^{-1} is assigned to the O-Xe-O and strongly-coupled Xe-O-I bending modes, by analogy with the corresponding band in $Xe(OTeF_5)_2$ occuring at 133 cm^{-1} (137). The band at 368 cm^{-1} is assigned to the IO_2 bending mode by comparison with the frequency of the F_{ax}-I=O bending mode in IOF_5 at 341 cm^{-1} (210). The effective mass bonded to the -O-I=O moiety in cis- OIF_4O is greater than that of the F-I=O moiety in IOF_5 (i.e., the O-I=O moiety is bonded to $XeOIOF_4$), and as a result, the frequency of the IO_2 bend is expected to occur to low-frequency of the F-I=O bend. Further support for this assignment comes from the relative intensity of this band. The IO_2 bending motion in cis-OIF_4O is expected to induce a large change in polarizability resulting in an intense Raman vibration (272 (48) cm^{-1}). In addition, a similar band in the solid state Raman spectrum of $FOIOF_4$ (333 (40) cm^{-1}) (186), although not assigned, also supports our assignment. The bands in the spectrum between 317 and 377 cm^{-1} are collectively assigned to F-I-O and F-I-F bending modes. It is expected that considerable coupling would occur between these modes thus resulting in a number of bands in the same region of the spectrum. In comparison, the analogous modes in IOF_5 (210) also occur in this region of the spectrum. The low-frequency vibrations (<100 cm^{-1}) are assigned to external modes (lattice vibrations) and/or low-frequency bending or torsional modes.

(vi) Preparation and Isolation of $FXeOIOF_4$

The successful preparation of a homogeneous mixture of cis- and trans-$FXeOIOF_4$ has been accomplished by one of two routes. The mixture has been characterized by recording the ^{129}Xe and ^{19}F NMR spectra in SO_2ClF and BrF_5 solvents at -40°C, and as a solid at -196°C by Raman spectroscopy. These results are discussed in detail in a subsequent section.

The first method of preparation is a single-step synthesis involving the stoichiometric reaction of XeF_2 and IO_2F_3 in HF solvent according to equation (4.7).

$$XeF_2 + IO_2F_3 \xrightleftharpoons[HF]{0^\circ C} FXeOIOF_4 \qquad (4.7)$$

As the HF solvent was removed, a yellow liquid consisting of a mixture of cis- and trans-$FXeOIOF_4$ separated. This preparation differs from that of cis, cis-$Xe(OIOF_4)_2$ in a number of respects. The preparation of cis, cis-$Xe(OIOF_4)_2$ could only be accomplished by an acid displacement (equation 4.6) and only in solvents of low polarity in which the formation of cis, cis-$Xe(OIOF_4)_2$ is favored, i.e., $CFCl_3$. In HF solvent, the formation of $Xe(OIOF_4)_2$ was presumably prevented by the competitive acid displacement equilibrium (4.8) which lies far to the right and yielded a mixture of $FXeOIOF_4$ and $HOIOF_4$.

$$Xe(OIOF_4)_2 + HF \rightleftharpoons FXeOIOF_4 + HOIOF_4 \qquad (4.8)$$

In contrast, cis-/trans-$FXeOIOF_4$ can be formed readily and quantitatively in HF solvent (equation 4.7). Aside from the differences in the methods of preparation, the cis, cis-isomer of $Xe(OIOF_4)_2$ is the only instance in which a pure derivative can be isolated, whereas for $FXeOIOF_4$, a mixture of cis- and trans-isomers are always formed.

A second route has been used for the preparation of cis- and trans-$FXeOIOF_4$. This method involves the stoichiometric reaction of XeF_2 with cis, cis-$Xe(OIOF_4)_2$ according to equation (4.9). This method has the disadvantage

$$XeF_2 + Xe(OIOF_4)_2 \xrightarrow[SO_2ClF]{0°C} 2\ FXeOIOF_4 \qquad (4.9)$$

in that it requires the preparation of cis, cis-$Xe(OIOF_4)_2$ as a precursor and its subsequent weighing and manipulation near room temperature (see Chapter 2).

The compound, cis-/trans-$FXeOIOF_4$, is a light-yellow liquid at room temperature (m.p. -5 - 0°C) which dissociates into XeF_2 and IO_2F_3 under dynamic vacuum at 0°C (see Chapter 5) and in BrF_5 solution (vide infra). It is stable with respect to decompostion at room temperature for periods exceeding 1 hour and reacts explosively with organic material. It does not readily attack glass but, nevertheless, was routinely stored in FEP under an atmosphere of dry nitrogen at -78°C.

(vii) Characterization of $FXeOIOF_4$ by ^{129}Xe and ^{19}F NMR Spectroscopy

The ^{129}Xe NMR parameters for the mixture of cis- and trans-$FXeOIOF_4$ recorded in SO_2ClF and BrF_5 solvents at -40°C are summarized in Table 4.3. Figure 4.13 illustrates the ^{129}Xe NMR spectrum recorded on the mixture in SO_2ClF at -40°C. The most prominent features of this spectrum are the mono-derivatives $FXeOSO_2F$ (A), trans-$FXeOIOF_4$ (B) and cis-$FXeOIOF_4$ (C). The assignments of these species are based on the ^{129}Xe chemical shifts and ^{129}Xe-^{19}F coupling constants (Table 4.3) previously recorded for the IO_2F_3/XeF_2 system in SO_2ClF. The

Figure 4.13

Xenon-129 NMR spectrum recorded at -40°C on a cis/trans-$FXeOIOF_4$ mixture dissolved in SO_2ClF ~~solvent~~. The peak assignments are given below.

Peak	Assignment
A	$FXeOSO_2F$
B	trans-$FXeOIOF_4$
C	cis-$FXeOIOF_4$
E	trans, trans-$Xe(OIOF_4)_2$
F	cis-$F_4OIOXeOSO_2F$
G	cis, trans-$Xe(OIOF_4)_2$
H	cis, cis-$Xe(OIOF_4)_2$
I	XeF_2

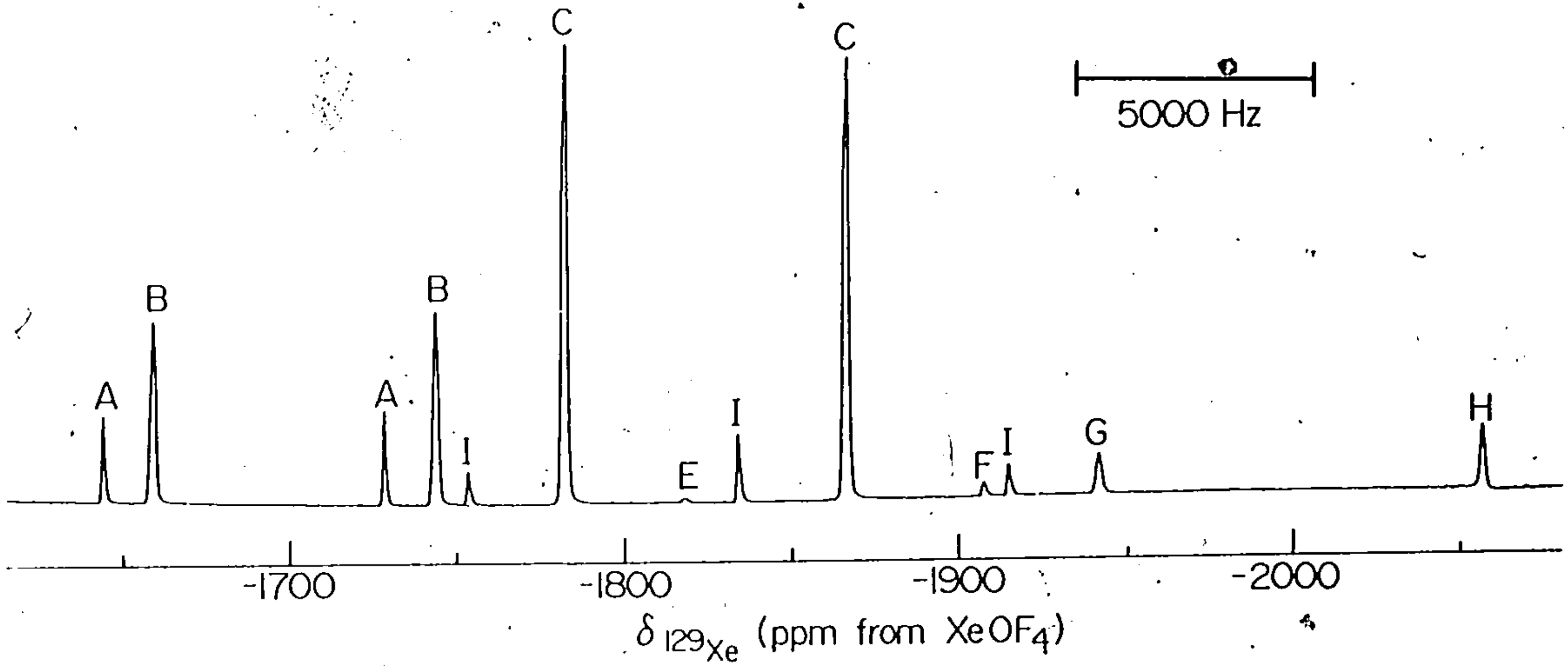
A
B
A
B
I
C
E
I
C
F
I
G
H
5000 Hz
-1700
-1800
-1900
-2000
$\delta_{^{129}Xe}$ (ppm from $XeOF_4$)

integrated ratios for the mono-derivatives were 1:2.3:5 for $FXeOSO_2F$, trans-$FXeOIOF_4$ and cis-$FXeOIOF_4$, respectively. As in the case of the IO_2F_3/XeF_2 system in SO_2ClF, the formation of $FXeOSO_2F$ arises from the reaction of $FXeOIOF_4$ with SO_2ClF, as previously noted, and as illustrated by equation (4.3). In addition to mono-derivatives, there is evidence for XeF_2 (I) and the bis-derivatives trans, trans-$Xe(OIOF_4)_2$ (E), cis-$F_4OIOXeOSO_2F$ (F), cis, trans-$Xe(OIOF_4)_2$ (G) and cis, cis-$Xe(OIOF_4)_2$ (H) (see Figure 4.13). The 1:2:1 triplet labelled I ($\delta^{129}Xe$ = -1834.29, $^1J(^{129}Xe-^{19}F$ = 5613 Hz) was assigned to XeF_2 by comparison with the previously reported chemical shift and one-bond xenon-fluorine coupling constant of this species in SO_2ClF solvent ($\delta^{129}Xe$ = -1905 ppm, $^1J(^{129}Xe-^{19}F)$ = 5630 Hz) (57,167). The appearance of a small amount of XeF_2 in this spectrum is consistent with the dissociation of $FXeOIOF_4$ to give XeF_2 and IO_2F_3. The latter point is supported by the presence of both IO_2F_3 and XeF_2 in the ^{19}F NMR spectrum (Table 4.4) and is discussed in detail in Chapter 5. The bis-derivatives in Figure 4.13 were assigned by comparison of their ^{129}Xe chemical shifts to those made for the same derivatives in the IO_2F_3/XeF_2 system in SO_2ClF. The compounds trans, trans-, cis, trans- and cis, cis-$Xe(OIOF_4)_2$ are presumed to result from the reaction of $FXeOIOF_4$ with IO_2F_3 as illustrated by equation (4.2). The mixed derivative cis-$F_4OIOXeOSO_2F$ is thought to arise from the reaction of $FXeOSO_2F$ with IO_2F_3 according to equation (4.4). The ^{129}Xe NMR spectrum for cis- and trans-$FXeOIOF_4$ recorded in BrF_5 solvent is similar to that shown in Figure 4.13 except that in the BrF_5 spectrum, there is no evidence for the fluorosulfate species and the ^{129}Xe chemical shifts occur to low frequency of their counterparts recorded in SO_2ClF. This is consistent with the previously established solvent-dependent shielding trends for Xe(II) chemical shifts (57,167).

The ^{19}F NMR spectra of cis/trans-$FXeOIOF_4$ were recorded in SO_2ClF and BrF_5 solvents at -40°C. The ^{19}F NMR parameters for the pure isomers are summarized in Table 4.4. The F-on-I(VII) region of the ^{19}F NMR spectrum recorded in SO_2ClF solvent is depicted in Figure 4.14. The most prominent features of this spectrum are the resonances (A) and (B) which represent cis-$FXeOIOF_4$ and trans-$FXeOIOF_4$, respectively. The assignment of resonance (B) to trans-$FXeOIOF_4$ stems from the fact that a trans-OIF_4O group is expected to display a singlet in the F-on-I(VII) region. The assignment of three (A) multiplets to cis-$FXeOIOF_4$ in the F-on-I(VII) region of the spectrum arises from the fact that a cis-OIF_4O group possesses three magnetically non-equivalent fluorine environments in the ratio 1:1:2 (F_1, F_2 and F_3 in structure 4.9). While the fluorine environments F_1 and F_3 for cis-$FXeOIOF_4$ are shifted slightly to low frequency of their counterparts in cis, cis-$Xe(OIOF_4)_2$, the environment representing F_2 is shifted to high frequency of environment F_2 in cis, cis-$Xe(OIOF_4)_2$ (Table 4.4). The two-bond fluorine-fluorine coupling constants for

Figure 4.14

Fluorine-19 NMR spectrum recorded at -40°C on a cis/trans-$FXeOIOF_4$ mixture dissolved in SO_2ClF solvent showing the F-on-I(VII) region of the spectrum. The peak assignments are given below.

Peak	Assignment
A	cis-$FXeOIOF_4$
B	trans-$FXeOIOF_4$
C	cis, cis-$Xe(OIOF_4)_2$
D	cis, trans-$Xe(OIOF_4)_2$
E	IO_2F_3
F	trans, trans-$Xe(OIOF_4)_2$
S	solvent

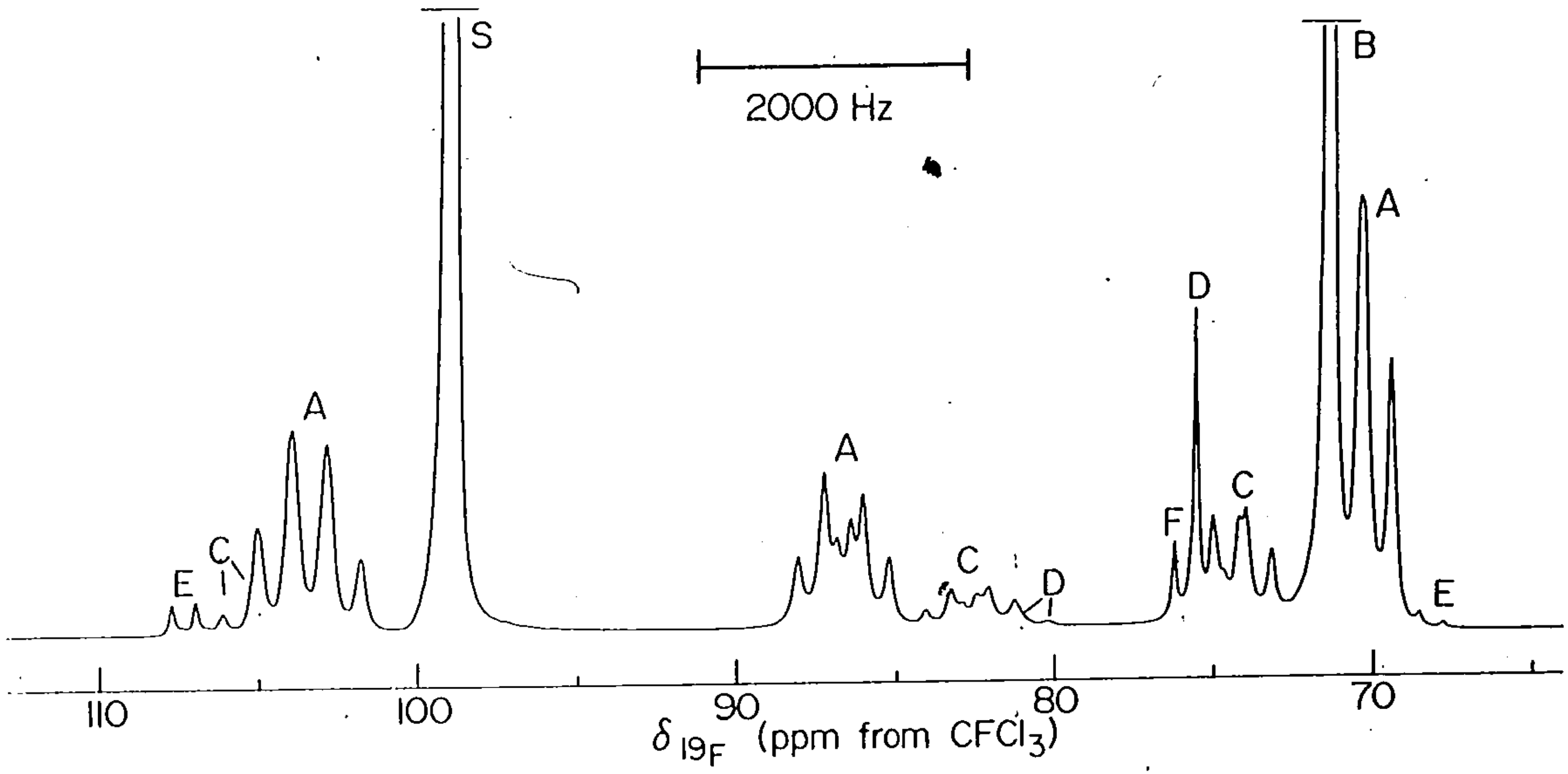
S
2000 Hz
B
A
D
C
F
E
C
D
A
C
E
110
100
90
80
70
$\delta_{^{19}F}$ (ppm from $CFCl_3$)

cis-$FXeOIOF_4$ (Table 4.4) are approximately the same magnitude as the two-bond couplings in cis, cis-$Xe(OIOF_4)_2$. Figure 4.14 also shows ^{19}F NMR resonances which can be assigned to the bis-derivatives trans, trans-$Xe(OIOF_4)_2$ (F) ($\delta^{19}F$ = 76.13 ppm), cis, trans-$Xe(OIOF_4)_2$ (D) ($\delta^{19}F$ (A_4) = 75.44 ppm) and cis, cis-$Xe(OIOF_4)_2$ (C) (Table 4.4). In addition to Xe(II) species, the weak resonances in Figure 4.14 labelled (E) are assigned to IO_2F_3 (AX_2, $\delta^{19}F$ = 107.27 ppm (X_2); 68.49 ppm (A)) which is formed in the dissociation of $FXeOIOF_4$, and is discussed in greater detail in Chapter 5. The ^{19}F NMR spectrum of the cis- and trans-$FXeOIOF_4$ mixture recorded in BrF_5 is depicted in Figure 4.15. This spectrum is provided to illustrate the similarity in spectra between the two solvents with respect to the positions and intensities of the ^{19}F NMR resonances. Aside from the fact that all resonances in the BrF_5 spectrum are shifted slightly to low frequency of those recorded in SO_2ClF, the two spectra are essentially identical. In SO_2ClF and BrF_5 solvents, the differences in chemical shift between environments F_1 and F_2 (15.71 ppm in BrF_5 and 16.77 in SO_2ClF) and environments F_2 and F_3 (15.36 ppm in BrF_5 and 16.30 ppm in SO_2ClF) is approximately equal, implying that the shielding effect on the fluorine environments in cis-$FXeOIOF_4$ increases linearly in the order $F_1 < F_2 < F_3$. A similar linear effect is not observed in the ^{19}F NMR resonances for cis, cis-$Xe(OIOF_4)_2$. In this case, $\delta(F_1 - F_2)$ is 21 ppm whereas $\delta(F_2 - F_3)$ is only 8 ppm. In addition to the resonances assigned to

Figure 4.15

Fluorine-19 NMR spectrum recorded at -40°C on a cis/trans-$FXeOIOF_4$ mixture dissolved in BrF_5 solvent showing the F-on-I(VII) region of the spectrum. The peak assignments are given below.

Peak	Assignment
A	cis-$FXeOIOF_4$
B	trans-$FXeOIOF_4$
C	cis, cis-$Xe(OIOF_4)_2$
D	cis, trans-$Xe(OIOF_4)_2$
E	IO_2F_3
F	trans, trans-$Xe(OIOF_4)_2$

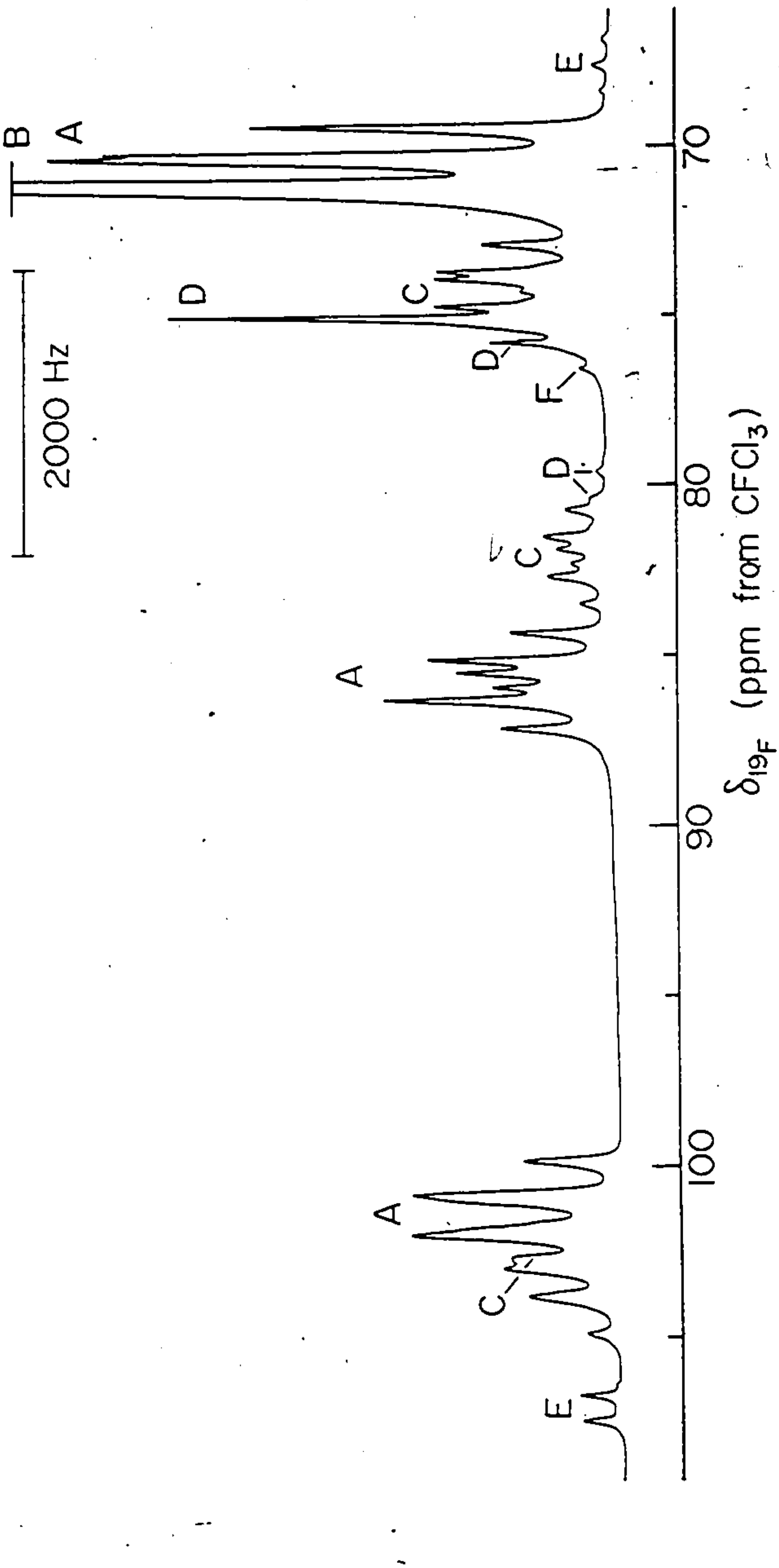
B
A
E
D
C
D
F
D
C
A
A
C
E
2000 Hz
70
80
90
100
$\delta_{^{19}F}$ (ppm from $CFCl_3$)

Xe(II) species, there is again evidence for IO_2F_3 dimer in the BrF_5 spectrum (Figure 4.15) which suggests that the dissociation of $FXeOIOF_4$ is largely independent of solvent and is further addressed in Chapter 5. A particularily informative part of the ^{19}F NMR spectrum can be found in the F-on-Xe(II) region. Figure 4.16 depicts the F-on-Xe(II) region of the ^{19}F NMR spectrum of cis- and trans-$FXeOIOF_4$ recorded in SO_2ClF solvent at -40°C. This spectrum shows four F-on-Xe(II) resonances with accompanying ^{129}Xe satellites (A,a,a), (B,b,b), (D,d,d) and (E,e,e). The assignment of these resonances is based on the intensities of the resonances with cis- and trans-$FXeOIOF_4$ expected to be the most intense (also supported by the intensities in the ^{129}Xe spectrum), the comparison between the ^{129}Xe satellite couplings and the one-bond xenon-fluorine couplings established in the ^{129}Xe NMR spectrum and by comparison of the ^{19}F NMR chemical shifts for XeF_2 and $FXeOSO_2F$ reported previously (94). Resonance (E) ($\delta^{19}F$ = -176.26 ppm), is assigned to XeF_2 by virtue of its ^{129}Xe satellite spacing ($^1J(^{129}Xe-^{19}F)$ = 5613 Hz) which is identical to that determined for this species in the ^{129}Xe NMR spectrum. Resonance (D) ($\delta^{19}F$ = -170.80 ppm) is assigned to $FXeOSO_2F$ by comparison of its ^{129}Xe satellite spacing ($^1J(^{129}Xe-^{19}F)$ = 5848 Hz) with that of the one-bond xenon-fluorine coupling of the same species (5837 Hz) as determined in the ^{129}Xe NMR spectrum. Resonance (A) in Figure 4.16 ($\delta^{19}F$ = -158.50 ppm) is assigned to the terminal fluorine on xenon of cis-$FXeOIOF_4$ since this is

Figure 4.16

Fluorine-19 NMR spectrum recorded at -40°C on a cis/trans-$FXeOIOF_4$ mixture dissolved in SO_2ClF solvent showing the F-on-Xe(II) region of the spectrum. The peak assignments are given below.

Peak	Assignment
A (a,a)	cis-$FXeOIOF_4$
B (b,b)	trans-$FXeOIOF_4$
D (d,d)	$\overline{F}XeOSO_2F$
E (e,e)	XeF_2

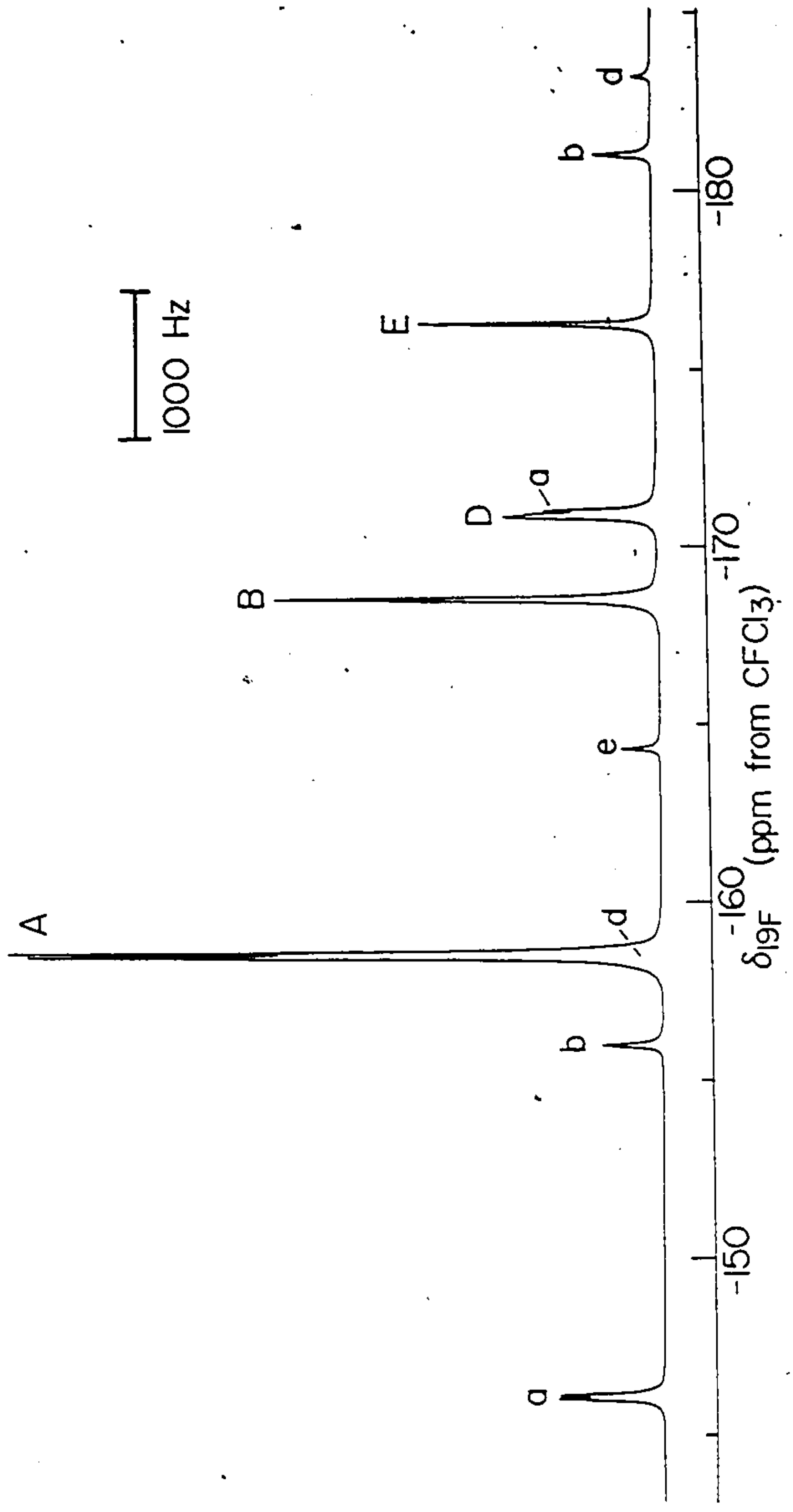
1000 Hz
A
B
D
E
a
b
d
e
-150
-160
-170
-180
$\delta_{^{19}F}$ (ppm from $CFCl_3$)

the most intense resonance in the F-on-Xe(II) region of the spectrum and by comparison of the ^{129}Xe satellite spacing, $J(^{129}Xe-^{19}F)$ = 5852 Hz, with that of the one-bond xenon-fluorine coupling constant (5851 Hz) determined for cis-$FXeOIOF_4$ in the ^{129}Xe NMR spectrum. Resonance (A) and its accompanying satellites also show an additional partially resolved doublet splitting (26 Hz) which arises from the four-bond spin-spin coupling of a unique fluorine on the cis-OIF_4O group to the fluorine directly-bonded to xenon. It is unclear why none of the other resonances in Figure 4.16 show such a resolved long-range spin-spin coupling. The doublet fine structure on A is indicative of a unique four-bond spin-spin coupling between either F_1 or F_2 of the cis-OIF_4O group (structure 4.9) and the terminal fluorine on xenon. Such a long range coupling is not unprecedented and had been noted previously in this work between the fluorine on sulfur of $FXeOSO_2F$ ($^4J_{FF}$ = 14 Hz). In view of the fact that fluorines cis to the I-O bond (F_3) do not give rise to a resolvable coupling, it is assumed that the remaining cis-coupling with F_2 is also not resolved. Consequently, the doublet splitting is attributed to F_1, which is trans to the I-O single bond. Intuitively, the through-space couplings between the terminal fluorine on xenon and F_2 and F_3 are expected to be larger than with F_2 owing to their close proximity and if free rotation about the Xe-O and I-O single bonds is assumed. It is interesting to note, however, that additional corroboration for this observation is found in the ^{129}Xe spectra of cis-FXeOIOF$_4$. The ^{129}Xe resonance appears as a doublet due to $^1J(^{129}Xe-^{19}F)$ which, under high resolution, shows additional fine structure on each doublet branch resembling a broadened, partially resolved doublet (41 Hz) with accompanying unresolved fine structure (Figure 4.3). Again, the doublet structure on each branch is assumed to arise from coupling with F$_1$ and the coupling to xenon ($^3J(^{129}Xe-^{19}F_2)$ arising from the fluorines cis to the I-O single bond (F$_1$ and F$_3$) are not large enough to be resolved, but contribute to the line broadening. It is presently not possible to account for the relative magnitudes of these "through-space" couplings.

Resonance (B) ($\delta^{19}F$ = -168.50 ppm) is assigned to trans-FXeOIOF$_4$ by comparison of its ^{129}Xe satellite spacing, $^1J(^{129}Xe-^{19}F)$ = 5902 Hz, with the one-bond xenon-fluorine coupling determined in the ^{129}Xe NMR spectrum (5893 Hz).

The ^{19}F NMR spectra recorded on the mixture of cis- and trans-FXeOIOF$_4$ has served to verify the assignments made in the ^{129}Xe NMR investigation. In addition, the ^{19}F NMR chemical shifts of these species have been used to corroborate the group electronegativty trends discussed in section C of this Chapter.

(viii) Characterization of $FXeOIOF_4$ by Raman Spectroscopy

The Raman spectrum of the mixture of cis- and trans-$FXeOIOF_4$ was recorded at -196°C in an FEP tube and is illustrated in Figure 4.17. The vibrational frequencies and intensities as well as tentative assignments are given in Table 4.6. The Raman spectrum consists of broad and poorly resolved vibrational bands in comparison to the spectrum of cis, cis-$Xe(OIOF_4)_2$ (Figure 4.12). This is likely the combined effect of having a mixture of cis- and trans-isomers with near-coincident vibrational frequencies and the fact that the mixture does not crystallize at -196°C but rather, forms a glass which would give rise to increased vibrational motions and line broadening.

The cis- and trans-$FXeOIOF_4$ molecules of symmetry C_s should each possess a maximum of 21 fundamental modes, all Raman active, classified as 14 A' + 7 A". The complexity of the spectrum depicted in Figure 4.17 does not permit a full assignment of all modes associated with the mixture of isomers. Wherever possible however, tentative assignments have been made by comparisons with the vibrational spectra of other monofluoro Xe(II) derivatives.

The high-frequency bands at 889 and 894 cm^{-1} are assigned to I=O stretches by analogy with the I=O stretching frequency determined for cis, cis-$Xe(OIOF_4)_2$ (889 cm^{-1}). These bands are assigned to the cis- and trans-isomers, respectively, by comparison with the frequencies for the I=O stretches in

Figure 4.17

Raman spectrum recorded on a cis/trans-$FXeOIOF_4$ mixture in an FEP tube at -196°C. * denotes bands arising from FEP.

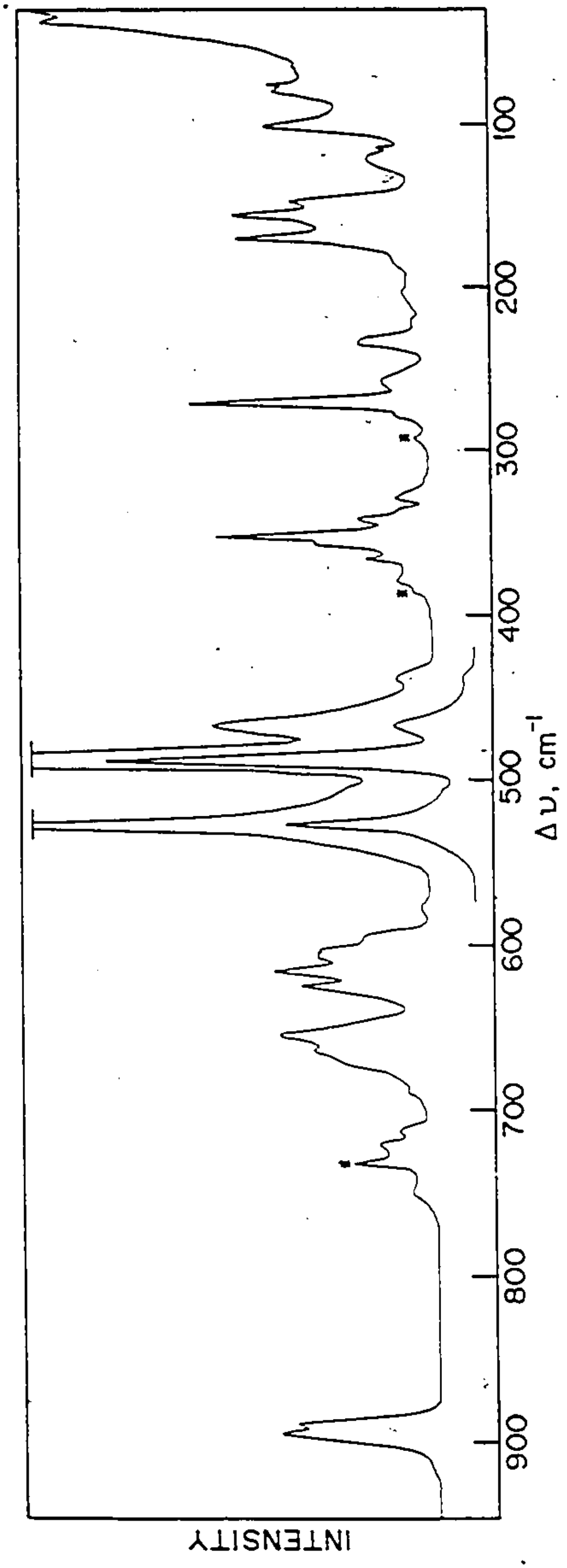
100
200
300
400
500
600
700
800
900
Δν, cm⁻¹
INTENSITY

Table 4.6

Vibrational Frequencies and Tentative Assignments for the Raman Spectrum Recorded on cis-/trans-$FXeOIOF_4$

Frequency,[a] cm^{-1}	Tentative Assignment
894 (15)	ν I=O, trans
889 (11)	ν I=O, cis
720 (4)	
712 (2)	
664 (15)	
654 (22)	
625 (14)	I-F stretches
616 (17)	
605 (13)	
595 (sh)	
578 (1)	
527 (49)	ν Xe-F, cis and trans
488 (100)	ν Xe-O, I-O[b]
467 (37)	
438 (3)	
379 (3)	
356 (sh)	
352 (11)	
341 (4)	
328 (2)	IF_2, FIO, IO_2 and IF_4 bending modes
278 (1)	
270 (13)	
257 (3)	
233 (5)	
205 (1)	
185 (1)	

continued...

Table 4.6 continued

Frequency,[a] cm^{-1}	Tentative Assignment
170 (12)	δ F-Xe-O, Xe-O-I[b]
156 (15)	
148 (8)	
122 (4)	
101 (11)	
80 (6)	

a: The Raman spectrum was recorded in FEP at -196°C.
* denote FEP bands.

b: These modes are presumably strongly coupled.

cis-$FOIOF_4$ (914 cm^{-1}) (186), trans-$FOIOF_4$ (924 cm^{-1}) (186) and cis, cis-$Xe(OIOF_4)_2$ (889 cm^{-1}). Furthermore, the observation of two bands in the I=O stretching region is supportive of a cis-/trans- mixture. The vibrational bands in the region 590-680 cm^{-1} are most certainly I-F stretches, however, a definite assignment cannot be made for these bands since the I-F stretches of both cis- and trans-$FXeOIOF_4$ are expected to occur in this region and may in some cases be coincident. The broad, intense vibrational band at 527 cm^{-1} is assigned to the overlapping Xe-F stretches of the cis- and trans-isomers by analogy with the frequencies of the corresponding modes in $FXeOSO_2F$ (521, 527, 532 and 539 cm^{-1} (168)), $FXeOSO_2CF_3$ (534 cm^{-1} (151)) and $FXeOTeF_5$ (520 cm^{-1} (138)). The bands at 467 and 488 cm^{-1} are assigned to the strongly coupled I-O and Xe-O stretches by analogy with the corresponding modes in $FXeOTeF_5$ (457 cm^{-1} (138)), $FXeOSO_2F$ (434 cm^{-1} (168)), $Xe(OTeF_5)_2$ (440 cm^{-1} (178)) and cis, cis-$Xe(OIOF_4)_2$ (464 cm^{-1} (205)). The vibrational bands below 400 cm^{-1} correspond to bending and/or torsional modes. The intense bands at 156 and 170 cm^{-1} are assigned to F-Xe-O and Xe-O-I bending modes by analogy with the corresponding Xe-O-I and O-Xe-O modes in cis, cis-$Xe(OIOF_4)_2$ (148 cm^{-1}). The vibrations in the region of the spectrum from 230-280 cm^{-1} and 320-380 cm^{-1} are assigned to the IF_2, IF_4, IO_2 and/or IOF bends by analogy with the corresponding modes in cis- and trans-$[OIOF_4]^-$ (186), IOF_5 (210,211) and cis, cis $Xe(OIOF_4)_2$. It is important to note that in Figure 4.17, there is no evidence for XeF_2 which is expected to have a strong stretching vibration at 496 cm^{-1} and no evidence of IO_2F_3 which is expected to show a moderately strong vibration at 920 cm^{-1} (192). These results clearly indicate that the IO_2F_3 and XeF_2 observed in the ^{19}F NMR spectra discussed above. must result from the dissociation of $FXeOIOF_4$ as suggested in the previous section and are not the result of residual reactants in the cis- and trans-$FXeOIOF_4$ mixture.

(D) CHEMICAL SHIFT TRENDS AND GROUP ELECTRONEGATIVITIES

(i) General

It has been shown in previous studies (57,94,96,109, 151,167) that ^{129}Xe and ^{19}F NMR chemical shifts and xenon-fluorine coupling constants can be used as effective measures of the ionicity of xenon-ligand bonds. That is, a decrease in ^{19}F chemical shift and increase in ^{129}Xe-^{19}F coupling constant is consistent with a greater degree of ionic character in the terminal Xe-F bond and that a decrease in ^{129}Xe chemical shift is indicative of an increasingly more covalent xenon-ligand atom bond. This measure can then be correlated with the electron-withdrawing ability or group electronegativity of a substituent group. The ^{129}Xe and ^{19}F NMR studies of the xenon(II) derivatives FXeL and XeL_2, where L = $-OIF_4O$, $-OSO_2F$ and $-OTeF_5$ can therefore be used to assess the group electronegativity trends for the series $-OSO_2F$, $-OTeF_5$ and $-OIF_4O$.

(ii) The Relative Electronegativities of the $-OIF_4O$ and $-OSO_2F$ Groups

The mixed xenon(II) derivatives containing one $-OSO_2F$ and one $-OIF_4O$ group provide a convenient means by which the shielding of the xenon nucleus can be compared for these two groups uder the same conditions. From the ^{129}Xe NMR studies on the IO_2F_3/XeF_2 system performed in SO_2ClF, it is evident that the ^{129}Xe chemical shifts of the fluorosulfate derivatives ~~are~~ consistently to high frequency of the $-OIF_4O$ group derivatives (Table 4.1). The average chemical shift differences are 16 ppm between $FXeOSO_2F$ and trans-$FXeOIOF_4$ and 33 ppm between trans-$F_4OIOXeOSO_2F$ and trans, trans-$Xe(OIOF_4)_2$. This implies the electronegativity of the $-OSO_2F$ group is greater than that of the trans-OIF_4O group. Furthermore, the ^{129}Xe chemical shifts for the bis-isomers of $-OIF_4O$ were found to be additive, progressing to lower frequency with increasing cis-substitution. This frequency shift was found to be 126 ppm on substitution of one trans-ligand for one cis-ligand and with substitution of the second trans-ligand, the ^{129}Xe resonance shifted a further 117 ppm to lower frequency. This near additivity trend was found to be independent of temperature and concentration. This trend implies the effective group order cis-OIF_4O < trans-OIF_4O < $-OSO_2F$ and is further supported by examining the ^{19}F NMR results for these species recorded in SO_2ClF solvent at -5°C for a 1 : 3.53 molar mixture of XeF_2 and IO_2F_3 (Table 4.2). The ^{19}F chemical shift for $FXeOSO_2F$ ($\delta^{19}F$ -

-171.9 ppm) occurs to low-frequency of the chemical shifts of both trans-$FXeOIOF_4$ ($\delta^{19}F$ = -168.9 ppm) and cis-$FXeOIOF_4$ ($\delta^{19}F$ = -159.4 ppm). This result can be interpreted in terms of the ionicity of the terminal Xe-F bonds which can in turn be related to the group electronegativity. The high electron-withdrawing ability of the fluorosulfate group, as compared to cis- or trans-OIF_4O, results in the $FXeOSO_2F$ molecule having substantially more XeF^+ character than in either cis- or trans-$FXeOIOF_4$. The increased XeF^+ character is reflected in the low-frequency (shielded) ^{19}F chemical shift for the fluorosulfate derivative. This can be further related to the covalency of the Xe-O bond, being the most covalent in cis-$FXeOIOF_4$ and least covalent (most ionic) in $FXeOSO_2F$.

(iii) The Relative Electronegativities of the $-OIF_4O$ and $-OTeF_5$ Groups; the cis- and trans-$F_4OIOXeOTeF_5$ Derivatives

In order to compare the electronegativities of the $-OIF_4O$ and $-OTeF_5$ groups, the series of mixed derivatives $(F_4OIO)_xXe(OTeF_5)_{2-x}$ were prepared in $CFCl_3$ and studied by ^{129}Xe NMR spectroscopy at 24°C. The ^{129}Xe NMR spectrum of a 1:1 molar mixture of cis, cis-$Xe(OIOF_4)_2$ and $Xe(OTeF_5)_2$ recorded in $CFCl_3$ solvent at 24°C is depicted in Figure 4.18. The ^{129}Xe NMR parameters for this system as well as the parameters for the same mixture recorded at 5°C are summarized in Table 4.7. In Figure 4.18, four resonances are shown

Figure 4.18

Xenon-129 NMR spectrum of a 1:1 molar mixture of cis, cis-Xe$(OIOF_4)_2$ and Xe$(OTeF_5)_2$ recorded in $CFCl_3$ solvent at 24°C.

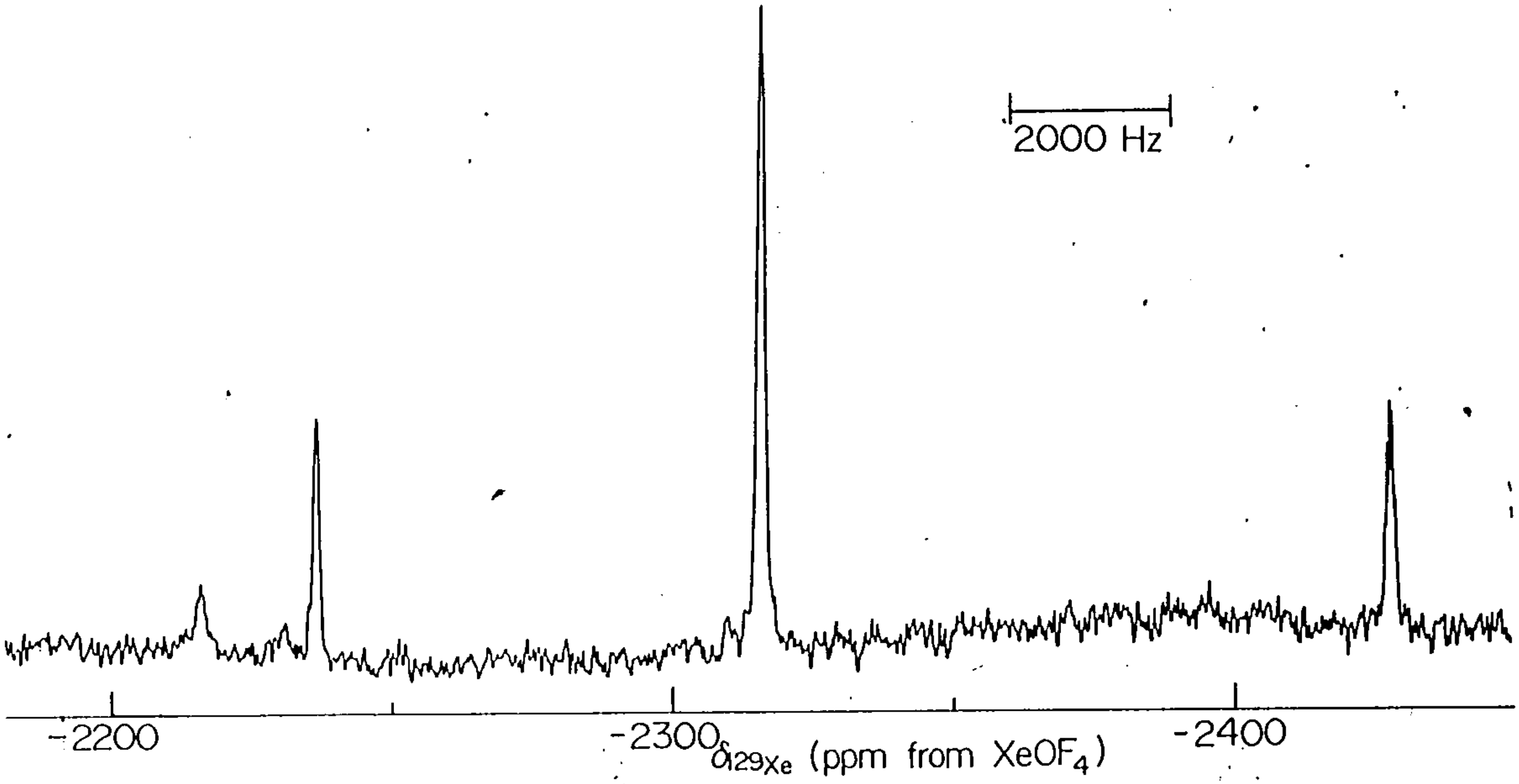
2000 Hz
-2200
-2300
-2400
$\delta_{^{129}Xe}$ (ppm from $XeOF_4$)

Table 4.7

Xenon-129 NMR Parameters for the $Xe(OTeF_5)_2$/$Xe(OIOF_4)_2$ System Recorded in $CFCl_3$ Solvent at 24 and 5°C

Species	$\delta^{129}Xe$(ppm)[a]	Temperature (°C)
$Xe(OTeF_5)_2$	-2423.2	5
	-2428.2	24
cis-$F_4OIOXeOTeF_5$	-2298.7	5
	-2315.7	24
cis, cis-$Xe(OIOF_4)_2$	-2219.5	5
	-2236.4	24
trans-$F_4OIOXeOTeF_5$	-2205.3	5
	-2217.5	24
cis, trans-$Xe(OIOF_4)_2$	-2119.8	5
	-2131.3	24

a: Referenced with respect to neat $XeOF_4$ at 24°C.

(one resonance of very low intensity, $\delta^{129}Xe$ = -2131.3 ppm is not shown) which represent the derivatives $(F_4OIO)_xXe(OTeF_5)_{2-x}$ (x = 0,1,2). The high frequency peak (δ129Xe = -2428.2 ppm) with resolved fine structure ($^3J(^{129}Xe-^{19}F)$ = 32 Hz) is assigned to $Xe(OTeF_5)_2$ by comparison with the ^{129}Xe chemical shift (-2447.4 ppm) and three-bond xenon-fluorine coupling (31 Hz) previously reported for this species (127). The peak at $\delta^{129}Xe$ = -2236.4 ppm is assigned to cis, cis-$Xe(OIOF_4)_2$ by comparison of its chemical shift with that established for the same species in the IO_2F_3/XeF_2 system, also recorded in $CFCl_3$ solvent (-2231.1 ppm). The peak which occurs in the frequency range between that of cis, cis-$Xe(OIOF_4)_2$ and $Xe(OTeF_5)_2$ ($\delta^{129}Xe$ = -2315.7 ppm) is assigned to the mixed derivative cis-$F_4OIOXeOTeF_5$. Further support of this assignment stems from the fact that this species is expected to be the most intense in the near-statistical scrambling of an equimolar mixture of cis, cis-$Xe(OIOF_4)_2$ and $Xe(OTeF_5)_2$. The low-intensity peak, which occurs at $\delta^{129}Xe$ = -2131.3 ppm, but is not shown in Figure 4.18, is assigned to cis, trans-$Xe(OIOF_4)_2$ by comparison with the chemical shift of this species established in the IO_2F_3/XeF_2 system, also recorded in $CFCl_3$ (-2113.6 ppm). The peak at $\delta^{129}Xe$ = -2217.5 ppm is therefore assigned to the mixed derivative trans-$F_4OIOXeOTeF_5$, since the ^{129}Xe chemical shift for this species is expected to occur to high-frequency of cis-$F_4OIOXeOTeF_5$ ($\delta^{129}Xe$ = -2315.7 ppm) but to low-frequency of cis, trans-$Xe(OIOF_4)_2$ ($\delta^{129}Xe$ = -2131.3

ppm).

Although the ^{129}Xe chemical shifts for the mixed derivatives, $(F_4OIO)_xXe(OTeF_5)_{2-x}$, progress to lower frequency with increasing $-OIF_4O$ substitution, these frequency shifts are not additive, as was found for the cis- and trans-isomers of $Xe(OIOF_4)_2$. For instance, a frequency shift of 125 ppm was found on substitution of one $-OTeF_5$ group of $Xe(OTeF_5)_2$ for one cis-OIF_4O ligand and with the substitution of the second $-OTeF_5$ group, the frequency was shifted a further 79 ppm to lower frequency. In comparison, the frequency shift associated with substituting one $-OTeF_5$ group of $Xe(OTeF_5)_2$ for one trans-OIF_4O group was 218 ppm.

The chemical shift order is observed to decrease as follows: trans-OIF_4O > cis-OIF_4O > $-OTeF_5$. From this ordering it may be inferred that the relative group electronegativities increase in the order $-OTeF_5$ < cis-OIF_4O < trans-OIF_4O.

(iv) Electronegativity Trends: Summary

The NMR parameters for the xenon(II) mixed derivatives containing cis-OIF_4O, trans-OIF_4O, $-OTeF_5$ and $-OSO_2F$ have been used to compare the electron-withdrawing ability of these groups under the same solvent and temperature conditions. These results suggest the group electronegativities increase in the order: $-OTeF_5$ < cis-OIF_4O < trans-OIF_4O < $-OSO_2F$. Furthermore, if one considers the Xe-F stretching frequency of the mono-derivatives to be a reflection of the ionicity of the

Xe-F bond, then the frequency is expected to increase as the xenon-ligand atom bond and terminal Xe-F bond become more ionic, i.e., more XeF^+ character. The stretching frequencies of the terminal Xe-F bonds do increase in the order of increasing group electronegativity, i.e., $-OTeF_5$ 520 cm^{-1} (138) < cis/trans-OIF_4O 527 cm^{-1} (205) < $-OSO_2F$ 530 cm^{-1} (134) which further supports the proposed trend.

CHAPTER 5

THE DECOMPOSITION PRODUCTS OF cis/trans $FXeOIOF_4$ AND cis, cis-$Xe(OIOF_4)_2$ AND THE PREPARATION AND CHARACTERIZATION OF $F_4OIOOIOF_4$

(A) INTRODUCTION

The decomposition pathways for most Xe(II) derivatives are well known. The mono-fluoro derivatives, with few exceptions, are thermally more stable than their bis counterparts, this, in part, is the result of the increased ionicity of F-Xe-L as compared to L-Xe-L, i.e., the valence bond structure FXe^+L^- is favored over LXe^+L^-. For instance, the decomposition of $FXeN(SO_2F)_2$ is slow at room temperature whereas the decomposition of $Xe[N(SO_2F)_2]_2$ occurs rapidly (149). The thermal decompositions of $FXeOSO_2F$ (134) and $FXeN(SO_2F)_2$ (149), according to equations (5.1) and (5.2), are typical of mono-fluoro derivatives leading to the formation of XeF_2, Xe gas and the peroxide or N-N bonded product. Analogous decompositions also occur according to equation (5.1)

$$2\ FXeOSO_2F \longrightarrow XeF_2 + Xe\uparrow + FO_2SOOSO_2F \qquad (5.1)$$

$$2\ FXeN(SO_2F)_2 \longrightarrow XeF_2 + Xe\uparrow + (FO_2S)_2NN(SO_2F)_2 \qquad (5.2)$$

for F-Xe-L, where L = $-OSO_2F$ (134), $-OTeF_5$ (225), $-OPO_2F$ (143) and $-OCOCF_3$ (147). Again, thermal decomposition pathways analogous to equations (5.1) and (5.2) are followed by most bis Xe(II) derivatives, L-Xe-L, with formation of Xe gas and either the peroxide (L = $-OSO_2F$), oxide (L = $-OTeF_5$ (225), $-OSeF_5$ (225,226), $-OPO_2F$ (143) or the N-N bonded product, $[N(SO_2F)_2]_2$, arising from the decomposition of $Xe[N(SO_2F)_2]_2$ (149).

The pure $-OIF_4O$ derivatives, $FXeOIOF_4$ and $Xe(OIOF_4)_2$, prepared in this work were found to be unstable with respect to thermal decomposition. A preliminary assessment of these decomposition products has been given in Chapter 4. The controlled thermal decompositions of these derivatives have been performed under a variety of conditions and monitored by ^{19}F NMR spectroscopy and Raman spectroscopy and are discussed in detail in this Chapter.

(B) THE DECOMPOSITION OF cis/trans $FXeOIOF_4$

During the characterization of mixtures of cis- and trans-$FXeOIOF_4$ in solution by ^{19}F NMR spectroscopy (Chapter 4), quantities of IO_2F_3 and XeF_2 were always detected. The formation of these species was thought to arise from the dissociation of $FXeOIOF_4$ according to equation (5.3). In

$$FXeOIOF_4 \rightleftharpoons IO_2F_3 + XeF_2 \qquad (5.3)$$

order to test this proposal, $FXeOIOF_4$, which had been previously checked by Raman spectroscopy and shown to contain no IO_2F_3 or XeF_2, was dynamically pumped under vacuum at 0°C.

The volatile products, which were trapped at -196°C, were characterized by ^{19}F NMR spectroscopy and Raman spectroscopy. The Raman spectrum recorded on the residue at -196°C in an FEP tube is depicted in Figure 5.1. Comparison of the vibrational frequencies from Figure 5.1 (Table 5.1) with the vibrational spectra reported for IO_2F_3 (192) and XeF_2 (53) confirm that this residue corresponds to a simple mixture of XeF_2 and IO_2F_3. The absence of the characteristic vibrational bands arising from the I(V) species IF_5, IO_2F or IOF_3 (220,227) suggests that $FXeOIOF_4$ dissociates under dynamic vacuum according to equation (5.3) and that no alternative decomposition occurs under these conditions. The results from the ^{19}F NMR spectrum recorded at -40°C on the residue dissolved in BrF_5 are summarized in Table 5.2. In addition to two AX_2 spectra in the F-on-I(VII) region, which are assigned to IO_2F_3 by comparison with the ^{19}F chemical shifts determined in Chapter 3, and a singlet with accompanying satellites in the F-on-Xe(II) region assigned to XeF_2 (Chapter 4), there is an AX_4 pattern in the F-on-I(V) region assigned to IF_5 (208). The IF_5 in this system is thought to have arisen from the decomposition of IO_2F_3 according to equation (1.19) yielding IOF_3 and O_2 gas (192). The IOF_3 formed is rapidly fluorinated in BrF_5 solvent to give IF_5 (228,229). Although $BrOF_3$ is presumably formed in the fluorination of IOF_3 with BrF_5, it is not observed in Figure 5.1. Instead, the $BrOF_3$ formed immediately decomposes to BrO_2F (228) which undergoes fast

Figure 5.1

The Raman spectrum of the volatile products from the dissociation of $FXeOIOF_4$ trapped at -196°C. * denotes an FEP band.

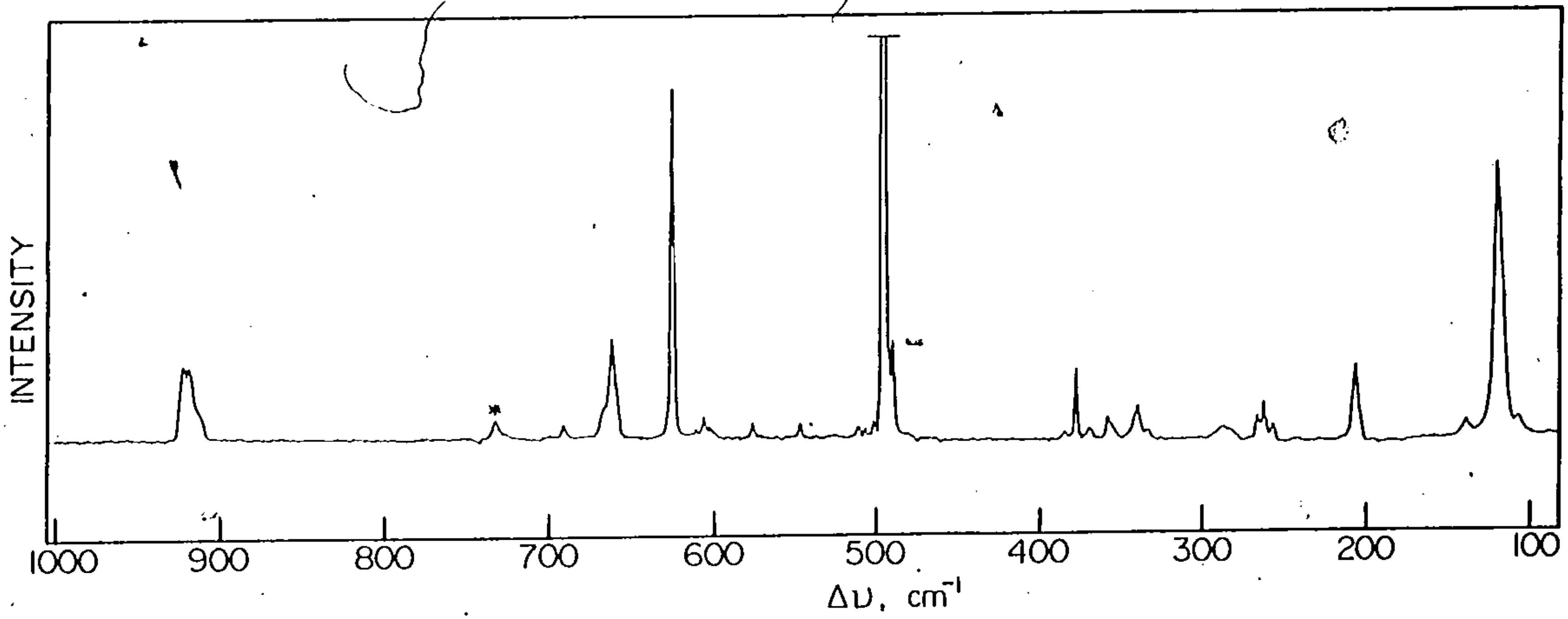
INTENSITY
*
1000
900
800
700
600
500
400
300
200
100
Δν, cm⁻¹

Table 5.1

Vibrational frequencies and assignments for the Raman spectrum recorded on the dissociation products of $FXeOIOF_4$ trapped at -196°C

Frequency^a (cm^{-1})	Assignment
917 (27)	ν (I=O)^b
911 (sh)	b
693 (1)	
661 (35)	ν (I-F_{ax})^b
625 (100)	ν (I-F_{eq})^b
601 (2)	ν (IO_2)^b
576 (1)	
547 (1)	
496 (>100)	ν (Xe-F)^c
494 (33)	
383 (<1)	b
380 (26)	b
378 (1)	b
360 (4)	b
341 (6)	b
290 (1)	
273 (4)	
270 (6)	b
267 (2)	
206 (25)	b
140 (2)	
109 (73)	c

a: Spectrum recorded at -196°C in an FEP tube.

b: Band arising from IO_2F_3 (this work and ref 208).

c: Band arising from XeF_2 (this work).

Table 5.2

Fluorine-19 NMR parameters for the dissociation products of $FXeOIOF_4$ recorded in BrF_5 solvent at -40°C

Species	$\delta^{19}F^a$ (ppm)	$^2J_{FF}$ (Hz)	$^1J(^{129}Xe-^{19}F)$ (Hz)
IO_2F_3	(A) 66.9	179	
	(X) 106.1		
	(A') 67.7	181	
	(X') 106.4		
XeF_2	-185.0		5625
IF_5	(A) 57.4	86	
	(X) 8.3		

a: Referenced with respect to neat $CFCl_3$ at 24°C.

fluoride-ion exchange with BrF_5 solvent resulting in a broad unobservable resonance.

The Raman spectroscopic and ^{19}F NMR results have shown that the product obtained in the dissociation of $FXeOIOF_4$ is a mixture of XeF_2 and IO_2F_3. There was no evidence in either spectrum for species which could be assigned to a peroxide ($F_4OIOOIOF_4$) or oxide ($F_4OIOIOF_4$), ruling out the thermal decomposition of $FXeOIOF_4$ according to equation (5.4) (c.f. equation (5.1)) and equation (5.4).

$$2\ FXeOIOF_4 \longrightarrow XeF_2 + F_4OIOOIOF_4 + Xe \uparrow \qquad (5.4)$$

$$F_4OIOOIOF_4 \longrightarrow F_4OIOIOF_4 + \tfrac{1}{2}\ O_2 \uparrow \qquad (5.5)$$

(C) THE THERMAL DECOMPOSITION OF cis, cis-$Xe(OIOF_4)_2$ LEADING TO THE FORMATION OF $F_4OIOOIOF_4$

(i) The Decomposition Routes of cis, cis-$Xe(OIOF_4)_2$

The stability of cis, cis-$Xe(OIOF_4)_2$ is low as a pure compound in the solid state and only marginal in solution at 0°C. The decomposition routes have been studied by ^{19}F NMR spectroscopy and Raman spectroscopy and are discussed in this Section.

When pure cis, cis-$Xe(OIOF_4)_2$ is allowed to stand in a static vacuum at room temperature, the ensuing decomposition is rapid yielding a mixture of gaseous products, a volatile liquid component and a colorless solid. The gaseous products have been identified as O_2, which is non-condensible at -196°C, and Xe, which is non-condensible at -78°C but condensible at -196°C. The other products have been identified by ^{19}F NMR spectroscopy and Raman spectroscopy as follows: The ^{19}F NMR spectrum of the solid and liquid components were recorded in $CFCl_3$ solvent at 24°C and is depicted in Figure 5.2. The spectrum shows an AX_4 pattern (A) assigned to IF_5 ($\delta^{19}F$: (A) = 58.2 ppm, (X_4) = 12.4 ppm; $^2J(FF)$ = 86 Hz) as well as a singlet resonance labelled (B) ($\delta^{19}F$ = 48.6 ppm) which is assigned to the three equivalent fluorines (by intramolecular exchange averaging) of IOF_3 (208). The Raman spectrum recorded on the solid component resulting from this decomposition corresponded to a mixture of IOF_3 and IO_2F, which were identified by comparison with the vibrational spectra previously reported for these compounds (207,208). The ^{19}F NMR and Raman spectroscopic results suggest that the fast decomposition of cis, cis-$Xe(OIOF_4)_2$ occurs according to equation (5.6). The diminished

$$Xe(OIOF_4)_2 \longrightarrow IF_5 + IOF_3 + Xe\uparrow + 3/2\ O_2\uparrow \qquad (5.6)$$

amounts of IOF_3 that are observed in the ^{19}F NMR spectrum is a result of the facile decomposition of this species (208) yielding IO_2F and IF_5 according to equation (5.7). The absence

$$2\ IOF_3 \longrightarrow IO_2F + IF_5 \qquad (5.7)$$

Figure 5.2

The ^{19}F NMR spectrum of the products resulting from the rapid decomposition of cis, cis-Xe($OIOF_4$)$_2$ recorded in $CFCl_3$ solvent at 24°C. The peak assignments are given below.

Peak	Assignment
A	IF_5
B	IOF_3

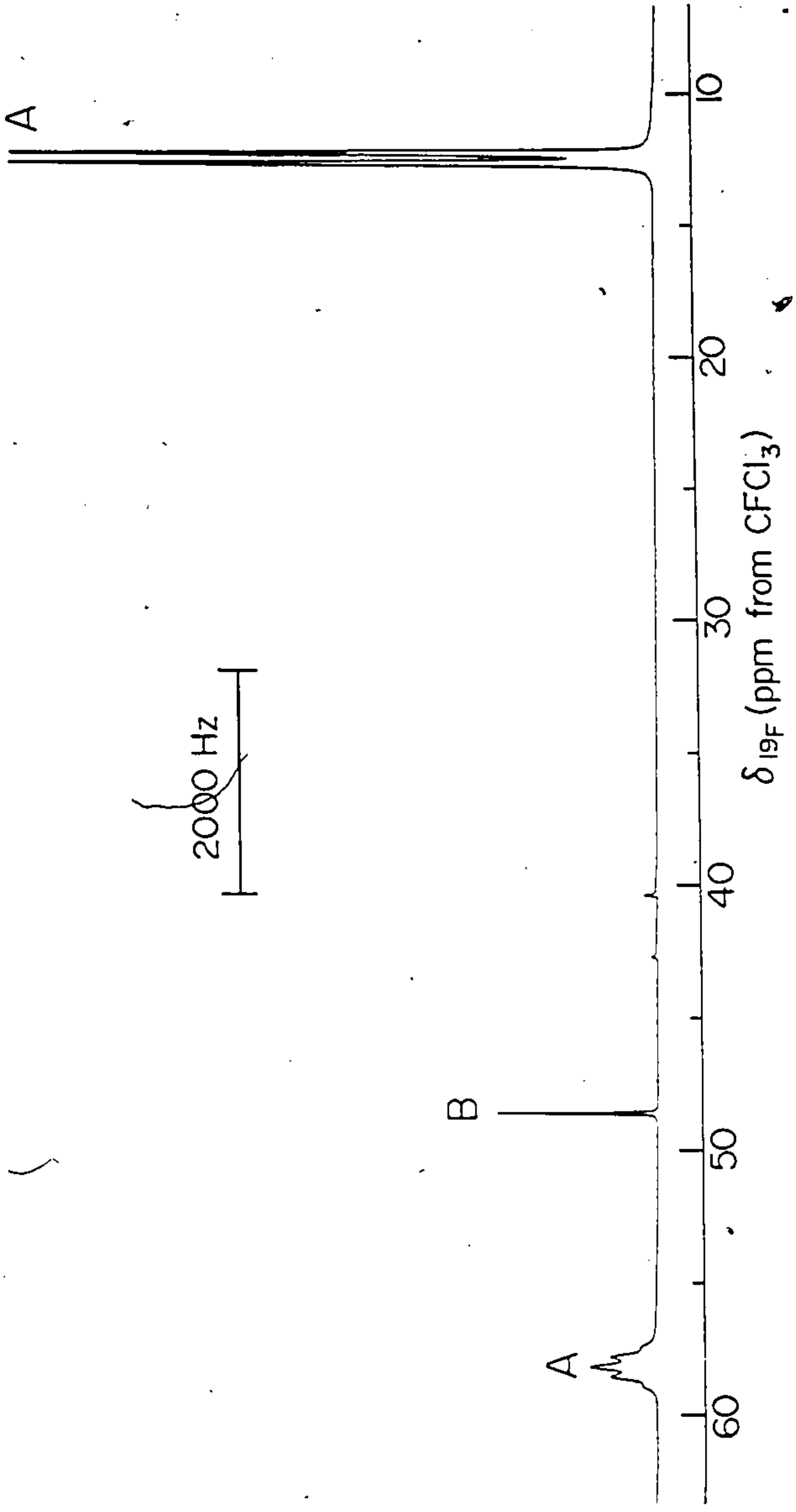
A
B
A
2000 Hz
10
20
30
40
50
60
$\delta_{^{19}F}$ (ppm from $CFCl_3$)

of a ^{19}F resonance associated with IO_2F is attributed to the very low solubility of this species in $CFCl_3$ (an insoluable white residue was observed in these samples).

The rapid decomposition of cis, cis-$Xe(OIOF_4)_2$ producing only I(V) species and giving no evidence for intermediate formation of a peroxide or oxide, is primarily attributed to radical formation (see Chapter 4). That is, in the initial stages of decomposition, radical formation occurs slowly but increases in concentration as the reaction proceeds. At some point in the decomposition, the concentration of the radical builds to a level that is sufficient to catalyze the rapid and sustained decomposition of the remaining bulk sample. It was presumed, however, that if the radical concentration could be controlled, then so also could the rate of decomposition. It was obvious that the radical concentration could not be maintained at a low enough level simply by dynamic pumping of the sample although the instantaneous decomposition cited could be avoided under these conditions. As a result, alternative methods were devised to enable the observation of the intermediate species generated, under controlled decomposition conditions.

A solid sample of cis, cis-$Xe(OIOF_4)_2$ was dissolved in SO_2ClF solvent and the decomposition initiated by warming the sample to 0°C for given time intervals followed by quenching at -196°C. The decomposition products were monitored by recording their ^{19}F NMR spectra after each quenching at -40°C. The ^{19}F

Figure 5.3

The ^{19}F NMR spectra recorded at -40°C showing the decomposition products resulting from warming a solution of cis, cis-$Xe(OIOF_4)_2$ in SO_2ClF to 0°C for: a, 0 minutes; b, 10 minutes; c, 70 minutes; d, 520 minutes. The peak assignments are given below.

Peak	Assignment
C	cis, cis-$Xe(OIOF_4)_2$
D	cis, trans-$Xe(OIOF_4)_2$
F	trans, trans-$Xe(OIOF_4)_2$
G	$F_4OIOOIOF_4$
S	SO_2ClF solvent

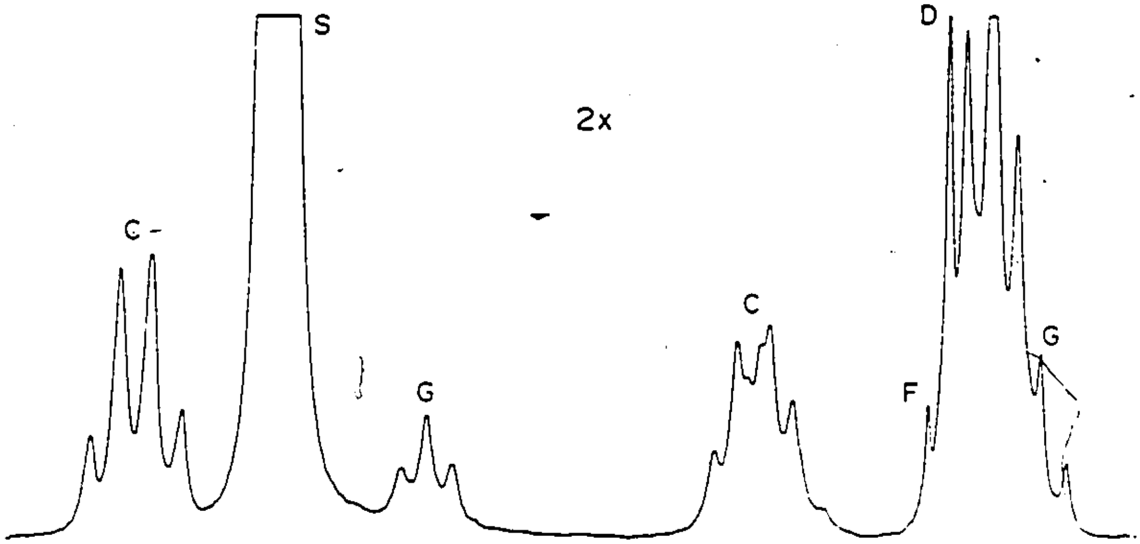

5.3 (a)

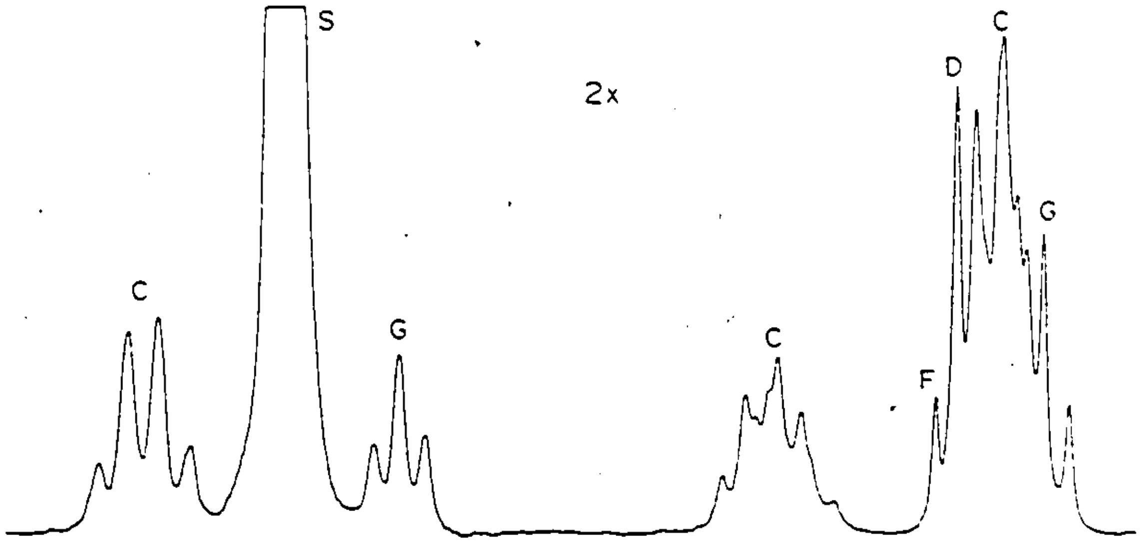

5.3 (b)

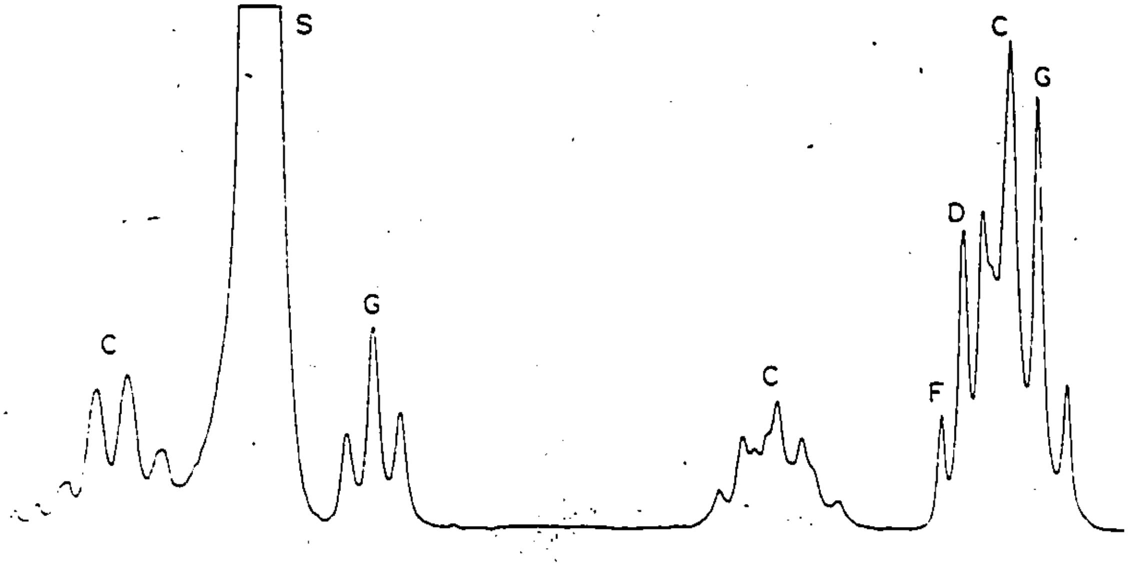

5.3 (c)

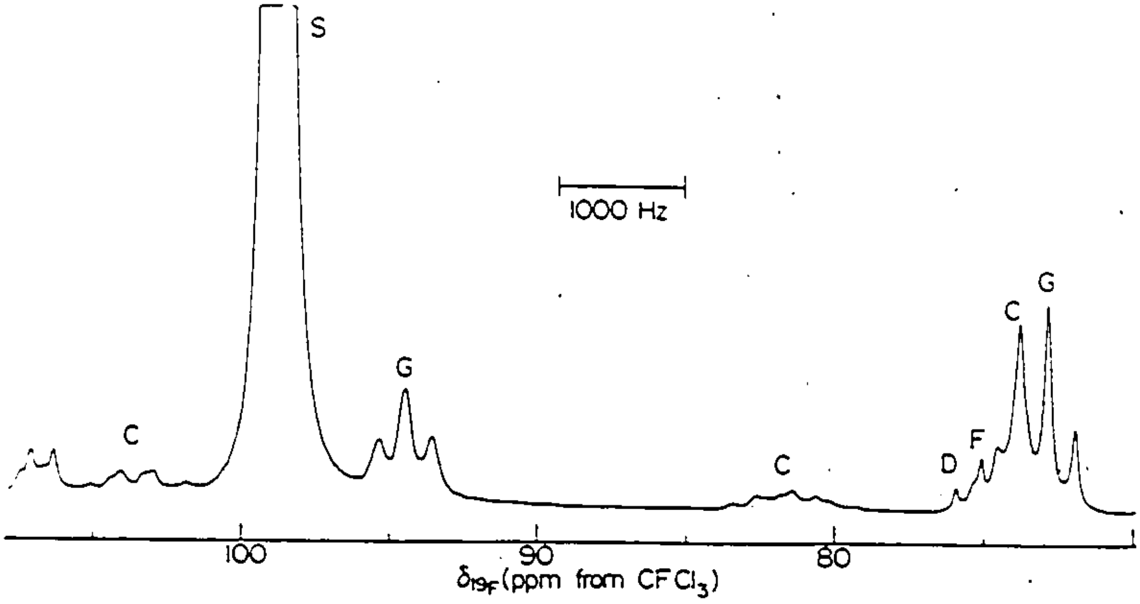

5.3 (d)

Table 5.3

Fluorine-19 NMR parameters for the species observed in the decomposition of cis, cis-$Xe(OIOF_4)_2$

Species	$\delta^{19}F^{a}$ (ppm)		$^{2}J_{FF}$ (Hz)	
cis, cis-$Xe(OIOF_4)_2$	(F_1)	103.6	(1,2)	271
			(1,3)	260
	(F_2)	81.9	(1,2)	274
			(2,3)	b
	(F_3)	73.6	(1,3)	245
			(2,3)	197
trans, trans-$Xe(OIOF_4)_2$		76.6		-
cis, trans-$Xe(OIOF_4)_2$		75.1		-
cis, cis-$F_4OIOOIOF_4$	(A_2)	93.4		216
	(X_2)	71.9		

a: Recorded in SO_2ClF solvent at -40°C and referenced with respect to neat $CFCl_3$ at 24°C.

b: Coupling not resolved.

NMR spectra depicted in Figure 5.3.(a-d) correspond to the products of decomposition after the following time intervals at 0°C: 0 minutes, 10 minutes, 70 minutes and 520 minutes. The ^{19}F NMR parameters are summarized in Table 5.3.

Figure 5.3(a) displays the ^{19}F NMR spectrum recorded on the sample at -40°C before warming to 0°C. The three multiplet resonances (C) correspond to the three fluorine environments associated with cis, cis-$Xe(OIOF_4)_2$ (Chapter 4). The singlet resonances, D and F, are assigned to the fluorines on the trans-OIF_4O groups in cis, trans- and trans, trans-$Xe(OIOF_4)_2$, respectively. In addition to these resonances and the F-on-S(VI) resonance of SO_2ClF (S), two triplets ($\delta^{19}F$ = 93.4 and 71.9 ppm, $^2J_{FF}$ = 216 Hz) labelled G and corresponding to an A_2X_2 pattern (similar to the pattern of cis-$HOIOF_4$) were observed. The possibility that this pattern arises from $HOIOF_4$ contamination has been ruled out since the cis, cis-$Xe(OIOF_4)_2$ used for this experiment had been previously shown by Raman spectroscopy to contain no impurities and the ^{19}F NMR parameters for $HOIOF_4$, recorded in SO_2ClF solvent at -40°C, are sufficiently different (c.f. Table 3.3). The cis, cis-peroxide molecule, $F_4OIOOIOF_4$ (structure 5.1), is expected to display an AMX_2-spin coupling pattern in its ^{19}F NMR spectrum. The observed A_2X_2-pattern is attributed to rapid exchange averaging of fluorine environments and presumably results from the rapid intramolecular exchange of oxygens in the peroxide linkage and the double-bonded oxygens on the -OIF_4O groups. This exchange

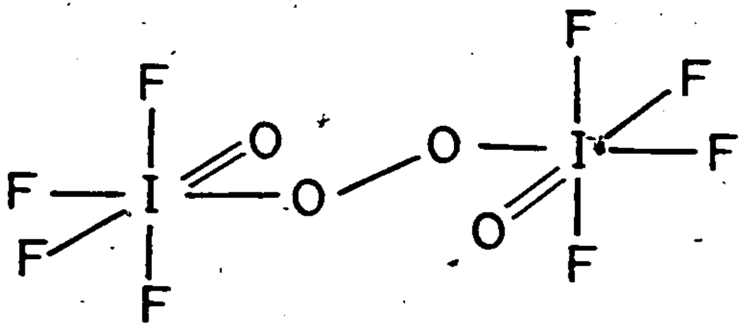

5.1

of the O-O bond, which is unprecedented in any other peroxide species may be envisaged to occur by means of the mechanism represented by scheme (5.8). Alternatively, a dissociative mechanism such as that represented by equation (5.9) may

$$F_4OI\text{-}{}^*O\text{-}O\text{-}IOF_4 \rightleftharpoons [F_4OI\text{-}{}^*O\cdot + F_4OI\text{-}O] \rightleftharpoons F_4{}^*OI\text{-}O\text{-}O\text{-}IOF_4 \quad (5.9)$$

apply. It is believed, however, that the associative intramolecular mechanism depicted in scheme (5.8) would be favored and, in either case, averaging would only be apparent for the cis, cis-peroxide isomer.

Figures 5.3.b - 5.3.d illustrate the intermediate features of the decomposition reaction from the point of Figure 5.3.a onwards. As the reaction proceeds, the decreasing intensities of the resonances arising from $Xe(OIOF_4)_2$ isomers are accompanied by an increase in intensity of the A_2X_2 pattern assigned to cis, cis-$F_4OIOOIOF_4$. This result is consistent with the slow decomposition of the bis Xe(II) compound according to equation (5.10).

$$Xe(OIOF_4)_2 \longrightarrow F_4OIOOIOF_4 + Xe\uparrow \quad (5.10)$$

To gain further support for the above proposal, it was necessary to confirm that the observed ^{19}F NMR resonances truly originate from the peroxide and were not simply a consequence of the manner in which the decomposition was performed. If the

Scheme (5.8)

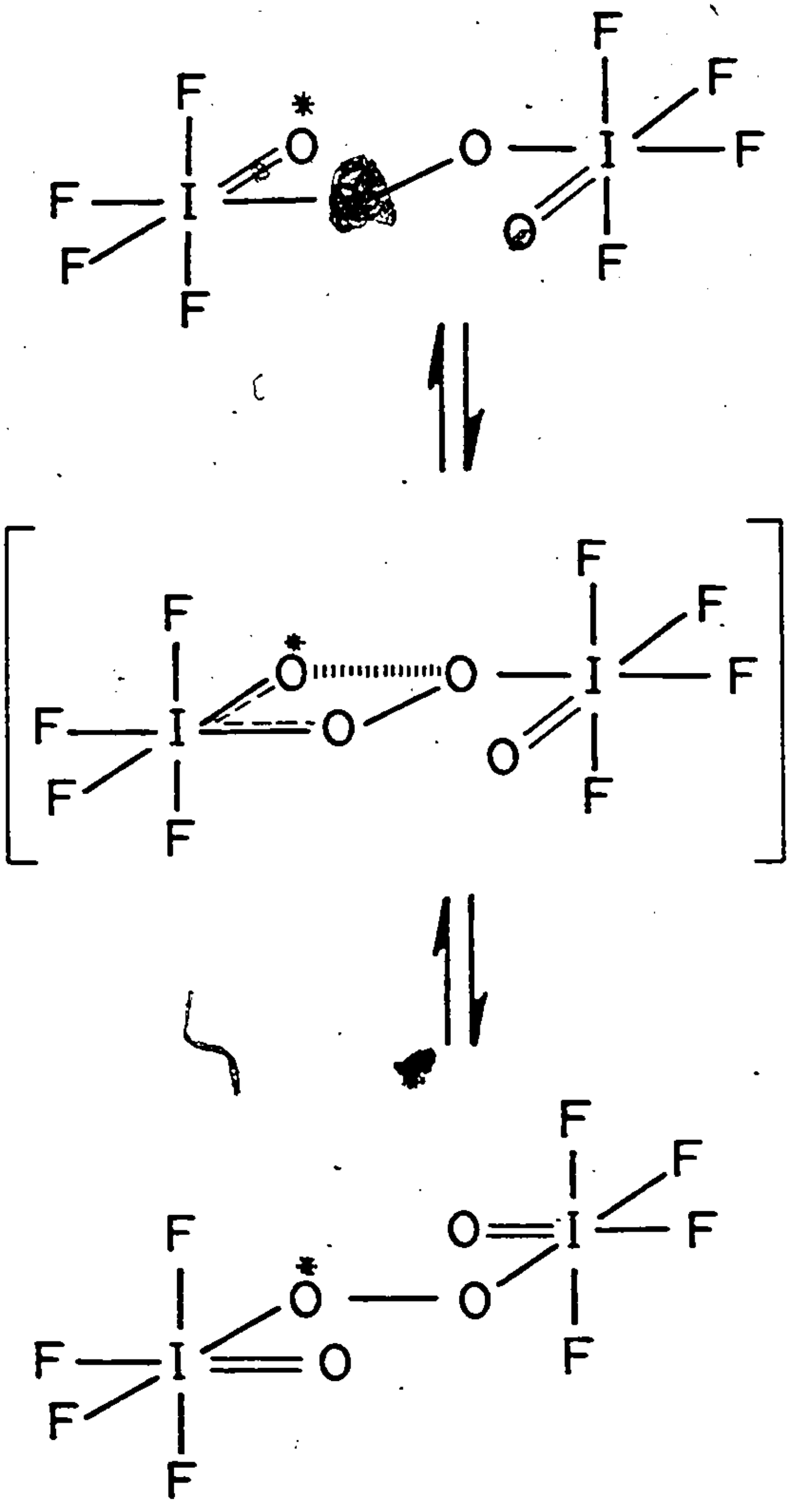

same A_2X_2 resonances could be observed under conditions where peroxide formation is expected to be favored, and by employing a route which is significantly different from that above, then a definitive statement as to whether or not the A_2X_2 pattern represents the peroxide could be made.

(D) THE REACTION OF IO_2F_3 AND KrF_2

In the reactions between KrF_2 and $B(OTeF_5)_3$, Seppelt and Lentz (140,141) have reported the quantitative formation of the peroxide, $F_5TeOOTeF_5$. This result implies the intermediate krypton(II) derivative, $Kr(OTeF_5)_2$, which is thermally unstable decomposing to the peroxide and Kr gas. Although there is no $-OIF_4O$ analogue of $B(OTeF_5)_3$, there is an alternative method for preparing $-OIF_4O$ derivatives.

In an attempt to prepare krypton derivatives containing $-OIF_4O$, by analogy with the xenon(II) derivatives, mixtures of IO_2F_3 and KrF_2 were investigated in SO_2ClF and BrF_5 solvents by ^{19}F NMR spectroscopy. By analogy with the IO_2F_3/XeF_2 system (Chapter 4), IO_2F_3 was expected to insert into a Kr-F bond according to equations (5.11) and (5.12). It was anticipated

$$IO_2F_3 + KrF_2 \rightleftharpoons FKrOIOF_4 \qquad (5.11)$$

$$IO_2F_3 + FKrOIOF_4 \rightleftharpoons Kr(OIOF_4)_2 \qquad (5.12)$$

that the krypton derivatives formed may also be unstable decomposing according to equation (5.13).

$$Kr(OIOF_4)_2 \longrightarrow Kr\uparrow + F_4OIOOIOF_4 \qquad (5.13)$$

The ^{19}F NMR spectrum resulting from a mixture of KrF_2 and excess IO_2F_3, recorded at -45°C and before the contents were allowed to warm, is depicted in Figure 5.4. The ^{19}F NMR parameters are summarized in Table 5.4. Figure 5.4 depicts resonances which can be assigned to IO_2F_3 (A) and the solvent, SO_2ClF (S), by comparison of the ^{19}F chemical shifts with those determined for these species in Chapter 3. The intense singlet resonance (C, $\delta^{19}F$ = 85.4 ppm) is assigned to unreacted KrF_2 by comparison with the previously reported chemical shifts of this species (114). In addition to these resonances, two triplets (B) representing an A_2X_2 pattern are observed whose chemical shifts are identical to those obtained in the bis decomposition reaction discussed above. After warming the sample to room temperature, gas evolution was apparent and was controlled by intermittent cooling in liquid nitrogen. The warming and quenching cycles were repeated until gas evolution ceased (^{19}F NMR spectra were recorded after each cooling), at which time the decomposition was judged to be complete. The ^{19}F NMR spectrum was again recorded at -45°C and is depicted in Figure 5.5. In Figure 5.5, excess IO_2F_3 (A) is still observed as well as an intensified A_2X_2 pattern (B), but no KrF_2 is evident. The intensity of the A_2X_2 pattern has

Table 5.4

Fluorine-19 NMR parameters for the IO_2F_3/KrF_2 system recorded in SO_2ClF solvent at -45°C

Species		$\delta^{19}F^{a}$ (ppm)	$^2J_{FF}$ (Hz)
KrF_2		85.4	-
cis, cis-$F_4OIOOIOF_4$	(A2)	93.8	214
	(X_2)	72.5	
IO_2F_3[b]	(X_2)	108.2	175
	(X_2')	107.8	174

a: Referenced with respect to neat $CFCl_3$.

b: The A and A' resonances are not resolved.

Figure 5.4

The ^{19}F NMR spectrum of the IO_2F_3/KrF_2 system recorded in SO_2ClF solvent at -45°C before warming. The peak assignments are given below.

Peak	Assignment
A	IO_2F_3
B	$F_4OIOOIOF_4$
C	KrF_2
S	SO_2ClF solvent

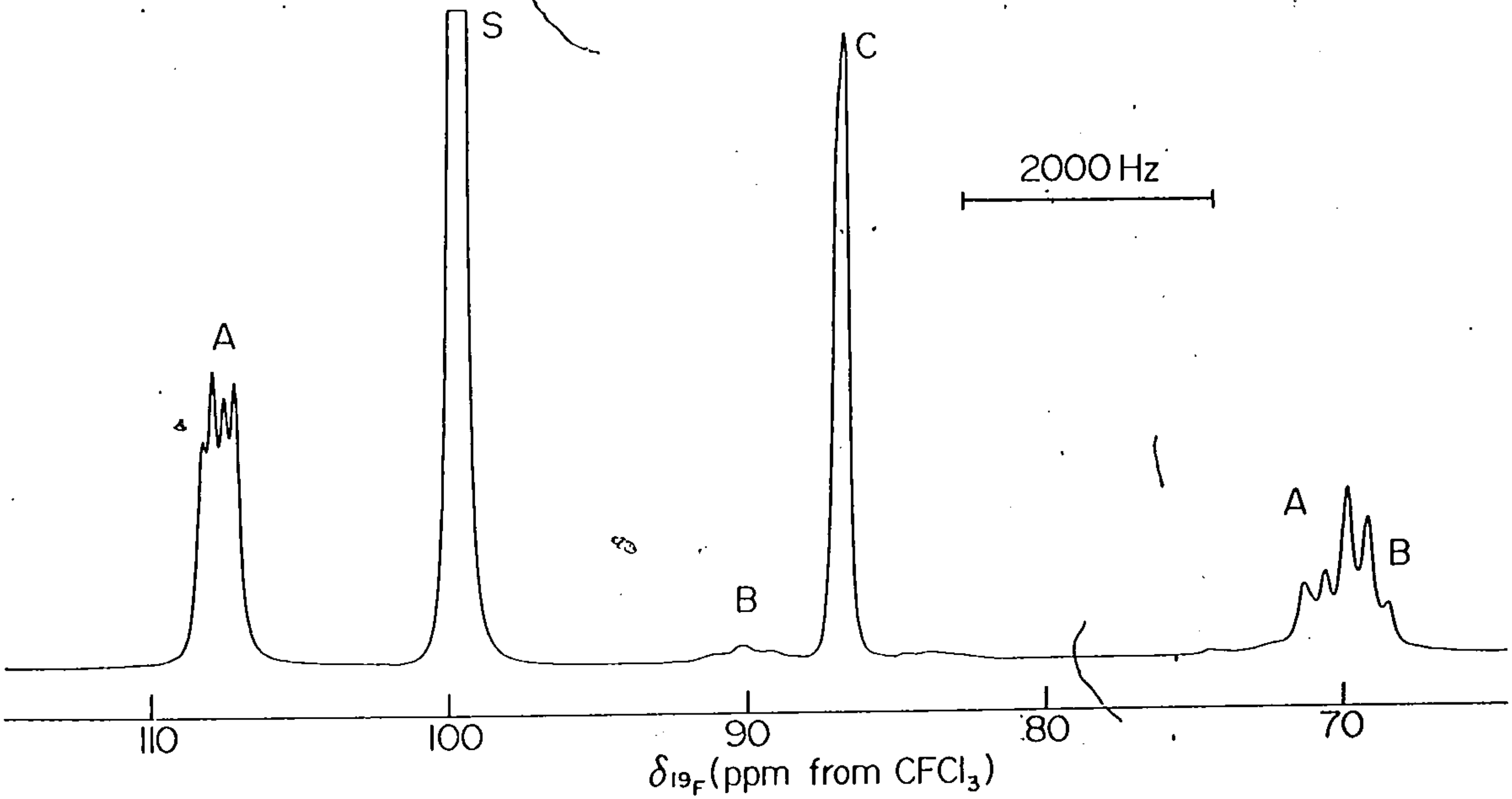

A
S
C
2000 Hz
B
A
B
110
100
90
80
70
δ_{19F} (ppm from CFCl$_3$)

Figure 5.5

The ^{19}F NMR spectrum of the IO_2F_3/KrF_2 system recorded in SO_2ClF solvent at -45°C after warming to the point where gas evolution had ceased. The peak assignments are given below.

Peak	Assignment
A	IO_2F_3
B	$F_4OIOOIOF_4$
S	SO_2ClF solvent

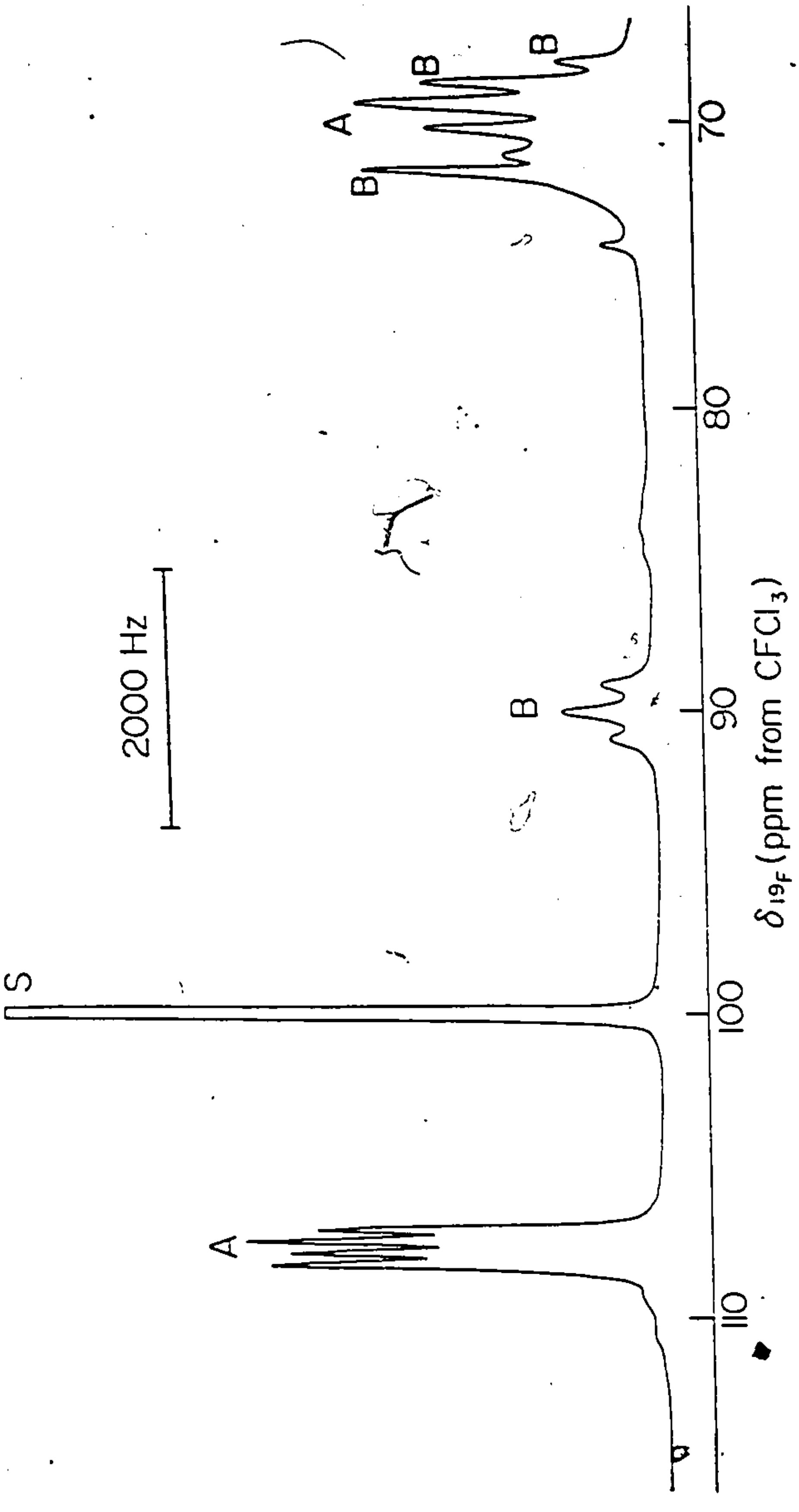

A
B
B
A
B
B
S
A
2000 Hz
70
80
90
100
110
$\delta_{^{19}F}$ (ppm from $CFCl_3$)

increased significantly over that in the initial spectrum (Figure 5.4), confirming that the species associated with this pattern was indeed formed by reaction with KrF_2. Furthermore, the close similarity of the chemical shifts and splittings of the A_2X_2 patterns in Figures 5.3 and 5.5 confirm these resonances arise from the same species, namely, $F_4OIOOIOF_4$. At no time in the course of this reaction could species corresponding to the intermediates $FKrOIOF_4$ and $Kr(OIOF_4)_2$ be observed.

(E) THE ISOLATION AND CHARACTERIZATION OF $F_4OIOOIOF_4$

In an effort to obtain further definitive evidence for the peroxide, attempts were made to isolate it as a pure compound. Routes which involved the use of solvents were avoided in light of the complicating features which may arise as a result of solvent attack (Chapter 4). Solid samples of pure cis, cis-$Xe(OIOF_4)_2$ were allowed to decompose at 0°C under dynamic vacuum with cold-trapping of the products at -196°C. In each case, after the decomposition was complete, small amounts of involatile white material remained in the decomposition vessel which were subsequently identified by Raman spectroscopy as IO_2F and IOF_3. The material which was trapped at -196°C consisted of a gaseous component, identified as Xe gas (pumped off at -78°C), as well as a solid component which was examined by ^{19}F NMR spectroscopy and Raman spectroscopy.

The ^{19}F NMR spectrum of the solid residue dissolved in $CFCl_3$ solvent and recorded at -40°C is shown in Figure 5.6 and the ^{19}F NMR parameters are summarized in Table 5.5. The spectrum, which shows several multiplets and singlets, is much more complex than any of the previous peroxide spectra, and it is evident that the spectrum cannot be attributed to a single species. A number of possibilities exist which may account for the complexity of this spectrum. The cis-OIF_4O groups, associated with the cis., cis- and cis, trans-isomers of $F_4OIOOIOF_4$, are each expected to display A_2X_2 patterns in the ^{19}F NMR spectrum for the reasons given earlier. In addition, the trans-isomers are expected to yield singlet resonances in the ^{19}F NMR spectrum as a result of four equivalent fluorines in a single equatorial environment. The appearance of complex multiplets in Figure 5.6 can therefore not be accounted for in terms of peroxide species only. The multiplet patterns (B) in this spectrum resemble the patterns which were previously assigned to the cis-OIF_4O groups of $FXeOIOF_4$ and $Xe(OIOF_4)_2$ in Chapter 4. One group of compounds which could account for these "extra" resonances are the cis, cis-, cis, trans- and trans, trans-isomers of the oxide, $F_4OIOIOF_4$, which could form according to equation (5.14). Analogous thermal decompositions

$$F_4OIOOIOF_4 \longrightarrow F_4OIOIOF_4 + \tfrac{1}{2} O_2 \qquad (5.14)$$

occur for the peroxides, $F_5TeOOTeF_5$ and $F_5SeOOSeF_5$, yielding

Table 5.5

Fluorine-19 NMR parameters for the species observed in the thermal decomposition of cis, cis-$Xe(OIOF_4)_2$

Species	$\delta^{19}F^{a}$ (ppm)	$^{2}J_{FF}$ (Hz)
cis, cis-$F_4OIOOIOF_4$	(A_2) 88.3	216
	(X_2) 69.0	
trans, trans-$F_4OIOOIOF_4$	(A_4) 70.6	-
trans, trans-$F_4OIOIOF_4$	(A_4) 85.8	-
$IO_2F_3{}^{b}$	(X_2') 108.3	171
	(X_2) 107.9	181
IF_5	(A) 57.9	87
	(X_4) 11.2	
IOF_3	48.6	-
IO_2F	40.8	-

a: Recorded at -40°C in $CFCl_3$ and referenced with respect to neat external $CFCl_3$ at 24°C.

b: The A and A' resonances are not resolved.

Figure 5.6

The ^{19}F NMR spectrum of the products of the controlled thermal decomposition of cis, cis-Xe($OIOF_4$)$_2$ recorded in $CFCl_3$ solvent at -40°C. The peak assignments are given below.

Peak	Assignment
A	$F_4OIOOIOF_4$
B	$F_4OIOIOF_4$

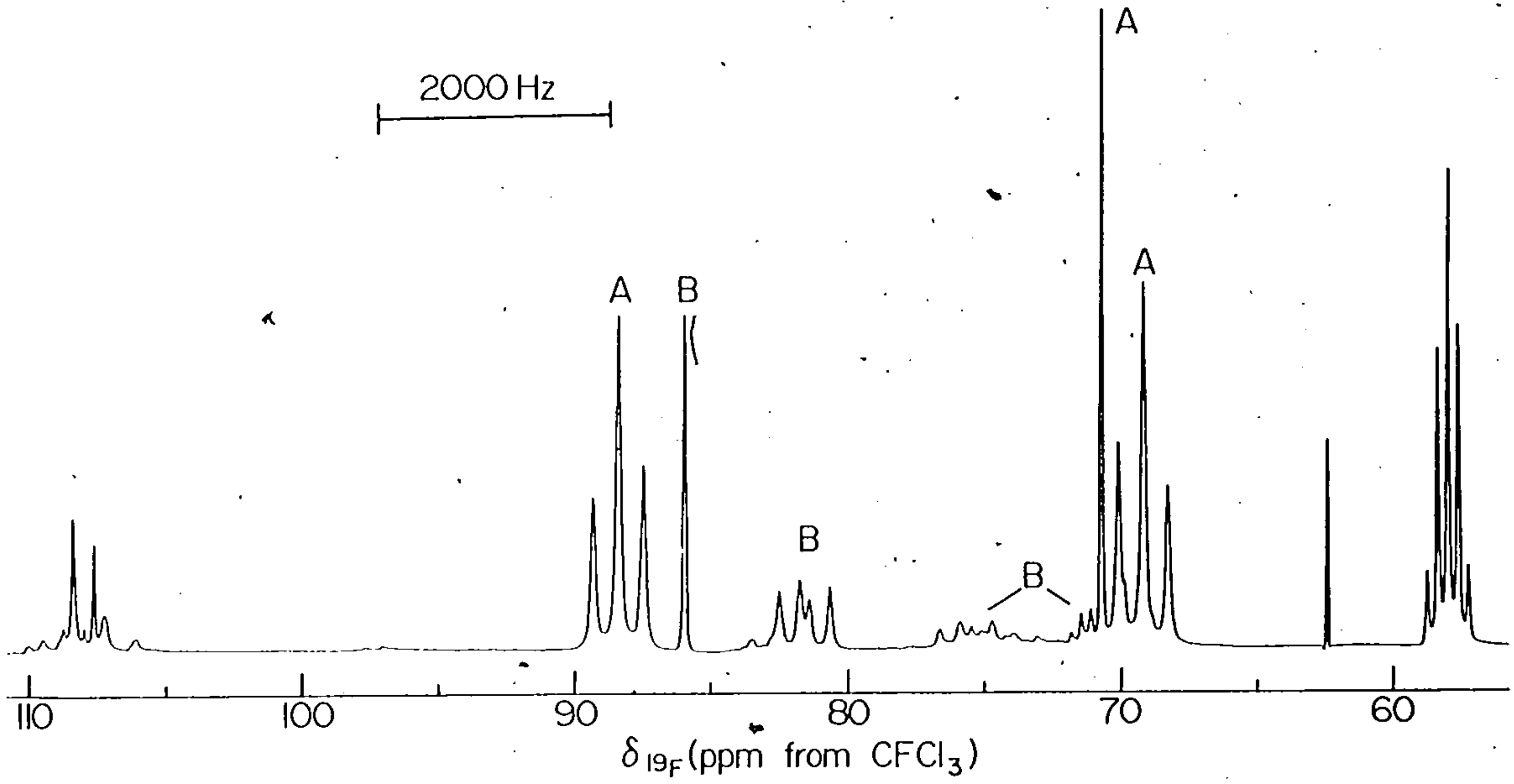
2000 Hz
A
A
A
B
B
B
B
110
100
90
80
70
60
δ19F (ppm from CFCl3)

the stable oxides, $F_5TeOTeF_5$ and $F_5SeOSeF_5$ (225,230,231). The trans-isomers of the oxides are expected to yield singlet resonances in the ^{19}F NMR spectrum as is the case for the trans-peroxides. The cis-OIF_4O groups associated with the cis, cis- and cis, trans-isomers of $F_4OIOIOF_4$ are, however, expected to display AMX_2-type patterns in the ^{19}F NMR spectrum, since in these cases, the exchanging of oxygens observed in the peroxide cases is not expected to occur.

In Figure 5.6, the A_2X_2 pattern ($\delta^{19}F$ (A_2) = 88.3 ppm, (X_2) = 69.0 ppm; $^2J(FF)$ = 216 Hz), labelled A, is assigned to the peroxide, cis, cis-$F_4OIOOIOF_4$, by comparison with the chemical shift and $^2J(FF)$ coupling constant previously determined for this species. The singlet at $\delta^{19}F$ = 70.6 ppm, also l~~abelled~~ A, represents an A_4 spin system associated with a trans-OIF_4O group and is tentatively assigned to trans, trans-$F_4OIOOIOF_4$. The assignments for the three multiplet resonances and the singlet resonance (B) are uncertain. These multiplet resonances collectively resemble an AMX_2-type pattern and therefore must represent a cis-OIF_4O group. Of the two possibilities in this case, cis, cis- or cis, trans-$F_4OIOIOF_4$, the assignment is tentatively made to the cis, cis-isomer since this isomer is the one expected to result from the decomposition of cis, cis-$F_4OIOOIOF_4$ according to equation (5.14). Using similar arguments, the singlet resonance (B, $\delta^{19}F$ = 85.8 ppm) could be assigned to trans, trans-$F_4OIOIOF_4$ since this species is expected to result from the decomposition of trans, trans-$F_4OIOOIOF_4$ according to equation (5.14). At high-frequency, there is a partially resolved triplet ($\delta^{19}F$ = 107.1 ppm) of unknown origin as well as two doublets ($\delta^{19}F$ = 108.3, $^2J(FF)$ = 171 Hz; $\delta^{19}F$ = 107.9 ppm, $^2J(FF)$ = 181 Hz) which are assigned to the X_2' and X_2 portions, respectively, of the $A'X_2'$ and AX_2 patterns of IO_2F_3. The triplets arising from the A' and A portions of the IO_2F_3 spectrum are presumably overlapped by the low-frequency triplet of cis, cis-$F_4OIOOIOF_4$ and are therefore not observed. The IO_2F_3 resonances as well as the low-frequency quintet (δ^{19} = 57.9 ppm, $^2J(FF)$ = 87 Hz) assigned to IF_5 and the singlets ($\delta^{19}F$ = 40.8 and 48.6 ppm) assigned to IO_2F and IOF_3 suggest two possible modes of decomposition for the oxide according to equations (5.15) and (5.16).

$$F_4OIOIOF_4 \longrightarrow IO_2F_3 + IF_5 + \tfrac{1}{2}\, O_2 \uparrow \qquad (5.15)$$

$$F_4OIOIOF_4 \longrightarrow IF_5 + IOF_3 + O_2 \uparrow \qquad (5.16)$$

The ^{19}F NMR results discussed to this point have provided strong evidence for peroxide species. The Raman spectrum recorded on the decomposition product of cis, cis-$Xe(OIOF_4)_2$ is depicted in Figure 5.7 and also supports the presence of a peroxide as well as the proposed I(V) decomposition products IOF_3 and IO_2F. The vibrational frequencies and tentative assignments are given in Table 5.6.

A peroxide molecule containing a cis $O\text{-}OIF_4O$ moiety of

Table 5.6

The vibrational frequencies for the Raman spectrum recorded on the decomposition products of cis, cis-$Xe(OIOF_4)_2$

Frequency[a] (cm^{-1})	Tentative Assignment
921 (5)	b
908 (79)	ν (O--O)
873 (12)	b
805 (25)	c
786 (6)	c
748 (16)	c
696 (19)	ν asym $(IF_2)_{ax}$. cis
677 (100)	ν sym (IF_4) trans
650 (sh)	b
647 (38)	ν sym $(IF_2)_{ax}$. cis
639 (15)	ν asym $(IF_2)_{eq}$. cis
630 (10)	b
619 (32)	
604 (37)	ν sym $(IF_2)_{eq}$. cis
599 (32)	
545 (12)	b
507 (7)	b
424 (6)	
419 (10)	
377 (5)	b

continued...

Table 5.6 continued

Frequency[a] (cm^{-1})	Tentative Assignment
342 (5)	b
332 (8)	c
290 (10)	b
279 (2)	
265 (3)	
235 (2)	
177 (3)	
165 (1)	
160 (1)	
148 (1)	
121 (4)	
115 (4)	
105 (3)	b
88 (3)	
76 (5)	
49 (22)	
37 (23)	

a: Recorded at -196°C in glass tube.

b: This band is coincident with IOF_3 (from ref 208).

c: This band is coincident with IO_2F (from ref 208).

Figure 5.7

The Raman spectrum recorded on the decomposition products of cis, cis-$Xe(OIOF_4)_2$ in a glass tube at -196°C.

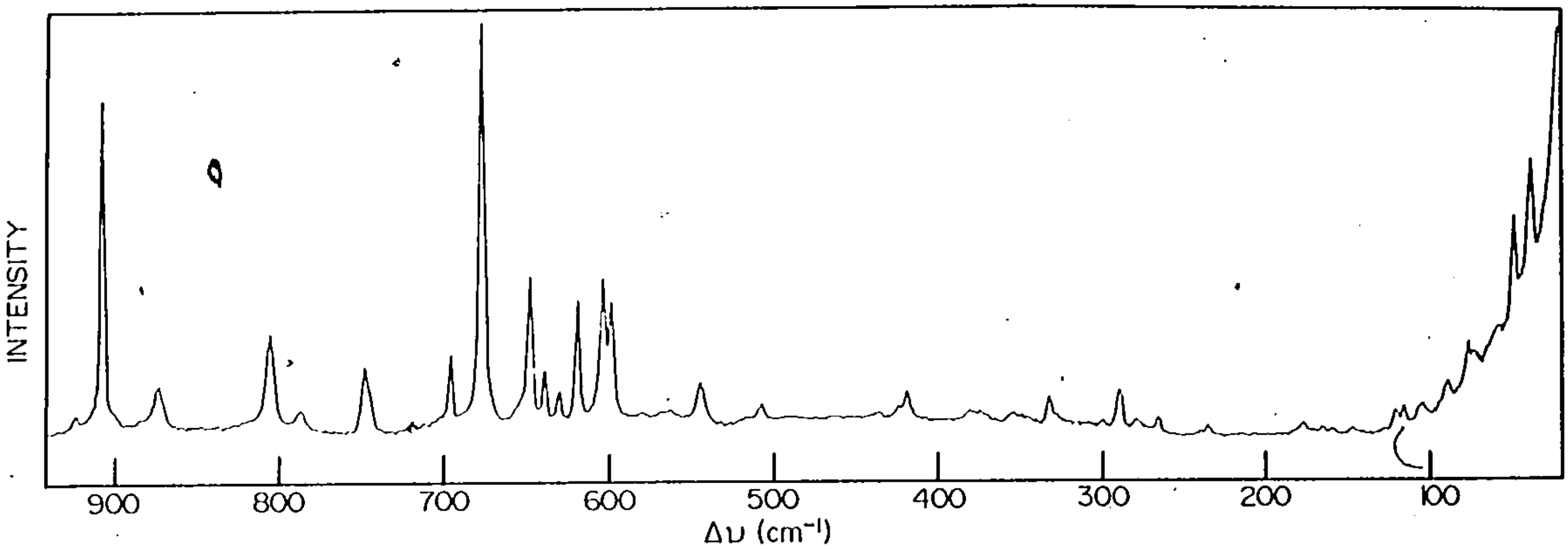
INTENSITY
900
800
700
600
500
400
300
200
100
Δυ (cm⁻¹)

symmetry C_s should possess 18 fundamental modes classified as 12 A' + 6 A". All of these are active in the Raman. Alternatively, a trans O-OIF$_4$O moiety of approximate C_{4v} symmetry should possess 13 fundamentals, with symmetry classifications 5 A_1 + 2 B_1 + B_2 + 5 E, all of which are Raman active. A mixture of the two groups could therefore yield up to 31 vibrational bands (ignoring factor-group splitting and intramolecular coupling) in the Raman spectrum. In addition to these, a series of bands representing the I(V) species IO_2F, IOF_3 and IF_5 are also expected.

In Figure 5.7 there are 31 bands observed in the frequency range 100 and 927 cm^{-1} which includes those assignable to I(V) species (Table 5.6). The most outstanding feature of the spectrum is the intense band at 908 cm^{-1} which can be assigned to the O-O stretch of the peroxide linkage. The frequency is in excellent agreement with the O-O stretching frequencies for other ligand group peroxides, namely, $F_5TeOOTeF_5$ 907 cm^{-1} (225) and $F_5SeOOSeF_5$ 903 cm^{-1} (225). The bands which are assigned to the I(V) species are so designated in Table 5.6. These assignments were made on the basis of the vibrational spectra for IO_2F and IOF_3 reported previously (207,208). It is unclear why Figure 5.7 shows only some bands which can be assigned to IF_5 (227), since, the presence of both IOF_3 and IO_2F in this spectrum, requires that IF_5 be present as well. It must therefore be assumed that the IF_5 is present, but somehow occluded by other species in the sample. There are five bands in region 600 - 700 cm^{-1} which are not assignable to any of the I(V) species. Although the assignments of these bands cannot be made with any certainty, their positions are consistent with those expected for I-F stretches. For instance, the intense band at 677 cm^{-1} resembles the ν_2 mode of IOF_5 (210,211) in both intensity and frequency and may in fact represent the IF_4 symmetric stretching mode of a trans-OIF_4O group, or alternatively, may correspond to the overlapping I-F stretches of cis- and trans-isomers. The bands occurring at 604 and 639 cm^{-1} and 647 and 696 cm^{-1} can be envisaged as arising from the symmetric and asymmetric equatorial and axial I-F stretches, respectively, of a cis-OIF_4O group. The remainder of the bands in Figure 5.7 (<600 cm^{-1}), which cannot be assigned to I(V) species, most certainly represent bending modes, but again, cannot be assigned with any certainty and are therefore not attempted.

(F) SUMMARY

The results discussed in this Chapter are important to the overall understanding of -OIF_4O derivative chemistry and have been used as a basis, in other Chapters, for understanding the complex reaction chemistry that takes place. In particular, the proposed peroxide, which has been encountered in both the Xe(II) and higher oxidation state systems, will most certainly provide insight into other -OIF_4O derivative systems yet to be investigated. It is clear that a better characterization of the peroxide is necessary. This will have to involve refinement of a "clean" preparative method which would ultimately yield a pure derivative(s). The low-temperature photolytic decomposition of cis, cis-$Xe(OIOF_4)_2$ as well as other alternative methods are currently under investigation in this laboratory as viable routes to the peroxide.

CHAPTER 6

XENON(IV) (VI) AND (VIII) DERIVATIVES OF THE $-OIF_4O$ GROUP

(A) INTRODUCTION

Xenon compounds in their +4, +6 and +8 oxidation states are presently limited to the simple binary fluorides, oxides and oxide fluorides cited earlier, and the $-OTeF_5$ derivatives of Xe(IV) and Xe(VI) (139,140,142). Although a report by Eisenberg and DesMarteau (156) claimed that XeF_4 and XeF_6 react with HSO_3F to give the covalently bonded fluorosulfate derivatives $F_2Xe(OSO_2F)_2$ and $F_4Xe(OSO_2F)_2$, respectively, this claim was later shown to be erroneous (109,157). The $-OTeF_5$ derivatives, $Xe(OTeF_5)_4$ (139), $OXe(OTeF_5)_4$ (140), $Xe(OTeF_5)_6$ (140) and $O_2Xe(OTeF_5)_2$ (142) have been reported as the products obtained from the stoichiometric reactions of the respective fluorides or oxide fluorides with the ligand transfer reagent $B(OTeF_5)_3$ (equation 1.7). Since no $B(OTeF_5)_3$ analogue or other suitable ligand transfer reagent exists for any other potential ligand, it is not surprising that higher oxidation state derivatives of these groups have not yet been prepared. The $-OTeF_5$ derivatives $Xe(OTeF_5)_4$, $OXe(OTeF_5)_4$ and $O_2Xe(OTeF_5)_2$ have been characterized in the solid state by Raman spectroscopy, and in solution, together with all possible mixed $F/-OTeF_5$ derivatives, by ^{129}Xe and ^{19}F NMR spectroscopy (142).

In the present work, $-OIF_4O$ derivatives of Xe(IV) and Xe(VI), resulting from the insertion reactions of IO_2F_3 with the binary fluorides XeF_4 and $XeOF_4$, have been observed in solution by ^{129}Xe and ^{19}F NMR spectroscopy. In addition, mixed derivatives of xenon(VI), resulting from the displacement of $HOTeF_5$ from $OXe(OTeF_5)_4$ by the stronger protonic acid $HOIOF_4$, have been observed in solution with the use of ^{129}Xe NMR spectroscopy. A mixture of solid derivatives has also been isolated from the stoichiometric reaction of $OXe(OTeF_5)_4$ with $HOIOF_4$. The low-temperature Raman spectrum of the solid as well as the ^{129}Xe spectrum recorded in solution, suggest that a mixture of novel xenon(VIII) derivatives is formed containing both $-OTeF_5$ and cis- and trans- $-OIF_4O$ groups.

(B) THE PREPARATION OF $F_3XeOIOF_4$ AND THE POSSIBLE FORMATION OF $OXeF_3OIOF_4$ AND THEIR CHARACTERIZATION IN SOLUTION BY NMR SPECTROSCOPY

(i) The IO_2F_3/XeF_4 System

As a result of the previous success at preparing Xe(II) derivatives in solution by the reaction of IO_2F_3 and XeF_2 (Chapter 4), a similar approach was taken in pursuit of a Xe(IV) derivative. Consequently, IO_2F_3 and XeF_4 were combined in $CFCl_3$ solvent with the view to insert IO_2F_3 into the Xe-F bonds of XeF_4 according to equation (6.1). The ^{129}Xe NMR

$$XeF_4 + n\ IO_2F_3 \rightleftharpoons F_{4-n}Xe(OIOF_4)_n \qquad (6.1)$$

spectrum of a 1:1.978 molar mixture of XeF_4 and IO_2F_3 recorded in $CFCl_3$ solvent at 24°C is depicted in Figure 6.1 and the ^{129}Xe NMR parameters are summarized in Table 6.1. Figure 6.1 shows, in addition to the outermost peak of the XeF_4 quintet (*) ($\delta^{129}Xe$ = 186.45 ppm; $^1J(^{129}Xe-^{19}F)$ = 3808 Hz), a doublet of triplets with unresolved fine structure ($\delta^{129}Xe$ = 24.42 ppm) which is assigned to the Xe(IV) derivative, $F_3XeOIOF_4$ (structure 6.1), based on the observed spin-spin coupling pattern and a comparison with the NMR data for the analogous molecule $F_3XeOTeF_5$ recorded in $CFCl_3$ solvent at 24°C (142). In addition, although the long range spin-spin coupling between the fluorines on the $-OIF_4O$ group and the xenon nucleus is not resolved, the F-on-I(VII) region of the ^{19}F NMR spectrum (discussed below) indicates that the cis-isomer is formed exclusively.

A species such as $F_3XeOIOF_4$, which contains the F_3Xe moiety, is expected to display a doublet of triplets in its ^{129}Xe NMR spectrum by virtue of the spin-spin coupling of two directly bonded magnetically non-equivalent fluorines (F',F) with the xenon nucleus. A similar pattern is observed in the ^{129}Xe NMR spectrum of $F_3XeOTeF_5$ (142). Furthermore, no other Xe(IV) species would give rise to such a spin-spin coupling pattern. The ^{129}Xe chemical shift (24.42 ppm) occurs to high frequency of the analogous shift in $F_3XeOTeF_5$ ($\delta^{129}Xe$ = -25.5 ppm), indicating that the xenon nucleus in the $-OIF_4O$ derivative is less shielded than in the $-OTeF_5$ derivative.

Table 6.1

Xenon-129 (69.56 MHz) and ^{19}F (235.36 MHz) NMR Parameters for a 1:1.978 XeF_4/IO_2F_3 Mixture Recorded at 24°C

Species	$\delta^{129}Xe$ (ppm)[a]	$\delta^{19}F$ (ppm)[b]	$^1J(^{129}Xe-^{19}F)$ (Hz)	$^2J(^{19}F-^{19}F)$ (Hz)
$F'F_2XeOIOF_4$	24.42	8.98 (F') -8.65 (F)	3417 (F') 3658 (F)	370
XeF_4	186.45	-13.94	3808	-
$FXeOIOF_4$ cis-	-1941.8	-	5844	-
$FXeOIOF_4$ trans-	-1835.7	-	5874	-
$Xe(OIOF_4)_2$ (cis, trans-)	-2101.4	-	-	-
$Xe(OIOF_4)_2$ (cis, cis-)	-2208.9	-	-	-

a: Referenced with respect to neat $XeOF_4$ at 24°C.

b: Referenced with respect to neat $CFCl_3$ at 24°C.

Figure 6.1

The ^{129}Xe NMR spectrum (69.56 MHz) for a 1:1.978 molar mixture of XeF_4/IO_2F_3 recorded in $CFCl_3$ solvent at 24°C.

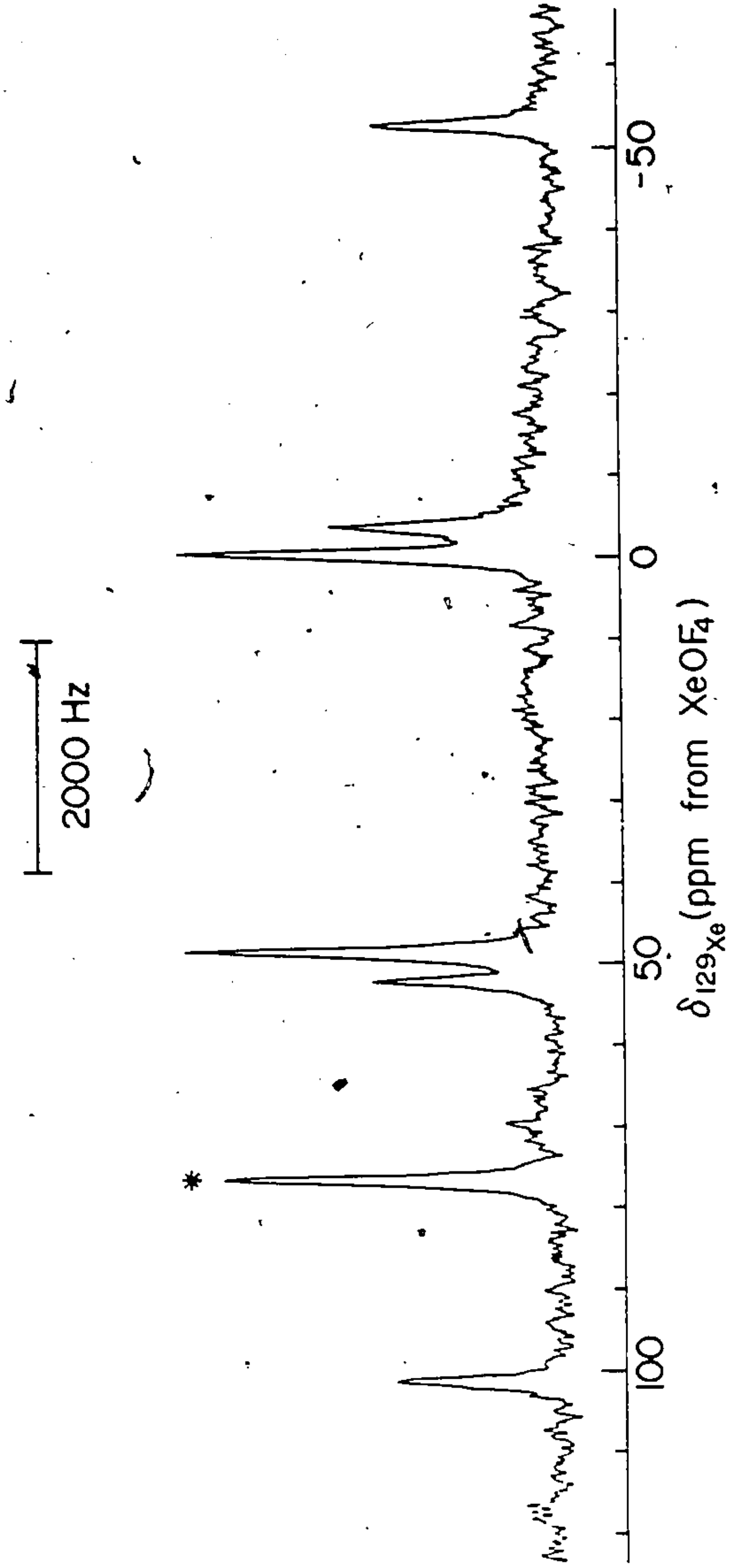
2000 Hz
*
-50
0
50
100
$\delta_{^{129}Xe}$ (ppm from $XeOF_4$)

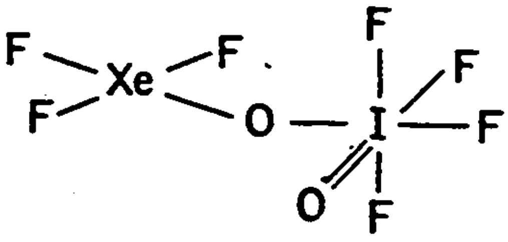

(6.1)

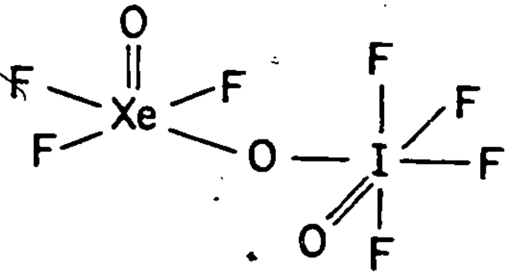

(6.2)

This is consistent with the electronegativity trend established in Chapter 4. The directly bonded spin-spin couplings between the xenon nucleus and the axial fluorine F' (3417 Hz) and two equatorial fluorines F (3658 Hz) are the same order of magnitude as the analogous couplings in $F_3XeOTeF_5$, 3733 and 3552 Hz, respectively. Further evidence in support of the formulation, $F_3XeOIOF_4$, was obtained from the ^{19}F NMR spectrum recorded on the same sample at 24°C. These results are summarized in Table 6.1. The ^{19}F chemical shifts of the axial fluorine F' (8.98 ppm) and equatorial fluorines F (-8.65 ppm) are similar to those reported for $F_3XeOTeF_5$ (-11.98 and 5.87 ppm, respectively). In addition, the fluorine-fluorine spin-spin coupling observed in the $F_3XeOIOF_4$ molecule, 370 Hz, is comparable to the analogous coupling in $F_3XeOTeF_5$ (355 Hz) (142). The F-on-I(VII) region of the spectrum containing several broad and overlapping multiplet patterns (similar to the IO_2F_3/XeF_2 system studied in $CFCl_3$ solvent, Chapter 4), nevertheless provides no evidence for a trans-isomer of $F_3XeOIOF_4$, which would display a singlet resonance in the F-on-I(VII) region. In addition, if both a cis- and trans-isomer of $F_3XeOIOF_4$ were formed in this system, the ^{129}Xe NMR spectrum would display two unique "doublets of triplets", which is clearly not the case. In light of these observations, the new derivative, $F_3XeOIOF_4$, is assigned as the cis-isomer (Structure 6.1). The fact that the long-range spin-spin coupling between the four fluorines-on-iodine(VII) and the xenon nucleus is not resolved in the ^{129}Xe spectrum, also supports assignment to the cis-isomer since, in the xenon(II) system (Chapter 4), the long range spin-spin coupling was not resolved for cis-$FXeOIOF_4$ or cis, cis-$Xe(OIOF_4)_2$.

The xenon(II) region of the ^{129}Xe NMR spectrum was recorded on the same sample immediately after the xenon(IV) data were obtained. This spectrum, also recorded at 24°C, is displayed in Figure 6.2 and the ^{129}Xe NMR parameters are provided in Table 6.1. The spectrum shows four xenon(II) resonances which are readily assigned by comparison with the ^{129}Xe NMR chemical shifts determined in Chapter 4 (Table 4.1) to trans-$FXeOIOF_4$ ($\delta^{129}Xe$ = -1835.7 ppm, $^1J(^{129}Xe-^{19}F)$ = 5874 Hz), cis-$FXeOIOF_4$ ($\delta^{129}Xe$ = -1941.8 ppm, $^1J(^{129}Xe-^{19}F)$ = 5844 Hz), cis, trans-$Xe(OIOF_4)_2$ ($\delta^{129}Xe$ = -2101.4 ppm) and cis, cis-$Xe(OIOF_4)_2$ ($\delta^{129}Xe$ = -2208.9 ppm). As was the case in the IO_2F_3/XeF_2 system studied in $CFCl_3$ solvent, the cis-isomers are favored over trans-isomers as reflected in the integrated ratios for cis:trans $FXeOIOF_4$ of 7.3:1 and for $Xe(OIOF_4)_2$, a cis, cis : cis, trans ratio of 7.1:1. Moreover, the bis-isomers are favored over the mono-isomers (5.5:1). The presence of bis xenon(II) species in the IO_2F_3/XeF_4 system implies that a higher substituted derivative was initially formed, possibly $F_2Xe(OIOF_4)_2$, which could be expected to decompose according to equation (6.2). Decomposition route

$$2\ F_2Xe(OIOF_4)_2 \longrightarrow Xe(OIOF_4)_2 + 2\ IF_5 + XeF_2 + 2\ O_2 \uparrow \qquad (6.2)$$

Figure 6.2

The ^{129}Xe NMR spectrum (69.56 MHz) of a 1:1.978 molar mixture of XeF_4/IO_2F_3 recorded in $CFCl_3$ solvent at 24°C showing the xenon(II) region.

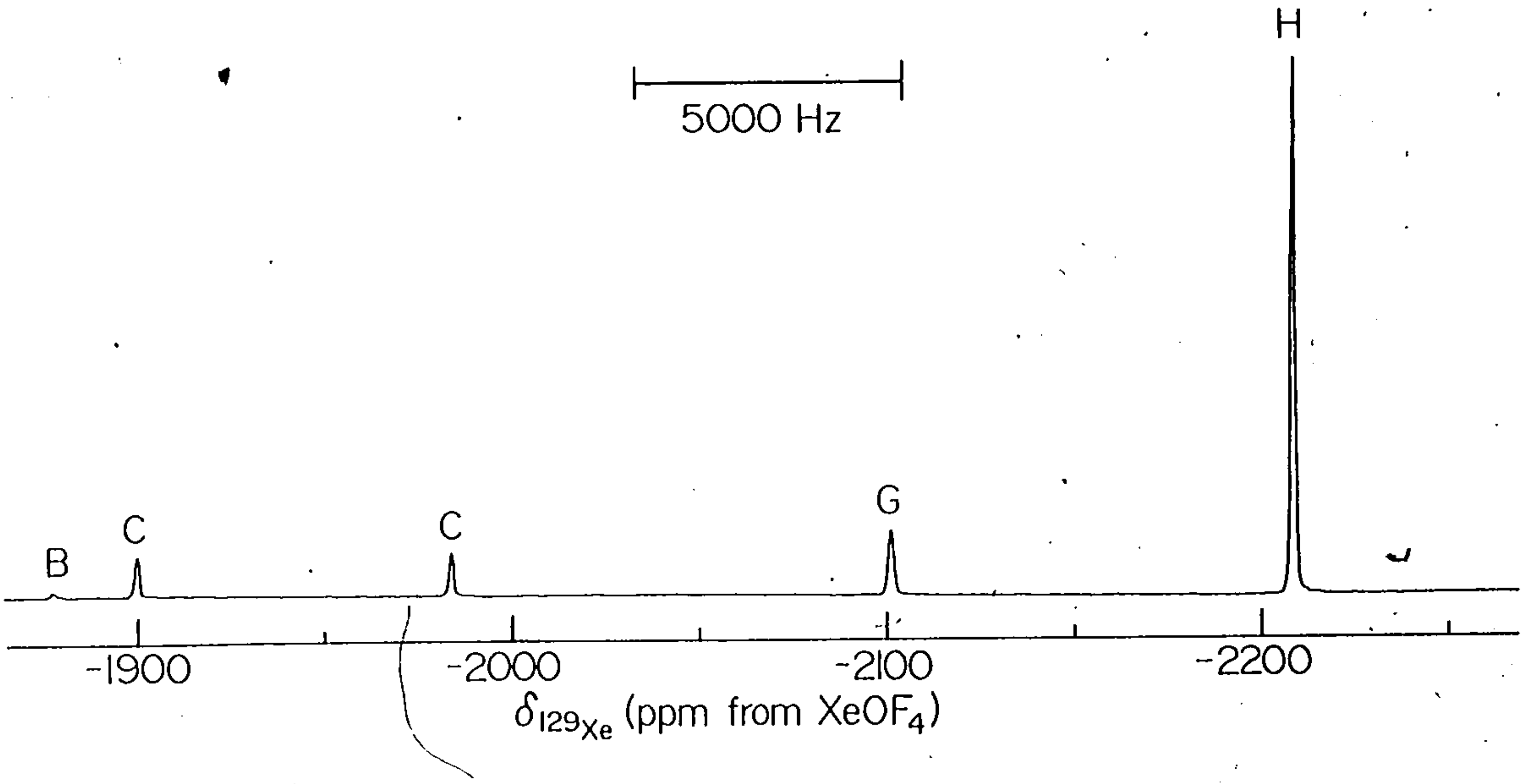
H
5000 Hz
G
C
C
B
-1900
-2000
-2100
-2200
$\delta_{^{129}Xe}$ (ppm from $XeOF_4$)

(6.2) is supported by evidence of Xe(II) species in the ^{129}Xe NMR spectrum (Figure 6.2) as well as the presence of an AX_4 pattern in the F-on-I(V) region representing IF_5 ($\delta^{19}F$ = 58.54 ppm, 13.39 ppm; $^2J(^{19}F-^{19}F)$ = 86 Hz). The decomposition of the trifluoro species, $F_3XeOIOF_4$, is expected to occur according to equation (6.3). This decomposition route is supported by the

$$2\ F_3XeOIOF_4 \longrightarrow XeF_4 + FXeOIOF_4 + IF_5 + O_2 \uparrow \qquad (6.3)$$

presence of $FXeOIOF_4$ and XeF_4 in the ^{129}Xe NMR spectra (Figures 6.1 and 6.2, respectively) and by the presence of IF_5 in the ^{19}F NMR spectrum.

The possibility that even higher substituted derivatives were formed cannot be entirely ruled out. For instance, if the tri- or tetra-substituted derivatives had been formed, i.e., $FXe(OIOF_4)_3$ or $Xe(OIOF_4)_4$, their stabilities would be expected to be substantially less than those of the di- and trifluoro derivatives, $F_2Xe(OIOF_4)_2$ and $F_3XeOIOF_4$. They would, in fact, be expected to decompose readily according to equations (6.4) and (6.5) by analogy with the reported

$$FXe(OIOF_4)_3 \longrightarrow FXeOIOF_4 + IF_5 + IOF_3 + 3/2\ O_2 \uparrow \qquad (6.4)$$

$$Xe(OIOF_4)_4 \longrightarrow Xe(OIOF_4)_2 + IOF_3 + IF_5 + 3/2\ O_2 \uparrow \qquad (6.5)$$

decomposition route of $Xe(OTeF_5)_4$, which occurs at 72°C according to equation (1.2) (139). Efforts to generate higher substituted derivatives by increasing the IO_2F_3 to XeF_4 ratio, as high as 4.2:1, were unsuccessful. In each case, the ^{129}Xe NMR spectrum showed evidence for the mono substituted derivative, $F_3XeOIOF_4$, but no higher derivatives.

(ii) The $IO_2F_3/XeOF_4$ System

In an effort to extend the IO_2F_3 insertions to include xenon(VI) derivatives, mixtures of IO_2F_3 and $XeOF_4$ were investigated in $CFCl_3$ solvent with the use of ^{129}Xe NMR spectroscopy. This reaction was expected to proceed with insertion of IO_2F_3 into an Xe-F bond of $XeOF_4$ according to equation (6.6). It was intially expected that reactions

$$IO_2F_3 \quad + \quad XeOF_4 \xrightarrow[0°C]{CFCl_3} OXeF_3(OIOF_4) \qquad (6.6)$$

between IO_2F_3 and $XeOF_4$ would be quite vigorous and they were therefore monitored closely during warm-up cycles for gas evolution and color changes. A mixture of IO_2F_3 and $XeOF_4$ corresponding to a molar ratio of 1:1, were combined in $CFCl_3$ solvent and warmed to 0°C for 10 minutes. Since there was no apparent gas evolution during this time, which would signal a decompostion, or no color change, which would represent solvent attack and the formation of chlorine, the ^{129}Xe NMR spectrum was recorded at 0°C. The region of the spectrum, recorded between 400 and -1038 ppm, showed only a binomial quintet, presumed to arise from $XeOF_4$, and no other xenon(VI) species. The xenon(II) region of the spectrum was also examined (-1600 to -2400 ppm) but provided no evidence for any xenon(II) species. The sample was then warmed to room temperature for 8 minutes and the xenon(VI) region of the spectrum recorded again at 0°C. Figure 6.3 illustrates the ^{129}Xe NMR spectrum recorded after the 8 minute warm-up at room temperature. The ^{129}Xe NMR parameters are summarized in Table 6.2. In addition to the binomial quintet of $XeOF_4$ ($\delta^{129}Xe$ = -21.26 ppm; $^{1}J(^{129}Xe-^{19}F)$ = 1143 Hz), a new pattern, appearing as a doublet of triplets ($\delta^{129}Xe$ = 52.8 ppm) was observed. The intensity of the doublet of triplets was much less than that of the binomial quintet and in addition, was complicated by a low signal-to-noise ratio.

The ^{129}Xe NMR spectrum depicted in Figure 6.3 can be assigned by comparison with the ^{129}Xe chemical shifts and $^{1}J(^{129}Xe-^{19}F)$ coupling constants previously reported for the $-OTeF_5$ derivatives of $XeOF_4$ and for XeOF4 itself (142). The binomial quintet is assigned to $XeOF_4$ as the ^{129}Xe chemical shift and $^{1}J(^{129}Xe-^{19}F)$ coupling constant compare well with the same values previously reported for $XeOF_4$ recorded in $CFCl_3$ solvent at 24°C ($\delta^{129}Xe$ = -29.9 ppm; $^{1}J(^{129}Xe-^{19}F)$ = 1131 Hz (142)). The high-frequency doublet of triplets is assigned to the mono-substituted derivative, $OXeF'F_2(OIOF_4)$ (structure 6.2, p. 227). An $OXeF'F_2$ moiety is expected to show a doublet

Table 6.2.

Xenon-129 and ^{19}F NMR parameters for the $IO_2F_3/XeOF_4$ System Recorded in $CFCl_3$ Solvent

	Chemical Shift, (ppm)		Coupling Constant, (Hz)	
Species	$\delta^{129}Xe^{a}$	$\delta^{19}F^{b}$	$^{2}J(FF)$	$^{1}J(^{129}Xe-^{19}F)$
$OXeF'F_2(OIOF_4)$	52.8	$(93.0)^{c}$ (F')	d	440 ± 10
		103.4 (F)	d	1166 ± 10
$XeOF_4$	-21.26	99.9	-	1143

a: Recorded at 0°C and referenced with respect to neat $XeOF_4$ at 24°C.

b: Recorded at -40°C and referenced with respect to neat $CFCl_3$ at 24°C. Fluorine chemical shifts are for F-on-Xe only.

c: Approximate chemical shift since this peak is overlaped.

d: Fluorine-fluorine coupling is not resolved.

<u>Figure 6.3</u>

Xenon-129 NMR spectrum of a 1:1 molar mixture of IO_2F_3 and $XeOF_4$ in $CFCl_3$ solvent recorded at 0°C.

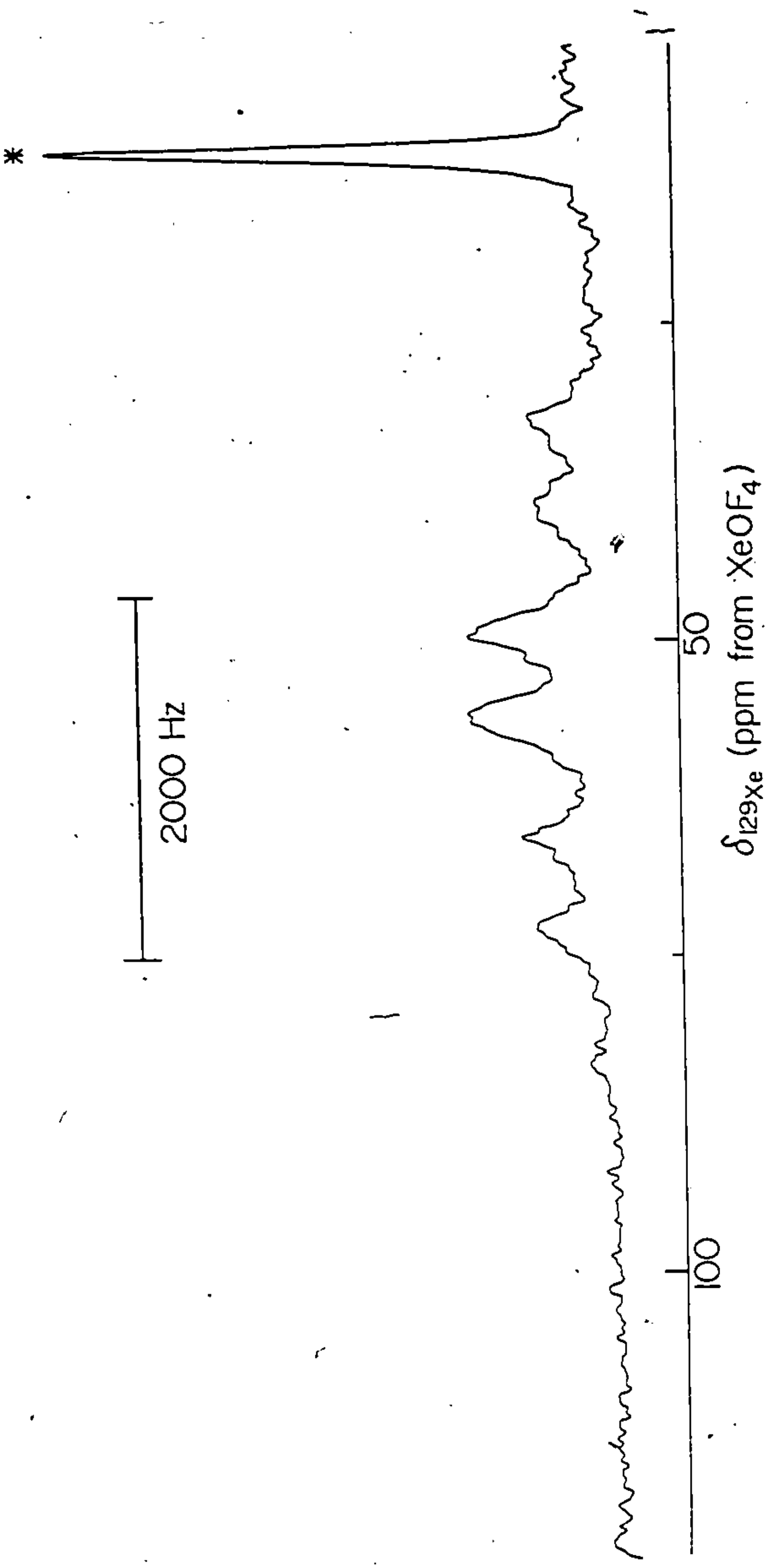
*
2000 Hz
50
100
$\delta_{^{129}Xe}$ (ppm from $XeOF_4$)

of triplets in the ^{129}Xe NMR spectrum resulting from the directly bonded spin-spin coupling of xenon with one fluorine in the axial position (F') and two fluorines in the equatorial postion (F_2) and is similar to that observed for $F_3XeOIOF_4$ discussed above. No other combination of fluorines, oxygens or $-OIF_4O$ groups would be expected to yield such a pattern. The ^{129}Xe chemical shift ($\delta^{129}Xe$ = 52.8 ppm) occurs to high-frequency of the corresponding shift previously assigned to $F_3XeOIOF_4$ ($\delta^{129}Xe$ = 24.4 ppm), which is to be expected with an increase in oxidation state from Xe(IV) to Xe(VI). It is unclear why the resonance of $OXeF_3(OIOF_4)$ occurs to high-frequency of $XeOF_4$. Since the relative electronegativity trends established in Chapter 4 places the $-OIF_4O$ group (both cis- and trans-) at lower electronegativity than fluorine, one would expect the chemical shift of the $-OIF_4O$ derivative to occur to low-frequency of $XeOF_4$. Furthermore, the $XeOF_4$ derivatives of the $-OTeF_5$ group, which is only slightly less electronegative than $-OIF_4O$ (also established in Chapter 4), occur consistently to low-frequency of $XeOF_4$ in the ^{129}Xe NMR spectrum (142). One possible explanation is that IO_2F_3 coordinates to the $XeOF_4$ molecule either through the xenon doubly-bonded oxygen or through the lone pair of electrons. This adduct would result in an overall increase in the covalent character of the xenon-fluorine bonds and consequently an increase in shielding of the xenon nucleus. The magnitudes of the directly bonded xenon-fluorine spin-spin coupling constants for $OXeF'F_2(OIOF_4)$ were determined as 440 ± 10 Hz for $^1J(^{129}Xe-^{19}F')$ and 1166 ± 10 Hz for $^1J(^{129}Xe-^{19}F)$. These values compare only reasonably well with the same values reported for $OXeF'F_2(OTeF_5)$, 1148 and 931 Hz, respectively (142), and are in fact, opposite in the sense that the equatorial coupling is larger than the axial coupling in the $-OIF_4O$ derivative. The couplings are similar to couplings reported for $XeOF_3^+$ (1018 and 434 Hz, respectively) (58), but again, the axial and equatorial magnitudes are reversed. This may again be attributed to IO_2F_3 coordination. If another IO_2F_3 molecule were to coordinate to $OXeF'F_2(OIOF_4)$ through the axial fluorine F', i.e., $F_3O_2I\cdots F'XeOF_2(OIOF_4)$, this would result in a weakening of the Xe-F' bond and subsequent reduction in the spin-spin coupling constant between the axial fluorine (F') and the xenon nucleus. This should in turn increase the strength of the equatorial fluorine-xenon coupling. The directly bonded spin-spin coupling observed in $OXeF'F_2(OIOF_4)$ between the equatorial fluorines and the xenon nucleus (1166 Hz) is considerably larger than that observed for either $OXeF'F_2(OTeF_5)$ (931 Hz) or $XeOF_3^+$ (434 Hz).

The ^{19}F NMR spectrum recorded at -40°C for the 1:1 mixture of IO_2F_3 and $XeOF_4$ in $CFCl_3$ solvent is illustrated in Figure 6.4 and the ^{19}F NMR parameters are summarized in Table 6.2. The spectrum shows mostly broad and unresolved multiplet resonances and is therefore only marginally useful in the characterization of this system. Tentative assignments have

Figure 6.4

The ^{19}F NMR spectrum for the 1:1 mixture of IO_2F_3 and $XeOF_4$ recorded in $CFCl_3$ solvent at -40°C. The peak assignments are given below.

Peak	Assignment
A (a,a)	$OXeF_3(OIOF_4)$
B (b,b)	$XeOF_4$
C (c,c)	$OXeF_3(OIOF_4)$

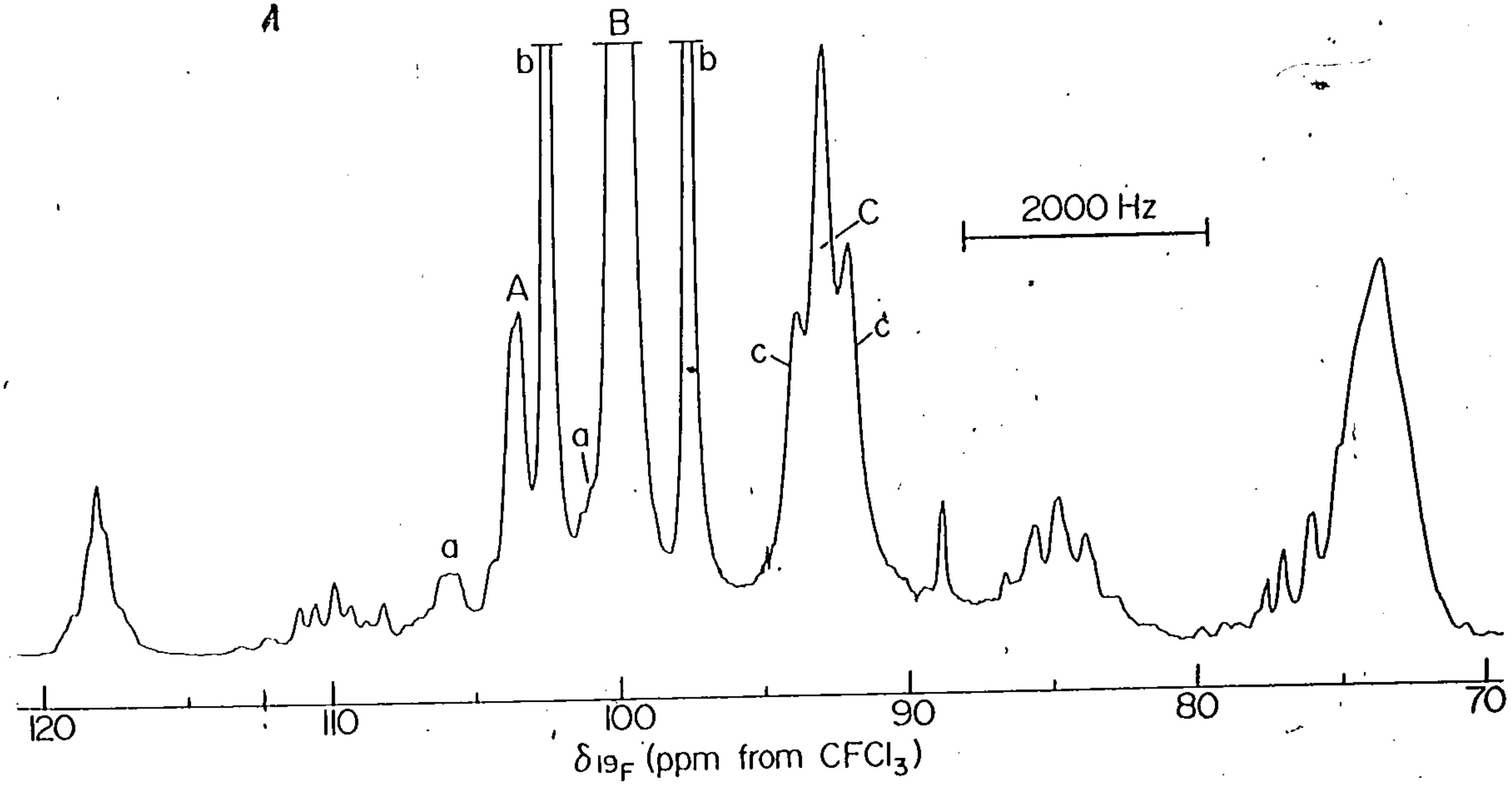
A
b
B
b
A
a
a
C
c
c
2000 Hz
120
110
100
90
80
70
$\delta_{^{19}F}$ (ppm from $CFCl_3$)

been made for the peaks labelled (A), (B) and (C) and are listed in Table 6.2.

The most abundant species in Figure 6.4 is the singlet resonance (B) and accompanying satellites (b,b) which are assigned to $XeOF_4$ by comparison with its previously reported ^{19}F chemical shift and $^{1}J(^{129}Xe-^{19}F)$ coupling constant (142). In addition to $XeOF_4$, there are many broad resonances which may represent fluorines directly bonded to Xe(VI) or fluorines directly bonded to I(VII). The resonances labelled (A) and (C), with accompanying satellites (a,a) and (c,c), respectively, are assigned to the fluorines directly bonded to xenon in $OXeF'F_2(OIOF_4)$. Resonance (A) is assigned to the equatorial fluorines on xenon (F) by comparison of the partially resolved satellite spacing (ca. 1180 Hz) with $^{1}J(^{129}Xe-^{19}F)$ (1166 Hz) determined in the ^{129}Xe spectrum. Resonance (C) is assigned to the axial fluorine (F') by comparison of the estimated satellite spacing (422 Hz) with $^{1}J(^{129}Xe-^{19}F)$ coupling constant determined in the ^{129}Xe spectrum (440 Hz). The other peaks in Figure 6.4 could not be assigned with any degree of certainty and are therefore left unassigned.

The low signal-to-noise ratio of the ^{129}Xe NMR spectrum in Figure 6.3 does not permit the assignment of $OXeF_3(OIOF_4)$ to either the cis- or trans-isomer. The fact that only one doublet of triplets is observed in the ^{129}Xe NMR spectrum, however, implies that only one isomer is formed. The ^{19}F NMR spectrum should, in this case, be able to provide this information insofar as the multiplet patterns associated with a cis-OIF_4O group have been established in Chapter 4 while a trans-OIF_4O group should show a singlet resonance in its ^{19}F NMR spectrum. In Figure 6.4, there is no singlet resonance observed which can be readily assigned to a trans-OIF_4O group. Furthermore, the presence of broad and unresolved peaks throughout the spectrum, prevents a definitive assignment to a cis-isomer.

(C) DISPLACEMENT REACTIONS INVOLVING $OXe(OTeF_5)_4$ AND $HOIOF_4$ AND THE POSSIBLE FORMATION OF $O_3Xe(OIOF_4)_x(OTeF_5)_{2-x}$ WHERE x = 1,2

(i) General

The fact that $HOIOF_4$ is capable of displacing $HOTeF_5$ from $Xe(OTeF_5)_2$ was established in Chapter 4. This displacement scheme provided the route by which the solid derivative, cis, cis-$Xe(OIOF_4)_2$, could be isolated as a pure compound and characterized more fully in the solid state by Raman spectroscopy and in solution by ^{129}Xe and ^{19}F NMR spectroscopy. It was hoped that similar acid displacements would occur with higher oxidation state xenon derivatives containing the $-OTeF_5$ group and that these reactions would ultimately lead to the isolation of Xe(IV) and/or Xe(VI) derivatives containing the $-OIF_4O$ group. These investigations are discussed below.

(ii) The Reactions of $Xe(OTeF_5)_4$ with $HOIOF_4$

The ^{129}Xe NMR studies performed on the XeF_4/IO_2F_3 system and discussed above have indicated that formation of a Xe(IV) derivative containing an $-OIF_4O$ group is possible. However, only the mono-substituted derivative, $F_3XeOIOF_4$, could be observed in solution. Nevertheless, mixtures of $Xe(OTeF_5)_4$ and $HOIOF_4$, corresponding to molar ratios 2.394:1, 4.357:1 and 7.378:1, were investigated in $CFCl_3$ solvent at -5°C by ^{129}Xe NMR spectroscopy. In each case, the ^{129}Xe NMR spectrum provided little or no evidence for the formation of $-OIF_4O$ derivatives. The most promising result was obtained in the 4.357:1 mixture of $HOIOF_4$ and $Xe(OTeF_5)_4$. In this system, the ^{129}Xe NMR spectra provided no evidence for Xe(IV) species but did however, reveal a distribution of Xe(II) products (similar to Figure 6.2) which are assumed to have arisen from the initial formation of Xe(IV) derivatives and their subsequent decomposition according to equations (6.2) to (6.5). Further attempts to generate Xe(IV) derivatives of the $-OIF_4O$ group were not made.

(iii) The Reaction of $OXe(OTeF_5)_4$ with $HOIOF_4$

The acid displacement reaction between $OXe(OTeF_5)_4$ and $HOIOF_4$ has been monitored in $CFCl_3$ solvent with the use of ^{129}Xe NMR spectroscopy. The displacement reaction was expected to proceed according to equation (6.7) and yield an equilibrium mixture of isomers of the general form $OXe(OIOF_4)x(OTeF_5)_{4-x}$.

$$OXe(OTeF_5)_4 + x\ HOIOF_4 \rightleftharpoons OXe(OIOF_4)_x(OTeF_5)_{4-x} + x\ HOTeF_5 \quad (6.7)$$

A mixture of $HOIOF_4$ and $OXe(OTeF_5)_4$, corresponding to the molar ratio 4.375:1, was prepared in $CFCl_3$ solvent and the ^{129}Xe NMR spectrum was recorded at -35°C. Attempts to record the spectrum at lower temperatures than -35°C resulted in deposition of colorless crystalline material while at higher temperatures, gas evolution, which signals decomposition, was always observed. The -35°C spectrum is illustrated in Figure 6.5 and the NMR parameters are summarized in Table 6.3. This spectrum shows seven major resonances labelled (A) - (G) in addition to a group of peaks of much lower intensity centered at $\delta^{129}Xe = 22$ ppm whose origin is uncertain. The chemical shifts of this weak set of peaks are too high for them to be assigned to a derivative such as $OXeL_4$ (L = $-OIF_4O$ and/or $-OTeF_5$), since, the ^{129}Xe chemical shifts for these species are expected to occur to low-frequency of that for $XeOF_4$ ($\delta^{129}Xe$ = -29.9 ppm) recorded under the same conditions. Furthermore, the chemical shifts of this group of resonances is too low to be considered a derivative such as O_2XeL_2 as these species would be expected to resonate to high-frequency of $O_2Xe(OTeF_5)_2$ ($\delta^{129}Xe$ = 131.0 ppm at -74°C in SO_2ClF (142)) in light of the group electronegativity trends established in Chapter 4. The ^{129}Xe chemical shift is similar to that determined for $F_3XeOIOF_4$ (24.4 ppm) but to postulate such a species in this system, in the absence of a strong fluorinating agent, would be

Figure 6.5

Xenon-129 NMR spectrum of a 4.375:1 molar mixture of $HOIOF_4$ and $OXe(OTeF_5)_4$ recorded in $CFCl_3$ solvent at -35°C. The peak assignments are given below.

Peak	Assignment
A	$OXe(OIOF_4)(OTeF_5)_3$
B	cis-$OXe(OIOF_4)_2(OTeF_5)_2$
C	trans-$OXe(OIOF_4)_2(OTeF_5)_2$
D	$OXe(OIOF_4)_3(OTeF_5)$
E,F,G	$OXe(OIOF_4)_4$

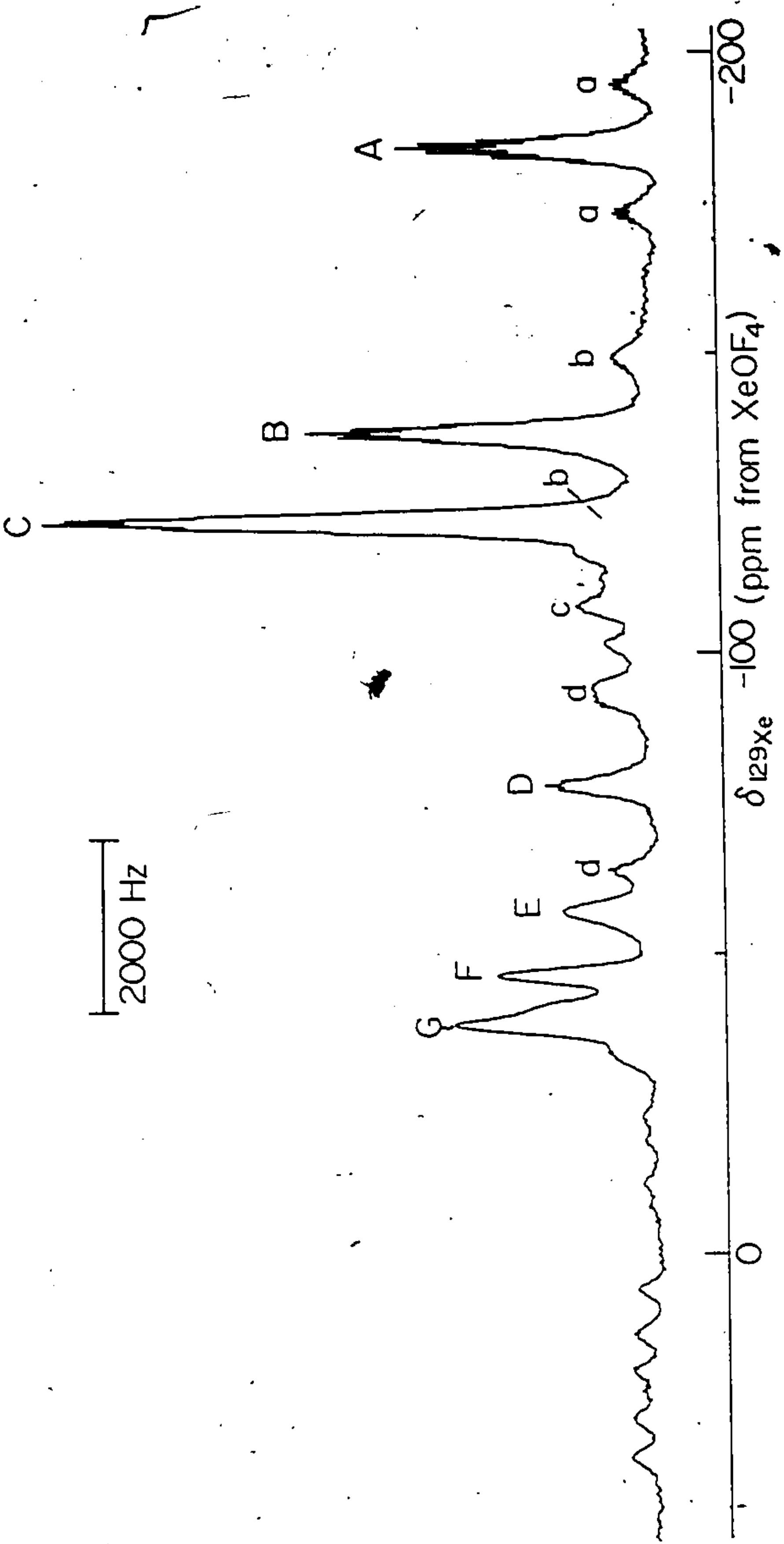

A
B
C
D
E
F
G
a
a
b
b
c
d
d
d
2000 Hz
0
-100
-200
δ129Xe (ppm from XeOF4)

Table 6.3

The ^{129}Xe NMR Parameters for the $OXe(OIOF_4)_x(OTeF_5)_{4-x}$ Derivatives Recorded at -35°C in $CFCl_3$ Solvent

Species	$\delta^{129}Xe^a$(ppm)	Coupling constant, Hz $^2J(^{129}Xe-^{125}Te)$	$^3J(^{129}Xe-^{19}F)$
$OXe(OIOF_4)(OTeF_5)_3$	-182.1	1503	50
cis-$OXe(OIOF_4)_2(OTeF_5)_2$	-134.2	(1810)[b]	50
trans-$OXe(OIOF_4)_2(OTeF_5)_2$	-118.9	(1828)[b]	(46)[b]
$OXe(OIOF_4)_3(OTeF_5)$	- 75.4	(2053)[b]	(34)[b]
$OXe(OIOF_4)_4$	- 53.3	-	c
	- 43.0	-	c
	- 35.0	-	c

a: Referenced with respect to neat $XeOF_4$ at 24°C.

b: Estimated coupling.

c: Not resolved.

too speculative. While this group of resonances must remain unassigned, the remaining peaks in Figure 6.5 can be tentatively assigned by comparison with the ^{129}Xe chemical shifts previously reported for the $OXeF_{4-x}(OTeF_5)_x$ system (142) and the group electronegativity trends for $-OIF_4O$ and $-OTeF_5$ established in Chapter 4.

Mixed $-OIF_4O/-OTeF_5$ derivatives of the general form $OXe(OIOF_4)_x(OTeF_5)_{4-x}$ are expected to have a total of 15 isomers resulting from ligand redistribution of cis- and trans- $-OIF_4O$ and $-OTeF_5$ groups at the four bonding sites of the $OXeX_4$ moiety (structure 6.3). Each isomer is expected to display a unique ^{129}Xe chemical shift and these shifts are expected to occur progressively to high-frequency as the ratio of $-OIF_4O$ groups to $-OTeF_5$ groups increases. The chemical shift range of this series is expected to have limits set by $OXe(OIOF_4)_4$ at highest frequency and $OXe(OTeF_5)_4$ at lowest frequency. The lowest frequency resonance in Figure 6.5 (A) ($\delta^{129}Xe = -182.1$ ppm) is assigned to $OXe(OIOF_4)(OTeF_5)_3$. Its chemical shift is midway between the ^{129}Xe chemical shifts reported for $OXe(OTeF_5)_4$ (-204.1 ppm) and $OXeF(OTeF_5)_3$ (-157.0 ppm) as expected, since, the electronegativity of the $-OIF_4O$ group was determined to lie between that of -F and $-OTeF_5$ (Chapter 4) and should have a shielding effect on the xenon nucleus which is intermediate between that of the -F and $-OTeF_5$ groups. The assignment of the $-OIF_4O$ group in this derivative to either the cis- or trans-isomer cannot be made with any certainty and is therefore not attempted. The resonances labelled B (δ^{129}Xe = -134.2 ppm) and C (δ^{129}Xe = -118.9 ppm) are assigned to cis- and trans-$OXe(OIOF_4)_2(OTeF_5)_2$ (cis and trans with respect to substitution on Xe), respectively, by comparison with the ^{129}Xe chemical shifts reported for the analogous derivatives cis-$OXeF_2(OTeF_5)_2$ (-117.8 ppm) and trans-$OXeF_2(OTeF_5)_2$ (-106.4 ppm). The resonance labelled D (δ^{129}Xe = -75.4 ppm) is assigned to $OXe(OIOF_4)_3(OTeF_5)$ since, on the basis of group electronegativity, the ^{129}Xe chemical shift of this derivative should occur between that of $OXeF_3(OTeF_5)$ (-66.3 ppm) and $OXeF_2(OTeF_5)_2$ (-106.4 ppm). Again, differentiation between cis- and trans-isomers of $-OIF_4O$ cannot be made. The resonances labelled E (δ^{129}Xe = -53.3 ppm), F (δ^{129}Xe = -43.0 ppm) and G (δ^{129}Xe = -35.0 ppm) are assigned collectively as the tetra-substituted derivatives $OXe(OIOF_4)_4$. These assignments stem from the fact that the ^{129}Xe chemical shifts of these species are in the range between the ^{129}Xe chemical shifts of $OXe(OIOF_4)_3(OTeF_5)$ (δ^{129}Xe = -75.4 ppm) and $XeOF_4$ (δ^{129}Xe = -29.9 ppm) as expected from group electronegativity considerations. The tetra-substituted derivative, $OXe(OIOF_4)_4$, has 6 possible isomers which result from all possible cis- and trans- combinations (cis- and trans- with respect to the bonding sites (1) - (4) in structure 6.3) of cis- and trans-OIF_4O groups. The fact that only 3 isomers are observed is understandable since, the ^{129}Xe chemical shifts for these isomers are expected to be quite similar. In fact,

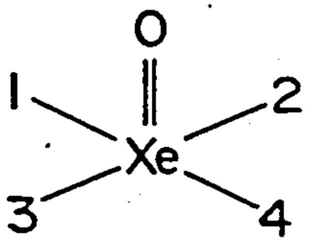

6.3

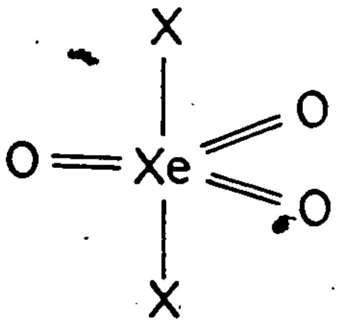

6.4

the shoulder on the low-frequency side of resonance G and the resonance labelled (d) (δ^{129}Xe = -61.8 ppm), which corresponds to the ^{125}Te satellite associated with $OXe(OIOF_4)_3(OTeF_5)$ (D), may represent two other resonance peaks of $OXe(OIOF_4)_4$.

In addition to the argument given above, the observed ^{125}Te satellites associated with resonance peaks A, B, C and D further support the proposed assignments of these peaks to the derivatives containing $-OTeF_5$ groups. The fact that these resonances occur close in frequency, and in some cases are overlapping with other peaks, prevented an accurate measurement of satellite intensities which could be used to determine the number of Te atoms corresponding to a given resonance peak.

Having determined that acid displacement reactions between $HOIOF_4$ and $OXe(OTeF_5)_4$ yielded $-OIF_4O$ group derivatives of xenon(VI), attempts were made to isolate one or more of these derivatives for a fuller characterization in the solid state by Raman spectroscopy, and as pure compounds, in solution by NMR spectroscopy. Mixtures of $HOIOF_4$ and $OXe(OTeF_5)_4$ were first reacted in varying mole ratios (4:1 to 12:1) in $CFCl_3$ solvent, however, these reactions produced no isolable products. This lack of success was attributed to the effect of solvent reactivity, which had been previously noted in the solvent-based attempts to isolate a Xe(II) derivative (Chapter 4). The successful isolation of a solid derivative from the $HOIOF_4/OXe(OTeF_5)_4$ system was, however, accomplished by a neat reaction of the two reagents (Chapter 2), much in keeping with the strategy used for the isolation of pure cis, cis-$Xe(OIOF_4)_2$ described in Chapter 2.

The reaction between a neat mixture of $HOIOF_4$ and $OXe(OTeF_5)_4$, corresponding to a mole ratio of 4.029:1, yielded a pale-yellow solid (Chapter 2) which has been studied in the solid state by low-temperature Raman spectroscopy and in solution by ^{129}Xe NMR spectroscopy. The high-frequency region of the ^{129}Xe NMR spectrum, recorded at 5°C on the pale-yellow solid dissolved in $CFCl_3$, is depicted in Figure 6.6. This spectrum shows three broad resonances with ^{129}Xe chemical shifts of 346.5, 338.2 and 283.4 ppm, respectively (Table 6.4). The ^{129}Xe chemical shifts do not correspond to those determined for the Xe(VI) derivatives, $OXe(OIOF_4)_4$ (Table 6.3), and in addition, are too high to be considered as any other neutral Xe(VI) species (58), i.e., XeO_2F_2 ($\delta^{129}Xe$ = 173.2 ppm), XeO_3 ($\delta^{129}Xe$ = 217 ppm). Although the ^{129}Xe chemical shifts for the neutral Xe(VIII) species, XeO_4 and XeO_3F_2, which could serve as a basis of comparison in this case, have never been reported, the resonances in Figure 6.6 are assigned to Xe(VIII) derivatives of the general form $O_3Xe(OIOF_4)_x(OTeF_5)_{2-x}$ (x = 1,2) for the following reasons: The decomposition of the Xe(VI) derivative, $OXe(OIOF_4)_4$, may proceed according to equation (6.8) yielding the Xe(VIII) derivative, $O_3Xe(OIOF_4)_2$ as well as IF_5, IOF_3 and oxygen gas. The subsequent decomposition of the Xe(VIII) derivative according to equation (6.9) is expected to

Figure 6.6

Xenon-129 NMR spectrum of the mixed Xe(VIII) derivatives $O_3Xe(OIOF_4)_x(OTeF_5)_{2-x}$ (x = 1,2) recorded in $CFCl_3$ solvent at 5°C.

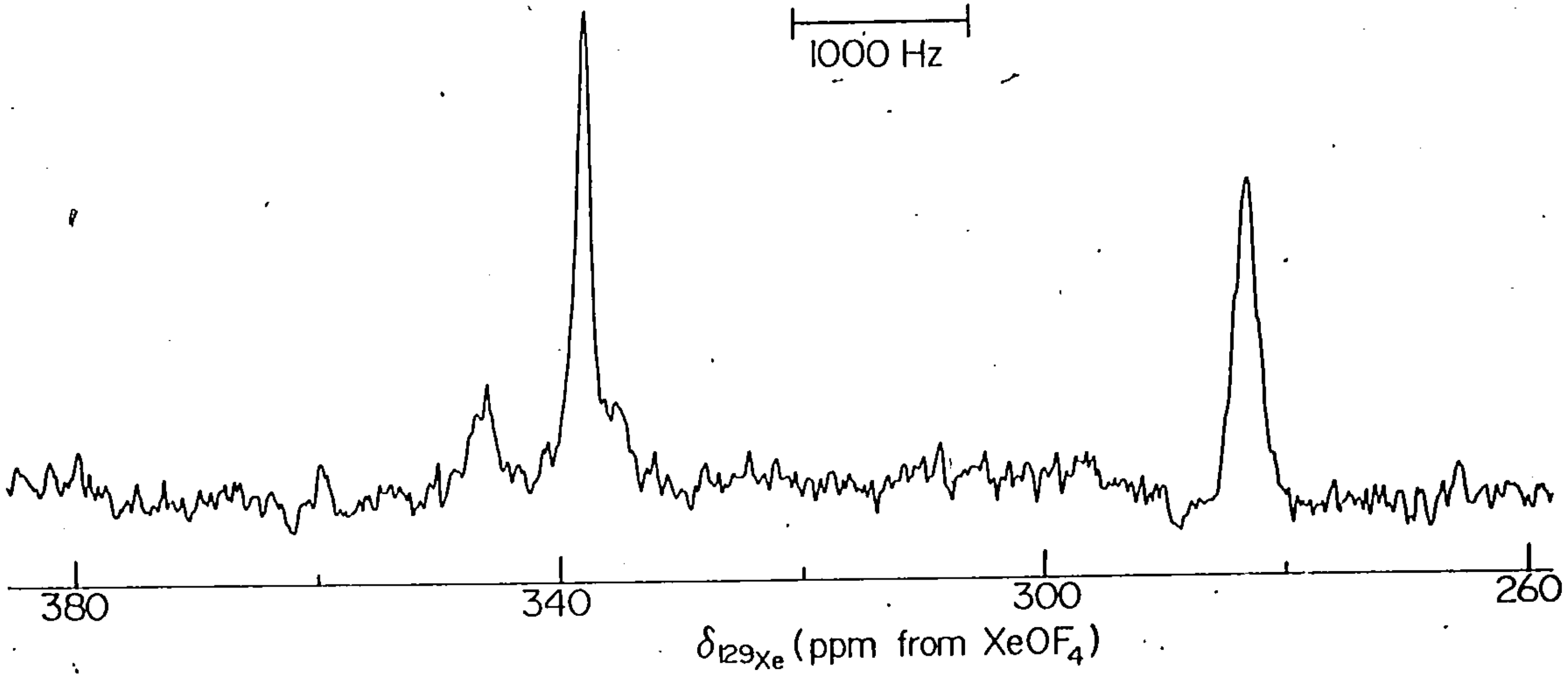
1000 Hz
380
340
300
260
$\delta_{^{129}Xe}$ (ppm from $XeOF_4$)

Table 6.4

Xenon-129 parameters for the species observed when $O_3Xe(OIOF_4)_x(OTeF_5)_{2-x}$ (x = 1,2) is dissolved in $CFCl_3$ solvent at 5°C

Species	$\delta^{129}Xe^{a}$ (ppm)	Relative Intensity
trans-$O_3Xe(OIOF_4)(OTeF_5)$	346.5	1
cis, cis-$O_3Xe(OIOF_4)_2$	338.2	4.6
cis-$O_3Xe(OIOF_4)(OTeF_5)$	283.4	6.7
cis, trans-$Xe(OIOF_4)_2$	-2134.3	1.3
trans-$F_4OIOXeOTeF_5$	-2225.2	1.0
cis, cis-$Xe(OIOF_4)_2$	-2228.7	6.2
cis-$F_4OIOXeOTeF_5$	-2308.4	5.1

a: Referenced with respect to neat $XeOF_4$ at 24°C.

$$OXe(OIOF_4)_4 \longrightarrow O_3Xe(OIOF_4)_2 + IF_5 + IOF_3 + \tfrac{1}{2}O_2\uparrow \quad (6.8)$$

$$O_3Xe(OIOF_4)_2 \longrightarrow Xe(OIOF_4)_2 + 3/2\ O_2\uparrow \quad (6.9)$$

occur readily based on the thermal instabilities of XeO_3F_2 and XeO_4 (61,67). If, in fact, $OXe(OIOF_4)_4$, or some mixed $-OTeF_5/-OIF_4O$ derivative such as $OXe(OIOF_4)_2(OTeF_5)_2$ are formed, and they do indeed decompose according to equations (6.8) and (6.9), the Xe(II) region of the ^{129}Xe spectrum should confirm the existence of these species. Figure 6.7 illustrates the Xe(II) region of the ^{129}Xe NMR spectrum recorded at 5°C. The four multiplet resonances in this spectrum are identified as cis, trans-$Xe(OIOF_4)_2$, trans-$F_4OIOXeOTeF_5$, cis-$F_4OIOXeOTeF_5$ and cis, cis-$Xe(OIOF_4)_2$ by comparison of their ^{129}Xe chemical shifts (Table 6.4) with the chemical shifts determined for these species in Chapter 4. This result suggests that initially, the pale-yellow solid consisted of a mixture of $O_3Xe(OIOF_4)_2$ and $O_3Xe(OIOF_4)(OTeF_5)$. The subsequent decomposition of these derivatives, according to equation (6.9) for $O_3Xe(OIOF_4)_2$, and equation (6.10) for $O_3Xe(OIOF_4)(OTeF_5)$, would then result in the four Xe(II) derivatives observed in the ^{129}Xe NMR spectrum. The three resonances in Figure 6.5,

$$O_3Xe(OIOF_4)(OTeF_5) \longrightarrow Xe(OIOF_4)(OTeF_5) + 3/2\ O_2\uparrow \quad (6.10)$$

Figure 6.7

Xenon-129 NMR spectrum showing the Xe(II) decomposition products of $O_3Xe(OIOF_4)_x(OTeF_5)_{2-x}$ (x = 1,2) recorded in $CFCl_3$ solvent at 5°C.

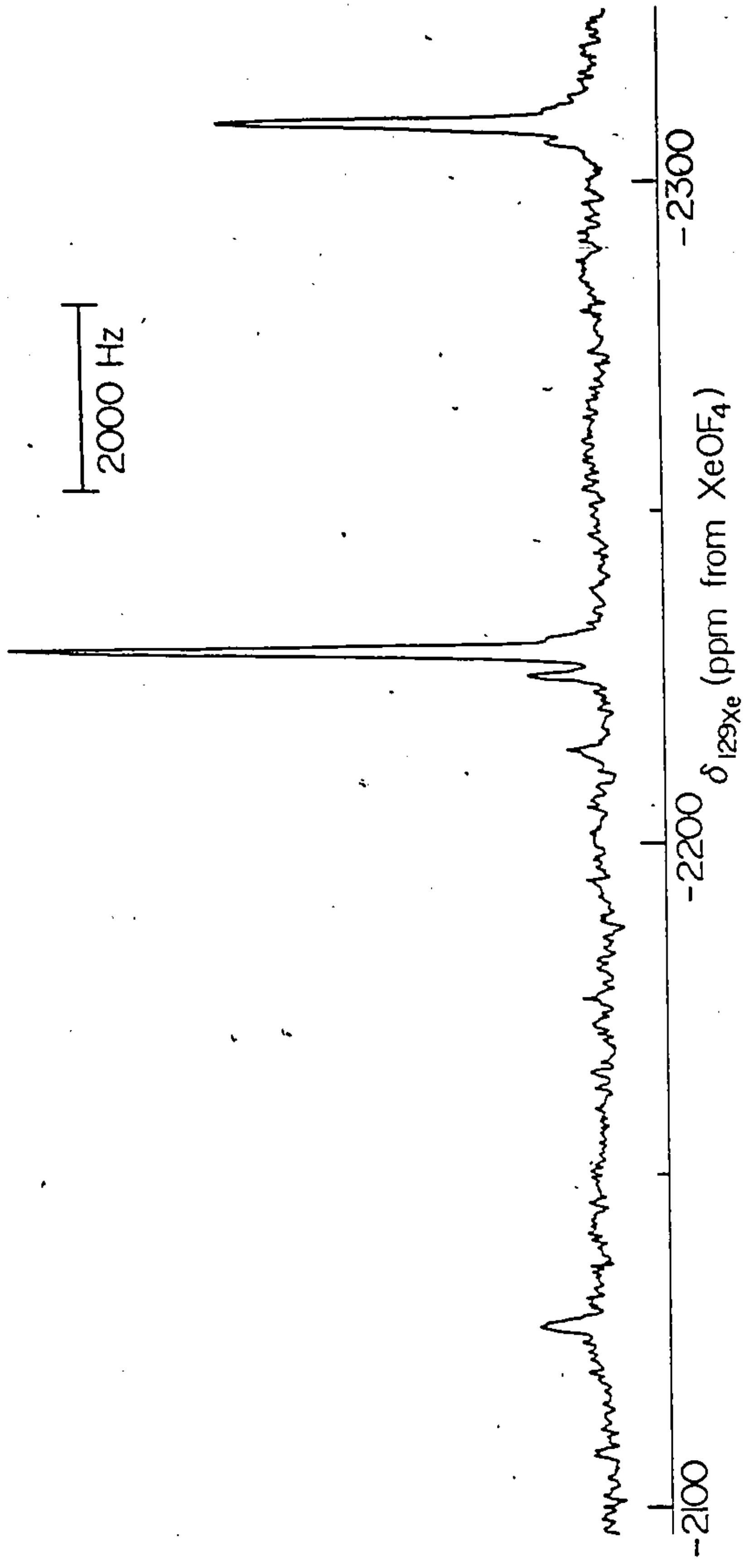
2000 Hz
−2300
−2200
−2100
$\delta_{^{129}\mathrm{Xe}}$ (ppm from $XeOF_4$)

corresponding to the Xe(VIII) derivatives, are therefore plausibly assigned to cis, cis-$O_3Xe(OIOF_4)_2$ ($\delta^{129}Xe$ = 338.2 ppm), trans, cis-$O_3Xe(OIOF_4)_2$ ($\delta^{129}Xe$ = 346.5 ppm) and $O_3Xe(OIOF_4)(OTeF_5)$ ($\delta^{129}Xe$ = 283.4 ppm). These assignments are made in accord with the ^{129}Xe shielding trends established for the $-OTeF_5$ and cis- and trans-OIF_4O groups in Chapter 4.

Additional evidence in support of the proposed formation of the novel Xe(VIII) derivatives has been obtained by recording the low-temperature Raman spectrum of the pale-yellow solid. The Raman spectrum is depicted in Figure 6.8 and the vibrational frequencies with some tentative assignments are given in Table 6.5. In addition to vibrational bands which are assigned to cis, cis-$Xe(OIOF_4)_2$ (Table 6.5) by comparison with the vibrational frequencies for this species determined in Chapter 4, there exists a number of bands in Figure 6.8 which are thought to arise from the xenon(VIII) derivatives. The region of the spectrum from 840 - 910 cm^{-1} shows seven well defined vibrational bands which are in the correct range for I=O stretches (c.f. ν I=O: IO_2F_3, 916 cm^{-1} (192); cis-$[OIF_4O]^-$, 855 and 875 cm^{-1} (186); IOF_3, 883 cm^{-1} (220)) and Xe=O stretches (c.f. XeO_2F_2, 882 and 850 cm^{-1} (55); $OXe(OTeF_5)_4$, 887 and 873 cm^{-1} (142)). The Xe(VIII) derivatives, $O_3Xe(OIOF_4)_x(OTeF_5)_{2-x}$ (x = 1,2), are assumed to adopt a trigonal-bipyramidal arrangement of oxygens and ligand groups (X) (structure 6.4, p. 247) by analogy with the known structure of XeO_3F_2 (67). Such an arrangement is expected to

Figure 6.8

The Raman spectrum of the pale-yellow solid isolated from the neat reaction of $HOIOF_4$ and $OXe(OTeF_5)_4$ (4.029:1) recorded in an FEP tube at -196°C. * denotes an FEP band.

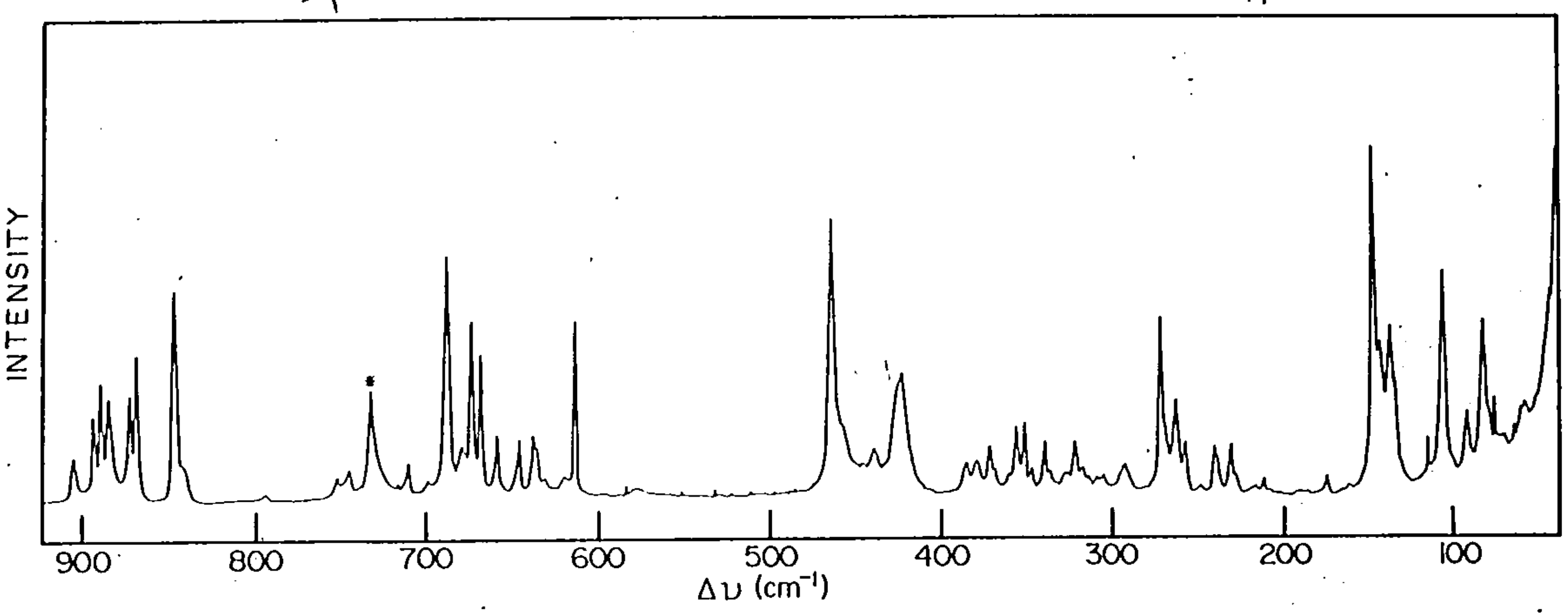
INTENSITY
*
900
800
700
600
500
400
300
200
100
Δυ (cm⁻¹)

Table 6.5

Vibrational data obtained from the Raman spectrum recorded on $O_3Xe(OIOF_4)_x(OTeF_5)_{2-x}$ (x = 1,2)

Frequency (cm^{-1})[a]	Tentative Assignment
906 (13)	ν Xe=0
894 (27)	
889 (37)	b
885 (29)	
873 (29)	ν I=0
868 (44)	ν I=0
848 (64)	ν Xe=0
840 (sh)	
792 (1)	
752 (3)	
745 (5)	b
711 (6)	
699 (1)	
688 (88)	I-F
680 (19)	and
675 (47)	Te-F
669 (42)	stretching
660 (21)	
647 (20)	b
639 (19)	
619 (4)	
614 (45)	b
579 (1)	
464 (92)	b
440 (13)	

continued...

Table 6.5 continued

Frequency (cm^{-1})^a	Tentative Assignment
425 (40)	
386 (9)	
379 (9)	
372 (16)	
369 (11)	b
360 (6)	
357 (21)	
353 (22)	b
347 (9)	
340 (15)	b
327 (4)	
321 (16)	
318 (8)	b
305 (1)	
292 (10)	
273 (46)	b
263 (30)	
258 (15)	
239 (14)	
231 (14)	
216 (1)	
174 (8)	
147 (100)	b
143 (48)	
138 (51)	
135 (sh)	
116 (8), 106 (81), 92 (14), 82^b (46)	Lattice modes

a: Recorded in an FEP tube at -196°C. * denotes FEP band.

b: Band corresponding to cis, cis-Xe(OIOF$_4$)$_2$.

display a symmetric and asymmetric Xe=O stretch by analogy with XeO_3F_2 (67). The bands at 848 and 906 cm^{-1} in Figure 6.8 are similar in intensity and relative separation to the Xe=O bands of XeO_3F_2 at 807 and 892 cm^{-1}, respectively (67). The frequency difference between the respective Xe=O modes for the different Xe(VIII) derivatives is expected to be small. The bands at 848 and 906 cm^{-1} may, in fact, represent overlapping Xe=O modes of $O_3Xe(OIOF_4)_2$ and $O_3Xe(OIOF_4)(OTeF_5)$. In addition, the I=O stretches for cis, cis-$O_3Xe(OIOF_4)_2$ and cis-$O_3Xe(OIOF_4)(OTeF_5)$ are expected to be similar in frequency yet different from the I=O stretches in either cis, cis-$Xe(OIOF_4)_2$ or cis-$F_4OIOXeOTeF_5$. The bands at 868 and 873 cm^{-1} could therefore represent the I=O stretches of cis, cis-$O_3Xe(OIOF_4)_2$ and cis-$O_3Xe(OIOF_4)(OTeF_5)$ and the bands at 885 and 894 cm^{-1}, represent the I=O stretches of the xenon(II) derivatives. The vibrational bands in the range 610 - 760 cm^{-1} are assumed to arise from the I-F and Te-F stretches of the various Xe(VIII) and Xe(II) derivatives in this system. Assignments for these bands, apart from those attributed to cis, cis-$Xe(OIOF_4)_2$, cannot be made with any certainty and are therefore not attempted. The number of bands in this region is however, consistent with a mixture of $-OTeF_5$ and $-OIF_4O$ derivatives as proposed above.

In the formation of the Xe(VIII) derivatives, according to equation (6.8), the concurrent formation of I(V) species, IF_5 and IOF_3 is expected. Iodine pentafluoride, IF_5, is volatile and is presumably pumped off under vacuum. On the other hand, IOF_3 is not volatile and should remain in the mixture along with the Xe(VIII) derivatives. The Raman spectrum depicted in Figure 6.8, however, provides no evidence for IOF_3 which should exhibit intense vibrational bands at 878 and 543 cm^{-1} (207,208). A highly speculative argument to account for the absence of IOF_3 in this spectrum is as follows: The IOF_3, which is formed according to equation 6.8, may immediately react with $OXe(OIOF_4)_4$ (equation 6.11) forming

$$OXe(OIOF_4)_4 + IOF_3 \longrightarrow O_2Xe(OIOF_4)_2 + IF_3(OIOF_4)_2 \qquad (6.11)$$

the five-coordinate I(V) species, $IF_3(OIOF_4)_2$, which may or may not be stable. In the latter case, decomposition of this species would yield products which are expected to be volatile and thus pumped off. The Xe(VI) derivative, $O_2Xe(OIOF_4)_2$, should it also be unstable, could decompose yielding O_2 and $Xe(OIOF_4)_2$ according to equation (6.12). This proposed series

$$O_2Xe(OIOF_4)_2 \longrightarrow Xe(OIOF_4)_2 + O_2 \uparrow \qquad (6.12)$$

of decompositions, though highly speculative, are nevertheless supported by the approximate ratio of Xe(VIII) to Xe(II) species (1:2), determined in the respective ^{129}Xe NMR spectra.

(D) SUMMARY

High oxidation state xenon derivatives containing the $-OIF_4O$ group have been prepared either through insertion reactions between IO_2F_3 and XeF_4 or $XeOF_4$, or by way of acid displacement reactions involving $OXe(OTeF_5)_4$ and $HOIOF_4$. These novel derivatives have been characterized in solution by ^{129}Xe and, in several cases, ^{19}F NMR spectroscopy. The $-OIF_4O$ group thus represents the second ligand-group known to stabilize the higher oxidation states of xenon. The proposed Xe(VIII) derivatives would represent the only such ligand-group derivatives known. In addition, their apparent stability would be unprecedented for Xe(VIII), excepting the perxenate anion, $[XeO_6]^{4-}$. Further work is therefore necessary to confirm their existence and to properly characterize these novel species. The HF solvolysis of the proposed Xe(VIII) derivatives would be expected to yield XeO_3F_2. The identification of this species in solution could be accomplished with the use of ^{129}Xe and ^{19}F NMR spectroscopy recorded at low temperature. The ^{129}Xe and ^{19}F chemical shifts derived from these studies as well as the expected binomial triplet pattern and directly-bonded $J(^{129}Xe-^{19}F)$ spin-spin coupling would be readily assignable to XeO_3F_2.

CHAPTER 7

PRELIMINARY EVIDENCE FOR $-OIF_4O$ COMPOUNDS OF MERCURY, BORON AND TELLURIUM

(A) INTRODUCTION

In the previous Chapters it has been shown that the $-OIF_4O$ group is capable of stabilizing xenon in its +2, +4, +6 and, even possibly, +8 oxidation states. The preparations of these derivatives has been accomplished with the use of either IO_2F_3 or $HOIOF_4$ as the $-OIF_4O$ ligand precursor. Unfortunately, however, the aggressive oxidizing nature of IO_2F_3 and $HOIOF_4$ (a result of the high oxidation potential of I(VII)) appear to preclude the use of either IO_2F_3 or $HOIOF_4$ in extending $-OIF_4O$ derivative chemistry to other more easily oxidizable elements. Similar difficulties are encountered in preparations of $-OSeF_5$ derivatives (132) owing to the high oxidation potential of selenium in the +6 oxidation state. This problem can, in some cases, be avoided with the use of the ligand-transfer reagent, $Hg(OSeF_5)_2$ (132,232). For instance, although the reaction of $AsCl_3$ and $HOSeF_5$ results in rapid oxidation of chlorine on arsenic, the reaction of $Hg(OSeF_5)_2$ with $AsCl_3$ in $C_2F_4Cl_2$ solvent at 0°C (equation (7.1)) yields the arsenic (III) derivative, $As(OSeF_5)_3$, with no degradation of $AsCl_3$ (233).

$$2\ AsCl_3 + 3\ Hg(OSeF_5)_2 \xrightarrow{C_2F_4Cl_2} 2\ As(OSeF_5)_3 + 3\ HgCl_2 \qquad (7.1)$$

The extensive derivative chemistry of the $-OTeF_5$ group can be accredited to the existence of two non-oxidative ligand-transfer reagents, $B(OTeF_5)_3$ (162) and $Hg(OTeF_5)_2$ (225,234). In addition, the oxidative $-OTeF_5$ ligand-transfer reagents, TeF_5OX (X = F, Cl) and $Xe(OTeF_5)_2$, have recently been shown to provide convenient routes to $-OTeF_5$ substituted fluorocarbons (182,183,235). Thus, $-OTeF_5$ derivatives can be prepared from either fluoride or chloride precursors and are now known for most of the main-group elements and many transition metal elements (132).

In this work, initial efforts have been directed towards extending the chemistry of the $-OIF_4O$ group beyond the limits of Group 18 with emphasis on the preparation of the potential ligand-transfer reagents, $B(OIOF_4)_3$ and $Hg(OIOF_4)_2$. The preliminary results of these investigations are discussed in this Chapter.

(B) BORON DERIVATIVES OF THE $-OIF_4O$ GROUP

The ligand-transfer reagent, $B(OTeF_5)_3$, was first prepared by Sladky *et al.* (162) by the stoichiometric reaction of $HOTeF_5$ and BCl_3 (equation (1.6)). By analogy, the stoichiometric reaction between $HOIOF_4$ and BCl_3 was attempted at -78°C according to equation (7.2). Upon mixing the two

$$BCl_3 + 3\ HOIOF_4 \xrightarrow{-78°C} B(OIOF_4)_3 + 3\ HCl \qquad (7.2)$$

reactants, a yellow deposit (on the order of milligrams) was observed on the upper portion of the reaction vessel followed by a particularily violent and luminous detonation. Presumably, $HOIOF_4$ is capable of oxidizing chlorine in BCl_3 forming one or more of the known thermally unstable chlorine oxides (219). Other attempts, which included the acid displacement of $HOTeF_5$ from $B(OTeF_5)_3$ with $HOIOF_4$ in $CFCl_3$ solvent were also unsuccessful. The lack of success in the latter attempt was thought to arise from the problem of solvent reactivity, as was noted for the preparation of cis, cis-$Xe(OIOF_4)_2$ performed in $CFCl_3$ solvent (Chapters 2 and 4). To circumvent the problem of solvent reactivity, the stoichiometric reaction of neat $HOIOF_4$ and $B(OTeF_5)_3$ was performed according to equation (7.3). Upon removal of $HOTeF_5$

$$B(OTeF_5)_3 + 3\ HOIOF_4 \xrightarrow{0^\circ C} B(OIOF_4)_3 + 3\ HOTeF_5 \quad (7.3)$$

under vacuum, a bright-yellow viscous liquid remained which showed no appreciable decomposition at 0°C. The ^{11}B NMR spectrum of this liquid recorded in $CFCl_3$ solvent at -40°C is depicted in Figure 7.1. In this spectrum a broad set of resonances consisting of three partially resolved peaks ($\delta^{11}B$ = 10.4, -46.8 and -110.5 ppm) is observed which is thought to arise from a series of mixed $-OIOF_4$/$-OTeF_5$ derivatives of the general form $B(OIOF_4)_x(OTeF_5)_{3-x}$. Since there are ten possible

Figure 7.1

The ^{11}B NMR spectrum of $B(OIOF_4)_x(OTeF_5)_{3-x}$ recorded in $CFCl_3$ solvent at -40°C.

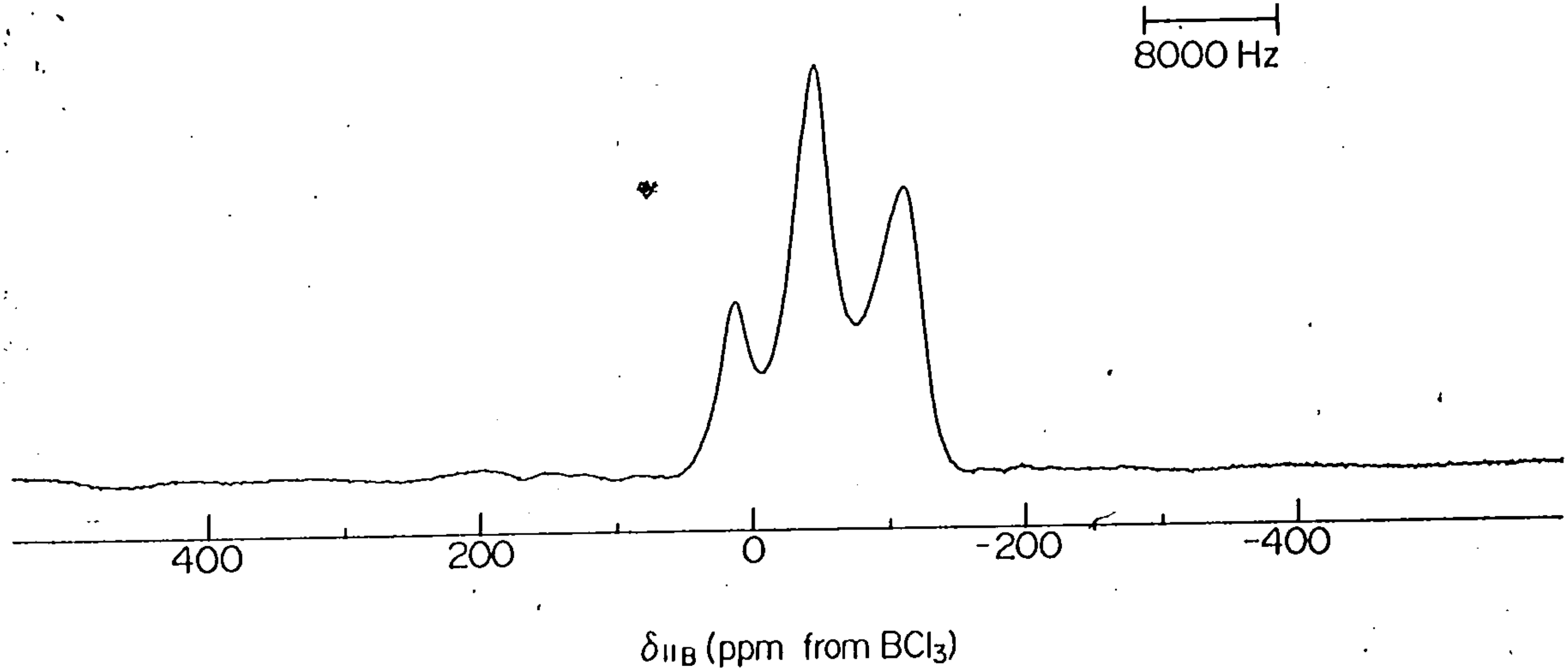
8000 Hz
400
200
0
-200
-400
δ_{11B} (ppm from BCl_3)

isomers of $B(OIOF_4)_x(OTeF_5)_{3-x}$ resulting from all possible combinations of cis- and trans-OIF_4O groups and one, two or three $-OTeF_5$ groups, and only three resonances in Figure 7.1 are resolved, definitive assignments for these resonances can not be made. In light of the relative group electronegativity trends (Chapter 4) it is expected that the ^{11}B chemical shifts should become less shielded as the number of $-OIF_4O$ groups increases. By comparison with the ^{11}B chemical shift for $B(OTeF_5)_3$ ($\delta^{11}B$ = -32.5 ppm in $CFCl_3$ at 0°C), this does not appear to be the case here. The ^{19}F NMR spectrum recorded at -40°C is depicted in Figure 7.2 which shows, in addition to the AX_4 ($\delta^{19}F$ = 69.4 ppm) and A_2X_2 ($\delta^{19}F$, (A_2) = 86.6 ppm, (X_2) = 67.8 ppm) patterns of trans- and cis-$HOIOF_4$, several singlet and multiplet resonances in the fluorine on iodine(VII) region. Assignments for the resonances in the F-on-I(VII) region, other than those of cis- and trans-$HOIOF_4$, cannot be made at this time since the isomer composition of the mixture is unknown. The presence of $HOIOF_4$ in this spectrum, and F-on-Te(VI) resonances in the region of the spectrum from $\delta^{19}F$ = -33 to -50 ppm (not shown), suggests that the bright-yellow liquid consists of an equilibrium mixture of $B(OIOF_4)_x(OTeF_5)_{3-x}$ derivatives.

Although only preliminary evidence has been obtained for boron derivatives containing the $-OIF_4O$ groups, the results nevertheless indicate that the formation of such derivatives appears feasible. In addition, the apparent thermal stability

Figure 7.2

The ^{19}F NMR spectrum of $B(OIOF_4)_x(OTeF_5)_{3-x}$ recorded in $CFCl_3$ solvent at -40°C.

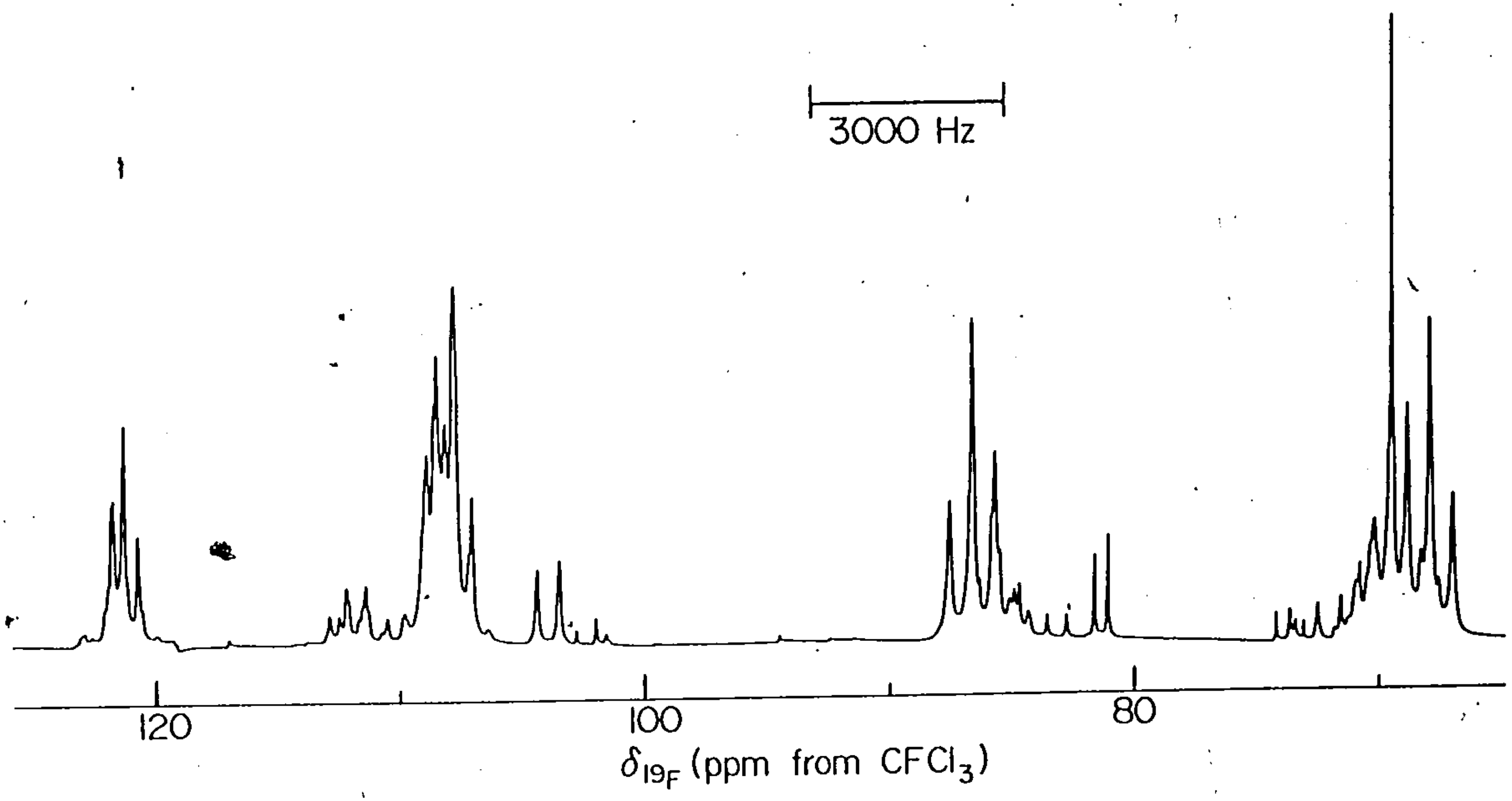
3000 Hz
120
100
80
$\delta_{^{19}F}$ (ppm from $CFCl_3$)

of the proposed mixed derivative suggests that with further efforts in this area, a stable isolable $-OIF_4O$ derivative may be forthcoming.

(C) EVIDENCE FOR THE MERCURY(II) DERIVATIVE: $Hg(OIOF_4)_2$

In attempts to prepare mercury derivatives of the $-OIF_4O$ group, $Hg(OIOF_4)_2$, acid displacement reactions such as that shown in equation (7.4) were employed. Upon removal of

$$Hg(OTeF_5)_2 + 2\ HOIOF_4 \xrightarrow[CFCl_3]{0^\circ C} Hg(OIOF_4)_2 + 2\ HOTeF_5 \qquad (7.4)$$

the solvent at 0°C, a pale-yellow solid was deposited which was examined by Raman spectroscopy. The vibrational frequencies with some tentative assignments are given in Table 7.1. Although the analogous derivatives, $Hg(OTeF_5)_2$ and $Hg(OSeF_5)_2$, are known and the vibrational frequencies for both compounds have been reported (225,232), assignments for these spectra have not been made. The most prominent feature of the spectrum is the very intense band at 312 cm^{-1} which is assigned to the Hg-O stretch. This band, like its counterpart in $Hg(OTeF_5)_2$ (ν Hg-O = 315 cm^{-1} (100), this work) is expected to be very intense in the Raman. This mode occurs to low frequency of the analogous stretching mode in cis, cis-$Xe(OIOF_4)_2$ (ν Xe-O, 464 cm^{-1}) which indicates a greater degree of ionic character

Table 7.1

Raman Frequencies and Assignments for $Hg(OIOF_4)_2$

Frequency[a] (cm^{-1})		Tentative Assignments[b]
803	(72)	ν I=O
785	(63)	ν I=O
775	(sh)	ν asym (IF_2)
703	(38)	ν sym (IF_2)
649	(4)	ν asym (IF_2)
601	(33)	ν sym (IF_2)
546	(64)	
536	(sh)	
408	(9)	
380	(6)	
359	(2)	
312	(100)	ν sym (Hg-O)
255	(11)	ν asym (Hg-O)
163	(3)	δ (I-O-Hg)
120	(sh)	
118	(28)	δ (O-Hg-O)
105	(2)	
71	(63)	lattice mode

a: Recorded at room temperature in a ¼" glass tube.

b: Tentative assignments were made by comparison with the Raman spectrum of $Hg(OTeF_5)_2$ recorded in this work. The Raman frequencies for $Hg(OTeF_5)_2$ are: 815(sh), 811(6), 710(53), 705(33), 698(6), 638(31), 630(2), 616(29), 483(36), 381(3), 352(68), 346(35), 339(7), 335(8), 321(sh), 315(100), 296(3), 231(29), 150(33), 145(sh), 127(38), 122(sh), 98(10).

associated with the mercury compound. The asymmetric Hg-O stretch is assigned to the band at 255 cm^{-1} by analogy with cis, cis-$Xe(OIOF_4)_2$ in which the asymmetric Xe-O stretch occurs to low-frequency of the symmetric stretch and by comparison with the frequency of the corresponding mode in $Hg(OTeF_5)_2$ (ν asym Hg-O = 231 cm^{-1}, this work). The bands at 118 and 163 cm^{-1} are assigned to O-Hg-O and I-O-Hg bends, respectively, by comparison with the corresponding modes determined for $Hg(OTeF_5)_2$ at 127 and 231 cm^{-1} (Table 7.1). In the region of the spectrum from 563 to 775 cm^{-1}, there are six bands which could represent I-F stretches. In particular, the bands at 601 and 649 cm^{-1} and at 703 and 775 cm^{-1} could possibly represent symmetric and asymmetric stretches associated with a cis-OIF_4O group. The presence of an additional band at 546 cm^{-1}, indicates that a trans-isomer may also be present. This is further supported by the presence of two bands at 785 and 803 cm^{-1} which also could indicate a cis- and trans-OIF_4O mixture. The possibility that this sample is contaminated with the most likely impurities, IO_2F and IOF_3, has been ruled out in the absence of bands at 690 cm^{-1} (corresponding to the I-F stretch of IO_2F (208)) and 873 cm^{-1} (corresponding to the I=O stretch of IOF_3 (208)). In addition, the absence of bands at 710, 638, 616, 483, 352, 346, 315, 150 and 127 cm^{-1}, which have been determined as the intense bands in the Raman spectrum of $Hg(OTeF_5)_2$ (this work, Table 7.1)), precludes the possibility that this sample still contains starting material.

Attempts to obtain ^{199}Hg and ^{19}F NMR spectra on this compound were unsuccessful owing to the very low solubility of this compound in all solvents attempted including $CFCl_3$, SO_2ClF and CH_2Cl_2. Further efforts in this area are therefore required which should be focused on obtaining NMR spectra of this derivative in more polar solvents.

(D) EVIDENCE FOR TELLURIUM DERIVATIVES OF THE $-OIF_4O$ GROUP

Two routes were investigated in attempts to prepare tellurium derivatives of the $-OIF_4O$ group. The first route attempted was an acid displacement of $HOTeF_5$ from $Te(OTeF_5)_4$ with $HOIOF_4$ in SO_2ClF solvent according to equation (7.5).

$$Te(OTeF_5)_4 + 4\ HOIOF_4 \xrightarrow[0°C]{SO_2ClF} Te(OIOF_4)_4 + HOTeF_5 \qquad (7.5)$$

The reaction, which proceeded with rapid evolution of oxygen gas, resulted in the deposition of a pale-yellow solid which was shown by Raman spectroscopy to contain primarily IOF_3 and IO_2F. In addition, the resulting solid was found to be only marginally soluble in SO_2ClF. The ^{125}Te NMR spectrum recorded on this solid in SO_2ClF showed no evidence that it contained either Te(IV) or Te(VI). In a second attempt at Te derivative formation, an excess of IO_2F_3 was allowed to react with TeF_4 (actual mole ratio IO_2F_3:TeF_4 was 8.26:1) in SO_2ClF solvent at room temperature. It was thought that IO_2F_3 may insert into the Te-F bond (equation (7.6)) by analogy with the insertion reactions of IO_2F_3 and XeF_2 (Chapter 4). During the

$$TeF_4 + n\ IO_2F_3 \xrightleftharpoons{SO_2ClF} TeF_{4-n}(OIOF_4)_n \qquad (7.6)$$

course of the reaction at room temperature, little gas evolution was apparent and the color of the reaction mixture, which was initially yellow, faded. Upon removal of the solvent at 0°C, a pale-yellow solid was deposited which was examined by Raman spectroscopy. The vibrational frequencies obtained from the Raman spectrum recorded on this solid (Table 7.2) showed it to contain no TeF_4 (236), IO_2F (208) or IOF_3 (208). It did, however, indicate the presence of unreacted IO_2F_3 as well as other unidentified species. The vibrational frequencies assignable to IO_2F_3 are indicated in Table 7.2. The most promising part of the spectrum with respect to $-OIF_4O$ derivative formation is the high-frequency portion. In the region of the spectrum from 595 to 765 cm^{-1}, there are eight bands which cannot be assigned to IO_2F_3. These bands presumably represent I-F stretches associated with $-OIF_4O$ groups, and in addition, the number of bands in this region suggest that more than one isomer is present. This is not unreasonable if one considers there is a possibility of 12 different cis- and trans-isomers of $Te(OIOF_4)_4$ alone. The high-frequency region of the spectrum also supports a mixture

Table 7.2

Raman Frequencies for the Pale-Yellow Solid Obtained from the Reaction Of TeF_4 with IO_2F_3 Recorded at 24°C

Frequency[a] (cm^{-1})	Possible Assignment
931 (5)	
913 (40)	b
865 (26)	I=O stretches
839 (45)	
825 (35)	
788 (8)	
765 (11)	
740 (8)	
695 (14)	
681 (36)	
668 (72)	I-F stretches
655 (92)	b
645 (21)	
623 (79)	b
619 (100)	
595 (sh)	
429 (7)	
382 (sh)	b
369 (26)	b

continued...

Table 7.2 continued

Frequency[a] (cm^{-1})	Possible Assignment
363 (17)	
345 (13)	
335 (15)	
327 (9)	
279 (4)	b
260 (15)	b
255 (50)	b
249 (sh)	b
235 (10)	b
200 (49)	b
189 (sh)	
149 (10)	
126 (16)	

a: Recorded in an FEP tube at room temperature.

b: A Raman band of IO_2F_3 occurs at this frequency (208).

of $-OIF_4O$ isomers. Thus, the bands at 825, 839, 865, 913, 927 and 931 cm^{-1}, could all represent the I=O stretches of the $-OIF_4O$ groups associated with different isomers.

Additional evidence for $-OIF_4O$ derivative formation has been obtained from the reaction of $HOIOF_4$ with TeF_4 in SO_2 solvent studied in situ by ^{125}Te NMR spectroscopy. The NMR spectrum recorded at -10°C consisted of a single line ($\Delta\nu_{\frac{1}{2}}$ = 110 Hz) at $\delta^{125}Te$ = 774.83 ppm. This peak does not correspond to that of TeF_4 ($\delta^{125}Te$ = 1317.5 ppm in SO_2 at -73°C (237)), but rather, is more representative of a Te(VI) species by virtue of its low-frequency chemical shift (237).

CHAPTER 8

SUMMARY AND CONCLUSIONS

(A) INTRODUCTION

Prior to this work, derivative formation of the $-OIF_4O$ group was limited to $HOIOF_4$ (184-186), $K^+[IO_2F_4]^-$ (187), $Cs^+[IO_2F_4]^-$ (186,188), $FOIOF_4$ (186,189) and $ClOIOF_4$ (186). The majority of work in this thesis describes the preparation and characterization of novel series of xenon derivatives containing the $-OIF_4O$ group. These derivatives were first prepared and observed in solution by ^{129}Xe and ^{19}F NMR spectroscopy and in some cases, where possible, isolation of these compounds lead to further characterization by Raman spectroscopy.

(B) THE $-OIF_4O$ GROUP PRECURSORS $HOIOF_4$ AND IO_2F_3

At the outset of this work, an improved synthesis of both $-OIF_4O$ group precursors, $HOIOF_4$ and IO_2F_3, was developed and optimized with the use of ^{19}F NMR spectroscopy. This synthesis leads to higher yields of these compounds than the original preparative method described by Engelbrecht and Peterfy (184,185). In addition, this improved synthesis makes use of reagents that are commerically available and does not require the preparation of starting materials as in the original preparative method (184,185).

The cis- and trans-isomer ratio dependence of $HOIOF_4$ on solvent and temperature was studied by ^{19}F NMR spectroscopy. It was found that the ratio of cis:trans increased as the solvent polarity decreased and as the temperature decreased. These effects were attributed to the lower acidity and group electronegativity of the cis-isomer.

The structure of IO_2F_3 was studied in solution by ^{19}F NMR spectroscopy. The use of high-field instrumentation in this work has provided well resolved NMR spectra of this species in solution which were lacking in all previous studies. The structure of IO_2F_3 in solution was determined to consist of an equilibrium mixture of cis-oxygen bridged dimers which was found to be, in general, consistent with the solid-state X-ray crystal structure (190).

(C) XENON DERIVATIVES CONTAINING THE $-OIF_4O$ GROUP

With extensive use of ^{129}Xe and ^{19}F NMR spectoscopy, a novel series of covalent Xe(II) derivatives including cis- and trans-$FXeOIOF_4$, trans, trans-, cis, trans- and cis, cis-$Xe(OIOF_4)_2$ were prepared and characterized in solution. The equilibrium distribution of these isomers was found to be dependent on solvent medium. The isolation of the pure derivative, cis, cis-$Xe(OIOF_4)_2$, was accomplished by an acid displacement of $HOTeF_5$ from $Xe(OTeF_5)_2$ with $HOIOF_4$, and represents the only example of a neutral xenon derivative prepared by this method. The solid-state structure was determined with the use of Raman spectroscopy and was found to be consistent with that established in solution. A mixture of cis/trans-$FXeOIOF_4$ was also isolated and studied by Raman spectroscopy.

The controlled thermal decomposition of cis, cis-$Xe(OIOF_4)_2$ has been studied with the use of ^{19}F NMR spectroscopy and Raman spectroscopy. The primary products of this decomposition have been identified as a mixture of peroxides, cis- and trans-$F_4OIOOIOF_4$ which decompose further yielding the corresponding oxides, cis- and trans-$F_4OIOIOF_4$. The peroxides are of particular interest since they are potential $-OIF_4O$ ligand-transfer reagents and could be used to expand the derivative chemistry of the $-OIF_4O$ group beyond that presently known. In the same respect, $Xe(OIOF_4)_2$ and $FXeOIOF_4$ are also potential ligand-transfer reagents, both in the oxidative sense and as reagents to add to the C=C bonds of chlorofluoro-olefins, by analogy with the demonstrated ability of $Xe(OTeF_5)_2$ to function as an $-OTeF_5$ ligand-transfer reagent (182,183).

In addition to Xe(II) derivatives, the higher oxidation state species $F_3XeOIOF_4$ and $OXeF_3(OIOF_4)$ have been observed in solution by ^{129}Xe and ^{19}F NMR spectroscopy. Other than simple oxide, fluoride and oxide fluoride derivatives, these derivatives represent the only examples, apart from $-OTeF_5$, where higher oxidation state xenon derivatives are known. It was not possible to observe higher substituted derivatives, such as those known for $-OTeF_5$, which would seem to indicate that these derivatives are less stable than the $-OTeF_5$ counterparts. As a result, the isolation of high oxidation state $-OIF_4O$ derivatives of xenon was not accomplished during the course of this work. A mixture of cis- and trans-OIF_4O/$-OTeF_5$ derivatives of Xe(VIII) have been proposed on the basis of their ^{129}Xe chemical shifts and solid-state Raman spectra. In view of the fact that of the Xe(VIII) examples presently known, only $[XeO_6]^{4-}$ salts are thermodynamically stable, the proposed assignments are deemed tentative. Verification of these assignments is currently underway.

Xenon-129 and ^{19}F NMR studies carried out on the $-OIF_4O$ derivatives have indicated that this group possesses a high effective group electronegativity. Furthermore, the ^{129}Xe and ^{19}F NMR parameters for the mixed $-OTeF_5$/$-OIF_4O$ and $-OSO_2F$/$-OIF_4O$ xenon(II) derivatives have been used to establish the relative order of increasing group electronegativity: $-OTeF_5$ < cis-OIF_4O < trans-OIF_4O < $-OSO_2F$.

(D) OTHER DERIVATIVES

Preliminary evidence has been given for the existence of $-OIF_4O$ derivatives of boron, mercury and tellurium. These results, although only preliminary, indicate that a potentially extensive derivative chemistry of the $-OIF_4O$ group is yet to be discovered.

(E) FUTURE DIRECTIONS FOR RESEARCH

A rich derivative chemistry of the $-OIF_4O$ group awaits discovery. Although insertion and displacement methods utilizing $HOIOF_4$ and IO_2F_3 may yield new derivatives of $-OIF_4O$, it is believed that these routes may be of limited success as a result of the high oxidizing potential of both these species. Thus, those elements which exist in their highest oxidation states as fluorides or ligand-group derivatives, i.e., UF_6 and $U(OTeF_5)_6$ (238), are foreseen as the most likely candidates for these methods of derivative formation.

The greatest potential for $-OIF_4O$ derivative formation perhaps lies in the use of ligand transfer reagents. Of the known $-OIF_4O$ derivatives, four compounds in particular may function in this capacity: $Xe(OIOF_4)_2$, $F_4OIOOIOF_4$, $B(OIOF_4)_3$ and $Hg(OIOF_4)_2$. The use of the xenon(II) derivative, $Xe(OTeF_5)_2$, as an oxidative $-OTeF_5$ group transfer reagent has already been well established in previous work (129,179-183). The $-OIF_4O$ group analogue, $Xe(OIOF_4)_2$ could potentially function in the same way as illustrated by equation (8.1).

$$Xe(OIOF_4)_2 + ML_x \longrightarrow ML_x(OIOF_4)_2 + Xe\uparrow \qquad (8.1)$$

In a similar manner, the peroxide $F_4OIOOIOF_4$ would seemingly function as a mild oxidative ligand transfer reagent as illustrated by equation (8.2).

$$R_2C{=}CR_2 \quad + \quad F_4OIOOIOF_4 \longrightarrow (F_4OIO)R_2C{-}CR_2(OIOF_4) \qquad (8.2)$$

(where $R_2C{=}CR_2$ is a chlorofluoro-olefin)

The ligand transfer reagents $B(OTeF_5)_3$ and $Hg(OSeF_5)_2$ have been used to develop extensive derivative chemistries of the $-OTeF_5$ and $-OSeF_5$ groups as cited previously. By analogy, the potential ligand transfer reagents $B(OIOF_4)_x(OTeF_5)_{3-x}$ or $B(OIOF_4)_3$ and $Hg(OIOF_4)_2$ would likewise serve to perpetuate the derivative chemistry of the $-OIF_4O$ group, which at present, is surely in its infancy.

REFERENCES

1. Lord Rayleigh and W. Ramsay, Phil. Trans., A186, 187 (1895).
2. H. Moissan, Bull. Soc. Chim. France, <u>13</u>, 976 (1895).
3. M. Berthelot, Ann. Chim. Phys., <u>11</u>, 15 (1897); Compt. Rend., <u>120</u>, 581, 662, 1386 (1895).
4. E.H. Boomer, Proc. Roy. Soc. London, <u>A109</u>, 198 (1925).
5. F. Paneth, Z. angew Chem., <u>37</u>, 421 (1924).
6. A. von Antropoff, K. Weil and H. Frauenhof, Naturwiss., <u>20</u>, 688 (1932).
7. C.L. Chernick, J. Chem. Ed., <u>41</u>, 185 (1964).
8. D.M. Yost and A.L. Kaye, J. Am. Chem. Soc., <u>55</u>, 3891 (1933).
9. W. Kossel, Ann. Phys., <u>49</u>, 229 (1916).
10. C.B. Hunt, Ed. in Chem., September 1983, 177.
11. N. Bartlett and D.H. Lohmann, Proc. Chem. Soc., 115 (1962).
12. N. Bartlett and D.H. Lohmann, J. Chem. Soc., 5253 (1962).
13. N. Bartlett, Proc. Chem. Soc., 218 (1962).
14. C.L. Chernick <u>et al.</u>, Science, <u>138</u>, 136 (1962).
15. D.F. Smith, J. Chem. Phys., <u>38</u>, 270 (1963).
16. H.H. Claassen, H. Selig and J.G. Malm, J. Am. Chem. Soc., <u>85</u>, 1927 (1963).
17. D.F. Smith, Science, <u>140</u>, 899 (1963).

18. J.L. Weeks, C.L. Chernick and M.S. Matheson, J. Am. Chem. Soc., 84, 4612 (1962).

19. H.H. Claassen, H. Selig and J.G. Malm, J. Am. Chem. Soc., 84, 3593 (1962).

20. J.G. Malm, I. Sheft and C.L. Chernick, J. Am. Chem. Soc., 85, 110 (1963).

21. E.E. Weaver, B. Weinstock and C.P. Knop, J. Am. Chem. Soc., 85, 111 (1963).

22. F. Schreiner, J.G. Malm and J.C. Hindman, J. Am. Chem. Soc., 87, 25 (1965).

23. N. Bartlett, Endeavour, 23, 3 (1964).

24. J.H. Holloway, "Noble-Gas Chemistry", Methuen and Co. Ltd., London (1968).

25. J.G. Malm and E.H. Appelman, At. Energy Rev., 8, 3 (1969).

26. H.H. Hyman, in "Physical Chemistry", H. Eyring, D. Henderson and W. Jost, Eds., Academic Press Inc., New York (1970), Vol. 5, Chapter 11.

27. N.K. Jha, R. I. C. Rev., 4, 147 (1971).

28. F. Sladky, in "MTP International Review of Science, Inorganic Series One", H.J. Emeleus and V. Gutmann, Eds., Butterworths, University Park Press, Baltimore (1972), Vol. 3, Chapter 1.

29. H.H. Hyman, Ed., "Noble-Gas Compounds", University of Chicago Press, Chicago (1963).

30. H. Selig, J.G. Malm and H.H. Claassen, Scientific American, 210, 66 (1964).

31. C.L. Chernick, Record Chem. Progr., 24, 139 (1963).

32. J.H. Holloway, Prog. Inorg. Chem., 6, 241 (1964).

33. H.H. Hyman, Science, 145, 773 (1964).

34. H. Selig, Fluoride Chemistry of the Noble-gases, in "Halogen Chemistry", V. Gutmann, Ed., Academic Press, New York (1968), Vol. 1, pp. 403-430.

35. G.J. Moody and J.D.R. Thomas, Rev. Appl. Chem., 16, 1 (1966).

36. J.L. Weeks and M.S. Matheson, in "Inorganic Synthesis", H.F. Holtzclaw, Ed., McGraw-Hill, New York (1966), Vol. 8, p. 260.

37. S.M. Williamson, in "Inorganic Synthesis", W.L. Jolly, Ed., McGraw-Hill, New York (1968), Vol. 11, p. 147.

38. W.E. Falconer and W.A. Sunder, J. Inorg. Nucl. Chem., 29, 1380 (1967).

39. Ref. (28), p. 8.

40. E.H. Appelman, Inorg. Chem., 10, 1881 (1971).

41. E.H. Appelman, J. Am. Chem. Soc., 90, 1900 (1968).

42. E.H. Appelman and J.G. Malm, in "Preparative Inorganic Chemistry", (1966), Vol. 3, Chapter 9, p. 341.

43. J.G. Malm and C.L. Chernick, in "Inorganic Synthesis", H.F. Holtzclaw, Ed., McGraw-Hill, New York (1966), Vol. 8, p. 254.

44. E.H. Appelman and J.G. Malm, J. Am. Chem. Soc., 86, 2141 (1964).

45. J.S. Ogden and J.J. Turner, J. Chem. Soc., Chem. Commun., 693 (1966).

46. Ref. (43), p. 258.

47. K. Seppelt, Angew. Chem., Int. Ed. Engl., 18, 186 (1979).

48. R.D. Burbank and G.R. Jones, J. Am. Chem. Soc., 96, 43 (1974).

49. R.J. Gillespie, "Molecular Geometry", Van Nostrand Reinhold, London, 1972.

50. W. Harshbarger, R.K. Bohn and S.H. Bauer, J. Am. Chem. Soc., 89, 6466 (1967).

51. K. Hedberg, S.H. Peterson, R.R. Ryan and B. Weinstock, J. Chem. Phys., 44, 1726 (1966).

52. J.G. Malm, B.D. Holt and R.W. Bane, in ref. (18), p. 167.

53. G.J. Schrobilgen, Ph.D. Thesis, McMaster University, Hamilton, Ontario, Canada (1973).

54. H.H. Claassen, C.L. Chernick and J.G. Malm, in ref (18), p. 287.

55. H.H. Claassen, E.L. Gasner, H. Kim and J.L. Huston, J. Chem. Phys., 49, 253 (1968).

56. H.D. Frame, Chem. Phys. Lett., 3, 182 (1969).

57. K. Seppelt and H.H. Rupp, Z. Anorg. Allg. Chem., 409, 331 (1974).

58. G.J. Schrobilgen, J.H. Holloway, P. Granger and C. Brevard, Inorg. Chem., 17, 980 (1978).

59. H.D. Frame, J.L. Huston and I. Sheft, Inorg. Chem., 8, 1549 (1969).

60. R.J. Gillespie and G.J. Schrobilgen, J. Chem. Soc., Chem. Commun., 595 (1977).

61. S.R. Gunn, J. Am. Chem. Soc., 87, 2290 (1965).

62. E. Jacob and R. Opferkuch, Angew. Chem., Int. Ed. Engl., 15, 158 (1976).

63. C.L. Chernick, H.H. Claassen, J.G. Malm and P.L. Plurien, in ref. (29), p. 106.

64. Ref. (26), pp. 601-605.

65. J.L. Huston, J. Phys. Chem., 71, 3339 (1967).

66. J.L. Huston, J. Am. Chem. Soc., 93, 5255 (1971).

67. J.L. Huston and H.H. Claassen, J. Chem. Phys., 55, 1505 (1971).

68. R.J. Gillespie, in ref. (29), p. 333.

69. J.L. Huston, 160th National Meeting of the American Chemical Society, Chicago, September 14-18, 1970.

70. S.M. Williamson and C.W. Koch, Science, 139, 1046 (1963).

71. S.R. Gunn, in ref. (29), p. 149.

72. H. Selig, H.H. Claassen, C.L. Chernick, J.G. Malm and J.L. Huston, Science, 143, 1322 (1964).

73. N. Bartlett and N.K. Jha, in ref. (18), p. 23.

74. N.N. Greenwood and A. Earnshaw, Eds., in "Chemistry of the Elements", Pergamon Press, Oxford (1984), Chapter 18.

75. J.J. Turner and G.C. Pimentel, Science, 140, 975 (1963).

76. D.R. MacKenzie, Science, 141, 1171 (1963).

77. J. Slivnik, A. Smalc, K. Lutar, B. Zemva and B. Frlec, J. Fluorine Chem., 5, 273 (1975).

78. L.V. Streng and A.G. Streng, Inorg. Chem., 5, 328 (1966).

79. Dokl. Akad. Nauk SSSR, 235, 96 (1977).

80. R.J. Gillespie and G.J. Schrobilgen, Inorg. Chem., 13, 1230 (1974).

81. J.H. Holloway and G.J. Schrobilgen, J. Chem. Soc., Chem. Commun., 623 (1975).

82. A.V. Grosse, A.D. Kirshenbaum, A.G. Streng and L.V. Streng, Science, 139, 1047 (1963).

83. E.N. Sloth and M.H. Studier, Science, 141, 528 (1963).

84. P.R. Fields, L. Stein and M.H. Zirin, in ref. (18), p. 113.

85. P.R. Fields, L. Stein and M.H. Zirin, J. Am. Chem. Soc., 84, 4164 (1962).

86. H. Selig, Inorg. Chem., 5, 183 (1966).

87. L. Stein, Science, 168, 362 (1970).

88. F. Sladky, P.A. Bulliner and N. Bartlett, J. Chem. Soc., Dalton Trans., 2179 (1969).

89. Ref. (24), p. 157 and references therein.

90. R.J. Gillespie, D. Martin and G.J. Schrobilgen, J. Chem. Soc., Dalton Trans., 1898 (1980).

91. J.H. Holloway and J.G. Knowles, J. Chem. Soc., Dalton Trans., 756 (1969).

92. F. Sladky, P.A. Bulliner, N. Bartlett, B.G. DeBoer and A. Zalkin, J. Chem. Soc., Chem. Commun., 1048 (1968).

93. N. Bartlett, B.G. DeBoer, F.J. Hollander, F. Sladky, D.H. Templeton and A. Zalkin, Inorg. Chem., 13, 780 (1974).

94. R.J. Gillespie, A. Netzer and G.J. Schrobilgen, Inorg. Chem., 13, 1455 (1974).

95. R.J. Gillespie and G.J. Schrobilgen, Inorg. Chem., 13, 1694 (1974).

96. J.H. Holloway and G.J. Schrobilgen, Inorg. Chem., 19, 2632 (1980).

97. Yu.M. Kiselev et al., Dokl. Akad. Nauk SSSR, 278, 881 (1984).

98. N. Bartlett and F. Sladky, J. Am. Chem. Soc., 90, 5316 (1968).

99. D. Gibler, B. Morrell, N. Bartlett and A. Zalkin, Abstracts, 162nd National Meeting of the American Chemical Society, Washington, D.C., Sept. 13-17, 1971, No. FLUO 1.

100. R.J. Gillespie, B. Landa and G.J. Schrobilgen, J. Chem. Soc., Chem. Commun., 1543 (1971).

101. R.J. Gillespie and G.J. Schrobilgen, Inorg. Chem., 13, 2370 (1974).

102. P. Boldrini, R.J. Gillespie, P.R. Ireland and G.J. Schrobilgen, Inorg. Chem., 13, 1690 (1974).

103. R.J. Gillespie, B. Landa and G.J. Schrobilgen, Inorg. Chem., 15, 1256 (1976).

104. D.E. McKee, A. Zalkin and N. Bartlett, Inorg. Chem., 12, 1713 (1973).

105. D.E. McKee, C.J. Adams and N. Bartlett, Inorg. Chem., 12, 1722 (1973).

106. R.J. Gillespie, D. Martin, G.J. Schrobilgen and D.R. Slim, J. Chem. Soc., Dalton Trans., 2234 (1977).

107. N. Bartlett and M. Wechsberg, Z. Anorg. Allg. Chem., 385, 5 (1971).

108. H.H. Hyman and L.A. Quarterman in ref. (18), pp. 275-278.

109. R.J. Gillespie and G.J. Schrobilgen, Inorg. Chem., 13, 765 (1974) and references therein.

110. J. Slivnik, B. Zemva, M. Bohinc, D. Hanzel, J. Grannec and P. Hagenmuller, J. Inorg. Nucl. Chem., 38, 997 (1976).

111. K. Leary and N. Bartlett, J. Chem. Soc., Chem. Commun., 903 (1972).

112. K. Leary, A. Zalkin and N. Bartlett, Inorg. Chem., 13, 775 (1974).

113. R.J. Gillespie and G.J. Schrobilgen, J. Chem. Soc., Chem. Commun., 90 (1974).

114. R.J. Gillespie and G.J. Schrobilgen, Inorg. Chem., 15, 22 (1976).

115. J.H. Holloway and G.J. Schrobilgen, Inorg. Chem., 20, 3363 (1981).

116. L. Stein, Radiochim. Acta, 32, 163 (1983).

117. R.J. Gillespie, B. Landa and G.J. Schrobilgen, J. Chem. Soc., Chem. Commun., 607 (1972).

118. R.D. Peacock, H. Selig and I. Sheft, Proc. Chem. Soc., 285 (1964).

119. R.D. Peacock, H. Selig and I. Sheft, J. Inorg. Nucl. Chem., 28, 2561 (1966).

120. S.W. Peterson, J.H. Holloway, B.A. Coyle and J.M. Williams, Science, 173, 1238 (1971).

121. G.J. Moody and H. Selig, Inorg. Nucl. Chem. Lett., 2, 319 (1966).

122. G.J. Schrobilgen, D. Martin-Rovet, P. Charpin and M.J. Lance, J. Chem. Soc., Chem. Commun., 894 (1980).

123. J.H. Holloway, V. Kaucic, D. Martin-Rovet, D.R. Russell, G.J. Schrobilgen and H. Selig, Inorg. Chem., 24, 678 (1985).

124. D.J. Hodgson and J.A. Ibers, Inorg. Chem., 8, 326 (1969).

125. S.H. Strauss, M.D. Noirot and O.P. Anderson, Inorg. Chem., 24, 4307 (1985).

126. P. Huppmann, H. Hartl and K. Seppelt, Z. Anorg. Allg. Chem., 524, 26 (1985).

127. T. Birchall, R.D. Myers, H. De Waard and G.J. Schrobilgen, Inorg. Chem., 21, 1068 (1982) and references therein.

128. F. Sladky and H. Kropshofer, Inorg. Nucl. Chem. Lett., 8, 195 (1972).

129. D. Lentz and K. Seppelt, Angew. Chem., Int. Ed. Engl., 17, 355 (1978).

130. K. Seppelt, Acc. Chem. Res., 12, 211 (1979).

131. R. Damerius, P. Huppmann, D. Lentz and K. Seppelt, J. Chem. Soc., Dalton Trans., 2821 (1984).

132. K. Seppelt, Angew. Chem., Int. Ed. Engl., 21, 877 (1982), and references therein.

133. N. Bartlett, M. Wechsberg, F.O. Sladky and P.A. Bulliner, J. Chem. Soc., Chem. Commun., 703 (1969).

134. M. Wechsberg, P.A. Bulliner, F.O. Sladky, R. Mews and N. Bartlett, Inorg. Chem., 11, 3063 (1972).

135. F. Sladky, Angew. Chem., Int. Ed. Engl., 8, 373 (1969).

136. F. Sladky, Angew. Chem., Int. Ed. Engl., 8, 523 (1969).

137. F. Sladky, Monatsh. Chem., 101, 1559 (1970).

138. F. Sladky, Monatsh. Chem., 101, 1571 (1970).

139. D. Lentz and K. Seppelt, Angew. Chem., Int. Ed. Engl., 17, 356 (1978).

140. D. Lentz and K. Seppelt, Angew. Chem., Int. Ed. Engl., 18, 66 (1979).

141. E. Jacob, D. Lentz, K. Seppelt and A. Simon, Z. Anorg. Allg. Chem., 472, 7 (1981).

142. G.A. Schumacher and G.J. Schrobilgen, Inorg. Chem., 23, 2923 (1984).

143. M. Eisenberg and D.D. DesMarteau, Inorg. Chem., 11, 1901 (1972).

144. K. Seppelt, Angew. Chem., Int. Ed. Engl., 11, 723 (1972).

145. K. Seppelt and D. Nothe, Inorg. Chem., 12, 2727 (1973).

146. J.J. Musher, J. Am. Chem. Soc., 90, 7371 (1968).

147. M. Eisenberg and D.D. DesMarteau, Inorg. Nucl. Chem. Lett., 6, 29 (1970).

148. R.D. LeBlond and D.D. DesMarteau, J. Chem. Soc., Chem. Commun., 555 (1974).

149. D.D. DesMarteau, R.D. LeBlond, S.F. Hossain and D. Nothe, J. Am. Chem. Soc., 103, 7734 (1981).

150. J.F. Sawyer, G.J. Schrobilgen and S.J. Sutherland, J. Chem. Soc., Chem. Commun., 210 (1982).

151. J.F. Sawyer, G.J. Schrobilgen and S.J. Sutherland, Inorg. Chem., 21, 4064 (1982).

152. G.A. Schumacher and G.J. Schrobilgen, Inorg. Chem., 22, 2178 (1983).

153. J. Foropoulos and D.D. DesMarteau, J. Am. Chem. Soc., 104, 4260 (1982).

154. C.T. Goetschel and K.R. Loos, J. Am. Chem. Soc., 94, 3018 (1972).

155. L.J. Turbini, R.E. Aikman and R.J. Lagow, J. Am. Chem. Soc., 101, 5833 (1979).

156. M. Eisenberg and D.D. DesMarteau, J. Am. Chem. Soc., 92, 4759 (1970).

157. M. Eisenberg and D.D. DesMarteau, Inorg. Chem., 11, 2641 (1972).

158. F.A. Cotton and G. Wilkinson, Eds., in "Advanced Inorganic Chemistry", Wiley-Interscience, J. Wiley & Sons (1980), p. 555.

159. R.C. Weast, "CRC Handbook of Chemistry and Physics", CRC Press Inc., Boca Raton, Florida, 64th Edition (1984).

160. K. Seppelt, Angew. Chem., Int. Ed. Engl., 13, 92 (1974).

161. K. Seppelt, Z. Anorg. Allg. Chem., 406, 287 (1974).

162. F. Sladky, H. Kropshofer and O. Leitzke, J. Chem. Soc., Chem. Commun., 134 (1973).

163. P. Huppmann, D. Lentz and K. Seppelt, Z. Anorg. Allg. Chem. 472, 26 (1981).

164. K. Seppelt and H.H. Rupp, Z. Anorg. Allg. Chem., 409, 338 (1974).

165. N.F. Ramsey, Phys. Rev., 77, 576 (1950); 78, 699 (1950).

166. A. Saika and C.P. Slichter, J. Chem. Phys., 22, 26 (1954).

167. G.J. Schrobilgen, "NMR and the Periodic Table"; R.K. Harris and B.E. Mann; Eds.: Academic Press: London, 1978; Chp 14.

168. R.J. Gillespie and B. Landa, Inorg. Chem., 12, 1383 (1973).

169. C.L. Chernick, C.E. Johnson, J.G. Malm, G.J. Perlow and M.R. Perlow, Phys. Lett., 5, 103 (1963).

170. G.J. Perlow, C.E. Johnson and M.R. Perlow, in ref. (29), p. 279.

171. S.L. Ruby and H. Selig, Phys. Rev., 147, 348 (1966).

172. J.H. Holloway, G.J. Schrobilgen, S. Bukshpan, W. Hilbrants and H. de Waard, J. Chem. Phys., 66, 2627 (1977).

173. N. Bartlett, M. Wechsberg, G.R. Jones and R.D. Burbank, Inorg. Chem., 11, 1124 (1972).

174. L.K. Templeton, D.H. Templeton, K. Seppelt and N. Bartlett, Inorg. Chem., 15, 2718 (1976).

175. R. Faggiani, D.K. Kennepohl, C.J.L. Lock and G.J. Schrobilgen, Inorg. Chem., 25, 563 (1986).

176. F. Sladky, Angew. Chem., Int. Ed. Engl., 9, 375 (1970).

177. F. Sladky, Monatsh. Chem., 101, 1578 (1970).

178. N. Keller and G.J. Schrobilgen, Inorg. Chem., 20, 2118 (1981).

179. D. Lentz, H. Pritzkow and K. Seppelt, Inorg. Chem., 17, 1926 (1978).

180. D. Lentz, H. Pritzkow and K. Seppelt, Angew. Chem., Int. Ed. Engl., 16, 729 (1977).

181. D. Lentz and K. Seppelt, Z. Anorg. Allg. Chem., 460, 5 (1980).

182. C.J. Schack and K.O. Christe, J. Fluorine Chem., 26, 19 (1984).

183. C.J. Schack and K.O. Christe, J. Fluorine Chem., 27, 53 (1985).

184. A. Engelbrecht and P. Peterfy, Angew. Chem., Int. Ed. Engl., 8, 768 (1969).

185. A. Engelbrecht, P. Peterfy and E. Schandara, Z. Anorg. Allg. Chem., 384, 202 (1971).

186. K.O. Christe, R.D. Wilson, and C.J. Schack, Inorg. Chem., 20, 2104 (1981).

187. R.J. Gillespie and J.P. Krasznai, Inorg. Chem., 16, 1384 (1977).

188. H.A. Carter, J.M. Ruddick, J.R. Sams and F. Aubke, Inorg. Nucl. Chem. Lett., 11, 29 (1975).

189. K.O. Christe and R.D. Wilson, Inorg. Nucl. Chem. Lett., 15, 375 (1979).

190. L.E. Smart, J. Chem. Soc., Chem. Commun., 519 (1977).

191. I. Beattie *et al.*, J. Chem. Soc., Dalton Trans., 1380 (1976).

192. R.J. Gillespie and J.P. Krasznai, Inorg. Chem., 15, 1251 (1976).

193. M.J. Vasile, W.E. Falconer and F.A. Stevie, J. Chem. Soc., Dalton Trans., 1233 (1977).

194. I.R. Beattie and G.J. van Schalkwyk, Inorg. Nucl. Chem. Lett., 10, 343 (1974).

195. B.M. Rode, Monatsh. Chem., 105, 807 (1974).

196. A. Finch, P.N. Gates, A.J. Edwards and A.A.K. Hana, J. Chem. Soc., Dalton Trans., 869 (1980).

197. A. Engelbrecht, O. Mayr, G. Ziller and E. Schandara, Monatsh. Chem., 105, 796 (1974).

198. A.J. Edwards and A.A.K. Hana, J. Chem. Soc., Dalton Trans., 1734 (1980).

199. J. Barr, R.J. Gillespie and R.C. Thompson, Inorg. Chem., 3, 1149 (1964).

200. A. Engelbrecht and F. Sladky, Angew. Chem., Int. Ed. Engl., 3, 383 (1964).

201. C.F. Hoffman, in "Inorganic Sunthesis". H.F. Holtzclaw, Ed., McGraw-Hill, New York (1953), Vol. 4. p. 150.

202. G. Brauer, Academic Press, New York, (1963) Vol. 1, p. 202.

203. H. von Wartenberg, Z. Anorg. Allg. Chem., 244, 344, (1940).

204. U. Elgad and H. Selig, Inorg. Nucl. Chem. Suppl., 91 (1976).

205. This work.

206. Allied Chemical Corporation, Fluosulfonic Acid-Product Information Technical Bulletin TA-30711, written ca. 1964.

207. H.A. Carter and F. Aubke, Inorg. Chem., 10, 2296 (1971).

208. J.P. Krasznai, Ph.D. Thesis, McMaster University, (1975).

209. P.M.A. Sherwood and J.J. Turner, Spectrochim. Acta, Part A., 26, 1975 (1970).

210. D.F Smith and G.M. Begun, J. Chem. Phys., 43, 2001 (1965).

211. J.H. Holloway, H. Selig and H.H. Claassen, J. Chem. Phys., 54, 4305 (1971).

212. J. Goubeau and J.B. Milne, Can. J. Chem., 45, 2321 (1967).

213. N. Bartlett, S. Beaton, L.W. Reeves and E.J. Wells, Can. J. Chem., 42, 2531 (1964).

214. T.E. Peel and R.J. Gillespie, J. Am. Chem. Soc., 95, 5173 (1973).

215. T.E. Peel and R.J. Gillespie, Adv. Phys. Org. Chem., 9, 1, (1972).

216. A. Engelbrecht and O. Mayer, 7th International Symposium on Fluorine Chemistry., Santa Cruz, California., 15-20 July 1973. Abstract 1-18.

217. Ref. (159). Dipole moments were measured in the gas phase and are estimated to be accurate within ± 0.5 D.

218. P. Bladon, D.H. Brown, K.D. Crosbie and D.W.A. Sharp, Spectrochim. Acta, Part A., 26, 2221 (1970).

219. K.O. Christe, Adv. Inorg. Chem. Radiochem., 18, 319 (1976).

220. H.A. Carter and F. Aubke, Inorg. Chem., 10, 2296 (1971).

221. L.E. Alexander and I.R. Beattie, J. Chem. Soc., Dalton Trans., 3091 (1971).

222. K.O. Christe, Private Communication.

223. W. Porcham and A. Engelbrecht, Monatsh. Chem., 102, 333 (1971).

224. B.M. Rode, A. Engelbrecht and I. Schantl, Z. Phys. Chem., 253, 17 (1973).

225. K. Seppelt and D. Nothe, Inorg. Chem., 12, 2727 (1973).

226. K. Seppelt, Chem. Ber., 106, 157 (1973).

227. G.M. Begun, W.H. Fletcher and D.F. Smith, J. Chem. Phys., 42, 2236 (1965).

228. P.H. Spekkens, Ph.D. Thesis, McMaster University, (1977).

229. R.J. Gillespie and P.H. Spekkens, Isr. J. Chem., 17, 11 (1978).

230. H. Oberhammer and K. Seppelt, Inorg. Chem., 17, 1435 (1978).

231. H. Oberhammer and K. Seppelt, Angew. Chem., Int. Ed. Engl., 17, 69 (1978).

232. K. Seppelt, Chem. Ber., 105, 2431 (1972).

233. K. Seppelt, Chem. Ber., 110, 1470 (1977).

234. F. Sladky, H. Kropshofer, O. Leitzke and P. Peringer, J. Inorg. Nucl. Chem., Supplement (1976).

235. C.J. Schack and K.O. Christe, J. Fluorine Chem., 24, 467 (1984).

236. C.J. Adams and A.J. Down, Spectrochim. Acta., 28A, 1841 (1972).

237. M.J. Collins and G.J. Schrobilgen, Inorg. Chem., 24, 2608 (1985).

238. K. Seppelt, Chem. Ber., 109, 1046 (1976).